# GEOSPATIAL TECHNIQUES

## for Managing Environmental Resources

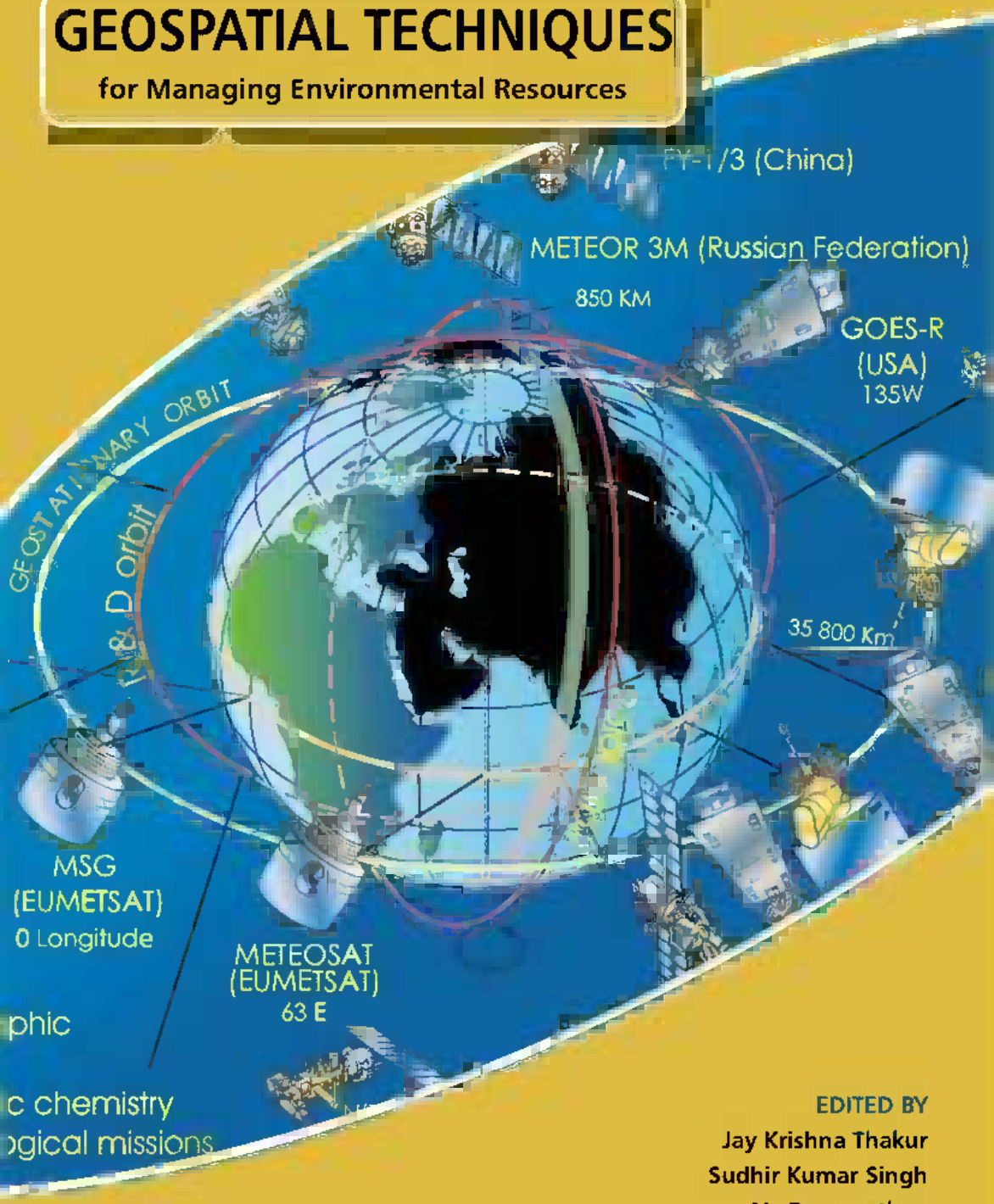



EDITED BY

Jay Krishna Thakur

Sudhir Kumar Singh

AL. Ramanathan

M. Bala Krishna Prasad

Wolfgang Gossel



Springer

# Geospatial Techniques for Managing Environmental Resources

# Geospatial Techniques for Managing Environmental Resources

Edited by

**Jay Krishna Thakur**
*Department of Hydrogeology and Environmental Geology*
*Institute of Geosciences and Geography*
*Martin Luther University, Halle (Saale), Germany*

**Sudhir Kumar Singh**
*Centre of Atmospheric and Ocean Science*
*KBCAOS, IIDS, University of Allahabad, India*

**AL. Ramanathan**
*School of Environmental Sciences*
*Jawaharlal Nehru University, New Delhi, India*

**M. Bala Krishna Prasad**
*Earth System Science Interdisciplinary Center*
*University of Maryland, USA*

**Wolfgang Gossel**
*Department of Hydrogeology and Environmental Geology*
*Institute of Geosciences and Geography*
*Martin Luther University, Halle (Saale), Germany*

A C.I.P. Catalogue record for this book is available from the Library of Congress.

ISBN 978-94-007-1857-9 (HB)
ISBN 978-94-007-1858-6 (e-book)

Copublished by Springer,
P.O. Box 17, 3300 AA Dordrecht, The Netherlands
with Capital Publishing Company, New Delhi, India.

Sold and distributed in North, Central and South America by Springer,
233 Spring Street, New York 10013, USA.

In all other countries, except SAARC countriesó Afghanistan, Bangladesh, Bhutan, India, Maldives, Nepal, Pakistan and Sri Lankaó sold and distributed by Springer, Haberstrasse 7, D-69126 Heidelberg, Germany.

In SAARC countriesó Afghanistan, Bangladesh, Bhutan, India, Maldives, Nepal, Pakistan and Sri Lankaó sold and distributed by Capital Publishing Company, 7/28, Mahaveer Street, Ansari Road, Daryaganj, New Delhi, 110 002, India.

*www.springer.com*

***Cover photo credit:*** http://www.wmo.int/pages/prog/www/images/GOS/Figure%20II-10%20Satellites.jpg

*Printed on acid-free paper*



Printed in India.

# Foreword

ì Geospatial informationî is spatial data concerning a place or, in space, collected in real time. Geospatial techniques together with remote sensing, geographic information science, Global Positioning System (GPS), cartography, geovisualization, and spatial statistics are being used to capture, store, manipulate and analyze to understand complex situations to solve mysteries of the universe. These techniques have been applied in various fields like metrology, forestry, air-water-land management, agriculture, health, homeland security etc. around the globe. This book has made an effort to provide a single record of current research status, technologies and applications of geospatial techniques in various fields and will be useful to academics, researchers and industry practitioners who are involved or interested in the study, use, design and development of advanced and emerging geospatial technologies around the world with ultimate aim to empower individuals and organizations in building competencies for exploiting the opportunities of the knowledge society.

The chapters in this book demonstrate the need for the integrating environmental management approaches in combination with other fields using geospatial techniques. This book presents case studies and examples from various parts of the world and provides a broad overview of various geospatial management approaches and tools used to promote environmental sustainability in the context of global environmental change and natural hazards. These case studies provide an insight into present day issues, challenges and opportunities; and highlight the key features, application of commercial and non-commercial satellite and sensors, principles and new approaches that need to be considered in future efforts for efficient integrated management in these fields. It is necessary to address the scientific strategies which underpin the implementation of geospatial techniques development for overall integrated management of various fields.

I would like to congratulate the great efforts of the editorial team of this volume which will serve as a scientific information base for future planning of the geospatial techniques development around the world and energize

synergy among academicians, researchers, stakeholders, INGOs, policy makers and the corporate sector for documentation and dissemination of knowledge for the global welfare management.

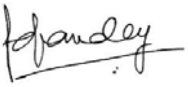

**Dr. Prem Chand Pandey**
Emeritus Professor, Indian Institute of Technology, Kharagpur, India
Founder Director, National Centre for Antarctic & Ocean Research (NCAOR), Goa, India

# Preface

The recent advancement of geospatial techniques and geodatasets have grown dramatically in size and number and become more widely distributed. The term Geospatial is generally used to describe the combination of spatial analytical methods and software with geographic datasets in conjunction with Geographic Information Systems (GIS), spatial statistics, remote sensing, cartography, geo-visualization and geomatics for aquatic and terrestrial environment especially for a civilian, business, government and military organizations. GIS as a system is integrating hardware, software, and data that captures, stores, analyzes, manages, and presents data that are linked to the locations with the merging of statistical analysis, and database technology. It is being used in cartography, remote sensing, land surveying, utility management, natural resource management, photogrammetry, geography, urban planning, emergency management, navigation, and localized search engines. Remote sensing is the acquisition of information of an object or phenomenon, by the use of either recording or real-time sensing device(s) that are wireless, or not in physical or intimate contact with the object. While, Geomatics is a fairly new terminology which is the combination of geodesy and geoinformatic terms and includes the tools and techniques used in land surveying, remote sensing, cartography, GIS, Global Navigation Satellite Systems (GNSS), photogrammetry, and related forms of earth mapping. Integration of these research and developments to real world application in these fields are now required for local, regional and global development. In this umbrella book of geospatial techniques, there are total seventeen chapters presenting the recent advancement in the GIS, remote sensing, Global Positioning System (GPS), geovisualization and geomatics for application in the field of Agriculture, Business GIS, Climate change, Energy, Environmental services, Geology, Glaciology, Health, Land information system, Natural hazard management, Natural resource management, Corporate studies, Urban planning and Utility management.

This book represents the inter- and multi-disciplinary view of authors for a meaningful and practical guidance for the better application of geospatial techniques that comprises contribution from distinguished scientists from both academia and institutions from around the globe who are actively working in this area. This volume presents the case studies and examples from various

parts of the globe and provides a broader overview of various approaches involved in data acquiring, monitoring and dissemination methods. This book provides a detailed knowledge of various platforms, satellites, and sensors; tools and techniques and application to various fields for the sustainable management of environmental resources in the context of global environmental change and natural hazards.

To the beginners, we suggest not to be panicked by seeing advanced methods, applications and integrated approaches. It is necessary to understand from basics and link presented methods and application of techniques to other fields, as there are amalgamation of various processes and thoughts. The book provides a holistic application of geospatial techniques in managing natural resources in the present scenario. This book is a comprehensive collection of articles from around the world, which reflects importance of this technology in making the earth habitable. These case studies provide an insight into present-day issues, challenges and opportunities; and highlight the key features, principles, and new approaches that need to be considered in future efforts to make the earth a livable place.

We would like to thank all the contributors to this volume and take this opportunity to acknowledge all our colleagues for their time-consuming efforts to review the manuscripts of the chapters for this volume. Their efforts with high quality review of the manuscripts contributed significantly to keep the high scientific contents of the book. The editors also would like to thank collaborators and research scholars for supporting their research activities that helped in bringing out this volume successfully.

The book is scientific and research-oriented, yet appealing to a broad audience interested in environmental applications of geospatial technologies, thus making it an important reference source for the fields of GIS, remote sensing, geography, environmental policy, and environmental science. We hope that this book will be useful for geospatial scientists, remote sensing and GIS scientists, engineers, managers and administrators in both academia and industries, decision and policy makers and for government and regulatory bodies dealing with geospatial issues by providing an opportunity to acquire relevant scientific information and experiences in ì Geospatial Techniques for Managing Environmental Resourcesî .

Lastly, the editors wish to thank the publishers for bringing out this volume successfully.

**Jay Krishna Thakur**
**Sudhir Kumar Singh**
**AL. Ramanathan**
**M. Bala Krishna Prasad**
**Wolfgang Gossel**

# About the Editors

**Jay Krishna Thakur** is Higrade Fellow at Department of Hydrogeology and Environmental Geology, Martin Luther University, Halle, Germany and visiting scientist at Helmholtz Centre for Environmental Research, UFZ, Leipzig, Germany. He has specialized on application of geospatial techniques in hydrogeology, hydrology, water resources and environmental management and worked extensively on the wetland management studies, quantification of water cycle components and its dynamics, modelling of surface water and groundwater, groundwater monitoring network optimization, GEONETCast environmental data streams for climate, water and environmental studies, clouds process, climate change impacts and adaptation, analysis and monitoring techniques of climate change etc. He has been awarded with various research fellowships including Netherlands Fellowship Program and Higrade Fellowship Program. He has also contributed in conference papers, book chapters and papers in reputed peer-reviewed journals.

**Sudhir Kumar Singh** is working at the Centre of Atmospheric and Ocean Science, University of Allahabad, Allahabad, India. He has also worked at Department of Forestry, Mizoram Central University, Aizwal, India. His main research areas are Remote Sensing and GIS applications in the field of resource management, environmental modelling and environmental pollution studies in order to solve real world problems. He has received many prestigious scholarships and has national and international collaboration with leading institutes in the United Kingdom, Germany, Turkey and Nepal. He has contributed many research papers in peer-reviewed journals and has reviewed papers, CVs and research proposal for several journals and various research institutions including the National Research Foundation, South Africa. As a supervisor, he guided over fifteen Diploma and MSc theses.

**AL. Ramanathan**, PhD in sedimentary geochemistry from Centre of Advanced Studies, Panjab University, worked as faculty in Geology Department, Annamalai University, for a decade. He is currently Professor of environmental geology, hydrogeochemistry, biogeochemistry, glaciology and application of geospatial techniques in environmental hydrogeology in the School of Environmental Sciences, Jawaharlal Nehru University, New Delhi, India. He has specialized on application of geospatial techniques in hydro-

geology, hydrology, environmental resources management and worked extensively on the mangroves, estuaries, coastal ground waters, surface and groundwater contamination modelling of India for the past two decades. He is engaged in coastal research with a number of universities and research organisations in India, Australia, France, Japan, Sweden, Russia, USA, etc. He has guided over thirty PhDs and MPhils in the above subject and published more than seventy papers in referred reputed journals. He has also published twelve books and contributed several chapters in many others. He has thrice received the IFS Sweden (Project) Awards to work on mangrove biogeochemistry besides working in national and international projects from Indo-Australian, Indo-Russian, DST, MoEF, MoWR, etc. He has been guest editor for the International Journal of Ecology and Environmental Sciences. He is a member of editorial board in the Indian Journal of Marine Sciences and served as referee for many national and international journals as well.

**M. Bala Krishna Prasad** is a Research Associate at Earth System Science Interdisciplinary Center, University of Maryland, College Park, USA. He did PhD in Biogeochemistry at School of Environmental Sciences, Jawaharlal Nehru University, India. His primary research interest is evaluation and modelling of climate change and anthropogenic impacts on the water quality and aquatic ecosystem dynamics. He is a recipient of the Young Scientist Award from the Ministry of Science & Technology (India), Linnaeus-Palme Research Fellowship from Department of Earth Sciences, Uppsala University (Sweden), Berkner Fellowship of AGU (USA) and Junior Research Fellowships as well. He has contributed more than a dozen papers in reputed peer-reviewed international journals.

**Wolfgang Gossel**, habilitated in 2008 in Applied Geosciences at Martin Luther University, Halle (Germany) and worked for nearly 20 years in hydrogeology. He is a specialist in groundwater flow and transport modelling, GIS data processing and the application of interpolation techniques in hydrogeology. He is mainly working on the regional scale and since 2002 has got published several papers about the numerical groundwater flow models of the Nubian Aquifer System in Northeast Africa and the map Hydrogeology of Germany. He has also collaborated with the Jawaharlal Nehru University in New Delhi, Assiut University and Ain Shams University in Egypt, Universidad Autonoma de Merida and Universidad Autonoma de San Luis Potosi in Mexico. He was Associate Editor of Hydrogeology Journal and Grundwasser. As a supervisor he guided about 50 Diploma and MSc theses.

# Contents

# 1

# Environmental Informatics: Advancing Data Intensive Sciences to Solve Environmental Problems

**Chaowei Yang, Yan Xu[1] and Daniel Fay[1]**
Center for Intelligent Spatial Computing, and Department of Geography and GeoInformation Sciences, George Mason University
Fairfax, VA, USA
[1]Earth, Energy and Environment at Microsoft Research Connections
Microsoft Corporation, Redmond, WA, USA

## Introduction

The 21st Century witnesses emergence of geospatial cyberinfrastructure and other relevant geospatial technologies (Yang et al., 2010) for collecting data, extracting information, simulating phenomena scenarios, and supporting decision making (Caragea et al., 2005; Stadler et al., 2006). The advancements of the geospatial technologies not only provide great opportunities for us to better understand environmental issues and better position us to solve global to local environmental problems (Pecar-Ilic and Ruzic, 2006), but also pose great challenges for us to handle terabytes to petabytes of heterogeneous environmental data. Environmental informatics (Green and Klomp, 1998; Hilty, Page and Hŗebíçek, 2006) should be revisited to efficiently and effectively manage, integrate, and mine information and knowledge from the vast amount of data for supporting environmental decisions (Hey, Tansley and Tolle, 2008).

Information/knowledge mining often starts with heterogeneous data from various resources, and ends with re-aggregated data in numbers and/or intuitive graphics adopted by decision makers. On one hand, there are many conventional geospatial techniques that can be used to facilitate generating information and knowledge from environmental data to produce social impact. There are also many computing technologies that are not specifically designed for managing environmental data but can be used innovatively to significantly accelerate the mining process. On the other hand, it is a challenge to decide what techniques to choose and to integrate with, so that strategies could be taken to

J.K. Thakur et al. (eds.), *Geospatial Techniques for Managing Environmental Resources*,
DOI 10.1007/978-94-007-1858-6_1, © Capital Publishing Company 2012

design solution by leveraging the techniques efficiently in managing environmental data.

Based on our past decade's investigation on utilizing geospatial technologies for managing environmental data, this chapter illustrates how to utilize a set of computational geospatial techniques to manage and process environmental data through presenting five examples. The chapter concludes with a discussion on future directions of environmental informatics to handle potential problems from the arena of data intensive, computing intensive, spatiotemporal intensive and concurrent access intensive (Yang et al., 2011).

## Background

Environmental data are of essential values in support of environmental decisions by providing historical and real-time representation of the facts about environmental phenomena. The data have the characteristics of: (1) global distribution (Pillmann, Geiger and Voigt, 2006; Zhizhin et al., 2007), for example, dust storm generated from northern Africa could travel to Europe and forest fire emissions in Washington state can impact air quality in Iowa (Xie et al., 2010); (2) multi-dimensionality, though many datasets are two dimensional, the collection of three and four dimensional data has begun, for example, a four dimensional dataset is measured of daily nitrogen concentrations at different depths within Chesapeake Bay; (3) heterogeneity, which exists in many ways such as within data formats, data contents, data accuracy, data spatial resolution and time scale (Devarakonda et al., 2010; Yang et al., 2008), geographic coverage, and jurisdiction or culture boundaries; and (4) large volume, intensive data up to petabytes in size may be collected to record observations in four dimensions of space and time (Goodchild, Yuan and Cova, 2007).

The emerging requirements for data of high resolution and collected as a time series when compared to existing information may result in gaps in time, geographic coverage, and jurisdiction or culture boundaries. The time scales over which relevant environmental data may be collected also varies by the type of observations that are required (Karatzas, Nikolaou and Moussiopoulos, 2004), for example, data in response to environmental disasters, climate change and/or policy decisions may require daily, yearly or decadal measurements. Spatial constraints and scientific principles must also be represented within environmental datasets (Yang et al., 2011b). An illustration of this is how toxic material will travel in rivers at a much faster speed than hazardous material percolating through soil, but slower than hazardous gas emissions travelling through the atmosphere. These movements of material are governed by different geophysical principles and therefore require different models of various complexities to simulate and produce accurate predictions in support of decision making.

From an informatics perspective, these problems are also reflected as data intensive, computing intensive, spatiotemporal intensive, and concurrent access intensive (Yang et al., 2011a): (1) the data in terabytes to petabytes are volume intensive; (2) the various geophysical models and interpolation methods require cutting-edge computer or high end computing support to simulate environmental phenomena; (3) data are increasingly demanded to be tagged up with both spatial and temporal information in order to be useful (Rasuly, Naghdifar and Rasoli, 2010). Near-real time data requirements are becoming more common for environmental emergency responses that happened much more frequently within our globalized world (Karatzas et al., 2004); and (4) some datasets and model predictions are of public interest to be accessed by thousands to millions of citizens in a very short time period. For example, the air quality information, just like the weather information, is essential for the public to make personal decisions about their outdoor activities and travel plans based on individual health considerations.

Best handling environmental data with such characteristics and satisfying the requirements from the users require us to revisit environmental informatics, the science studying how to utilize information technologies and methodologies to process environmental data for better informed decision making (Wang 2007). In general, environmental informatics includes the procedure (Fig. 1) to: (1) extract, interpolate, and aggregate data to generate information for specific environmental decision needs; (2) analyze or simulate environmental issues to obtain knowledge about environmental issues; (3) support specific environmental decisions with potential scenarios and domain knowledge; and (4) making social impact by contributing valuable information and collecting citizen feedbacks to improve the environmental observations, data processing techniques, model simulation algorithms, or to revise decision making procedure with a more scientifically sound approach.

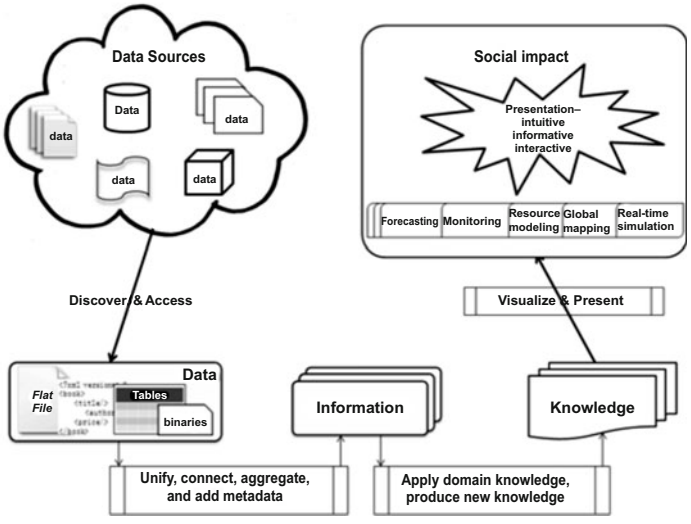


**Figure 1.** Information flow within environmental informatics.

## Research Examples

Observing the characteristics of environmental data, the requirements for data processing, and the procedure to address user requirements, we review environmental informatics in the context of data intensive science that includes transforming environmental data, to information, to knowledge, to decision support, and ultimately to social impact. Each of the four steps is exemplified through literature reviews and research examples from the Environmental Informatics Framework, a Microsoft eScience initiative and George Mason University (GMU) Center for Intelligent Spatial Computing (CISC)'s research projects: (1) A virtual Earth observatory project shows the discovery and integration of data from widely distributed services for environmental operations based on interoperability and on-the-fly integration; (2) A United States ozone observation and interpolation project illustrates data to information transformation; (3) An on-demand MODIS science project demonstrates how cloud computing can help to enable science question answered in near real-time; (4) A Chinese land cover change project demonstrates how to utilize intensive data and sophisticated models to support decision making; and (5) A citizen sensing flooding project is used to demonstrate how the data, information, modelling, and knowledge can produce social impact and benefit from citizen sciences. Scenarios with integrative solutions based on cutting-edge Microsoft data and information technologies are laid out in the examples to illustrate the future of environmental informatics.

### Data Discovery, Access and Utilization with Virtual Observatory

Global Earth observations collect petabytes of geospatial data that are important for tackling environmental issues. But the datasets are widely distributed, in diverse volume, and served through heterogeneous approaches. Efficient discovery, access and utilization of the data are great challenges. The efficient integration of the data on the fly will provide enabling capability to facilitate global to local level decision support (Yang et al., 2011b). Under the sponsorship from Microsoft and NASA, GMU CISC developed a spatial web portal to integrate the data services from around the global to serve as a virtual Earth observatory.

Figure 2 illustrates the interface of the spatial web portal, which is able to search against global Earth observation data in collaboration with the clearinghouse of Global Earth Observation System of Systems (GEOSS). Found datasets can be accessed and integrated from around the world (denoted red icons) when served through interoperable interfaces, such as Open Geospatial Consortium (OGC)'s Web Services, including Web Map Service (WMS), Web Coverage Services (WCS), and others.

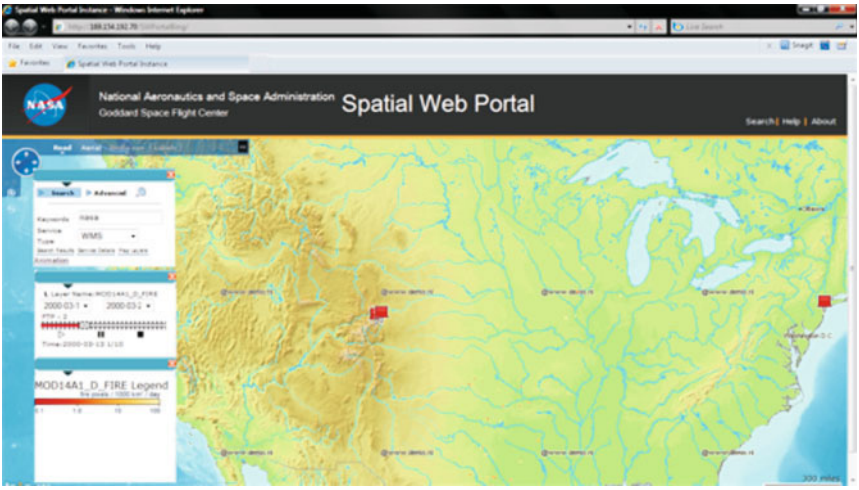


**Figure 2.** A virtual observatory of Earth science data based on spatial web portal.

Figure 2 illustrates that forest fire information, detected through MODIS, is integrated on a daily basis through the spatial web portal and decision makers can, for example, use it to generate historical animations (controlled by the three small windows) as well as ingest real-time Earth observations to assist emergency response for allocating fire suppression resources. The system can also be used for other environmental problems because of its characteristics of interoperability, and the advanced capabilities provided by Microsoft Bing Maps.

## Ozone Observation and Country-wide Interpolation

Ozone concentration is an important air quality factor that has impact on our breathing and other public health related activities. In collaboration with NOAA, EPA established about 100 observation sites around the United States. These sites generate point data on a minute basis and most of them have time series observations. With the outage variations and the uneven distribution of the sites (denoted in dots in Fig. 3), it is difficult to get an overview about the ozone distribution around the entire country with the point data.

Starting from a course project, a team of students at GMU collected daily data from the sites for the past 10 years and developed a graphics user interface (Fig. 3) for end users to: (1) pinpoint the ozone concentration within the map, (2) choose the specific dates for the observation (through upper left calendar), (3) animate the ozone concentration on a daily basis, and (4) choose different interpolation methods and accuracy to interpolate the point data to get area coverage for the entire nation (lower left).

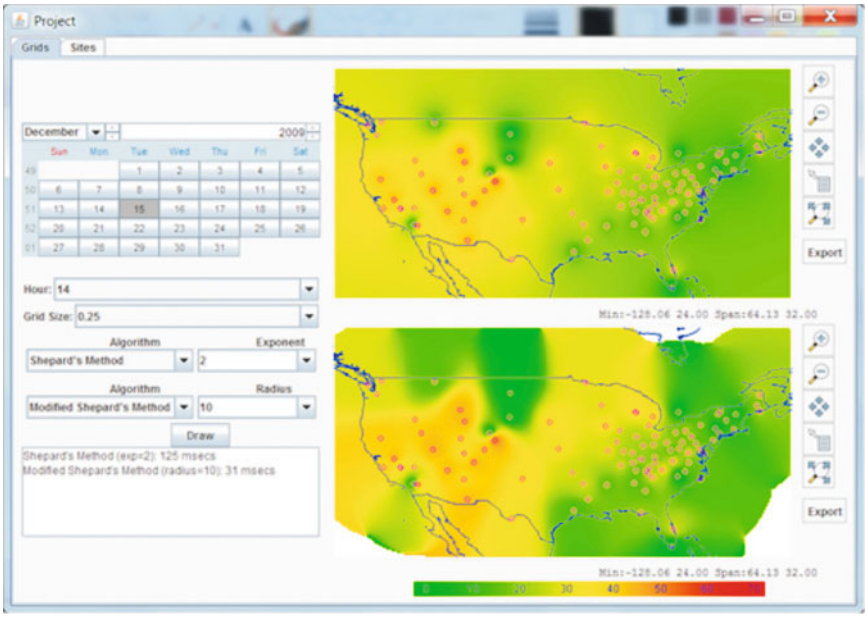


**Figure 3.** Ozone interpolation and navigation tool for the United States.

This tool could help us to have a better view of the entire nation for ozone concentration based on the site point observations and statistical interpolation. To some degree, it helps us to interpolate or extract information for missing places. But on the other hand, it demonstrates, through comparison of interpolation methods (right side images of Fig. 3), that simple interpolation is too arbitrary to generate accurate ozone concentration maps. Therefore, follow-on studies are needed to incorporate weather information and other source of observations, such as satellite remote sensing, to generate more accurate interpolations and eventually to forecast the ozone concentrations based on the historical and weather forecasting (Slini, Karatzas and Moussiopoulos, 2003). Making the data and interpolation services available through OGC web services would also help them to be easily discovered, accessed and utilized through, for example, virtual observatory described in previous section.

## Knowledge Generation from Long-term Observation

Earth observations are invaluable for scientists to track the phenomena facts of the Earth surface. Complex data processing algorithms, such as subsetting and parameter extracting, are needed to process the observations before final products can be used by scientists or decision makers. And these products requirements are quite different. Therefore, an infrastructure is needed to provide on-demand science queries for specific parameters or products.

As an example of real-time data intensive project where not only large amount of data but also complex processing algorithms are needed, the Microsoft Research MODISAzure project demonstrated that cloud computing technology can dramatically change the scale and the pace of the environmental research. It enables scientists to ask more exciting and important questions and will help to answer them by providing an automated closed processing loop to support the observation, data selection, reprojection, derivation reduction, and analysis reduction for science results given specific scientific questions (Fig. 4).

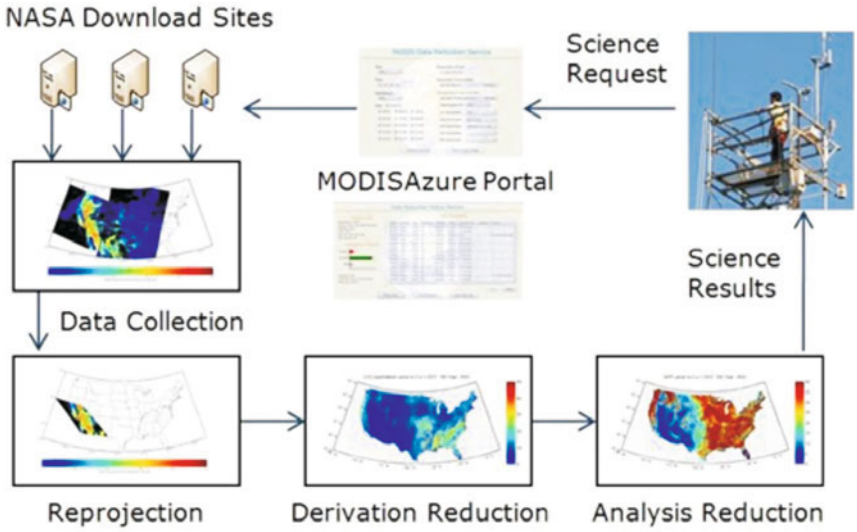


**Figure 4.** The workflow of MODISAzure is implemented on the Azure cloud computing platform.

This science on-demand scenario includes data subsetting/selection, reprojection, derivation and analyses components based on complex algorithms, which are data intensive and computing intensive. Spatiotemporal intensive is also a characteristic that is considered within the project to provide real time response for science questions. The data intensive, computing intensive and spatiotemporal intensive issues are resolved within this project using Azure cloud computing platform.

The solution automates the main components of the pipeline including data download, image reprojection, on-demand execution of the algorithms, and delivery of final results to scientists' desktops. It helps solve several obstacles to accessing the vast and varied remote sensing data from the MODIS satellites and other sources. More details about the MODISAzure project can be found at *http://research.microsoft.com/projects/azure/azuremodis.aspx*. This project demonstrates that the data discovery, access and utilization can be conducted in an automated fashion with support from cloud computing.

## Forecasting Changes in Urban Land Use

Land use/cover change is a driving factor for many environmental issues. Forecasting the environmental consequence due to fast urban expansion is a serious challenge for decision makers in many fast developing countries. A capability to simulate/forecast land use and land cover change based on specific policies and constraints is important to make informative decisions (Rasuly, Naghdifar and Rasoli, 2010).

Figure 5 shows a screen shot of an online Bing Maps based land use application. High Performance Computing (HPC) technologies are applied to combine urban land expansion module and environmental forecast module to provide computing support. It enables real-time simulation of the effect selected by heterogeneous environmental variables (shown on the upper-right corner in the picture). The application provides an interactive user interface for decision makers and the general public to investigate and better understand how the changes in urban land use may impact the environment. The platform is accessible via Internet browser with user access control. The application can be easily scaled to incorporate more environmental factors and regions.

The project integrates historical and observation data from different resources including in-situ sensor and satellite images. In addition, land use and land change knowledge based on different driving factors, such as policy constraints and spatial distribution, are built into a model that is running on a high performance computing facility at Tsinghua University.

More detailed description on this application can be found in the proceedings of Microsoft Environmental Research Workshop 2010 (*http://research.microsoft.com/en-US/events/environmentalresearch2010/default.aspx*)

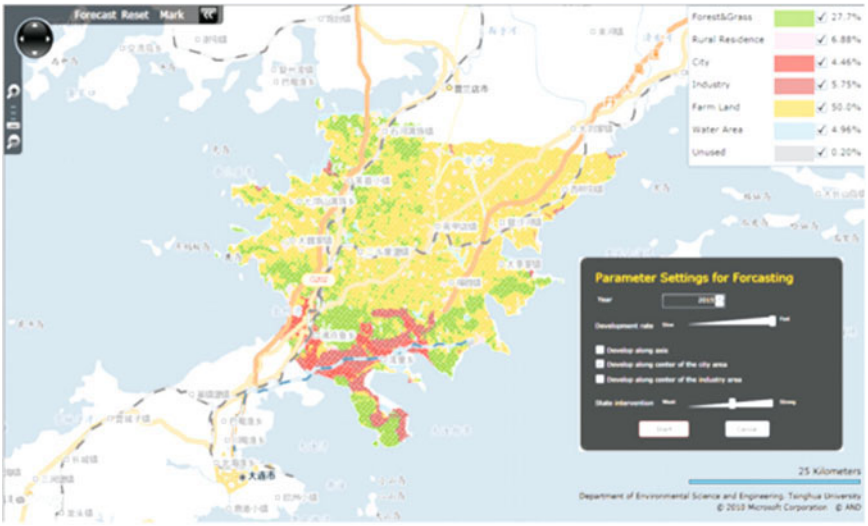


**Figure 5.** The land use change simulation based on different parameters setting.

### Social Impact and Citizen Sensing for Flooding Management

Many environmental issues have personal touch and broad impact. It is challenging to integrate information from masses of individuals within a broad area impacted. For example, in regions such as south Florida, before a hurricane hits, the city receives large number of calls from residents to report house flooding. Such citizen call-in data are location and time sensitive during the emergency, which can be leveraged to democratize emergency management, flooding control and decision support; raise localized, timely and socially relevant situational awareness; and critically complement physics-based modelling forecasts (Barros, 2005). A better visualization of the call-in data in time series will help decision makers or emergency planners to manage emergency preparedness. In this case, Microsoft Research World Wide Telescope (WWT, http://www.worldwidetelescope.org) is found to be the ideal tool to produce the desired visualization effect. Figure 6 shows a screen shot of the citizen call-in data in 2005-2008 animated in a WWT guided tour with different colours denoting different years. The tour can be interactively enriched with scientific models to simulate and forecast potential storm hits.


**Figure 6.** Citizen sensing helped with the flooding management of southern Florida.

## Solutions with Microsoft Advanced Technologies

Through five examples, previous section illustrates how Microsoft technologies are utilized to solve data intensive, computing intensive, spatiotemporal intensive and concurrent access intensive issues facing us for advancing environmental informatics in the 21st century.

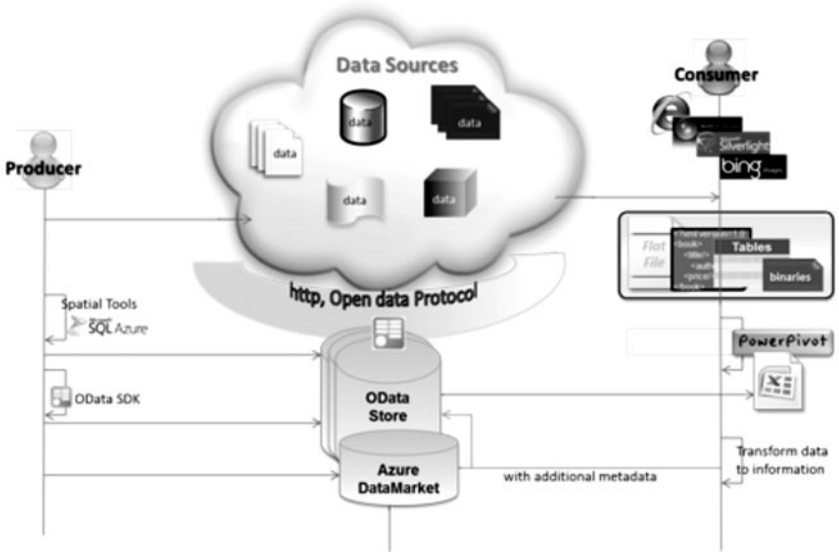


**Figure 7.** A flexible solution from Environmental Informatics Framework (EIF), a Microsoft eScience initiative.

Figure 7 illustrates a flexible configuration and possible components that can help environmental data processing and advancing environmental informatics. The solution is focussed on data generated from a variety of resources and produced by different users. Microsoft SQL and SQLAzure platform can be used to organize and manage the data kept in OData Store and DataMarket. OData Stores and Microsoft Azure DataMarket (formally codenamed Dallas) could provide connection to the data through the Open Data Protocol (OData), and consequently visualized in a variety of tools, such as Microsoft Excel, Excel with PowerPivot Add-in, Bing Maps, or WWT, for end users to intuitively access the datasets. If all components were running in a cloud computing environment, such as Azure, the data, services utilized can be discovered and utilized in an automatic fashion with minimum scripting development.

## Future Research Directions

Advanced IT technologies are providing enabling capabilities to better tackle environmental issues in the 21st century as illustrated through the examples in an environmental informatics fashion (Radermacher, 1994). Problems also emerged from the process of the data accumulation, scientific research, end user requirements, and requirements for more precise information and knowledge. The challenges of data intensive, computing intensive, spatiotemporal intensive, and concurrent intensive will continue to serve as driving demands for advancing environmental informatics. Opportunities and

challenges coexist within our efforts to tackle the issues (Yang et al., 2011b). The following directions need further attention for research and development in the following decade to advance environmental informatics.

- An environmental informatics *infrastructure* is needed for fast integration and aggregation of environmental observations from different organizations into a virtual simulation centre that can produce scientifically sound decision support information (MacDonell, Morgan and Newland, 2002). This can benefit from the recent geospatial cyberinfrastructure advancement at different agencies (Yang et al., 2010), especially within the environmental protection agency and companies, such as Microsoft, who are willing to contribute advanced technologies to address our global environmental issues.
- Advanced *computing technologies* are still needed to be further developed, especially in a spatial cloud computing fashion (Yang et al., 2011a and 2011b) to best leverage the distributed computing resources to handle environmental observations accumulated from local to global locations and to best handle environmental models, observations, and simulations in an optimized fashion.
- *Data integration and interoperability* is an inevitable task that will endure the entire life cycle of environmental informatics to solve data heterogeneous and service heterogeneous problems in the 21st century.
- *Spatiotemporal models* are becoming increasingly important from both theoretical and technological research and development to handle real-time and historical environmental data for better simulating potentially resulting scenarios from environmental decisions.
- *Human knowledge* about our planet is critical to the advancement of environmental informatics (Chen et al., 2007) and should be integrated in solutions (Tochtermann and Maurer, 2000). But our understanding of Earth has been very much divided according to different domains including, for example, biology, physics, ocean, atmosphere and land. *Model integration* is much needed to couple individualized models to form integrative systems to better simulate the response of geophysical systems from any event triggered by either human activities, such as hazardous material emission, or by nature, such as a tsunami.
- All resources supporting the advancements of environmental informatics will have their own relevant *quality and usage* limitation based on the providers, operational status and end users. The research on the quality and authority of data, service, information, knowledge and models will be critical to guarantee better decision making. Assessing the accuracy is essential within environmental informatics processes (Kalapanidas and Avouris, 2003).
- *Citizen science* is emerging as a phenomenon to involve citizens in popular scientific discoveries and science and policy comment and verification (Gruiz, 2009). For environmental science, this is especially true when

observations are still the best approach to obtain environmental information (Mayfield, Joliat and Cowan, 2001). Large amount of environmental issues are reported by citizen (Stockwell et al., 2006). Citizens could also contribute their computing resources in a Seti@Home fashion to solve public environmental issues, such as climate change through Climate@Home.

- *An automated and self-adaptive environment* for discovery, access and utilization of data and services will be needed in the future for quickly integrating data, information, knowledge, citizen sciences, and decisions made to produce knowledge for rapid, broad and precise environmental problems solving.

## Conclusion

Within the data explosion era, environmental informatics faces great challenges to better manage, integrate, simulate and forecast environmental information to extract knowledge for better environmental decisions. This chapter summarizes environmental informatics through analyzing the characteristics of environmental data and five research examples.

We report: (1) How the environmental data observed can be interpolated to have a reasonable geographic coverage; (2) How data can be discovered, accessed and integrated and visualized through Bing Maps to conduct information integration on the fly; (3) How to utilize Azure cloud computing and MODIS knowledge to produce decision support results in real time; (4) How to utilize cloud computing and distributed data integration to support environmental scenario simulations for decision making with potential scenarios; and (5) How to involve citizens in environmental sciences to help observe, respond and mitigate hazardous issues. Through advanced technologies provided by Microsoft, these projects demonstrate exemplary solutions for the four steps within environmental informatics.

The research benefits from recent advancements in computer science, data sciences, and information technologies and methodologies. To fully integrate observation data worldwide, utilize elastic cloud computing platforms, and serve users with right environmental information in the right place, at the right time will be a driving objective for the next decade in advancing environmental informatics for (1) solving environmental issues, (2) advancing environmental sciences, (3) responding to environmental emergency, and (4) protecting our home planet for future generations.

Research is needed in (1) bridging advanced technologies and environmental sciences, (2) advancing sciences and technology, information theory within a globalized context, and (3) improving end users awareness and utilization of environmental data, information and knowledge in a more creative and beneficial decision environment.

## Acknowledgements

Research reported is sponsored by Microsoft, NASA and Federal Geographic Data Committee. The authors would also like to acknowledge Yi Liu from Tsinghua University, China, for his contribution in the example as shown in Fig. 5; South Florida Water Management District, USA, and Yong Liu from National Center for Supercomputing Applications (http://www.ncsa.illinois.edu/), for their contribution in the example as shown in Fig. 6; Xi Zhou, Chen Xu, Jizhe Xia, Xin Qu, and Min Sun, Qunying Huang from George Mason University (cisc.gmu.edu) for their contributions to examples as shown in Figs 2 and 3.

## References

Barros, A.P. (2005, Jul. 31-Aug.4). Environmental informatics - Long-lead flood forecasting using Bayesian neural networks. Paper presented at the International Joint Conference on Neural Networks, Montreal, Canada.

Caragea, D., Zhang, J., Bao, J., Pathak, J. and Honavar, V. (2005). Algorithms and software for collaborative discovery from autonomous, semantically heterogeneous, distributed information sources. *Lecture Notes in Computer Science*, **3734**, 13–44.

Chen, Z., Gangopadhyay, A., Karabatis, G., McGuire, M. and Welty, C. (2007). Semantic integration and knowledge discovery for environmental research. *Journal of Database Management*, **18**, 43–68.

Devarakonda, R., Palanisamy, G., Green, J.M. and Wilson, B.E. (2010). Data sharing and retrieval using OAI-PMH. *Earth Science Informatics*, **3**, 1–5.

Dhanushkodi, S.R., Mahinpey, N., Srinivasan, A. and Wilson, M. (2008). Life cycle analysis of fuel cell technology. *Journal of Environmental Informatics*, **11**, 36–44.

Goodchild M., Yuan, M. and Cova, T.J. (2007). Towards a general theory of geographic representation in GIS. *International Journal of Geographical Information Science*, **21**, 239–260.

Green, D.G. and Klomp, N.I. (1998). Environmental informatics—A new paradigm for coping with complexity in nature. *Complexity International*, **6**.

Gruiz, K. (2009). Web-based information system and decision support tool: The structure and use of the MOKKA IT tool. *Land Contamination and Reclamation*, **17**, 695–702.

Hey, T., Tansley, S. and Tolle, K. (2009). The Fourth Paradigm: Data-Intensive Scientific Discovery. Microsoft Press, Redmond, WA.

Hilty, L.M., Page, B. and Hŧebíçek, J. (2006). Environmental informatics. *Environmental Modelling and Software*, **21**, 1517–1518.

Karatzas, K., Nikolaou, K. and Moussiopoulos, N. (2004). Timely and valid air quality information: The APNEE-TU Project. *Fresenius Environmental Bulletin*, **13**, 874–878.

Kalapanidas, E. and Avouris, N. (2003). Feature selection for air quality forecasting: A genetic algorithm approach. *AI Communications*, **16**, 235–251.

MacDonell, M., Morgan, K. and Newland, L. (2002). Integrating information for better environmental decisions. *Environmental Science and Pollution Research*, **9**, 359–368.

Mayfield, C., Joliat, M. and Cowan, D. (2001). The roles of community networks in environmental monitoring and environmental informatics. *Advances in Environmental Research*, **5**, 385–393.

Pecar-Ilic, J. and Ruzic, I. (2006). Application of GIS and Web technologies for Danube waterway data management in Croatia. *Environmental Modelling and Software*, **21**, 1562–1571.

Pillmann, W., Geiger, W. and Voigt, K. (2006). Survey of environmental informatics in Europe. *Environmental Modelling and Software*, **21**, 1519–1527.

Radermacher, F.J., Riekert, W.-F., Page, B. and Hilty, L.M. (1994). Trends in environmental information processing. *IFIP Transactions. A: Computer Science and Technology* **(A-52)**, 597–604.

Rasuly, A., Naghdifar, R. and Rasoli, M. (2010). Detecting of Arasbaran forest changes applying image processing procedures and GIS Techniques. *Procedia Environmental Sciences*, **2**, 454–464.

Stadler, M., Ahlers, D., Bekker, R.M., Finke, J., Kunzmann, D. and Sonnenschein, M. (2006). Web-based tools for data analysis and quality assurance on a life-history trait database of plants of Northwest Europe. *Environmental Modelling and Software*, **21**, 1536–1543.

Slini, T., Karatzas, K. and Moussiopoulos, N. (2003). Correlation of air pollution and meteorological data using neural networks. *International Journal of Environment and Pollution*, **20**, 218–229.

Stockwell, D.R.B., Beach, J.H., Stewart, A., Vorontsov, G., Vieglais, D. and Pereira, R.S. (2006). The use of the GARP genetic algorithm and Internet grid computing in the Lifemapper world atlas of species biodiversity. *Ecological Modelling*, **195**, 139–145.

Tochtermann, K. and Maurer, H. (2000). Knowledge Management and Environmental Informatics. *Journal of Universal Computer Science*, **6**, 517–536.

Wang, X. (2007). Environmental informatics for environmental planning and management. *Journal of Environmental Informatics*, **9**, 1–3.

Xie, J., Yang, C., Zhou, B. and Huang, Q. (2010). High performance computing for the simulation of dust storms. *Computers, Environment, and Urban Systems*, **34**, 278–290.

Yang, C., Goodchild, M., Huang, Q., Nebert, D., Raskin, R., Xu, Y., Fay, D. and Bambacus, M. (2011a). Spatial Cloud Computing – How geospatial science use and help to shape cloud computing. *International Journal of Digital Earth*, **4**, 305–329.

Yang, C., Raskin, R., Goodchild, M.F. and Gahegan, M. (2010). Geospatial Cyberinfrastructure: Past, Present and Future. *Computers, Environment, and Urban Systems*, **34**, 264–277.

Yang, C., Wu, H., Huang, Q., Li, Z. and Li, J. (2011b). Utilizing spatial principles to optimize distributed computing for enabling physical science discoveries. *Proceedings of National Academy of Sciences*, doi: /10.1073/pnas.0909315108.

Zhizhin, M., Kihn, E., Redmon, R., Poyda, A., Mishin, D., Medvedev, D. et al. (2007). Integrating and mining distributed environmental archives on Grids. *Concurrency Computation Practice and Experience*, **19**, 2157–2170.

# 2

# Hierarchical Geospatial Computing Environment for Data-intensive Geographic Process Simulation

**Mingyuan Hu, Hui Lin, Bingli Xu[1], Ya Hu[2], Sammy Tang[3] and Weitao Che**
Institute of Space and Earth in Information Science, the Chinese University of Hong Kong, China
[1]Department of Information Engineering, The Academy of Armored Forces Engineering, Beijing 100072, China
[2]Remote Sensing Information Engineering Department, Faculty of Geosciences and Environmental Engineering Southwest Jiaotong University, Chengdu 610031, China
[3]Information Technology Services Center, the Chinese University of Hong Kong, China

## Introduction

Geographic information system (GIS) professionals recognize that geographic process is essential for understanding what is happening in the world, learning how the environment is changing, modelling how complex systems work and giving context to other types of data. Consequently, geographic process models have been increasingly featured for the next generation geographic information science (system), as a method for phenomena simulation and mechanism analysis of the physical environment and its live activities, thereby driving conventional GIS based on data manipulation into the world of dynamic and computational processes (Goodchild, 2006; Yuan and Hornsby, 2008; Torrens, 2009; CSDGS et al., 2010).

However, geographic process models such as atmospheric models generally are toward computational models, large data-intensive sets based, and at multiple spatiotemporal scales, which often take time-consuming computing or need immediately simulated responses to explain these dynamic phenomena (Openshaw, 2000; Guan et al., 2006; Brimicombe, 2009). In order to make better and full use of the vast geographic data and exploit the

J.K. Thakur et al. (eds.), *Geospatial Techniques for Managing Environmental Resources*,
DOI 10.1007/978-94-007-1858-6_2, © Capital Publishing Company 2012

valuable information beyond the original data resources, data intensive computing is now considered as the "fourth paradigm" in scientific discovery after theoretical, experimental and computational science (Tony et al., 2009). New computing technologies such as cloud computing, grid technology and multicore processors have spawned GIS fields to meet the new scientific challenges, including computationally-intensive scientific, mathematical and academic problems through volunteer computing (Foster, 2002; Goodchild, 2010).

Some pilot studies in geospatial fields are spatial statistical analysis (Wang et al., 2008; Harris, 2010), air-borne laser scanning data sequential processing (Han et al., 2009), hyperspectral image processing (Plaza et al., 2006), parallel cellular automata modelling (Guan and Clarke, 2010; Li et al., 2010), as well as simulations with parallelized mesoscale environmental models (Xie et al., 2009; Xu et al., 2010) and wildland fire behaviour simulation (Douglas and Coen, 2010). Despite the existence of commercially available dispersed computing resources, they are highly priced and are largely inaccessible to general users (Sugato, 2005; Zhang, 2010). Furthermore, these systems cannot provide the entire solution in their generic forms (Foster and Kesselman, 2004) and they are also difficult for geographical tasks schedule, leveraging the built-in geospatial data management as well as inherent implementing computing tasks in heterogeneous environments (Curran and Shearer, 2009; Huang et al., 2009). On the other hand, when the number of processors go beyond a threshold, normalized speedups of grid/cloud computing could slow down significantly, which might be caused by the combined factors of communication/scheduling overheads, workload imbalances and contention of shared resources (Xie et al., 2009; Li et al., 2010). There is also an increasing recognition that the scalability and controllability of high PC clusters allow progress beyond remote computational resources limited by the network bandwidth, security authentication and queue requests, etc. (Marín et al., 2011). The low cost high performance PCs thus has fostered research to use them to drive immediately geographic process computing (Zhang, 2010). In particular, personal PC clusters computing advances the linkage across existing resources, but also offers the power of self-control to the management of geospatial data resources and dataflow for real time dynamic simulation at the local area. Consequently, in this chapter, a distributed problem-solving environment is proposed in order to reveal fully the real features of spatiotemporal geographic process and support both 3D analysis and hierarchical emergency decision making, comprising the geographic process models, the hierarchical geospatial computation involving grid computing layer and local PC clusters effectively coordinated, and Viz Wall for real-time data visualization and geographic analysis.

The remainder of this chapter is organized as follows. Second part describes the related background of geographic process models and high performance

hierarchical geospatial computing environment for data-intensive computing. A hierarchical geospatial computing environment for data-intensive geographic process simulation is introduced in third part. The fourth part discusses the case study: the grid computing based regional atmospheric simulation, PC cluster based parallel computation of a Gauss dispersion model, and the visual wall for geographic visualization. Final part gives the conclusion of this work with thoughts on the future prospects.

## Advanced Features in Geographic Process Computation

### Geographic Process Models

Geographic process models are not only geo-knowledge in them, but can also generate new geo-knowledge by changing the input initiate parameters. Therefore, being different from digital representation such as geometric construction, what a geographic process model highlights are dynamical geographical process simulation and geographical phenomenon analysis, so it focusses on not only the cities or communities, but also all geographical environments such as atmospheric pollution, oceans dynamics and soil horizon. In this case of air pollution simulation research, Mesoscale Model5 (MM5) and Gauss plume model for simulation and analysis are typically introduced.

### MM5 (Dudhia et al., 2005)

The PSU/NCAR mesoscale model5 (known as MM5) is a regional, nonhydrostatic, terrain-following sigma-coordinate model designed to simulate or predict mesoscale atmospheric circulation. The model is supported by several pre- and post-processing programs, which are referred to collectively as the MM5 modelling system. The MM5 modelling system software is mostly written in Fortran, and has been developed at Penn State and NCAR as a community mesoscale model with contributions from users worldwide. Since that time it has undergone many changes designed to broaden its applications. These include (i) a multiple-nest capability, (ii) nonhydrostatic dynamics, (iii) a four-dimensional data assimilation (Newtonian nudging) capability, (iv) increased number of physics options, and (v) portability to a wider range of computer platforms, including OpenMP and MPI systems. There are about eight modules for MM5, which are TERRAIN, REGRID, LITTLE_R/RAWINS, INTERPF, INTERPB, NESTDOWN, MM5 and GRAPH/RIP.

### Gauss Plume Model (Turner, 1994)

Based on statistic theory, in steady turbulence environment, particle dispersion and transport behaviours accord with Gaussian plume model, which is also called Gaussian dispersion model. Gaussian plume model does not include chemical reaction among pollutants and wet and dry deposition, and is an idealized simplified dispersion model. Gaussian plume model is relatively

simple and easy for calculation to point source emitters, such as coal-burning electricity-producing plants, which is the reason that it is still widely used.

## CU Grid

The facilities of the Grid of the Chinese University of Hong Kong (CUGrid) are provided for high-performance computing needs and for supporting computation-intensive research projects. It currently consists of 36 single CPU nodes in one logical batch, 70 dual core nodes in a second logical batch and another 48 dual core nodes in another batch. 56 of the quad-core nodes were added into the CUGrid recently. All these nodes are physically interconnected and managed with a grid middleware Globus ToolKit. The total CPUs available to user via OpenPBS queue is about 490 with total computational power of 2.5 TFLOPS (Tera Floating point Operations per Second) and its processing power is expected to be increased to 3-4 TFLOPs in the near future. The CUGrid environment now not only supports many of the research works or projects which would normally require large power on computational capabilities for confirming, verifying and validating the experimental patterns in evaluations. These works could range from an initial study to the potential final research areas and/or to support the validation or final examination of the model that is in investigation.

As shown in Fig. 1, CUGrid is connected to the Grid Testbeds of the Pacific Rim Applications and Grid Middleware Assembly (PRAGMA) via G/farm at the CUGrid PRAGMA Testbed extension, this effectively allowing CUHK research projects to be collaborated with other institutions in PRAGMA (e.g. UCSD and NCSA in US, AIST in Japan, KISTI in Koera, CNIC in China etc.). The result of computational and data resources could then be further

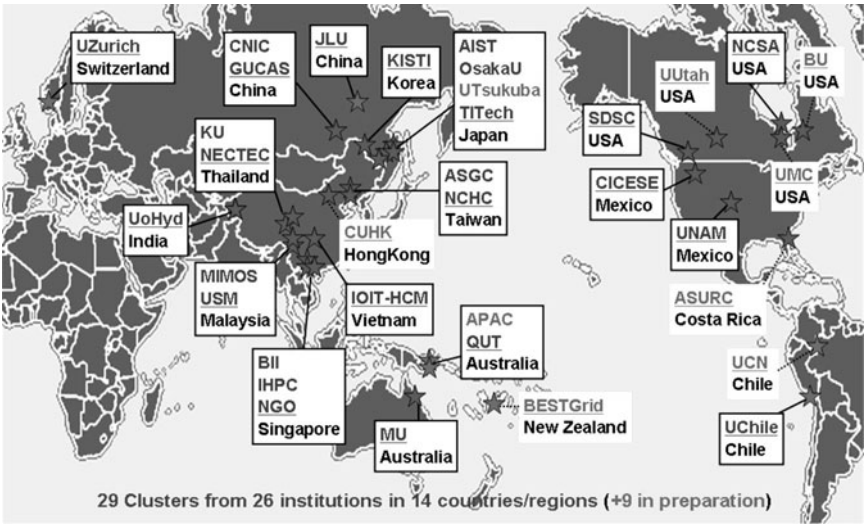


**Figure 1.** PRAGMA grid testbed.

expanded and utilized by the researcher for further needs which is beyond the CUGrid capacity.

### Globus ToolKit (Globus Toolkit, 2010)

Computing grids are often constructed by the general-purpose grid software libraries known as middleware. Globus Toolkit, currently at version 5, is an open source grid middleware for building computing grids developed and provided by the Globus Alliance. With the recent advancement on Grid computing technology and the maturity of the related supporting software environment of Globus ToolKit, CUHK has successfully built a 200 plus nodes grid environment, for supporting large scale scientific research projects.

### Rocks Clusters (Rocks, 2010)

Rocks clusters have played a pivotal role in the research of cluster computing. Driven by one goal: make clusters easy to deploy, manage, upgrade and scale, the Rocks group has been addressing the difficulties of deploying manageable clusters, which help deliver the computational power of clusters to a wide range of scientific users, improve the state of the art in parallel tools in supporting stable and manageable parallel computing platforms available to a wide range of scientists.

### SAGE (SAGE, 2010)

SAGE (Scalable Adaptive Graphics Environment) is a scalable pixel distribution architecture for supporting collaborative scientific visualization environments with potentially high display resolution on tiled walls. In collaborative scientific visualization, it is crucial to share high-resolution imagery as well as high-definition video among groups of collaborators at local or remote sites.

## The Conceptual Model of Hierarchical Geospatial Computing Environment for Data-intensive Geographic Process Simulation

This section provides a hierarchical geospatial computing environment applied to the data-intensive environmental processes, with support for a geographic process model for urban air pollution, hierarchical geospatial computation for data-intensive environmental processes, as well as the Viz Wall for 3D scientific visualization, as shown in Fig. 2.

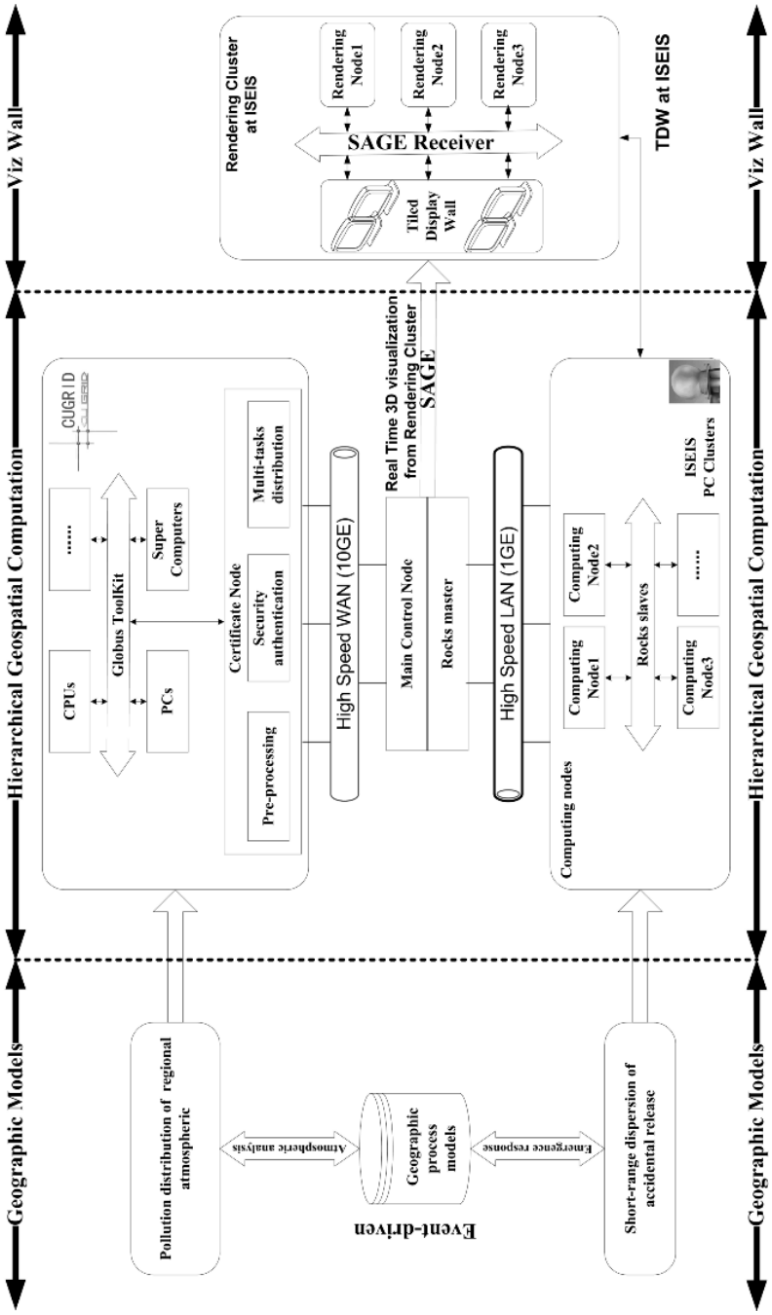


**Figure 2.** The conceptual graph of hierarchical geospatial computing architecture for data-intensive geographic process simulation.

### *Multi-scale Geographic Process Models*

Environmental phenomena are generally recognized as different cognitive scales and include very intricate spatiotemporal processes and continuously increasing geospatial data. The better way of presenting these changes is through geographic process models, not geo-data. For example, atmospheric simulation can be regarded as meso-scale urban pollution or micro-scale emergency response, especially for the case of an industrial hazard. As shown in Fig. 2, regional model (such as MM5) is adopted to quantify and explain variability in the distribution of atmospheric pollution in a given PRD city cluster area; the local dispersion model (such as Gauss model) aims to reveal the source-receptor (relationships) features of the short-range dispersion of accidental release for local emergency decision support.

### *Hierarchical Geospatial Computation*

It is based on a hierarchical design targeted at enhancing the flexibility and scalability of data-intensive computing. It provides the integration of grid computing based on the available distributed computational resources and self-organized PC clusters to solve time-consuming and complicated scientific problems. The hierarchical relationships among CUGrid, PC clusters and main control are illustrated in Fig. 2. The grid system of the Chinese University of Hong Kong (CUGrid) is introduced in the framework for high-performance computing needs and for supporting computation-intensive research projects, in which hybrid computers such as loosely coupled, heterogeneous, and geographically dispersed CPU nodes and massively parallel supercomputers are physically interconnected and managed with a grid middleware Globus ToolKit. In the completely computing environment, the CUGrid is responsible for the MM5 computing, which is deployed in the authorized master node of the CUGrid computers. The master node receives and executes commands, allocates jobs to other computers on the CUGrid, collects the computation output and stores this output and information to the main and high speed networked storage spaces for visualization, analysis and collaboration.

The PC computing clusters are related to the deployment of parallel computation on PCs for the Gauss plume model; such computation takes place in idle computers at the Institute of Space and Earth Information Science (ISEIS) in CUHK. The PC clusters computing nodes installation process is based on the Rocks clusters, after installing Rocks on the main control node (front-end), all computing nodes installation and configuration are handled automatically by Rocks (Rocks, 2010). Computing nodes are equipped with parallel computing algorithms, which are also responsible for the division and distribution of tasks and a summary of the computing results. The Rocks-based main control node is designed as the coordinator for the whole hierarchical computing structure (Rocks, 2010), which establishes a direct correlation between the CUGrid (with a 10 Gbps network) and PC clusters (1 Gbps network), controls and mediates all access to the CUGrid and PC

cluster resources and facilitates the system services provisioning, management, deployment and job scheduling for the stable and manageable parallel computing platforms available to a wide range of scientific users.

### *Viz Wall for Geo-visualization and Geo-analysis*

For the scientific visualization and geographic decision-making analysis, there is a significant challenge posed by data-intensive science applications, especially for the areas of high definition geographic process simulation such as atmospheric pollution simulation with large volume computing data stream and the low-latency networking impact. As shown in Fig. 2, in the proposed ISEIS Tiled Display Wall (TDW), backing up with the power of the background CUGrid computing power, user can also view multiple datasets in parallel for certain very complex and large images simultaneously with interactive control. The development of the ISEIS TDW, thus, on a relatively inexpensive easily useable tiled display would also be useful for departments seeking their own display facility for large datasets but without the financial resources to build a visualization portal. SAGE (Scalable Adaptive Graphics Environment) is an appropriate option for allowing the seamless display of various networked applications over the whole display, in which PC rendering nodes with graphics cards are responsible for the large data volume 3D rendering, where each PC powers one or two of the tiles in the display. Parallel visualization is thus designed to improve decision-making efficiency, and the TDW is deployed for distributing visualization to a large-scale, high-dimensional and high resolution display, which would be targeted to provide the necessary foundation to explore the possibility of creating a multi-pipe graphics engine that could either be driven by the CUGrid or to drive parallel PC cluster computing on its own to form the final display required for a particular visualization need.

### *Distributed Management*

Geographic process models are generally many program/function codes, and the management on geo-models can be referenced from open-source or commercial program developing platforms, such as Fortran, Python, Visual Studio.Net and Java. In these platforms, models are coded as functions and stored in function libraries or dynamic link libraries (DLL), which also provide description files (such as .h files for VC++ platform) as the metadata of models, to tell users what functions (models) are used for, what the meanings for input and output variables of models are. Based on the computing framework of Fig. 2, in the following case study, MM5, which is computation intensive, is suggested to be distributed on the computational grid of CUGrid. The environmental data to support the running of MM5 is also loaded on the CUGrid. The Gauss plume model is distributed on the PC clusters for the parallel computation. MM5 and the Gauss plume model are both well controlled in the system main control interface by using 2D/3D visualization node in

TDW, which integrate geographic information to visualize and analyse pollution results, including geo-model computation visualization, air pollution result (both distribution and dispersion) visualization, analysis visualization and collaboration visualization.

## Case Study: Towards the Improvement of Air Pollution Simulation and Data Visualization

In this case study area of Pearl River Delta (PRD) of China, we try to integrate MM5, Gauss plume model, geographic information and tiled display wall for 2D and 3D visualization into a comprehensive environment, to facilitate air pollution research and to shorten gaps between air pollution research and geo-located visualization and spatial-temporal analysis.

### CUGrid-based Regional Air Pollution Simulation

CUGrid is constructed for providing the fundamental computational facilities for all the computing needs in CUHK, which currently consists of 36 single CPU nodes, 70 dual core nodes, 48 dual core nodes, and another 56 quad-core nodes in multiple batches. As the set of input and outfile from MM5 are text base file, and with the scale of the problem, the files could be very large, this would greatly reduce the performance of the model analysis if the traditional file system is used (e.g. NFSV3). This not only limits the overall parallel process of the model analysis, but also reduces the total throughput of the model calculation. In the process of the computing in the CUGrid, we set up a parallel file and data access architecture, the output is confined to few files (domain output files); therefore, both reading and writing operations are concentrating on a set of few files.

*MM5 Setup:* The PSU/NCAR Meso-scale Model (known as MM5) is a regional, non-hydrostatic model designed to simulate or predict meteorological phenomenon and meso-scale atmospheric circulation (Dudhia et al., 2005). It significantly facilitates researchers to analyse the regional atmospheric environment. MM5 has a capability of multiple nesting with upto nine domains running at the same time and completely interacting (Dudhia et al., 2005). An actual configuration of three domains was adopted in the experiment as shown in Fig. 3: D03 is at the third level and its available simulation region is focussed on the scope of the Pearl River Delta (PRD) of China, which is fixed in the rectangle from (113.14, 21.96) at the bottom left corner and (114.59, 22.84) at the top right corner. There are 34 grids in the north-south direction and 49 grids in the west-east direction with a resolution of 3 km in both directions. Each sub-domain has a "Mother domain" used to prepare coarse parameters, which specify the boundaries into the nest domain interior to obtain precise results. As shown in Fig. 3, for domain 2(D02) the mother domain is D01, and for D03 it is D02. A sequential set of vertical layers from 2 m to 1000 m was set for model runs on all domains.

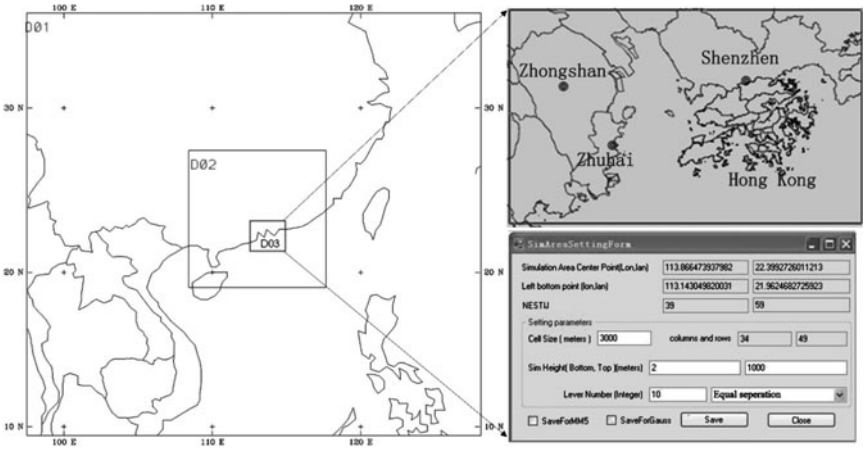


**Figure 3.** (a) Actual simulation area selection. (b) Parameters setting for selected area.

*Data Mapping and Parallel Implementation of MM5:* To run the MM5 model, lateral boundary values for each horizontal layer have to be set as initial values for running a simulation. As shown in Fig. 4, there are m × n

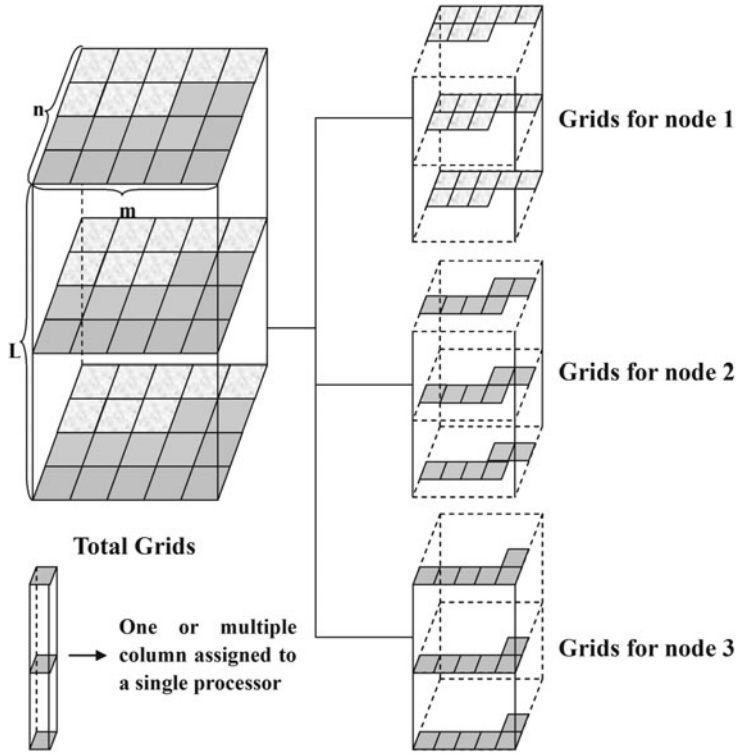


**Figure 4.** Grid-based allocation for parallel computation of Domain 3.

grids in each horizontal layer and each grid in the same vertical column has a similar boundary condition index as its mother domain. Based on the consideration described above, the prime goal of this parallel computing decomposition is to allow the computations in a vertical column (as shown in left-bottom) of grid nodes to easily acquire their boundary values, which can be assigned to a single processor as depicted by Fig. 4 left-bottom. For all layers of the selected simulation region, Fig. 4 also gives the parallel computing decomposition with computers.

Based on the MM5's meteorological computing outputs including three-dimensional wind, temperature, pressure and specific humidity fields, the air pollution transportation and dispersion is necessary for predicting time-varying trace gas concentrations for the PRD area.

In the experiment, an equation (see equation 1), which is specifically established and designed to simulate the single air pollutant dispersion in the troposphere, was integrated into MM5 system via its Terrain module. The computation results of geo-visualization for selected time series are shown in Fig. 5.

$$\frac{\partial c}{\partial t}+\frac{\partial uc}{\partial x}+\frac{\partial vc}{\partial y}+\frac{\partial wc}{\partial z}=\frac{\partial}{\partial x}\left(K\frac{\partial c}{\partial x}\right)+\frac{\partial}{\partial y}\left(K\frac{\partial c}{\partial y}\right)+\frac{\partial}{\partial z}\left(K\frac{\partial c}{\partial z}\right)+Q-L \quad (1)$$

where, $c$ is concentrations of an air pollutant (kg/kg); $u$, $v$ and $w$—wind velocity components in three dimensions (m/s); $K(x, y, z, t)$—Eddy diffusivity ($m^2/s$); $Q$—emission (1/s); and $L$ is deposition fluxes (1/s).

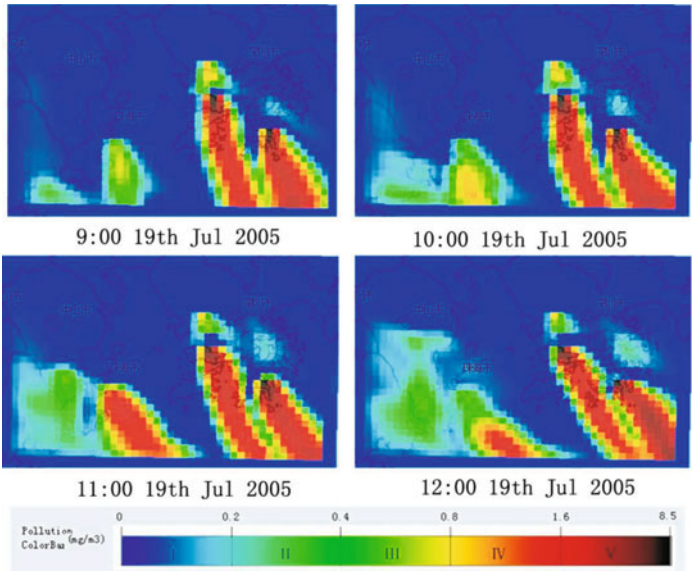


**Figure 5.** Simulated sulphur dioxide concentration dispersion from 9:00 19th July 2005 to 12:00 19th July 2005 on layer with sigma height of 700 meters above terrain.

## PC Clusters-based Parallel Computation of Gauss Pollution Dispersion Model for Multi-point Sources

The computational grid is efficient for high performance computation, but it is also complex and difficult to maintain. Compared with grid computation, PC clusters-based parallel computation is easier to control. Therefore, for the Gaussian plume model, parallel computation is used to minimize computation time.

The Gaussian dispersion model is generally used to estimate or to predict the downwind concentration of air pollutants emitted from stationary point emission sources such as industrial power plants. The point emission source generally affects the scope of the scale in space within 1 km and horizontal grid spacing within 1~10 m, which is usually associated with local areas for emergency response. In contrast to the MM5 computation on the CUGrid above, this system module focuses on a Gauss dispersion model parallelizing based on a separate PC clusters to simulate single or multiple point emission dispersion. The complete equation for multiple point source Gaussian dispersion modelling of continuous, buoyant air pollution plumes is shown below (Turner, 1994):

$$C(x,y,z) = \frac{Q}{2\pi\sigma_y\sigma_z u}\exp\left(-\frac{y^2}{2\sigma_y{}^2}\right) \times\left\{\exp\left[-\frac{(z-He)^2}{2\sigma_z{}^2}\right]+\exp\left[-\frac{(z+He)^2}{2\sigma_z{}^2}\right]\right\} \quad (2)$$

where, $C$ is concentration of emissions, in g/m³, at any receptor location: $x$ metres downwind from the emission source point, $y$ metres crosswind from the emission plume centre line, and $z$ metres above ground level; $Q$—emission rate of source pollutant; $u$—horizontal average wind velocity; He—effective height of emission plume centre line above ground level; and $\sigma_y/\sigma_z$ are horizontal and vertical standard deviations of the emission distribution.

The features of the Gaussian plume model, including the multiple input pollution sources, multiple layers for calculation and multiple grids on each layer, make it suitable for parallelization. The calculation efficiency of the Gaussian plume model is closely related to these features, which are parameterized as a number of point sources, a number of layers and a number of grids on each layer. Thus, the complete computation flow is depicted in Fig. 6. Firstly, the selected simulation region has to be gridded into m × n × l grid space, which represents multiple m × n grids of each layer from the ground. After setting the initial parameters of the Gaussian dispersion model such as wind speed and direction, source location and height, etc., the whole parallel computation process needs to be divided into sub-tasks and

these sub-tasks allocated to the connected PC computing nodes. Under the MPICH (common packages used in cluster computing are included such as MPICH and Ganglia), this set of PC is responsible for the computation of sub-tasks: the selected simulation area is separated into multiple vertical layers and each layer is assigned to a group of PCs responsible for the calculation of the final pollution concentration of each grid, which is the combined result of all point pollution resources to each layer. Further, when all of the sub-tasks computations are finished, the sub-results will be sent back to the task management for post sub-task combination and geo-visualization.

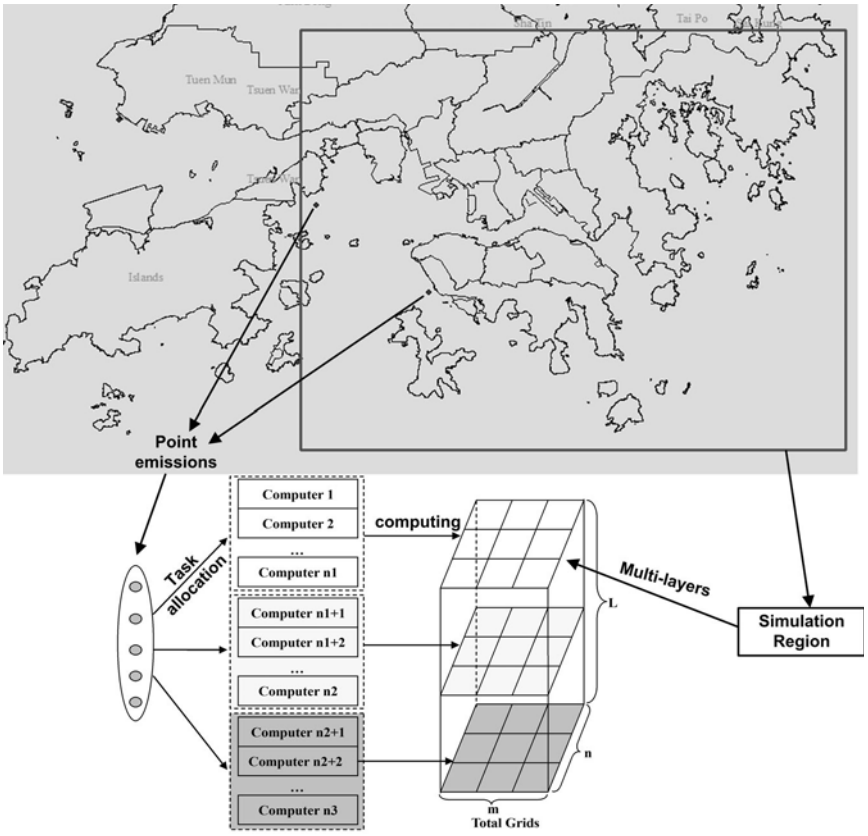


**Figure 6.** Parallel arithmetic of hybrid of multiple layers and point emissions.

Based on the task decomposition and parallel computing above, the visual result of the Gaussian dispersion model on point emissions is shown in Fig. 7.

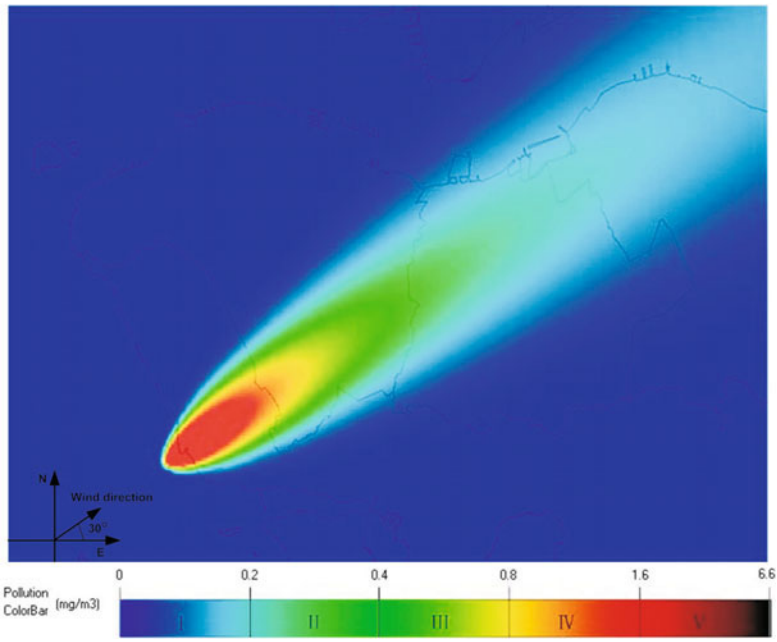


**Figure 7.** Geo-visualization of the result of Gaussian plume model computation.

## Viz Wall for Geo-visualization

Geo-visualization is the important method for accelerating rapid insight into complex phenomena and corresponding data, enabling the abstract information to be more actual, intuitive and professional. The Tiled Display Wall has been around for few years and a number of universities and other research institutions—especially for those participate to PRAGMA and those with high speed networks and high performance computing resources—involve in research areas like Earth-Science, Bio-medical, Remote Sensing and Medical imaging. Experiences from the researchers in those institutions reported that users with large data confirmed that the TDW displays are extremely useful. With the proper TDW setup, users could work on their research with lights on, and could get a global view of the data from far and rely on the true high definition (HD) images of the display to check and confirm on the details of specific area.

Therefore, the ISEIS TDW was set up as a productive visualization facility by building a tiled display and by starting with the fundamental and optimized useful size, a matrix of 3 by 3 high definition LCD monitors display wall (ISEIS TDW). To maximize its performance and to utilize the power of the CUGrid, the ISEIS TDW was designed to support multiple sources with parallel rendering which, in turn, utilizes the computational power of the CUGrid as well as a number of small cluster at the ISEIS.

As shown in Fig. 8, combining the visualization facilities with the PC rendering clusters capability, ISEIS TDW allows the creation of a collaborative visualization environment for supporting a large research group and for many researchers at the same time. In our TDW system, the whole visualization is based on the SAGE configuration for supporting collaborative scientific visualization. The 10G network is used as a high speed network connection to support the storage needs and the high bandwidth requirement for the transmission of the dataset between the computational nodes, the rendering nodes and the SAN storage. It would also be used to allow for multiple rendered streams of pixels from local and remote sites with similar display settings. With the ISEIS TDW, the rendering and display PCs in the display cluster perform the necessary parallel rendering for parallel session of the multiple dataset, while the PCs in the compute cluster in CUGrid compute the iso-surfaces from the scientific data, and the SAN storage holds the data.

Furthermore, since it is built with standard components (Viz Wall under Rocks cluster, EVL's SAGE), the underlying network can easily be expanded using flexible, inexpensive switches to accommodate additional servers for increased horizontal and overall performance on bandwidth and computational capacity.

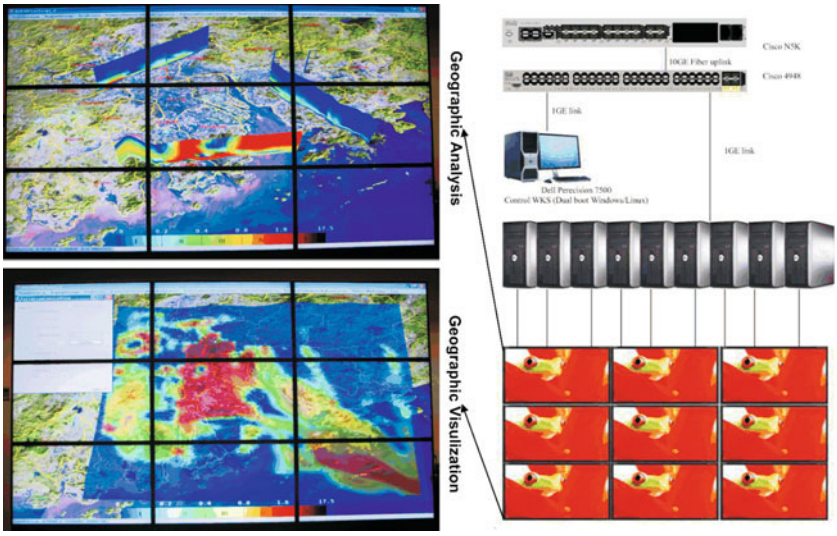


**Figure 8.** Tiled display wall-based geo-visualization and geographic analysis.

## Conclusions and Perspective Remarks

A scalable geospatial computation environment is proposed for solving the problems of increasingly complicated geo-referenced phenomenon simulation, with support for local computing clusters for point source simulation, meso-scale regional air pollution analysis for large data sets and intensive calculations,

as well as Viz Wall for dynamic visualization representation. By means of this geospatial computing environment, the general PC resources and the remotely accessed high performance computer are effectively managed in one integrated framework, and provide more flexible and extended geographic process computation. Experimental analysis proves that this integrated framework provides insight to the vertical dimension of geographic process simulation, and plays an important role in developing an appropriate hierarchical framework for urban atmospheric analysis in local regions and in large scale environments to support the development of sustainable environmental management strategies for city clusters.

Further research will be focussed on the multi-scale urban atmospheric environment simulation including micro-scale CFD simulation combined with real-time spatial process monitoring by sensor networks, to improve further the cognition ability between humans and their environments.

## Acknowledgements

The work described in this chapter is supported by the National High Technology Research and Development Program of China (973 program grant no. 2010CB731801), the National High Technology Research and Development Program of China (863 key program grant no. 2010AA122202), HKSAR RGC Project no. 447807, and the Research Fund of State Key Laboratory of Resources and Environmental Information System, Chinese Academy of Sciences.

## References

Brimicombe, A. (2009). GIS, environmental modeling and engineering. CRC Press, London, New York.

CSDGS and NRC (2010). Understanding the Changing Planet: Strategic Directions for the Geographical Sciences. The National Academies Press, Washington DC.

Curran, O. and Shearer, A. (2009). A workflow model for heterogeneous computing environments. *Future Generation Computer Systems*, **25(4)**, 414-425.

Douglas, C.C. and Coen, J.L. (2010). Computational modeling of large wildfires: A roadmap. *In:* 2010 Ninth International Symposium on Distributed Computing and Applications to Business Engineering and Science (DCABES) (pp. 113–117). Hong Kong, China.

Dudhia, J., Gill, D., Manning, K., Wang, W. and Bruyere, C. (2005). PSU/NCAR Mesoscale Modeling System Tutorial Class Notes and Users' Guide (MM5 Modeling System Version 3). Retrieved January 5, 2010, from http://www.mmm.ucar.edu/mm5/documents/tutorial-v3-notes.html.

Foster, I. (2002). The grid: A new infrastructure for 21st century science. *Physics Today*, **55(2)**, 42-47.

Foster, I. and Kesselman, C. (2004). *The Grid2: Blueprint for a New Computing Infrastructure* (2nd ed.). Kaufmann Publishers, Morgan.

Globus Toolkit (2010). About the Globus Toolkit. Retrieved January 2, 2010, from http://www.globus.org/toolkit/about.html.

Goodchild, M.F. (2006). Geographical information science: fifteen years later. *In:* P.F. Fisher (Ed.), *Classics from IJGIS: Twenty years of the International Journal of Geographical Information Science and Systems* (pp. 199–204). CRC Press, Boca Raton.

Goodchild, M.F. (2010). Twenty years of progress: Giscience in 2010. *Journal of Spatial Information Science,* **1**, 3–20.

Guan, Q., Zhang, T. and Clarke, K. (2006). GeoComputation in the Grid Computing Age. *Lecture Notes in Computer Science: Web and Wireless Geographical Information Systems*, *4295/2006*, 237–246.

Guan, Q. and Clarke, K. (2010). A general-purpose parallel raster processing programming library test application using a geographic cellular automata model. *International Journal of Geographic Information Science*, **24(5)**, 695–722.

Han, S.H., Heo, J., Sohn, H. and Yu, K. (2009). Parallel processing method for airborne laser scanning data using a pc cluster and a virtual grid. *Sensors*, **9(4)**, 2555–2573.

Harris, R., Singleton, A., Grose, D., Brunsdon, C. and Longley, P. (2010). Grid-enabling geographically weighted regression: A case study of participation in higher education in England. *Transactions in GIS*, **14(1)**, 43–61.

Huang, P., Peng, H., Lin, P. and Li, X. (2009). Static strategy and dynamic adjustment: An effective method for grid task scheduling. *Future Generation Computer Systems*, **25(8)**, 884–892.

Li, X., Zhang, X.H., Yeh, A. and Liu, X. (2010). Parallel cellular automata for large-scale urban simulation using load-balancing techniques. *International Journal of Geographic Information Science*, **24(6)**, 803–820.

Marín Pérez, J.M., Bernabé, J.B., Alcaraz Calero, J.M., Garcia Clemente, F.J., Pérez, G.M. and Gómez Skarmeta, A.F. (2011). Semantic-based authorization architecture for grid. *Future Generation Computer Systems*, **27(1)**, 40–55.

Openshaw, S. (2000). Geocomputation. *In:* Stan Openshaw and R.J. Abrahart (Eds.), *Geocomputation* (pp. 1–32). Taylor and Francis, London and New York.

Plaza, A.D., Valencia, J.P. and Martinez, P. (2006). Commodity cluster-based parallel processing of hyperspectral imagery. *Journal of Parallel and Distributed Computing*, **66(3)**, 345–358.

Rocks (2010). Rocks cluster distribution. Retrieved June 2, 2010, from http://www.rocksclusters.org.

SAGE (2010). SAGE introduction. Retrieved January 2, 2010, from http://www.sagecommons.org/.

Sugato, B. (2005). Simulation of grid computing infrastructure: challenges and solutions. *In:* Proceedings of the 37th conference on Winter Simulation (pp. 1773 London and New York: 1780), Orlando, Florida.

Tony, H., Stewart, T. and Krist, T. (Eds.) (2009). The Fourth Paradigm: Data-Intensive Scientific Discovery. United States of America, Microsoft Research.

Torrens, P.M. (2009). Process Models and Next-Generation Geographic Information Technology. Retrieved February 10, 2010, from http://www.esri.com/news/arcnews/summer09articles/process-models.html.

Turner, D.B. (1994). Workbook of Atmospheric Dispersion Estimates: An Introduction to Dispersion Modeling (2nd ed.). CRC Press, Boca Raton.

Wang, S.W., Cowles, M.K. and Armstrong, M.P. (2008). Grid computing of spatial statistics: using the TeraGrid for g(i)*(d) analysis. *Concurrency and Computation: Practice and Experience*, **20(14)**, 1697–1720.

Xie, J.B., Yang, C., Zhou, B. and Huang, Q. (2009). High-performance computing for the simulation of dust storms. *Computers Environment and Urban Systems*, **34(4)**, 278–290.

Xu, B., Lin, H., Chiu, L.S., Tang, S., Cheung, J., Hu, Y. and Zeng, L. (2010). Vgecugrid: An integrated platform for efficient configuration, computation, and visualization of mm5. *Environmental Modelling and Software*, **25(12)**, 1894–1896.

Yuan, M. and Hornsby, K.S. (2008). Computation and Visualization for Understanding Dynamics in Geographic Domains: A Research Agenda (1st ed.). CRC Press, New York.

Zhang, J. (2010). Towards personal high-performance geospatial computing (HPC-G): perspectives and a case study. *In:* Proceedings of *the ACM SIGSPATIAL International Workshop on High Performance and Distributed Geographic Information Systems* (pp. 3–10). San Jose, California.

# 3

# Integration of Geographic Information Systems for Monitoring and Dissemination of Marine Environment Data

**Marcin Kulawiak and Marek Moszynski**
Department of Geoinformatics, Gdansk University of Technology
Narutowicza 11/12 Str., 80-233 Gdansk, Poland

## Introduction

The issue of monitoring, analysis and visualization of marine activity, either for the purpose of environment protection or threat sensing, has been the subject of intensive research for many years. In the last decades, presented solutions have shown the advantages of dedicated software for storing and management of acoustic and spatial data (Stepnowski et al., 1996; Trygonis et al., 2009; Thakur et al., 2011) as well as the potential of web mapping in application to environmental modelling (Maceachren and Kraak, 1997; Doyle et al., 1998; Goodall et al., 2011). In more recent years, many commercial and scientific institutions have been continuously contributing to the process of development and application of various tools for aquatic sensing. Because of this, the variety of marine sensors is very wide, ranging from simple techniques such as direct sampling or hydrological measurements using CTD probes, through hydroacoustic surveys, air-borne photographs and satellite imaging to numerical modelling and simulation.

In this context, the acquisition, processing, integration and visualization of various kinds of aforementioned data is a key feature of applications dedicated to aquatic ecosystems management, as it has been shown e.g. by Tsou (2004). At the same time, Kraak (2004) has shown that a common geographical coordinate space is an excellent place to combine many types of information concerning the environment. In this context, it has become clear that the proper way of processing and visualization of data acquired from various marine sensors should involve the use of a Geographic Information

J.K. Thakur et al. (eds.), *Geospatial Techniques for Managing Environmental Resources*,
DOI 10.1007/978-94-007-1858-6_3, © Capital Publishing Company 2012

System. Since that time, Rao et al. (2007) used the ESRI ArcIMS platform to implement a web GIS Decision Support System (DSS) for use in resource management and assessment of environmental quality, while Kruger et al. (2007) demonstrated a web GIS dedicated for verification of hydrologic forecasts built with Open Source technologies. In the same year, Tuama and Hamre (2007) presented a web-based DSS for monitoring, integration and dissemination of marine pollution data collected from multiple sensors by means of non-proprietary technologies. Several months later Bakare et al. (2008) demonstrated the application of commercial technologies like ESRI ArcGIS to morphological modelling of the seabed, aiming to identify the areas which may require resurveying to maintain navigation safety in British territorial waters. A year afterwards, Hamre et al. (2009) presented a web GIS portal dedicated to integration and dissemination of multi-source data for the purpose of environmental risk management in marine and coastal areas of Europe. More recently, successful attempts at dynamic presentation of marine data collected from a variety of sensors by means of web GIS have been presented by Kulawiak et al. (2010a).

Nevertheless, dynamic processing and integration of remote sensor data remains one of the greatest challenges related to application of GIS to marine environment monitoring. The origin of this issue lies in the steady progress that the different methods of marine data acquisition have seen throughout the second part of the twentieth century. Tools such as the multibeam echosounder have acquired range and resolution high enough to produce megabytes of data per every second of survey. On the other hand, diverse methods of processing and analysis of such information have also been constantly evolving. The advent of high performance PC's with multicore CPU's, gigabytes of RAM and terabytes of hard drive storage space, coupled with widespread access to broadband Internet has made it possible to process and visualize high-resolution data from remote sensors in near-real time without the need for dedicated hardware.

Therefore, the greatest limitation of current technology lies not in lack of precision or processing powers, but in absence of common standards of data exchange and proper visualization. Without architecture-independent means of accelerated web-based three-dimensional presentation of geographical data, its remote visualization will always be a compromise between realistic complexity of source data and imperfect methods of its delivery to the end users. In the current situation, developers need to carefully balance between remote processing and presentation of impaired data and precise on-site 3D visualization of the entire available dataset.

This chapter presents the common types of marine data sensors, discusses popular technologies used for constructing GIS, and describes the results that may be obtained by application of the discussed technologies to processing, integration, analysis and visualization of data from the presented sources.

## Featured Technologies

There are many techniques of presenting and processing GIS data. Some of them are more suited towards visualization, others provide means for better spatial analysis and some, to an extent, allow for both. The technologies presented in this section are some of the most prominent in the GIS sector. But more importantly, they all have proven to effectively constitute advanced Geographical Information Systems dedicated to integration and processing of data pertaining to the marine environment.

### The ESRI ArcGIS Engine

The ArcGIS Engine is a set of libraries which can be used to create new GIS applications as well as extend the functionality of existing ones. The core components of ArcGIS are referred to as ArcObjects. They are platform-independent object-oriented libraries which may be accessed through available C++, COM, Java and .NET Application Programming Interfaces (API's). Because the libraries are platform-independent, they need to be invoked from the platform-specific ArcGIS Engine runtime, which is available on Windows, UNIX and Linux. ArcObjects realize a set of functionalities which allow the built application e.g. to display a map with multiple layers, transform between coordinate systems, create and update geographic features or interact with personal and enterprise geodatabases.

Building an application with ArcObjects involves choosing the desired functionality from the available controls and linking it with custom C++, C# or Java code. For example, a custom version of the ESRI ArcMap desktop GIS application may be created by joining the "Map" and "Table of Content" controls with a Map Navigation toolbar. In a similar manner, adding 3D display functionality to the application would require the inclusion of ArcScene control.

Being a commercial product, the ArcGIS Engine is available in several configurations, with the standard edition offering basic data creation and display functionality, and Geodatabase Update, Spatial, 3D and StreetMap USA extensions providing additional libraries for additional prices. An important aspect of ArcGIS Engine is that although purchasing an ESRI Developer Network (EDN) annual subscription grants access to these libraries, deploying a developed application to a client requires the purchase of a separate ArcGIS Engine license, as well as licenses for optional extensions.

### The ArcGlobe

The ESRI ArcGlobe is a part of the ArcGIS 3D Analyst package. The application presents the user with a freely explorable three-dimensional Earth globe in a way that is similar to the freely available Google Earth. However, ArcGlobe is a part of the ArcGIS package and therefore shares a lot of functionalities

with its other elements. In particular, ArcGlobe supports most data formats native to ESRI software, such as Shapefiles, TIN's and SDE databases. This means that data created e.g. with ArcMap may be easily imported into ArcGlobe and displayed in three dimensions. Base maps may also be imported through the Internet from ArcGIS Online services, with most recent versions of ArcGlobe also supporting Microsoft Bing Maps. The software allows to load and display three-dimensional features such as buildings and bridges and supports extrusion of two-dimensional features to three dimensions using attribute data. In addition, ArcGlobe allows to perform three-dimensional spatial analysis of viewshed and line-of-sight, as well as spot height interpolation, profiling, and steepest path determination. Integration with 3D Analyst provides tools for calculating surface area, volume, slope, aspect, and hillshade, as well as data query based on attributes or location.

Because any geographical data loaded in the ArcGlobe will be displayed in the context of a three-dimensional model of the Earth, the software is best suited for presentation and analysis of large environments such as cities or coastal areas.

## The GeoTools Open Source Java GIS Toolkit

GeoTools is an Open Source Java library which provides methods for manipulating various types of geospatial data. The functionality of GeoTools includes creation, modification, integration, analysis as well as styling and rendering of raster and vector data. The library provides the user with easy access to geographic data, whether it is stored in files or in geodatabases.

GeoTools is developed by the Open Source Geospatial Foundation and is usually the first software to implement new standards established by the Open Geospatial Consortium (OGC). Examples of such standards are the Web Map Service (WMS) and Web Feature Service (WFS) protocols, as well as the Common Query Language (CQL) format. The library also supports OGC's XML-based Styled Layer Descriptor (SLD) files, which may be used to customize the look of vector features. Classes provided by GeoTools allow to quickly build GIS applications which enable the composition and display of styled maps, as well as spatial analysis of geographical data such as graphs and networks. Data created with the GeoTools package may be easily referenced with and transformed between coordinate systems compatible with the European Petroleum Survey Group (EPSG) specifications. The streaming data readers used by GeoTools allow to avoid memory limitations on the amount of data that can be accessed by an application.

Due to its flexibility, the library may serve as a foundation of server as well as desktop GIS projects. The most prominent applications built with GeoTools are the Open Source GeoServer Web map server and uDig Open Source desktop application framework.

## The GeoServer

The GeoServer is a dynamically developing Open Source GIS server which fully supports OGC WMS, WFS, Web Coverage Service and Web Feature Service Transactional (WFS-T) protocols. Through the use of GeoTools, the GeoServer supports PostGIS, Shapefile, ArcSDE, DB2, Oracle, VPF, MySQL, MapInfo, and Cascading WFS data sources, as well as Web Map output as jpeg, gif, png, SVG, GeoJSON, GeoRSS and pdf, including support for antialiased images. The presentation of every layer stored in the GeoServer database can be individually customized using SLD files, which can be dynamically swapped and altered during web queries. An embedded EPSG database allows for real-time data reprojection between hundreds of existing as well as user-defined projections.

The GeoServer is based on Java Enterprise Edition (JEE) Servlet technology and can run in any Servlet container. Its open architecture allows for easy adoption of new data formats with GeoTools DataStore interfaces and helper classes. Existing GeoTools DataStores instantly plug-in to GeoServer, showing up as an option in the user-friendly configuration Graphical User Interface (GUI).

In order to fully utilize its GIS capabilities, the GeoServer should be used in conjunction with compatible client software. While this may be any application supporting open standards of data exchange, such as Google Earth, uDig, GVSig and others, the GeoServer is known for its effective integration with OpenLayers, which is also a dynamically developing Open Source project.

## The OpenLayers Web GIS Client Library

OpenLayers is an Open Source object-oriented JavaScript library for displaying map data in most modern web browsers, with no server-side dependencies. It implements a constantly developing JavaScript API for building rich web-based geographic applications. OpenLayers allows the developer to utilize many readily available and fully customizable components for easy construction of GIS client solutions which can be embedded into any Web page. As a framework, OpenLayers is intended to separate map tools from map data so that all the tools can operate on all the data sources by means of industry-standard methods, such as the OGC WMS and WFS protocols (Schmidt, 2008). Although it exhibits similarities to the Google Maps and MSN Virtual Earth APIs, OpenLayers has the advantage of being developed for and by the Open Source software community, which makes it free for modification and redistribution.

The default installation of OpenLayers provides only basic GIS features like zooming and panning, and advanced functionalities must be added manually by the developer, using a selection of existing controls as well as custom code. In practice, however, building a Web GIS client with OpenLayers

is very easy thanks to the vast library of examples. This, along with good documentation and support for tiled layer caches, makes this Open Source product a very flexible alternative to commercial solutions.

This innovative technology is becoming increasingly popular among developers of Web mapping systems and is now utilized in several major projects like the NOAA National Weather Service (http://radar.srh.noaa.gov/) and the European Union GeoPortal (www.inspire-geoportal.eu).

## Means of Monitoring the Marine Environment

Thorough monitoring of the marine environment is a complex task which not only consists of measurements but also analysis, validation and interpretation of information acquired by various sensors. The most commonly used sensors may be divided into two groups. The first group, dedicated to monitoring the underwater environment, includes sonar systems like echosounders and sidescan sonars. The second group deals with sensing of activities on the water surface and consists of radars, satellite images and Automatic Identification System (AIS) of marine vessels.

### Underwater Sensors

Producing maps of the sea floor has always been a unique challenge. Throughout the years different tools have been developed to meet these specific requirements. The produced tools include underwater devices like single-beam echosounder, sidescan sonar and bathymetric systems that remotely map the sea floor and subsurface. These systems are deployed from the fantail or a sidemount of a ship and towed continuously throughout a survey area. Navigational systems are run concurrently to precisely locate the gathered data.

Historically, the information on sea depth has been collected with the help of simple, relatively easy to use, low-cost echosounder equipped with a single piezoelectric transducer. These *single-beam bathymetry systems* measure the water depth directly beneath the vessel. The transceiver transmits a high-frequency acoustic pulse in a beam downward into the water column, the acoustic energy is reflected off the sea floor beneath the vessel and received at the transceiver. The continuous recording of water depth below the vessel yields high-resolution measurements, but only along the survey track. The operating frequency of single-beam systems ranges from 3.5 kHz to 400 kHz. A low-frequency system may also function as a subbottom profiler, as the energy can penetrate the sea floor and produce a very detailed map of surficial sediment thickness. The resulting depth values in the form of a point dataset represent accurate and reliable bathymetry. In order to show depths along the survey transects, bathymetry data can be displayed in the form of a coloured track or as a series of numbers called soundings (very common on marine charts). When the echosounder is equipped with bottom classification software,

an interpolated image with bottom types may be generated. Modern digital echosounders can produce detailed echograms in the form of raster images that represent a vertical transect of the whole survey. Although the echogram represents a vertical glimpse into the water column, sea bottom and sub-bottom areas, scientists very often embed the image in the horizontal untrue context of the map. It is very advantageous especially when the surveys are organized along map parallels and the track is sparse in meridians. The true presentation of an echogram data in three-dimensional geographic coordinates is still rare as the graphical rendering of such data in 3D GIS systems is highly demanding.

Data provided by a single-beam echosounder, in general, has limited uses because features lying between tracklines (which are often spaced between a few dozen and several hundred metres apart) are not visible to the system. Because of this, the provided data is quite sparse and requires a great degree of interpolation. Single beam surveys are still necessary for a number of applications; however more sophisticated devices are manufactured that use more than one transmitting and/or receiving piezoelectric element.

A *sidescan sonar* constitutes the optimal trade-off between resolution and swath coverage, with moderate complexity and cost. It produces data which allows to characterize surface sediment and identify sea floor objects. Imaging the sea floor with a sidescan sonar system is accomplished by towing a sonar (referred to as "tow-fish") over the study area. The tow-fish is equipped with a linear array of transducers that emit, and later receive, an acoustic energy pulse in a specific frequency range. The acoustic pulse is specifically designed so that it is wide in the across-track direction and narrow in the along-track direction. The acoustic backscattered energy received by the sidescan sonar tow vehicle provides information regarding the general distribution and characteristics of the surficial sediment and outcropping strata. Sidescan sonar systems typically operate in the 100 kHz to 1 MHz frequency range. Swath width depends on water depth and ranges from around 50 m to 500 m within these operating frequencies. The higher the frequency, the higher the resolution of the resultant sidescan sonar image. Such imagery data may be embedded in the map context as it represents near horizontal plane of sea floor with ranges that could be calculated from tow-fish track and the geometry of acquisition. However, although the acquired image is rectangular, its referencing in the map context is not straightforward because each pixel needs to be referenced according to the geometry of measurement. It means that nonlinear stretching of image is required, followed by application of graphical path technique to the whole image according to recorded geographical location. This process produces pixel holes in the image, which need to be removed via interpolation. A more sophisticated approach uses specialized software which creates a large image by assembling, or mosaicing, each swath of data into a georeferenced composite that represents the acoustic character of the sea floor within the study area.

Today, *multibeam echosounder* is the marine technology used by hydrographers to generate precise maps of the sea floor. Although it is characterized by high costs and high complexity of acquisition and processing, it is the most advanced and accurate solution for mapping the sea. The bathymetric maps produced by the multibeam instrument have a wide variety of applications. Marine geologists use these maps to study how the ocean crust was formed, how glaciers once moved over coastal areas and to find sites for sediment coring. Oceanographers can better model the flow of ocean currents. Marine biologists can use the data to map wildlife habitats and define fishing areas. A multibeam system sends out an array of sound pulses in a fan shape and returns depths from underneath the ship as well as from the sides. They can map a swath width of about four times the water depth, operating from 12 kHz (deep-water, low-resolution) to 400 kHz (shallow-water, high-resolution). As the ship is constantly moving, the transmitting beams have to correct for the ship's motion by steering the beams so they reflect off the correct part of the sea floor. The beams update many times per second (up to 50 Hz depending on water depth), allowing faster boat speed (over 10 knots) while maintaining full coverage of the sea floor. Multibeam bathymetry systems are now routinely used during research cruises to map areas of sea floor as large as thousands of square kilometres. The precise, high resolution bathymetry is obtained by processing echo data using signal amplitude and phase information from each beam, which can distinguish very small bottom features. The de-spiked and spline-filtered data represents dense point dataset, often present in the regular map context as a colourful, hill-shaded model view of bottom data. The visualization of complete multibeam data, including processed water column echoes requires substantial effort, as it can present 3D bathymetry along with 3D view of fish schools and other objects located between water surface and bottom. The state of the art in multibeam systems technology is currently represented by the multibeam sector scanning sonar, which produces a continuous animated 3D image of a wide sector of water column along with real-time DTM. The full use of data produced by such a system in the context of 3D GIS is still beyond the processing power of typical computers.

## Surface Sensors

The surface of a sea may be monitored through the analysis of ship movement patterns as well as by means of general surveillance. The former is done via mandatory broadcast of ship identification by every registered marine vessel. The latter involves the use of satellite images and radar data. Systems for detection and forecasting of oil spill spread fall somewhere between those two categories, as during a lifetime of an oil spill its elements submerge and may undergo sedimentation.

A *radar*, as an object-detection system, uses electromagnetic waves to determine the range, altitude, direction, or speed of both moving and fixed

objects. In marine environment nautical radars installed on-board are typically used to detect approaching ships and aircraft, observe weather formations and distant terrains as well as locate landmarks, as transmitted pulses of radio waves reflect from any object in their path as long as it exhibits different density from air medium. In a way similar to air traffic control, stationary installations of radars are present in coastal areas. Although the reflected radar signals captured by the receiving antenna are usually very weak, sophisticated methods of signal processing are used in order to recover useful information. The modern uses of radar are highly diverse, mostly because modern systems record and process radar image data in digital form. For example, commercial radar imaging satellites use active sensors that illuminate surface features with broadcast microwave energy at wavelengths which propagate through the atmosphere and clouds with almost no interaction or weakening. Because of this, they can record the returned signal during the day as well as night and under virtually any weather conditions. The image data that originates from rotating the transmitting/receiving antenna is typically internally processed to have rectangular coverage suitable for being stored as the false-scaled bitmap image. Its georeference is immediately obtained from known geographic position of the radar antenna and the radar range, typically expressed in nautical miles. Hence, the conversion to Universal Transverse Mercator projected marine maps is straightforward. However, as the stream of radar data is typically refreshed every 1 or 2 seconds, and additionally the radar range may be changed by the operator, the image georeferencing must be setup in real-time, what may be challenging in a real-time GIS system.

*Satellite sensors* provide means of measuring electromagnetic reflectance of objects on the Earth's surface as well as in the atmosphere. They offer good stability, capability for repeated measurements, potential of global coverage and spatial resolution ranging from 1 km to 1 m. The most prominent characteristic differentiating satellite platforms is mobility. Geostationary satellites maintain a fixed position over an area of the Earth, and thus are most useful in activities which involve among others continuous monitoring of the environment. Satellites which orbit the planet along fixed paths allow for surveillance of large portions of the globe, but at the cost of long delays between consecutive surveys of the same area. In addition, each platform may be equipped with several types of sensors providing information for different purposes. Some of the more popular platforms include the Meteosat Second Generation (MSG) geostationary satellites equipped with Spinning Enhanced Visible and InfraRed Imager (SEVIRI), the Meteorological Operational (MetOp) orbiting satellites equipped with Advanced Very High Resolution Radiometer (AVHRR), Terra and Aqua polar orbiting satellites equipped with Moderate-resolution Imaging Spectroradiometer (MODIS), the Envisat polar orbiting satellite with Advanced Synthetic Aperture Radar (ASAR), and the GeoEye-1 polar orbiting satellite equipped with sensor capable to capture very high resolution satellite photographs.

Satellites most often produce data in the form of photographs of an area in a given amount of spectral bands or groups of wavelengths. In most cases, images captured in the visible spectrum are ready for use (e.g. as background GIS imagery) shortly after their reception by a satellite ground station. Photographs of other spectra may require further processing (e.g identification and extraction of data such as vegetation zones). Although reception of satellite data generally requires access to a satellite ground station, many institutions publish satellite images through various media. An example is the EumetSat Broadcast System for Environmental Data (EumetCast), a multi-service dissemination system based on standard Digital Video Broadcast (DVB) technology. It uses commercial telecommunication geostationary satellites to multicast files received from meteorological satellites. Because of limited bandwidth, a full data scan is available every 15 minutes after reception by a satellite antenna. The data contains twelve spectral channels spread from the visible band centered on 0.6 μm to the carbon dioxide band centered on 13.4 μm, including one broadband high-resolution visible band channel. Data received from all channels is segmented to 8 or 24 (for high-resolution channel) strips, as a 3712 × 464 raster (5568 × 464 for high-resolution channel). Because of the utilized technology, access to this data is available to anyone equipped with a PC and a DVB-compatible receiver.

The *Automatic Identification System* is used for automatic recognition and tracking of marine vessels. It works by electronically exchanging data such as vessel name, position, speed and course with other nearby ships and Vessel Traffic Service (VTS) stations. By requirement of the International Maritime Organization (IMO), AIS is mandatory on all passenger ships as well as other vessels which exceed gross tonnage (GT) of 299 tonnes. In addition to vessel tracking, AIS may be used to assist the crew and port operators in traffic monitoring and avoidance of collisions.

Although AIS data requires a dedicated receiver, several institutions have made it available in semi real-time over the Internet. An example of such a service is www.marinetraffic.com, a website provided by the University of the Aegean in Greece. The marine traffic Web service manages radio signals obtained by AIS receivers from all over the world and makes them available through HTTP queries in the form of XML files.

An *oil spill simulation system* usually consists of several sub-modules which are responsible for modelling different elements of the marine environment. For example, the POSEIDON operational tool for prediction of floating pollutant transport, developed for the Aegean Sea by the Hellenic Centre for Marine Research (HCMR), consists of two discrete modules (Papadopoulos et al., 2002). The first one is a three-dimensional oil-spill weathering and drift module that simulates the dispersion of oil droplets and their chemical transformations. The second is a forcing module that provides data for wind, waves, currents and diffusivity to the oil-drift module. The oil-spill weathering and drift module is designed to simulate the drift of the oil as

well as its chemical reactions with the environment. The oil slick is simulated in the form of a thousand particles which have individual chemical and physical characteristics. The model uses advection and diffusion estimates to calculate the three-dimensional position of each particle, while information such as wind and wave conditions and hydrological characteristics are required for the simulation of its time-varying physiochemical properties. The latter include evaporation, emulsification, beaching and sedimentation, which correspond to the transfer of oil from the sea surface to the atmosphere, the mixing of water in the heavier fractions of the hydrocarbons, the trapping of oil along the coast and trapping of oil particles that reach the sea bottom (Pollani et al., 2001). The forcing module, which provides data for wind, waves and three-dimensional currents, collects information from three different operational models for the Greek Seas. These consist of a meteorological forecasting model, a wind-wave model, and a 3D hydrodynamic model. With this data the module is able to provide 72-hour forecasts for the Aegean and the Eastern Mediterranean Sea on a daily basis (Kulawiak et al., 2010b).

A different example of an oil spill simulation model is Computer Aided Rescue and Oil Combating System (CAROCS), designed and developed by the Maritime Institute in Gdansk (MIG) for the Baltic Sea. From among the processes influencing oil spill dispersion, this particular model considers (1) advection caused by sea currents and wind, (2) wave height and direction, (3) vertical and horizontal diffusion of oil spill droplets and (4) vapourization and dispersion. The model also utilizes the High Resolution Operational Model for the Baltic Sea (HIROMB) as well as WAM4 wave forecast model as input (see e.g., Chybicki et al., 2008). The model generates consecutive spill layers with a spatial resolution of 3 NM at one hour intervals.

## Integration of GIS for Monitoring of Marine Environment

This section describes several systems which utilize some of the technologies presented in this chapter for integration, processing and visualization of data from various marine sensors. The depicted Geographic Information Systems have been developed by the Gdansk University of Technology Department of Geoinformatics in the course of different projects.

### Visualization of Oil Spill Simulation Results

The Web-based Geographic Information System for monitoring and mapping of marine pollution was developed by GUT in cooperation with the HCMR as a dissemination and analysis backend for the oil spill spread forecasts produced by POSEIDON. The process of integrating the Web-GIS into a complex system for oil spill spread simulation and Web-based dissemination, designed as an advanced marine pollution awareness and emergency management tool

has been described in detail by Kulawiak et al. (2008). The oil spill operational model produces output data in the form of ASCII files containing simulation results for an oil spill spread during a given amount of time. Every oil spill is represented as a set of a thousand geographically oriented droplets and is accompanied by additional data, such as the simulated date and time, the total volume of the oil spill as well as the evaporated and emulsified volumes both in the sea and on land. All this information must be extracted, processed and visualized.

The discussed system utilizes custom JEE and JSE code for reception and parsing of the simulation data files. It then produces a series of vector data files which contain all of the information conveyed by the operational model. These files are ready to be registered in the system Map Server and remotely visualized through the Web client. The former is realized by means of the GeoServer, while the DHTML client is based on the OpenLayers Javascript library, as shown in Fig. 1.

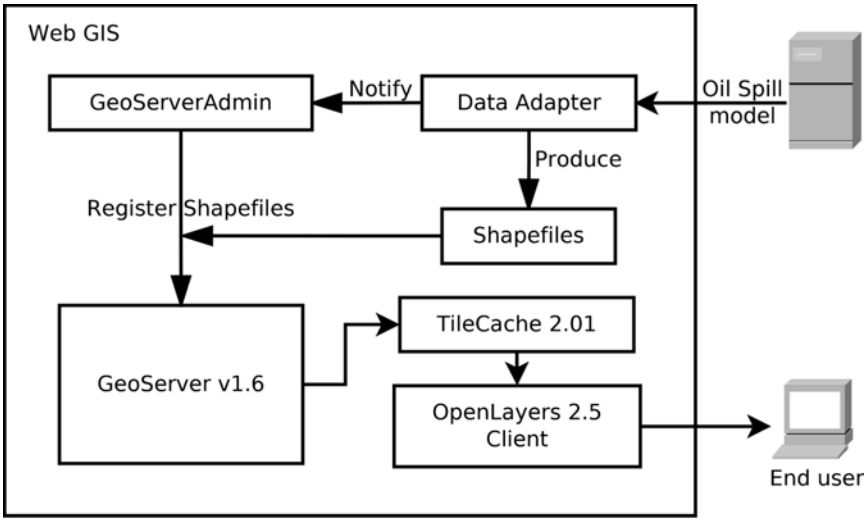


**Figure 1.** Architecture of the Web-based GIS for oil spill spread monitoring and forecasting.

This combination allows the system to utilize a broad range of existing formats for background data layers. Examples of such would be satellite imagery, electronic navigation charts, WMS servers, remote geodatabases as well as mapping services such as Google Maps. The application of GeoServer allows for easy integration of required data formats, and utilization of OpenLayers provides means to create dynamic multilayer visualizations of oil spill simulation results accessible to anyone equipped with only a modern Web browser, which constitutes one of the most distinctive features of this system. In consequence, the system allows authenticated end users to dynamically view the simulation results in a geographical context in the form

of thematic layers overlaid on background marine and land data. In addition to standard GIS operations like view zooming and panning, the user is presented with interactive elements like an animation of the oil spill spread as well as tools for querying each hour layer for parameters like the volume of selected oil spill, its geographic coordinates, elevation of its elements and many more, as shown in Fig. 2.

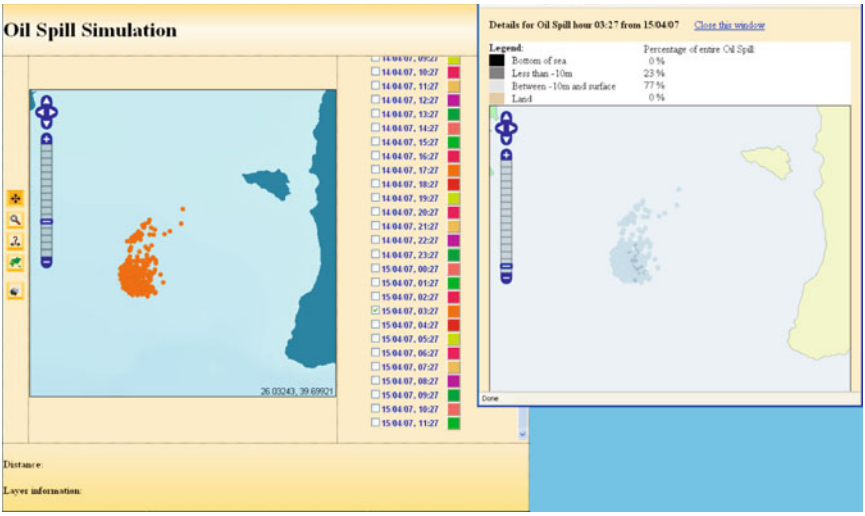


**Figure 2.** A sample view of an oil spill hour in the Web GIS (left) with a detailed view of the spill in a separate window (right).

## Three-dimensional Integration of Marine Survey Data

For purposes of monitoring the ecosystem of the Gulf of Gdansk, GUT developed a desktop GIS for integration, processing and 3D visualization of marine sensor data. The application was built upon the ESRI ArcGIS Engine technology to provide a complex solution for integration, analysis and visualization of spatial data acquired from sources such as sonar systems and CAROCS. It was developed in C# language using the .NET platform and utilizes ArcObjects for spatial processing and visualization. Using ArcGIS Engine technology allowed for creation of complex mechanisms for three-dimensional visualization of custom spatial objects, ranging from multibeam echosounder bathymetry, sidescan sonar and single-beam echosounder data to oil spill modelling results.

The presented system consists of several main elements, namely the Data Integration and Adaptation module, the Data Presentation module, the Geodatabase and remote data sources. The complete block diagram of the system, including relations between the system components, is shown in Fig. 3.

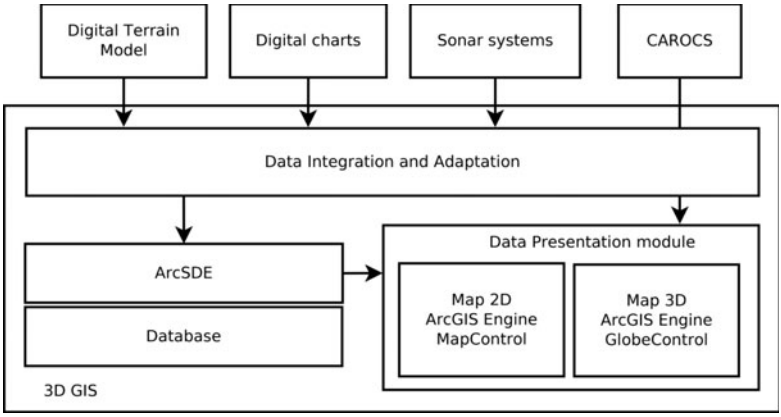


**Figure 3.** Architecture of the GIS for 3D integration, processing and visualization of marine sensor data.

The Data Integration and Adaptation module is developed using the Microsoft .NET platform and corresponding elements of ArcGIS Engine. The system employs custom algorithms for processing MBS data. After such data is extracted from a raw stream of bytes, it is filtered with the use of information such as the transducer depth relative to water level, number of valid beams, sample rate, quality factor, and reflectivity in order to minimize possible acquisition artifacts. Multibeam bathymetry is then validated and georeferenced using data acquired from the ship's GPS receiver. In a similar way the system processes data from the sidescan sonar and single-beam echosounder. Because the stream of survey data is typically processed in chunks, this results in a series of georeferenced vector and raster data. In the case of single-beam echosounders, the horizontal axis of each image represents the time of acquisition. With the use of navigational information from the surveying vessel, it is converted into geographic position on the map. The acquired information is then stored in ESRI ArcSDE, an application server that facilitates storing and managing spatial data in an underlying database. CAROCS oil spill data, being dynamic, is handled differently. After being generated by the Data Integration and Adaptation module, it is passed directly to the visualization subsystem. The Data Presentation module uses ArcGIS Engine MapControl and GlobeControl components to provide a standard set of GIS functionalities like map viewing, zooming and panning for two-dimensional and three-dimensional display, respectively. However, efficient visualization of certain data required the creation of dedicated OpenGL procedures for display and animation of three-dimensional objects. For example, the system allows to display MBS data in two forms, either as a series of points containing bathymetry data, or as a series of two-dimensional fan-shaped images (water-column) that can be used to visualize objects other than the seabed, such as fish or pollution. In order to maintain visibility, signal values below a certain threshold can be made completely transparent. This method can be used to

clearly show objects floating above the sea floor, like pelagic fish schools shown in Fig. 4.

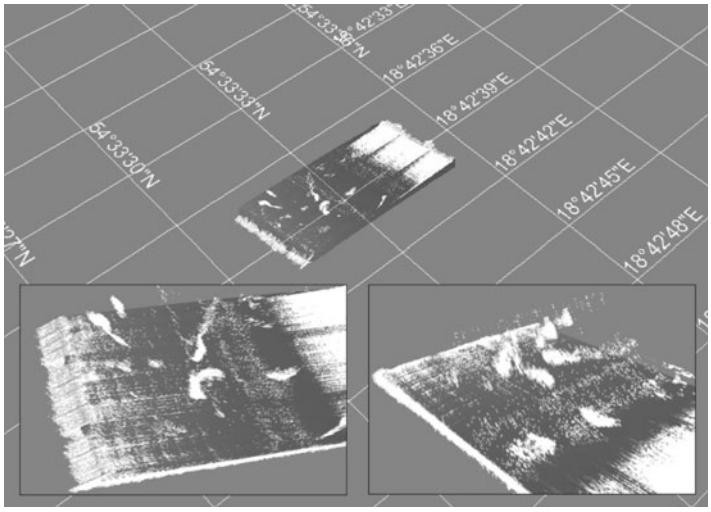


**Figure 4.** A three-dimensional presentation of pelagic fish schools in the Gulf of Gdansk, acquired from MBS water column data.

The combined functionalities of the system allow for creation of complex visualizations, e.g. an overview of the Gulf of Gdansk with overlaid three detailed views that present data from the single-beam echosounder, sidescan sonar and multibeam echosounder integrated in a three-dimensional coordinate space, as depicted by Fig. 5. The application allows seamless navigation between data acquired from various sources, at various times.

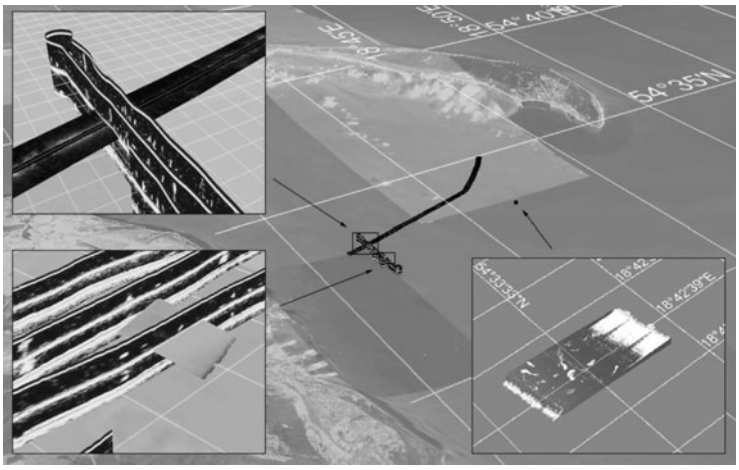


**Figure 5.** A three-dimensional view of the Gulf of Gdansk with overlaid data from single-beam echosounder, sidescan sonar and multibeam echosounder.

## Remote Monitoring of the Marine Ecosystem

In the course of a project funded by the State Committee for Scientific Research, GUT developed a web-based GIS for remote integration and processing of marine data. The system uses Open Source technologies, namely GeoServer, OpenLayers and Java, to combine data from sonar systems, CAROCS, radar, AIS and MetOp with nautical charts and background data. The results are visualized in the form of remotely available time-varying thematic layers presenting various aspects of the investigated marine region, overlaid on multiple background maps. The system also allows for visualization of different dynamic environment phenomena such as weather conditions or fish school movements. In the former case, the Web GIS provides means for presenting the data in the form of an animated layer consisting of historical satellite data. The latter is made available as an animated georeferenced marker on the Web GIS map. The different functionalities of the system are realized by several dedicated modules, all developed with use of Open-Source technologies, as shown in Fig. 6.

The Map Server, Web Client, and Integration modules are realized with the use of GeoServer, OpenLayers, and a custom JEE and JSE code, respectively. Interfaces for diverse distributed data sources and sensors allow for easy integration of various information regarding the marine environment.

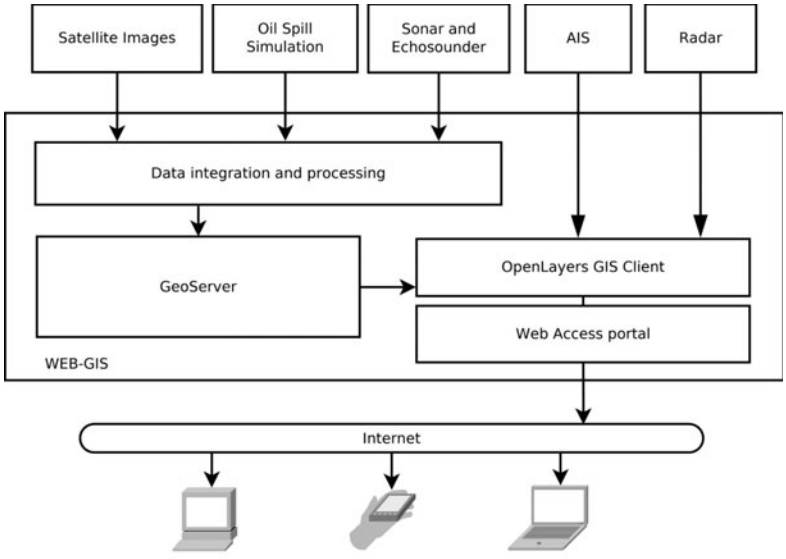


**Figure 6.** Architecture of the Web-based GIS for remote integration and processing of marine data.

The system transforms multibeam echosounder bathymetry data into Portable Network Graphic files with an additional world (*.pgw) and projection (*.prj) files that enable geographic positioning of spatial information by the GeoServer. Back-scattering data is presented in the form of a georeferenced

animation consisting of a series of 512 × 1024 pixel frames, generated from a number of consecutive swaths. Other acoustic parameters like TVG, gain and power are also available in the marker pop-up.

Radar data is fed to the system through a dedicated software server, which provides georeferenced imagery on user demand. Depending on the sensor's geographic orientation, each requested image frame needs to be projected before it can be overlaid on the base map. For example, a single 240 × 240 raw raster image headed from North by 11 degrees is fitted to a standard 256 × 256 tile that is geographically scaled on the map to its actual range setup.

Because AIS data is provided by an independent web service, it isn't readily compatible with the Web GIS coordinate system. Because of this, it needs to be pre-processed on the client side before it can be displayed. Thus, the data returned by AJAX requests to the MarineTraffic Web service is parsed and transformed through Javascript methods. It is then visualized using vendor-provided icons representing ship markers, with adequate size and orientation (rounded to 5 degrees) reflecting ship course. The HTTP queries are map extent and zoom level sensitive in order to conserve bandwidth. The layers, representing the state of ships, ports and AIS stations, are periodically refreshed in an automatic manner.

In a similar way to radar data, the information received from EumetCast is also stored on a dedicated web server. However, because the images are registered in a geostational projection, they require additional processing before integration with Plate-Care charts or Mercator projected marine maps. Because of this, the channels are organized into layers which can be geo-concatenated and reprojected by a dedicated WMS server. The server provides near real-time area snapshots in the form of 256 × 256 pixel tiles which may cover the greater part of the northern hemisphere. MetOp-A satellite data is also provided by a dedicated WMS server. The server pre-processes data acquired from the satellite ground station and makes it available in the form of WMS and WCS. In contrast to EumetCast, MetOp data available in the system is confined to the area of Europe. Sample integration of Satellite and AIS data within the Web GIS is shown in Fig. 7.

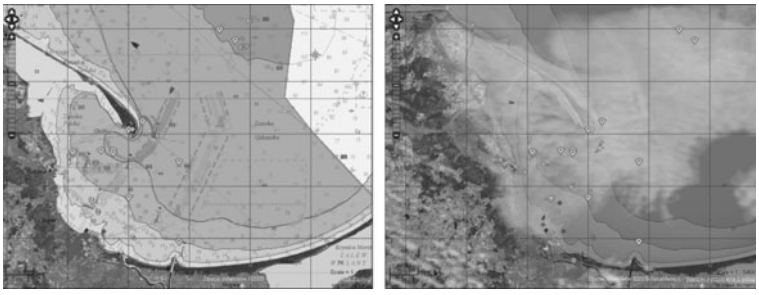

**Figure 7.** The main map of the Web GIS showing information from AIS, Radar (left) and Satellite (right) sensors integrated in a common coordinate space and overlaid on digitalized nautical charts and WMS data.

## Perspectives

Monitoring of marine environment and visualization of results is not a new field of research. During the years it has seen slow but stable evolution of means of collecting and processing data. At the same time Geographic Information Systems have evolved from specialized single-user workstation software into freely available tools for remote mapping, geocoding, and spatial analysis. Their expansion closely followed the progress of information technology, as they entered new niches when the opportunity presented itself. The introduction of 3D acceleration hardware enabled the creation of three-dimensional GIS. The advent of Dynamic HTML laid the foundations for Javascript-based services such as Google Maps. The development of Smartphones brought Web GIS to mobile devices. In a similar way the adoption of HTML5 and WebGL will catalyze the development of remotely accessible browser-based 3D GIS.

Thus, the foreseeable future trends do not involve a revolution but instead rely on further progress of existing solutions. Taking into account the progress of wireless Internet, remote three-dimensional visualization of data collected from mobile sensors in real time will likely become possible.

## Conclusion

This chapter presented common types of marine sensors which allow for monitoring and sensing of underwater as well as surface activities. The chapter also discussed several popular commercial and Open Source technologies used for constructing custom Geographic Information Systems. Finally, the chapter exemplified the application of the discussed technologies to processing, integration, analysis and visualization of data from the presented sources.

For a long time commercial solutions have seen little competition, especially in the area of desktop GIS. In the recent years this state of affairs has been rapidly changing, with organizations like the Open Source Geospatial Foundation concentrating efforts on the development of alternative solutions. In consequence, although commercial software still prevails in desktop applications, Open Source solutions such as GeoServer and OpenLayers hold a strong position in development of web-based GIS.

The technologies presented in this chapter are constantly evolving, developing methods of improved presentation and analysis of geographic data with the power of new generations of computer hardware. Thus far most functionalities of regular desktop GIS have been implemented in Web applications with the use of Server-side data processing and an interactive DHTML client. Even features like processing and visualization of back-scatter and bathymetry data based on various acoustic parameters like TVG, gain and water-column information may be implemented in the form of a Web service, as it has been exemplified by the presented Web-based GIS for monitoring of the marine ecosystem.

The only element of desktop GIS which still requires at least a standalone web client such as Google Earth is remote presentation of three-dimensional data. However, there is good chance that the possibilities brought by new standards like HTML5 and WebGL will alleviate this problem and in the near future the full functionality of three-dimensional marine GIS will be freely available to anyone equipped with a modern web browser.

## References

Bakare, A.M., Morley, J.G. and Simons, R.R. (2008). Developing a seabed resurvey strategy: A GIS approach to modelling seabed changes and resurvey risk. *Computers, Environment and Urban Systems*, **32(4)**, 293–302.

Chybicki, A., Kulawiak, M., Lubniewski, Z., Luba, M., Moszynski, M. and Dabrowski, J. (2008). GIS for Remote Sensing, Analysis and Visualization of Marine Pollution and Other Marine Ecosystem Components. Proceedings of 2008 1st International Conference on Information Technology, 223–226.

Doyle, S., Dodge, M. and Smith, A. (1998). The potential of Web-based mapping and virtual reality technologies for modelling urban environments. *Computer, Environment and Urban Systems*, **22(2)**, 137–155.

Goodall, J.L., Robinson, B.F. and Castronova, A.M. (2011). Modeling water resource systems using a service-oriented computing paradigm. *Environmental Modelling & Software*, **26(5)**, 573–582.

Hamre, T., Krasemann, H., Groom, S., Dunne, D., Breitbach, G., Hackett, B., Sørensen, K. and Sandven, S. (2009). Interoperable web GIS services for marine pollution monitoring and forecasting. *Journal of Coastal Conservation*, **13(1)**, 1–13.

Kraak, M.-J. (2004). The role of the map in a Web-GIS environment. *Journal of Geographical Systems*, **6**, 83–93.

Kruger, A., Khandelwal, S.G. and Bradley, A. (2007). AHPSVER: A web-based system for hydrologic forecast verification. *Computers & Geosciences*, **33**, 739–748.

Kulawiak, M., Luba, M., Stepnowski, A., Prospathopoulos, A., Kioroglou, S., Perivoliotis, L. and Grammatikaki, M. (2008). Integrating a Web-based GIS to a marine pollution monitoring and forecasting system. Proceedings of the International Conference on Marine Data and Information Systems, Athens (Greece).

Kulawiak, M., Chybicki, A. and Moszynski, M. (2010a). Web-based GIS as a tool for supporting marine research. *Marine Geodesy*, **33(2 and 3)**, 135–153.

Kulawiak, M., Prospathopoulos, A., Perivoliotis, L., Luba, M., Kioroglou, S. and Stepnowski, A. (2010b). Interactive visualization of marine pollution monitoring and forecasting data via a Web-based GIS. *Computers & Geosciences*, **36(8)**, 1069–1080.

Maceachren, A.M. and Kraak, M.-J. (1997). Exploratory cartographic visualization: Advancing the agenda. *Computers & Geosciences*, **23(4)**, 335–343.

Papadopoulos, A., Kallos, G., Katsafados, P. and Nickovic, S. (2002). The Poseidon weather forecasting system: An overview. *The Global Atmosphere and Ocean Systems*, **8(2-3)**, 219–237.

Pollani, A., Triantafyllou, G., Petihakis, G., Nittis, K., Dounas, K. and Koutitas, C. (2001). The POSEIDON Operational Tool for the Prediction of Floating Pollutant Transport. *Marine Pollution Bulletin*, **43(7-12)**, 270–278.

Rao, M., Fan, G., Thomas, J., Cherian, G., Chudiwale, V. and Awawdeh, M. (2007). A web-based GIS Decision Support System for managing and planning USDA's Conservation Reserve Program (CRP). *Environmental Modelling & Software*, **22**, 1270–1280.

Schmidt, C. (2008). OpenLayers: Free Maps for the Web. Retrieved October 22, 2009, from http://www.openlayers.org

Stepnowski, A., Burczynski, J., Ostrowski, M., Moszynski, M., Lenkiewicz, J. and Partyka, A. (1996). ECHOBASE – A Portable Geographic Fishery Research Database System. *Marine Geodesy*, **19**, 269–280.

Thakur, J.K., Srivastava, P.K., Singh, S.K. and Vekerdy, Z. (2011). Ecological monitoring of wetlands in semi-arid region of Konya closed basin, Turkey. Regional Environmental Change (DOI: 10.1007/s10113-011-0241-x).

Trygonis, V., Georgakarakos, S. and Simmonds, E.J. (2009). An operational system for automatic school identification on multibeam sonar echoes. *ICES Journal of Marine Science*, **66(5)**, 935–949.

Tsou, M.-H. (2004). Integrating Web-based GIS and image processing tools for environmental monitoring and natural resource management. *Journal of Geographical Systems*, **6**, 155–174.

Tuama, É.Ó. and Hamre, T. (2007). Design and Implementation of a Distributed GIS Portal for Oil Spill and Harmful Algal Bloom Monitoring in the Marine Environment. *Marine Geodesy*, **30**, 145–168.

# 4

# Estimation of Evapotranspiration from Wetlands Using Geospatial and Hydrometeorological Data

**Jay Krishna Thakur, P.K. Srivastava[1], Arun Kumar Pratihast[2] and Sudhir Kumar Singh[3]**

Department of Hydrogeology and Environmental Geology, Institute of Geosciences, Martin Luther University, Halle (Saale), Germany
[1]Water and Environment Management Research Centre
Department of Civil Engineering
University of Bristol, Bristol BS8 1TR, United Kingdom
[2]Center for Geo-information, Wageningen University
Wageningen, The Netherlands
[3]Department of Atmospheric and Ocean Science
University of Allahabad, Allahabad 211001, India

## Introduction

Over recent decades, wetlands have been recognized increasingly for their high biodiversity and for the important hydrological functions, including flood alleviation, low-flow support, nutrient cycling and groundwater recharge (Thakur, 2010; Thakur et al., 2011). Wetland hydrology is a primary driving force influencing wetland ecology, its development and persistence (Mitsch and Gosselink, 1993). For most wetlands, evapotranspiration (ET) is the major component of water loss, and when considered as its energy equivalent, the latent heat flux (LE), the largest consumer of incoming energy (Reynolds et al., 2000; Wilson et al., 2001). The radiation and the turbulent heating drive the dynamics of the land-atmosphere energy exchanges in the wetlands. Estimation of these radiation and turbulent heating through mass energy balance equations is the core of numerical weather forecast, climate research, water resources and environmental management and long-term agriculture production. Most of the conventional methods which use point measurement in measuring the energy balance, such as Bowen ratio, Penman-Monteith, Priestley and Taylor, give results that can be efficient on local level but could not be extended to large scale or global scale measurement in time and space (Stewart, 1989).

J.K. Thakur et al. (eds.), *Geospatial Techniques for Managing Environmental Resources*,
DOI 10.1007/978-94-007-1858-6_4, © Capital Publishing Company 2012

ET depends upon many factors including the availability of water at the evaporating surface, solar radiation, air temperature, humidity and wind speed, type and density of vegetation cover, rooting depth and reflective land surface characteristics (Hupet and Vanclooster, 2001; Kalmar and Currie, 2006; Yao, 1974).

Several scientists have demonstrated the relationship between land surface temperature, soil moisture and canopy based on a combination of a soil moisture-balance equation and energy-balance theory (Moran et al., 1994; Nemani and Running, 1989; Sandholt et al., 2002; Srivastava et al., 2009; Yue et al., 2007). The normalized deviation vegetation index (NDVI) and land surface temperature can be used to establish an integrated model to monitor land use/cover (Singh et al., 2010; Yue et al., 2007). The most commonly used one is land surface temperature (LST), which is shown in a two-dimensional space composed of NDVI and land surface temperature (Sandholt et al., 2002; Yue et al., 2007). The land surface temperature can be directly linked to ET; several scientists show that they are proportional to each other (Cox et al., 1999; Noilhan and Planton, 1989; Shukla and Mintz, 1982; Weng et al., 2004).

Various remote sensing algorithms have been used over the years to estimate the atmospheric turbulent fluxes. In this study, Surface Energy Balance System (SEBS) algorithm was employed to estimate actual ET ($ET_a$). The algorithm has been used for the application of evaporation estimates in Spain Barrax (Z. Su and Jacobs, 2001), Taiyuan basin in China (Jin et al., 2005), in estimation of sensible heat flux in Spain Tomelloso area (Jia et al., 2003), and for drought monitoring purposes in north west China (Zhongbo Su et al., 2003). SEBS has been evaluated for its application to ASTER imagery with flux-measurements in Barrax, Spain (van der Kwast et al., 2009).

The aim of this chapter is to describe method to quantify ET spatiotemporally in wetlands of semi-arid region using open source software and geospatial-hydrometeorological data and to study hydrological dynamics in term of ET in various types of wetlands around Tuz Lake in Konya closed basin, Turkey.

## Study Area

The wetlands, around Lake Tuz, irregular shape having total area of 7651 $km^2$, are located between 38º11′ - 39º18′ N latitudes and 32º15′ - 34º15′ E longitudes in the Konya closed basin to the south from Ankara in the heart of Turkey (Fig. 1). The study area is situated at an elevation of 905 m above mean sea level (Gökmen, 2009; Thakur and Singh, 2010). The climate in Konya closed basin represents a typical arid to semi-arid climate dominated by halophytic and simple steppes (Tektas, 2007). Sandstones and shales compose the surface layer whereas schist-quartz schist-mica schist, marble, calc schist-quartz schist-mica schist, dolomitic limestone and serpentinite-radiolarite-limestone-glaucophane schist sequences compose sub-surface layers of the wetlands floor in the study area (Zeki Camur and Mutlu, 1996). Aeolian

depositional landforms can be seen on the northern and western areas of the wetlands.

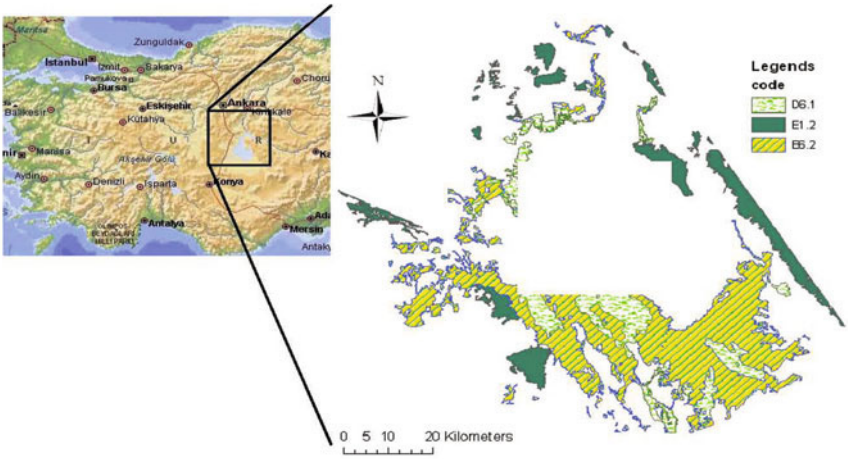


**Figure 1.** Location map of study area showing wetlands around Tuz Lake, in Konya closed basin, Turkey (Shape file source: Environmental Protection Agency for Special Areas (EPASA)). D6.1, E1.2 and E6.2 are habitat codes for inland salt marshes, perennial calcareous grassland and continental inland salt steppes respectively.

## Data and Methods

### Datasets Used and Analysis

SEBS requires the following set of input from remote sensing data: the land surface temperature, emissivity, land surface albedo, NDVI and vegetation proportion. Air pressure at surface and reference height, hourly air temperature and mean daily air temperature, specific humidity, wind speed at the reference height and sunshine hours per day are the second input provided by ground meteorological data. The air temperature and wind speed are scaled to the blending height (100 m) assumed to apply for all pixels of the image. Thirdly, downward solar radiation and long wave radiations are required input for the energy balance component. The downward solar radiation is taken from hourly meteorological data for each of the satellite pass time of the images, whereas the outgoing long wave radiation is derived from satellite data with some parameterization. In the study area, meteorological variables are measured from station having height 2 m above the ground surface (Thakur et al., 2011).

The methodology for the research consists of three different stages viz. pre-field work, field work and post-field work. Time series meteorological and hydrological data were collected to analyse the trend and the variability of rainfall, evaporation, temperature and groundwater level. Fieldwork was carried out in the wetlands of the Konya closed basin, Turkey for ground truth collection. The ground control points were collected using hand-held GPS for georeferencing of the images and land cover classification purposes. In this

study, major hydrological variables have been defined and different parameters of the wetlands quantified. During this stage the vegetation cover, type and height information was taken which is needed as input for SEBS algorithm. The third and final stage was the pre-processing and processing of the data collected; extracting meteorological information for the overpass time; atmospheric corrections for the visible and thermal bands; and applying SEBS in Integrated Land and Water Information System (ILWIS) open sources software. The time series meteorological data were used to derive the reference ET. The research stages, which were made to meet the objectives of the chapter, are shown in Fig. 2.

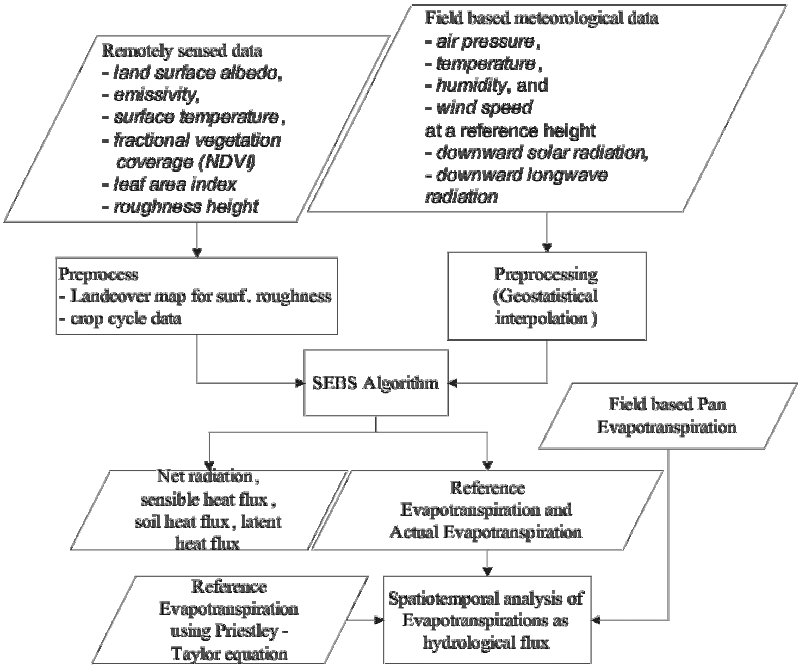


**Figure 2.** Flowchart of main steps to quantify ET spatiotemporally in wetlands in semi-arid region in Konya closed basin, Turkey (Thakur, 2010).

## Actual ET ($ET_a$) Using Surface Energy Balance System (SEBS)

The Surface Energy Balance System (SEBS) was developed by Z. Su (2002) using visible and infrared satellite remote sensing data. The SEBS algorithm is based on land surface energy balance theory combined with the in-situ meteorological data or the product of atmospheric numerical model to estimate land surface turbulent flux and the relative evaporation at different scales. The land surface parameters (albedo, emissivity, temperature, Vegetation Proportion (Pv) and NDVI) for the system are extracted from the reflectance and radiance measurement of the satellite (Z. Su et al., 1999). The other input used includes air pressure, temperature, humidity, wind speed at a reference height and

sunshine hours per day. These climatological data are accessed from the standard meteorological station at the reference height. SEBS is very sensible to the meteorological input like the air temperature. The difference between the surface and air temperature forces the sensible heat flux. SEBS is an extension of Surface Energy Balance Index (SEBI) concept with the improvement of estimation of thermal roughness length with a dynamic model which is based on the work of Massman (1999) and Z. Su and Jacobs (2001). The algorithm has an advantage of using both Bulk Atmospheric Similarity (BAS) of Brutsaert (1999) and the Monin-Obukhov atmospheric surface layer (ASL) similarity which can be used for regional and local scale estimation of the turbulent fluxes respectively.

The Surface Energy Balance System (SEBS), developed by Su (Z. Su, 2002), is used to estimate the atmospheric turbulent fluxes and evaporative fraction using satellite earth observation data, in combination with meteorological information of study area at proper scales (Qin et al., 2008). This system retrieves ET using measurements of incoming surface radiation, surface skin temperature, surface meteorology, and surface and vegetation properties (H. Su et al., 2005). SEBS also includes physical model that considers surface heterogeneity in the estimation of the roughness height for heat transfer. This system consists of a set of tools for the determination of the land surface physical properties and state variables, such as albedo, emissivity, temperature, vegetation coverage etc. from spectral reflectance and radiance—an extended model for the determination of the roughness length for heat transfer and evaporative fraction from the energy balance at limiting cases (Z. Su and Jacobs, 2001). The surface energy balance equation is written as

$$R_n = G_0 + H + \lambda E \tag{1}$$

where $R_n$ is the net radiation, $G_0$ is the soil heat flux, $H$ is the turbulent sensible heat flux, and $\lambda E$ is the turbulent latent heat flux ($\lambda$ is the latent heat of vapourization and $E$ is the actual ET).

Under the dry-limit, the latent heat becomes zero due to the limitation of soil moisture and the sensible heat flux is at its maximum value. From Eqn. (1), we can write

$$\lambda E_{dry} = R_n - G_0 - H_{dry} \equiv 0 \tag{2}$$

or $$H_{dry} = R_n - G_0$$

And under the wet-limit, where the evaporation takes place at potential rate, the sensible heat flux takes its minimum value, $H_{wet}$ and is given by,

$$\lambda E_{wet} = R_n - G_0 - H_{wet} \tag{3}$$

or $$H_{wet} = R_n - G_0 - \lambda E_{wet}$$

Then the relative evaporation $\Lambda_r$ can be written as

$$\Lambda_r = 1 - \frac{H - H_{wet}}{H_{dry} - H_{wet}} \tag{4}$$

And finally total radiation can be written as

$$\Lambda_r = \frac{\lambda E}{H + \lambda E} = \frac{\lambda E}{R_n - G} = \frac{\Lambda_r \cdot \lambda E_{wet}}{R_n - G} \tag{5}$$

The actual latent heat flux ($\lambda E$) can be obtained from Eqn. (5) also. The actual sensible heat flux ($H$) is determined with the bulk atmospheric similarity approach and is constrained in the range set by the sensible heat flux at the wet limit ($H_{wet}$), and that at the dry limit $H_{dry}$. Equation (2) gives $H_{dry}$ and $H_{wet}$ can be derived by a combination equation similar to the Penman–Monteith equation with the assumption of a completely wet situation. By assuming that the daily value of evaporative fraction is approximately equal to the instantaneous value, the daily evapotranspiration is determined as:

$$ET_a = 8.64 \times 10^7 \times \frac{\Lambda \cdot Rn_{day}}{\lambda \rho_W} \tag{6}$$

where $\rho_w$ is the density of water [kgm$^{-3}$], $Rn_{day}$ is the daily net radiation [Wm$^{-2}$]. The 24 hours net radiation is given by

$$Rn_{day} = (1 - c_1 \cdot r_0) \times K_{24}^{\downarrow} + L_{day} \tag{7}$$

where $r_o$ is the broad band surface albedo, $L_{day}$ is the average daily net long wave radiation [Wm$^{-2}$], $C_1$ is the conversion factor of instantaneous albedo to the daily average, $K_{day}^{\downarrow}$ is the measured incoming radiation [Wm$^{-2}$] and $L_{day}$ is usually estimated using the daily atmospheric transmittance as below:

$$L_{day} = -110\ \tau \tag{8}$$

where $\tau$ is determined from sunshine fraction as below:

$$\tau = \left(a_s + b_s \cdot \frac{n}{N}\right) \tag{9}$$

where the default values $a_s = 0.25$ and $b_s = 0.5$ are used.

By summing up the corresponding daily evapotranspiration for a certain period, the actual evapotranspiration for the period (i.e. a week, a month or a year) can be estimated.

## Reference ET Using Priestley-Taylor Equation

In Turkey, November, December, January and February are winter months. During these months in the years of 2000, 2004 and 2008, cloud-free images were not available. The maximum and minimum temperatures were 11.4 ºC, –13.8 ºC; 14 ºC, –10.7 ºC and 13.6 ºC, –12.8 ºC during the years 2000, 2004 and 2008 respectively. In the years 2000, 2004 and 2008, the average temperature of the winter months was 0.12 ºC, 2.05 ºC and 0.40 ºC respectively.

In the absence of cloud-free MODIS images when SEBS approach is not suitable, based on Priestley-Taylor equation, an empirical relation was formulated between ET factor and total amount of solar radiation considering solar radiation and surface temperature play a major role in ET processes. The

equation for ET factor ($ET_f$) can be estimated by using radiation based equation (Maidment, 1993) as below:

$$ET_f = F_{fpt} \cdot A \quad (\text{mm day}^{-1}) \tag{10}$$

and

$$F_{pt} = \alpha\left(\frac{\Delta}{\Delta+\gamma}\right) \tag{11}$$

where $\alpha$ = 1.74 for arid region, $\Delta$ and $\gamma$ are gradient of saturated vapour pressure and psychrometric constant expressed in kPa $^oC^{-1}$ unit respectively. The value of $\Delta$ and $\gamma$ at different temperatures is listed in Appendix 1. $A$ (= $R_n - G$) is the net solar radiation. During these months, as the land surface average temperature is near 0 $^o$C, the soil heat flux is neglected. Using these equations, $ET_f$ was calculated for all months in the years 2000, 2004 and 2008. The $ET_f$ obtained from Eqn. (10) and $ET_a$ obtained from SEBS processing was graphically plotted to find regression coefficient between these two quantities. The regression coefficient was used to extend $ET_a$ for winter months during the years 2000, 2004 and 2008.

Field-based pan evaporation values from the meteorological station near the wetlands for the years 2000, 2004 and 2008 have been used to study significance and correlation of the remotely sensed ET. The evaporation measurement was taken using US Class A pan evaporimeter.

## Results and Discussion

### ET Estimation

The temporal distribution of total monthly actual $ET_a$ in D6.1, E1.2 and E6.2 habitats in the wetlands for the years 2000, 2004 and 2008 shows high $ET_a$ in the months of May, June and July (Fig. 3).

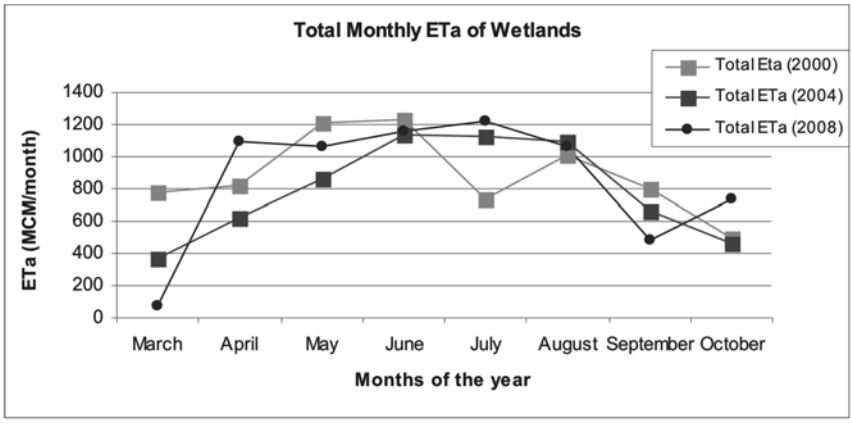


**Figure 3.** Total monthly $ET_a$ of wetlands (MCM is million cubic metre).

In the months January and February of year 2000, January of the year 2004; and January and February of 2008 the average atmospheric temperature was below 0 ºC. During these periods, the $ET_a$ of the wetlands is considered 0 mm/day. In the remaining months of these years (during the months of November, December, January and February) when average monthly temperature is above 0 ºC, the $ET_a$ was calculated on the basis of empirical equation explained in Eqns (10) and (11). The average and total $ET_a$ during the years 2000, 2004 and 2008 is graphically plotted in Fig. 4. The average $ET_a$ value represents average of daily $ET_a$ values for all the habitat types from the month March to November when MODIS images were available. In addition, the total $ET_a$ value represents sum of daily $ET_a$ values of all habitat types throughout the year, from both the $ET_a$ calculated by SEBS methods when MODIS images were available and $ET_a$ calculated by empirical method based on daily solar radiation when MODIS images were not available. The trend of average $ET_a$ and total $ET_a$ is in reverse direction. Although average $ET_a$ has increasing trend, the total $ET_a$ has decreasing trend. The value of total $ET_a$ during the year 2008 is lower than the year 2000. This is because, during the year 2008, the $ET_a$ contribution in the months of January, February, November and December was low. The $ET_a$ values in the years 2000, 2004 and 2008 ranges from 0.00 mm/day to 13.21 mm/day, 0.50 mm/day to 14.94 mm/day and 1.85 mm/day to 14.02 mm/day respectively. Moreover, the average $ET_a$ for overall study area is 5.17 mm/day, 4.44 mm/day and 5.51 mm/day during the years 2000, 2004 and 2008 respectively. The total $ET_a$ in the years 2000, 2004 and 2008 are 648 MCM (Million Cubic metres)/year, 551 MCM/year and 616 MCM/year in the overall study area.

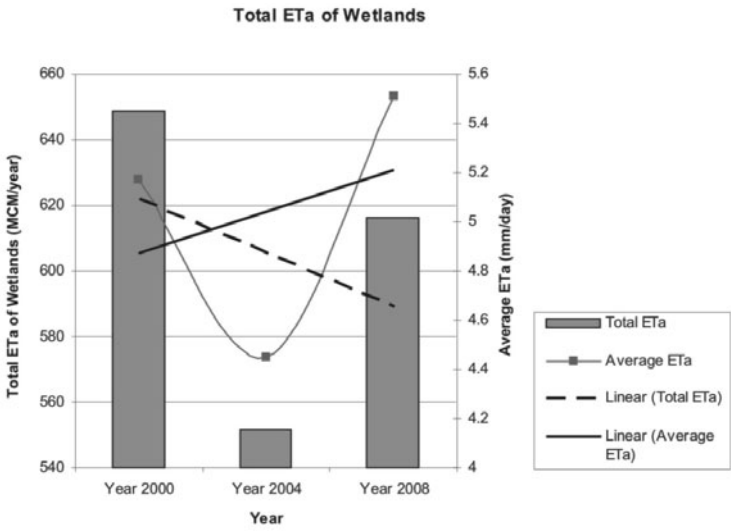


**Figure 4.** Total and average $ET_a$ of the wetlands (MCM is million cubic metre).

Both the rainfall and $ET_a$ have decreasing trend in these wetlands, as there are hydrological inflow and outflow components of the water cycle and area highly correlated. Similar type of relationship has also been studied in Ghana (Kakane and Søgaard, 1997). The $ET_a$ maps of wetlands depict higher $ET_a$ in the summer months as compared to the winter months in overall study area (Fig. 5). However, the annual variation in $ET_a$ for two different years can be seen in Fig. 6.

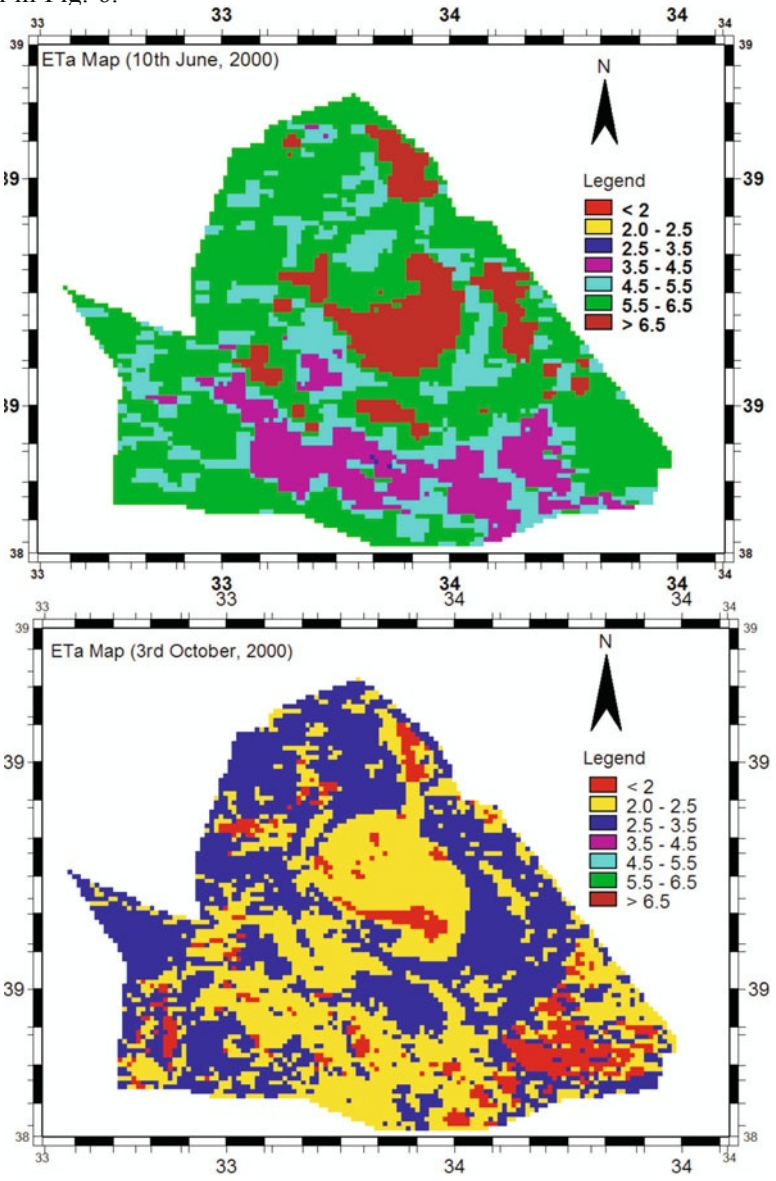


**Figure 5.** $ET_a$ maps of wetlands for 10th June and 3rd October 2000 showing spatial distribution and seasonal variation of $ET_a$ in the study area within a year.

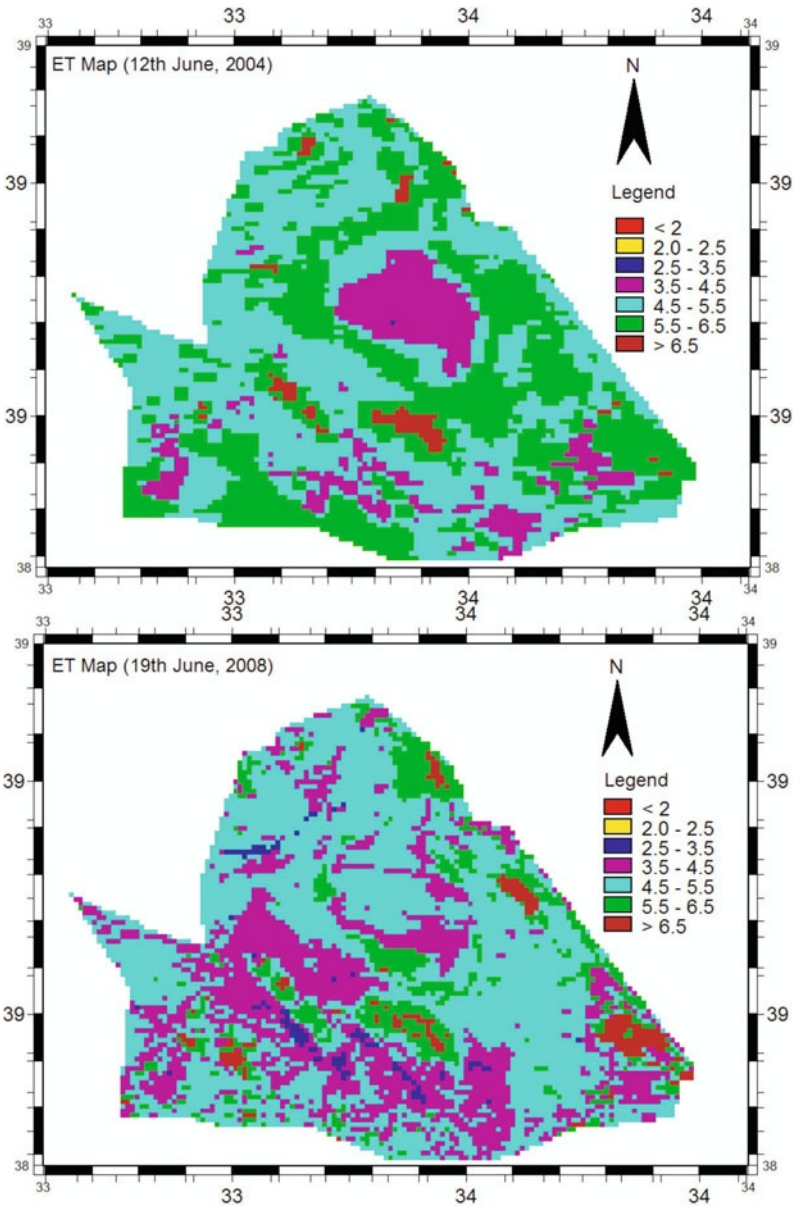


**Figure 6.** $ET_a$ maps of wetlands for 12th June 2004 and 19th June 2008 showing spatial distribution of $ET_a$ in the study area for two different years.

## Validation

The monthly average $ET_a$ and monthly average class A pan evaporimeter estimated evaporation of the study area during the years 2000, 2004 and 2008 are graphically plotted in Fig. 7.

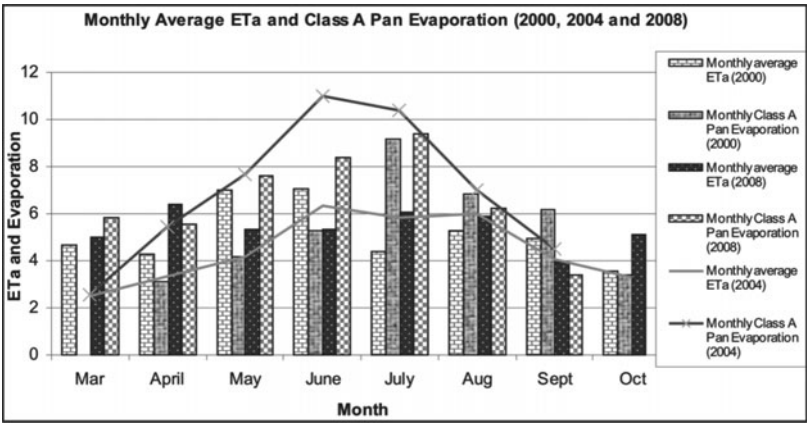


**Figure 7.** Monthly average $ET_a$ and Class A pan evaporations.

The correlation coefficient between $ET_a$ and class A pan evaporation during these years are 22.17%, 85.42% and 33.54% respectively. As the class A pan evaporation indicates only evaporation of the study area, the correlation between these two data sets can be considered good correlation. The similar correlation between evaporation and ET has been studied by Campbell and Sziligyi (Campbell and Phene, 1976; Szilagyi and Jozsa, 2008).

## Conclusion

Evapotranspiration represents a significant component of the water balance in wetland systems. The analysis showed that observed results are strongly dependent on the existing hydrometeorological conditions. This study revealed that the interrelationship among hydrological and ecological variables can be analyzed quantitatively. The hydrological variables like $ET_a$ and rainfall have been analyzed in relation with other hydrometeorological variables and can be used to monitor wetlands dynamics. The major hydrological variables on the basis of inflow and outflow in the water cycle of wetlands system in the semi-arid region was expressed as ET in this study. The ET rate was found to be higher in the basin than the observed rainfall. The analysis shows that surface energy balance system (SEBS) can be used for estimation of $ET_a$ of wetlands. This research can be used for improved understanding of spatial availability of water in the wetlands and in the hydrological cycles.

## Acknowledgement

The author (JKT) is highly thankful to Zoltan Vekerdy, Gabriel Norberto Parodi and Mustafa Gokmen for the guidance throughout the research period, data availability and field visit arrangements at Water Resources Department, Faculty of Geo-information Science and Earth Observation (ITC), Universiteit Twente, Enschede, The Netherlands.

## References

Brutsaert, W. (1999). Aspects of bulk atmospheric boundary layer similarity under free convective conditions. *Reviews of Geophysics*, **37(4)**, 439–451.

Campbell, R.B. and Phene, C.J. (1976). Estimating potential evaporation from screened pan evaporation. *Agricultural meteorology*, **16**, 343–352.

Cox, P., Betts, R., Bunton, C., Essery, R., Rowntree, P. and Smith, J. (1999). The impact of new land surface physics on the GCM simulation of climate and climate sensitivity. *Climate Dynamics*, **15(3)**, 183–203.

Gökmen, M., Vekerdy, Z. and Verhoef, W. (2009). Earth Observation for Quantifying Ecohydrological Fluxes. Paper presented at the European Geosciences Union (EGU) Conference.

Hupet, F. and Vanclooster, M. (2001). Effect of the sampling frequency of meteorological variables on the estimation of the reference evapotranspiration. *Journal of Hydrology*, **243(3-4)**, 192–204.

Jia, L., Yrisarry, J., Ibanez, M. and Cuesta, A. (2003). Estimation of sensible heat flux using the Surface Energy Balance System (SEBS) and ATSR measurements. *Physics and Chemistry of the Earth, Parts A/B/C*, **28(1-3)**, 75–88.

Jin, X., Wan, L. and Su, Z. (2005). Research on evaporation of Taiyuan basin area by using remote sensing. HAL - CCSD.

Kakane, V.C.K. and Søgaard, H. (1997). Estimation of Surface Temperature and Rainfall in Ghana. *Geografisk Tidsskrift, Danish Journal of Geography*, **97**, 76–85.

Kalmar, A. and Currie, D.J. (2006). A global model of island biogeography. *Global Ecology and Biogeography*, **15(1)**, 72–81.

Maidment, D.R. (Ed.). (1993). Handbook of Hydrology: McGraw-Hill Professional.

Massman, W.J. (1999). A model study of kBH-1 for vegetated surfaces using localized near-field Lagrangian theory. *Journal of Hydrology*, **223(1-2)**, 27–43.

Mitsch, W.J. and Gosselink, J.G. (Eds.). (1993). Wetlands (Second ed.): Van Nostrand Reinhold, New York.

Moran, M., Clarke, T., Inoue, Y. and Vidal, A. (1994). Estimating crop water deficit using the relation between surface-air temperature and spectral vegetation index. *Remote Sensing of Environment*, **49(3)**, 246–263.

Nemani, R.R. and Running, S.W. (1989). Estimation of Regional Surface-Resistance to Evapotranspiration from Ndvi and Thermal-Ir Avhrr Data. *Journal of Applied Meteorology*, **28(4)**, 276–284.

Noilhan, J. and Planton, S. (1989). A simple parameterization of land surface processes for meteorological models. *Monthly Weather Review*, **117(3)**, 536–549.

Qin, C., Jia, Y., Su, Z., Zhou, Z., Qiu, Y. and Suhui, S. (2008). Integrating Remote Sensing Information into a Distributed Hydrological Model for Improving Water Budget Predictions in Large-scale Basins through Data Assimilation. *Sensors*, **8(7)**, 4441–4465.

Reynolds, J.F., Kemp, P.R. and Tenhunen, J.D. (2000). Effects of long-term rainfall variability on evapotranspiration and soil water distribution in the Chihuahuan Desert: a modeling analysis. *Plant Ecology*, **150(1)**, 145–159.

Sandholt, I., Rasmussen, K. and Andersen, J. (2002). A simple interpretation of the surface temperature/vegetation index space for assessment of surface moisture status. *Remote Sensing of Environment*, **79(2-3)**, 213–224.

Shukla, J. and Mintz, Y. (1982). Influence of land-surface evapotranspiration on the earth's climate. *Science*, **215(4539)**, 1498.

Singh, S.K., Thakur, J.K. and Singh, U.K. (2010). Environmental Monitoring of Land cover/land use change in Shiwalik Hills, Rupnagar District of Punjab, India using Remote Sensing and Ancillary data. Paper presented at the International Conference on Global Climate Change.

Srivastava, P.K., Majumdar, T.J. and Bhattacharya, A.K. (2009). Surface temperature estimation in Singhbhum Shear Zone of India using Landsat-7 ETM+ thermal infrared data. *Advances in Space Research*, **43(10)**, 1563–1574.

Stewart, J.B. (1989). On the use of the Penrnan-Monteith equation for determining area! évapotranspiration. Paper presented at the Estimation of Areal Evapotranspiration Vancouver, B.C., Canada.

Su, H., McCabe, M.F., Wood, E.F., Su, Z. and Prueger, J.H. (2005). Modeling Evapotranspiration during SMACEX: Comparing Two Approaches for Local and Regional-Scale Prediction. *Journal of Hydrometeorology*, **6(6)**, 910.

Su, Z. (2002). The Surface Energy Balance System (SEBS) for estimation of turbulent heat fluxes. *Hydrology and Earth System Sciences*, **6**, 85–100.

Su, Z. and Jacobs, C. (2001). ENVISAT: actual evaporation. BCRS Report 2001: USP-2 Report 2001 01-02, Beleidscommissie Remote Sensing (BCRS) Delft.

Su, Z., Pelgrum, H. and Menenti, M. (1999). Aggregation effects of surface heterogeneity in land surface processes. *Hydrol. Earth Syst. Sci.*, **3(4)**, 549–563.

Su, Z., Yacob, A., Wen, J., Roerink, G., He, Y., Gao, B., Boogaard, H. and Diepen, C.V. (2003). Assessing relative soil moisture with remote sensing data: theory, experimental validation, and application to drought monitoring over the North China Plain. *Physics and Chemistry of the Earth*, **28**, 89–101.

Szilagyi, J. and Jozsa, J. (2008). New findings about the complementary relationship-based evaporation estimation methods. *Journal of Hydrology*, **354(1-4)**, 171–186.

Tektas, A. (2007). Determination of Biological diversity, Biyolojik Çeşitliliğin Tespiti/ Tuz Gölü Projesi: Corporate head office of special environmental protection.

Thakur, J.K. (2010). Eco-hydrological wetland monitoring in a semi-arid region (A case study of Konya Closed Basin, Turkey). Faculty of International Institute for Geo-Information Science and Earth Observation (ITC), Universiteit Twente, Enschede, the Netherlands.

Thakur, J.K. and Singh, S.K. (2010). Eco-hydrological monitoring of wetlands in a semi-arid region using remote sensing, GIS, GPS and various data sets: a case study of Konya closed basin, Turkey. Paper presented at the IAH 2010.

Thakur, J.K., Singh, S.K. and Diwakar, J. (2011). Estimation of actual evapotranspiration (ETa) using Surface Energy Balance System (SEBS) and remote sensing approach for Water Resources Management of Wetlands in Semi Arid region. Paper presented at the Sustainable Water Resource Management and Treatment Technology, Nagpur, India.

Thakur, J.K., Srivastava, P.K., Singh, S.K. and Vekerdy, Z. (2011). Ecological monitoring of wetlands in semi-arid region of Konya closed basin, Turkey. Regional Environmental Change (DOI: 10.1007/s10113-011-0241-x).

van der Kwast, J., Timmermans, W., Gieske, A., Su, Z., Olioso, A., Jia, L., Elbers, J., Karssenberg, D. and Jong, S.de (2009). Evaluation of the Surface Energy Balance System (SEBS) applied to ASTER imagery with flux-measurements at the SPARC

2004 site (Barrax, Spain). *Hydrology and Earth System Sciences Discussions*, **6(1)**, 1165–1196.

Weng, Q., Lu, D. and Schubring, J. (2004). Estimation of land surface temperature-vegetation abundance relationship for urban heat island studies. *Remote Sensing of Environment*, **89(4)**, 467-483.

Wilson, K.B., Hanson, P.J., Mulholland, P.J., Baldocchi, D.D. and Wullschleger, S.D. (2001). A comparison of methods for determining forest evapotranspiration and its components: Sap-flow, soil water budget, eddy covariance and catchment water balance. *Agricultural and Forest Meteorology*, **106(2)**, 153–168.

Yao, A.Y.M. (1974). Agricultural potential estimated from the ratio of actual to potential evapotranspiration. *Agricultural Meteorology*, **13(3)**, 405–417.

Yue, W., Xu, J., Tan, W. and Xu, L. (2007). The relationship between land surface temperature and NDVI with remote sensing: application to Shanghai Landsat 7 ETM+ data. *International Journal of Remote Sensing*, **28(15)**, 3205–3226.

Zeki Camur, M. and Mutlu, H. (1996). Major-ion geochemistry and mineralogy of the Salt Lake (Tuz Gölü) basin, Turkey. *Chemical Geology*, **127(4)**, 313–329.

# Appendix 1

Temperature ($T$ in $^oC$) dependence of saturated vapour pressure ($e_a$ in kPa), its temperature gradient ($\Delta$ in kPa $^oC^{-1}$), together with psychrometric constant ($\gamma$ in kPa $^oC^{-1}$) at standard atmospheric pressure are as follows:

| *T (°C)* | *$e_a$ (kPa)* | *$\Delta$ (kPa °C$^{-1}$)* | *$\gamma$ (kPa °C$^{-1}$)* |
|---|---|---|---|
| 0 | 0.611 | 0.044 | 0.0654 |
| 1 | 0.657 | 0.047 | 0.0655 |
| 2 | 0.706 | 0.051 | 0.0656 |
| 3 | 0.758 | 0.054 | 0.0656 |
| 4 | 0.814 | 0.057 | 0.0657 |
| 5 | 0.873 | 0.061 | 0.0658 |
| 6 | 0.935 | 0.065 | 0.0659 |
| 7 | 1.002 | 0.069 | 0.0659 |
| 8 | 1.073 | 0.073 | 0.066 |
| 9 | 1.148 | 0.078 | 0.066 |
| 10 | 1.228 | 0.082 | 0.0661 |
| 11 | 1.313 | 0.087 | 0.0661 |
| 12 | 1.403 | 0.098 | 0.0662 |
| 13 | 1.498 | 0.104 | 0.0663 |
| 14 | 1.599 | 0.11 | 0.0663 |
| 15 | 1.706 | 0.116 | 0.0664 |
| 16 | 1.819 | 0.123 | 0.0665 |
| 17 | 1.938 | 0.13 | 0.0665 |
| 18 | 2.068 | 0.137 | 0.0666 |
| 19 | 2.198 | 0.145 | 0.0666 |
| 20 | 2.339 | 0.153 | 0.0667 |
| 21 | 2.488 | 0.161 | 0.0667 |
| 22 | 2.645 | 0.17 | 0.0668 |
| 23 | 2.81 | 0.179 | 0.0668 |
| 24 | 2.985 | 0.189 | 0.0669 |
| 25 | 3.169 | 0.199 | 0.0669 |
| 26 | 3.363 | 0.209 | 0.067 |
| 27 | 3.567 | 0.22 | 0.067 |
| 28 | 3.781 | 0.232 | 0.0671 |
| 29 | 4.007 | 0.243 | 0.0672 |
| 30 | 4.244 | 0.256 | 0.0672 |
| 31 | 4.494 | 0.269 | 0.0674 |
| 32 | 4.756 | 0.282 | 0.0675 |
| 33 | 5.032 | 0.296 | 0.0675 |
| 34 | 5.321 | 0.311 | 0.0676 |
| 35 | 5.625 | 0.326 | 0.0677 |
| 36 | 5.943 | 0.342 | 0.0678 |
| 37 | 6.277 | 0.342 | 0.0678 |
| 38 | 6.627 | 0.358 | 0.0679 |
| 39 | 6.994 | 0.375 | 0.067 |

# 5

# Climbing the Water Ladder – The New GIS Approach

**Amos Kabo-bah and Kamila Lis**[1]
College of Hydrology and Water Resources, Hohai University
1 Xikang Road, Nanjing 210098, China
[1]Faculty of Biology and Earth Science, Department of Landscape Geography, Nicolaus Copernicus University in Torun
Gagarina Str. 9, 87-100 Torun, Poland

## Introduction

There are numerous precious natural resources in the world but the only resource which is needed by everybody, by every country, by rich or poor people and by all other living creatures is water. Water therefore becomes very essential part of daily lives. Unfortunately, our water resources have been struggling over the decades to fully reach the required attention it needed by all people around the world. This is because freshwater still faces challenges including increasing scarcity, lack of accessibility to adequate clean drinking water, deterioration of water quality, fragmentation of water management both nationally and globally, decline of financial resources allocation for water development, threat to world peace and security and a continuing lack of awareness of the magnitude of the problem by the decision makers and the public at large. Nations with abundance of freshwater resources can have an economic advantage over those less endowed. For instance most developed nations today enjoy a degree of abundance in renewable freshwater resources compared to developing nations especially in Africa (Abu-Zeid, 1998). The world population of about six billion is projected to double in the second half of this century and majority of this population will be in the developing nations. Unfortunately, developing nations currently face water and sanitation problems and water-borne diseases (Bouwer, 2000; Thakur et al., 2011).

Regardless, all human beings have an inherent right to have access to water of adequate quantity and quality necessary to meet their basic needs (Gleick, 1998). However, this is not always the case as seen in current challenges faced across the world. Water is central to improving of food security but this

J.K. Thakur et al. (eds.), *Geospatial Techniques for Managing Environmental Resources*,
DOI 10.1007/978-94-007-1858-6_5, © Capital Publishing Company 2012

is always complicated by water scarcity especially in regions in Sub-Saharan Africa that are currently hit by water scarcity (Gowing, 2003). There are number of new concepts that attempt to solve this challenge by adopting a principle of "water trade". For instance; water-scarce areas can minimize their use of water by importing commodities that take a lot of water to produce food and electric power from communities or countries that have more water. Water can then be economically shared among those *that have* and *those without* water resources. Since this water is `virtually' embedded in the commodity, it is called virtual water (Allan, 1998).

The world over countries will face serious water shortages with little prospect of having adequate water for their inhabitants. This can be achieved by either moving more water to people or by moving more people to water. Imports of virtual water embedded in food and other commodities may then economically and politically be a very good solution, and probably the easiest way to achieve peaceful solutions to water conflicts (Bouwer, 2000). After the World Summit on Sustainable Development (WSSD) held in Johannesburg in 2002, the international community took an important step towards more sustainable patterns of water management by including, in the WSSD Plan of Implementation, a call for all countries to "develop integrated water resource management and water efficiency plans by 2005", with support to developing countries. From then on, many countries have taken crucial steps to embark on the WSSD target (Jønch-Clausen, 2004). It is believed that sustainable development can be attained if water is managed in an integrated manner, or precisely through Integrated Water Resources Management (Rahaman and Varis, 2005). Savenije and Van der Zaag (2008) in their research on integrated water resources management realised that at least five of the eight Millennium Development Goals (MDGs) require good water management; they cannot be achieved without it.

These current challenges and proposals on best ways of addressing water management in a sustainable manner may be a failure when considering the current prevailing challenges in the water sector. For instance, by 2020, between 75 and 250 million people are projected to be exposed to an increase of water stress due to climate change in Africa; increase flooding and water scarcity in Asia; and inland flooding and more coastal flooding in nearly all European regions. Increases in temperature and associated decreases in soil water are projected to lead to gradual replacement of tropical forest by savannah in eastern Amazonia and loss of biodiversity through species extinction in many areas of tropical Latin America (IPCC, 2007).

The scale of water challenges and associated impact on people are more national and global as discussed previously. Therefore, the required actions too must also follow similar trend in order to address the use and management of water in a more efficient manner. The fast growing computer age, gives us a huge opportunity to better understand our water challenges in large scales. Geo-information Systems (GIS) together with space technology has shown

the enormous advantage in the understanding of the dynamics of natural resources including water resources. The only disadvantage to this technology in the past was that it was limited to few professionals and few commercial organisations. With the growing new trend, this technology can be used by any body in any part of the world. In fact, GIS is becoming a technology just like 'mobile phones'. To further facilitate this technology towards efficient understanding of the dynamics of our water resources, this chapter introduces two technologies that can greatly support water use and management; and also greatly improve the knowledge of grass root communities across the world to better understand their resource base. The authors believe that when grassroots better understand their environment and water associated challenges as spelt out in IPCC, 2007, they can within their own capacity develop coping strategies to adapt to these situations. In so doing better adoption of IWRM and Climate Change policies spelt out in the various protocols such as Kyoto and various conferences on Climate Change would be attained.

This chapter considers that to be able to clearly understand the crucial role water has in our lives, we need to adopt step by step approach to understand the complex water ecology. This step by step approach can better be achieved through the use of low cost technologies to inform people properly about what resources they have and what they can do with it. The chapter, therefore, presents two technologies: GEONETCast initiative and use of Public Participatory GIS as a way of better understanding what we have as water resource. The authors believe there are other green initiatives such as rainwater harvesting but concentrates on these new methods which promise huge opportunities for communities across the world.

## Water Resources – Issues and Challenges

Water is central to the achievement of MDGs as identified by Savenije and Van der Zaag (2008). It therefore means that significant progress towards the MDGs target implies a relative impact too on adequate water provision and sound water management. Some reports indicate significant improvements towards the meeting of the MDGs throughout east Asia and south Asia. However, there are huge disparities from continent to continent. Sub-Saharan Africa is in pervasive crisis, with rising extreme poverty, shockingly high child and maternal mortality, and many countries in the region are failing to meet most of goals of the MDGs. Additionally, Latin America, the Middle East, and north Africa have made little headway in reducing the rates of extreme poverty in recent years. Even Asia remains home to hundreds of millions of people living in extreme poverty. Virtually all countries are failing in the goal of achieving environmental sustainability, and most lag severely on the goals for gender equality and maternal mortality (Sachs and McArthur, 2005; Thakur, 2010; Thakur et al., 2011). In next five years when world leaders assess the progress that has been made in meeting the commitment enunciated in the Millennium Declaration of 2000 and encapsulated in the

eight Millennium Development Goals (MDGs), more emphasis need to be laid on how best water provision, use and management can be better enforced to ensure that the MDGs are met (MDG, 2010).

Though significant effort has been made by many organisations and individuals the world over, our world's fresh water is still under critical state. Throughout the world, the challenge of *too little water*, *too much water* and *too dirty water* continue to be one of the biggest challenges by communities and governments in various countries. As described in Fig. 1, these problems are often encapsulated by international and national agenda to become more economically powerful or are as a result of cultural and social norms of the country. The impact of natural phenomenon such as climate change also worsens the existing conditions of this three-pillar water paradigm. As identified by Abu-Zeid (1998), the following issues continue to be a core of problems still faced by various nations:

a. *Water scarcity:* Fresh water available for human consumption, for social, economic and cultural needs and for environmental requirements is rapidly becoming scarcer. In the 1950s, only a handful of countries faced water shortages. In the late 1990s, the number of countries facing a water deficit has grown to 26 with a total population of 300 million. It is predicted that two-thirds of the world's population will face water shortages in one form or another by the year 2050. Food production which consumes 70% of the world's fresh water is at risk if no measures are taken.
b. *Lack of accessibility to clean drinking water and sanitation:* Despite international efforts over the last decades, approximately 1.2 billion people lack access to clean drinking water, 2.2 billion lack adequate sanitation and four billion do not have sewerage service. Those most affected are particularly the poor (especially women and children).

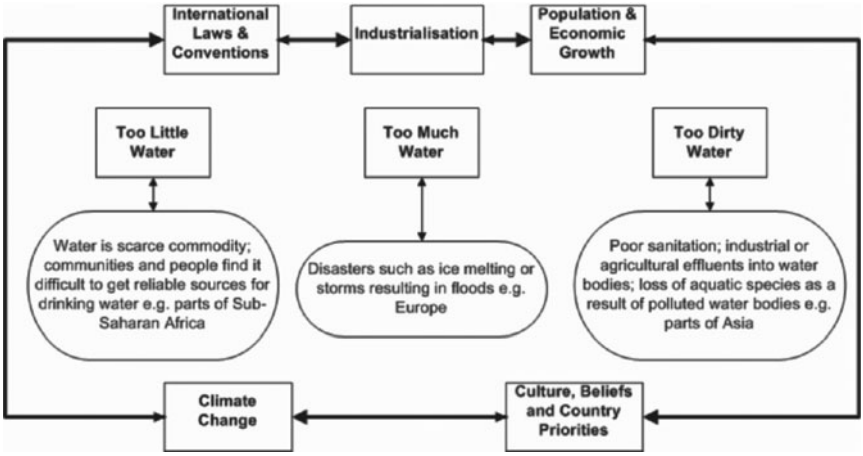


**Figure 1.** Simplified water problems and challenges likely to be faced by any country.

c. *Water quality problems:* Rapid industrialization, urbanization, the growth of mega-cities and the intensification of agriculture at the expense of the environment and water bodies result in highly polluted water rivers, lakes and streams. The impact of this on the human health and aquatic life is immeasurable.
d. *Decline of financial resources allocation and fragmentation of water management:* Addressing the water problems and challenges require significant financial investments. However, there is a steady decline in financial allocations to water projects since 1980s. Developing countries in particular suffer this decline. Apart from this problem, there has been enormous growth of various institutions e.g. Non-Governmental Organisations (NGOs) and others all working towards the goal of water use in a more efficient manner. As a result of the fragmentation of institutions nation-wide and globally, it is difficult to consolidate efforts towards efficient use of financial resources for water resources management.
e. *Lack of awareness by decision-makers and the public:* Water over the years has been taken for granted as being abundant and of good quality. This wrong perception continues to persist and more work is needed to properly educate all people to understand and then to reverse this phenomenon. This chapter therefore seeks to address this situation as a way of bringing to fore some tools that can enhance the understanding of the dynamics of our water resources. This will help educational institutions, professional associations and NGOs to incorporate the simple techniques into their working programmes and framework for better understanding of water issues and pending crises.
f. *Fragile world peace and security:* Water is the foundation of our very existence and the socio-economic foundation of society and its environment. The decline of its availability is a threat to peace and security to many parts of the world. It so happens that most countries facing water shortages also suffer from political instability, social tension and public unrest. National and international trans-boundary water conflicts are on a time bomb ready to explode at any moment.

As discussed the water problems are complicated and interlinked with various sectors of social and economic development. The issue of social learning and the importance of the involvement of informal sectors become very important towards this. As noticed by Pahl-Wostl et al. (2007), social learning and participation of informal actors is key to the implementation of integrated water policies and programmes in an eco-friendly manner. The next sections of this chapter look on how efforts from GEONETCast (http://www.earthobservations.org/geonetcast.shtml) and PPGIS can become an integral part of water management.

## GEONETCast Initiative

*Background*

Geographic Information Systems (GIS) have evolved as an important ingredient for socio-economic development and growth. Though there exist traditionally various forms of mapping systems since the 1960s, GIS technology evolved since the early 1980s has been growing rapidly. The potential of this technology to provide planners with up-to-date, reliable information about water resources and environment in small and large scale is eminent (Madon and Sahay, 1997). Various GIS-based multivariate applications for water resources and land suitability assessment with a public participation base have been developed over the years (Bojórquez-Tapia et al., 2001). In addition, numerous Decision Support Systems (DSS) developed for water resource management have been widely recognised. There is growing knowledge of the links between watershed components and advanced watershed simulation models (Mysiak et al., 2005).


**Figure 2.** Societal benefits of Global Earth Observation System of Systems. (*Source:* http://www.earthobservations.org/geoss.shtml)

Originally the use of real-time earth observation data, in combination with other geospatial ground information to inform society and public, have been used for many years by meteorological services for weather reporting and forecasting. Internet-based search engines and on-line communication media are also strongly contributing to an increased use of earth view, mapping and other geospatial end-user services. The Group on Earth Observation (GEO) is leading a worldwide effort to extend the use of near-real time Earth

Observation combined with i*n situ* ground data to a broad array of societal benefit areas, including climate, weather, water, health, energy, disasters, agriculture, biodiversity and ecosystems (Mannaerts et al., 2009). This initiative is called the GEONETCast Initiative. This is a global data dissemination system to deliver near-real time Earth observation (EO) and *in-situ* data and products derived from the Global Earth Observation System of Systems (GEOSS) to the user community. The information is relevant for policy formulation and management decision making and is covering the full range of societal benefit areas. Backbone of the data dissemination system is EUMETCast, already used globally by the meteorological organizations for near real-time data reception using low cost ground receiving stations. Large volumes of data are broadcasted and received using this one-way dissemination system. Delivery of self-training packages to users operating a ground reception system is currently possible using the so-called "training-channel" on EUMETCast (Ben Maathuis and Mannaerts, 2009).

The last two decades have shown an important shift towards stand-alone software systems to networked ones, often client/server applications using distributed geo- (web-) services. This allows organisations to combine without much effort their own data with remotely available data and processing functionality. Another important aspect of an integrated spatial data analysis is a low-cost access to data from within user-friendly and flexible software. Web-based open source software solutions are more often a powerful option for developing countries. The Integrated Land and Water Information System (ILWIS) is a PC-based GIS and Remote Sensing software, comprising a complete package of image processing, spatial analysis and digital mapping and was developed as commercial software from the early nineties onwards. Fortunately, recent project efforts have migrated ILWIS into a modular, plug-in-based open source software, and provide web-service support for OGC-based web mapping and processing. The core objective of the ILWIS open source project is to provide a maintainable framework for researchers and software developers to implement training components, scientific toolboxes and (web-) services. The latest plug-ins have been developed for multi-criteria decision making, water resources analysis and spatial statistics analysis. The development of this framework is done since 2007 in the context of 52°North, which is an open initiative that advances the development of cutting edge open source geospatial software, using the GPL license. GEONETCast makes available satellite images via Digital Video Broadcast (DVB) technology (see Fig. 3). An OGC WMS interface and plug-ins which convert GEONETCast data streams allow an ILWIS user to integrate various distributed data sources with data locally stored on the machine (Lemmens et al., 2009).

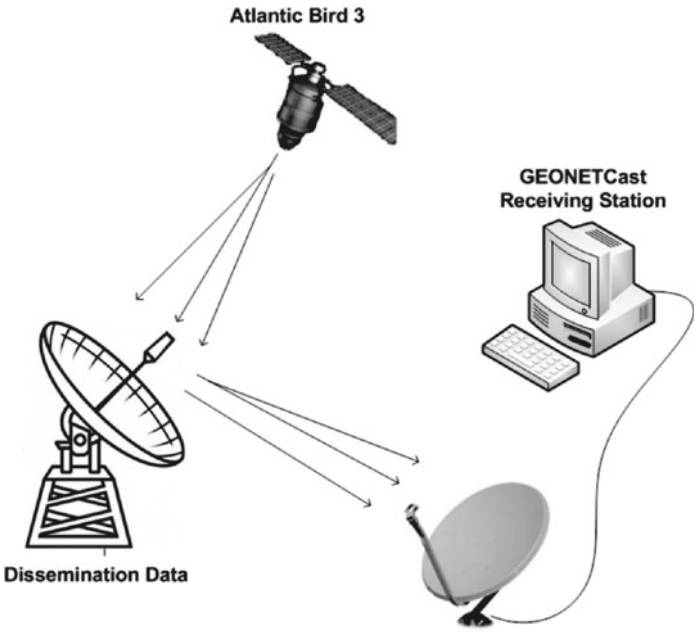


**Figure 3.** GEONETCcast Conceptual Set up.

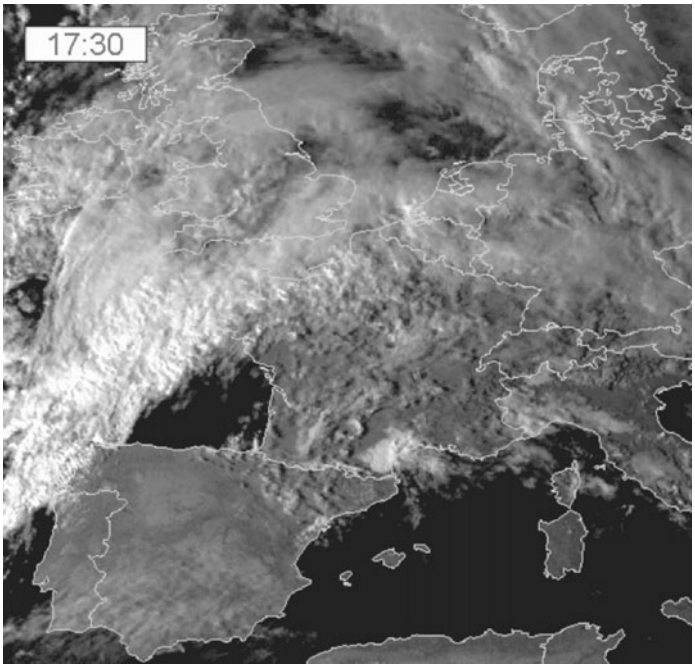


**Figure 4.** Weather on 3 October 2010 in Europe. © EUMETSAT. (http://www.itc.nl/GEONETCast-General-information)

### *Setup and Some Applications*

The EUMETCast service for Europe is based on Ku-band transmissions and is only guaranteed to cover the EUMETSAT Member States and Co-operating States. The dissemination service for Africa is a C-band based transmission also covering selective regions outside the EUMETSAT Member States and Cooperating States and recently even an extension of this service to South America has commenced. For Africa the EUTELSAT AtlanticBird-3 satellite carries the C-Band dissemination service for MSG. The format of the C-band dissemination is the same as for HotBird-6 dissemination. The data is re-transmitted to AtlanticBird-3 via the Fucino ground station in Italy. C-Band covers the frequencies 3.70 GHz to 4.2 GHz. The EUMETSAT Council decided to use EUTELSAT's AtlanticBird-3 satellite for the C-Band dissemination of MSG data to Africa as this frequency is less susceptible to intensive rainfall as it causes attenuation of the Ku-band signal which might result in reception failure.

This satellite is stationed at 5° West and is one of EUTELSAT's 'Atlantic Gate' series of satellites. The C-band beam used covers the whole of Europe and Africa. All of Europe and Africa – apart from parts of Morocco, southern Algeria, Mali and Niger – lie within the 39 dBW contour of the footprint. For the areas outside the 39 dBW, a larger diameter antenna is required (of three metre) for good signal reception in Africa (B Maathuis et al., 2006). For more information on installation procedure, the reader is referred to various documents available at http://52north.org/communities/earth-observation/overview.

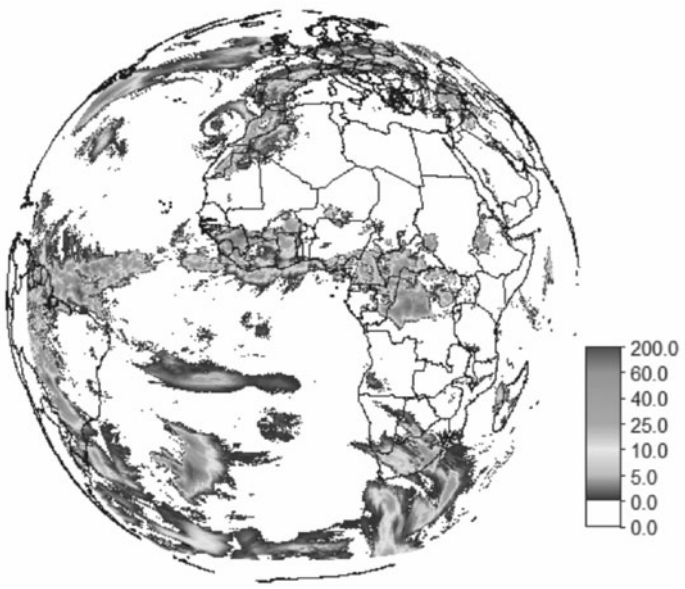


**Figure 5.** MPEF-Multi sensor precipitation estimate for June 16, 2009.

With the GEONETCast operational workstation fully working various products could be obtained. A brief description of some of the products is given in this chapter. Through the Meteorological Product Extraction Facility, automatically other relevant meteorological products are extracted using the GEONETCast Toolbox, the option "MPEF". The sub menu is providing seven import routines of various products that are generated by MPEF and disseminated through GEONETCast. Figure 5 is the MPEF-Multi Sensor Precipitation Estimate (MPEG) product derived from this system. This product is derived from individual products obtained at every 15 minutes. The aggregated product is then the total precipitation for the entire globe for that day. This not only creates a huge opportunity for all organisations working in the area of water and environment to only depend on information from meteorological departments but also have their own spatial datasets that can be used for their planning and monitoring of weather conditions.

Another product is the MPEF-Atmospheric Motion Vectors (AMV) which gives information on pressure, wind direction, wind speed and temperature extracted from the original file (see Fig. 6). There is an extracted table file which gives detailed information about all these parameters. This information is obtained every 15 minutes. Near-real time monitoring of AMV can be done and this could be combined with other data sets such as MPEG to better phantom our understanding of stormy weather conditions and floods.

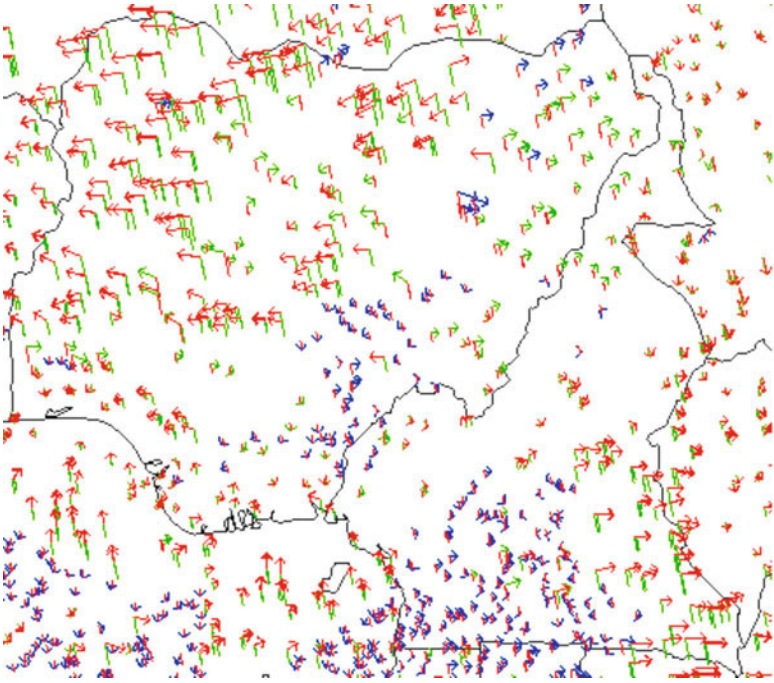

**Figure 6.** AMV map for parts of Nigeria and Cameroon.

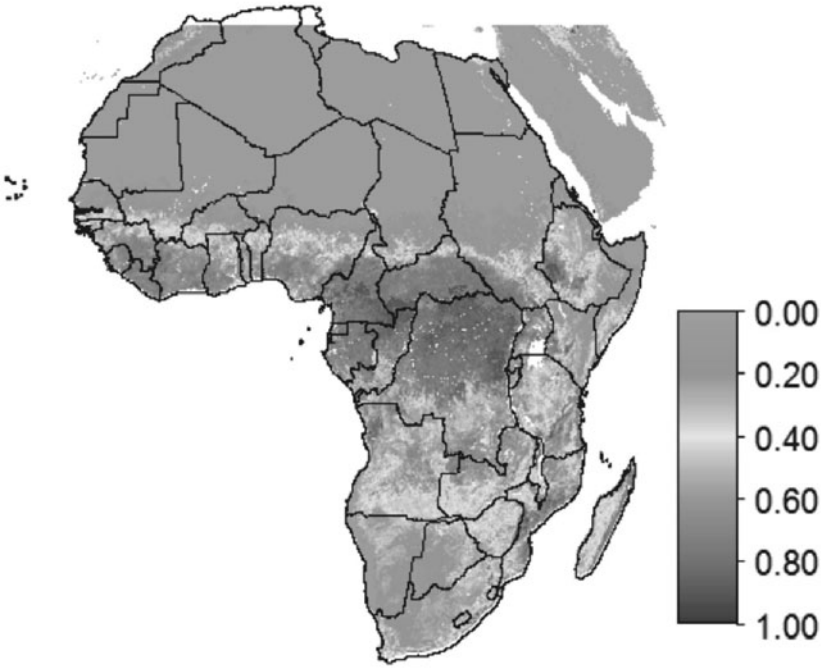


**Figure 7.** LSA SAF-Fraction of Vegetation Cover (FVC) for Africa on June 13, 2009.

Satellite Application Facilities (SAFs) are specialised development and processing centres within the EUMETSAT Applications Ground Segment. In the GEONETCast Toolbox you will find four menu items: "SAF Africa", "SAF Euro", "SAF South America" and "SAF SST MSG-GOES Combined". More detail description about these products can be obtained from the user manual of the GEONETCast toolbox. Figure 7 is one of these products for fraction of vegetation cover (FVC) for Africa obtained on the June 13, 2009 (see Fig. 7).

In water resources management, modelling and understanding the surface energy balance is important for assessing the re-distribution of moisture and heat in soil and atmosphere. The Surface Energy Balance System (SEBS) estimates turbulent heat fluxes using satellite earth observation data in the visible, near-infrared, and thermal spectral domain (B. Z. Su, 2009; Z. Su, 2002; van der Kwast and de Jong, 2004). SEBS is made up of two sets of tools for the determination of the land surface physical parameters, such as albedo, emissivity, temperature, vegetation coverage etc. from spectral reflectance and radiance; air pressure, temperature, humidity, and wind speed at a reference height can all be derived from GEONETCast toolbox. In a simple application, the GEONETCast toolbox was used to derive all the input requirements for SEBS to compute the daily evapotranspiration for Zambia region (see Fig. 8).

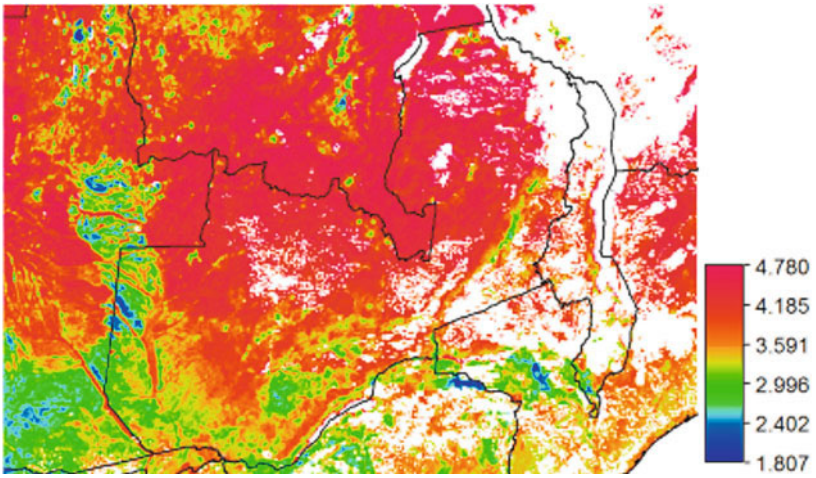


**Figure 8.** Daily evapotranspiration for Zambia.

Here we have presented few products and an application, but the toolbox gives the derivation of several products. These data sources can be applicable for various sectoral operations ranging from meteorological to water resources management. It is hoped that organisations be signed up for this system and begin to use this to understand the spatio-temporal variation of water-land use dynamics in their environment. This system, because of its low cost nature and full operational support from 52 North organisation (www.52north.org), can greatly help the communities and institutions across the world to better appreciate the complex dynamics in their environment. In this case, land surface temperature maps, land cover maps, humidity maps etc. could be combined in the same window to better understand the inter-relationship. Another important feature of this system of GEONETCast and ILWIS is that, information processed can be viewed in near-real time and displayed via a map service. Therefore processed information by organisations, individuals and communities can easily be shared with the larger community worldwide.

Also the availability of 3G-Network, providing wireless accelerated data speeds and simultaneous voice and data capabilities, offer new possibilities for Distance Education and E-Learning in Africa and other developing countries across the world. With relatively cheap 3G enabled modem or mobile phone, connected to a computer or laptop, larger bandwidth is obtained which can be utilized for these types of training activities, irrespective of available fixed network infrastructure. Through this community (http://52north.org/communities/earth-observation/overview), users share ideas and products and new applications developed from using the application. All tools and utilities to support the GEONETCast-Community are also available via this web address (Ben Maathuis and Mannaerts, 2009). As technology advancement in developing countries keep improving everyday, it implies that internet

availability will also become more accessible also. Therefore, the future of GEONETCast will be possible to extend to the remotest of places in developing countries as long as internet facilities are available and also specific ground stations are installed in every country. Technologies are changing very fast. The authors are optimistic that somehow in the future, users might not require the installation of a workstation before they can have access to data via GEONETCast. If that be the case, the availability of internet will be enough to allow users across the world to download data for free.

## Public Participatory GIS

The term Public Participatory GIS (PPGIS) originated at two meetings of the National Centre for Geographic Information and Analysis (NCGIA) as attendees struggled to frame the next generation of GIS that would ground technical advancements in social and political contexts. These meetings reported on a growing affinity of GIS practitioners with developing applications that "empower less privileged groups in society" and attendees declared that the next generation of GIS should be more inclusive to non-official voices. Multiple perspectives have illustrated that PPGIS is a highly localized activity, permeated with culture and socio-political influences. Systems developed in the United States may be employed in developing countries, in which the pre-existing group relationships, available skill levels, and technological infrastructure are markedly dissimilar. A PPGIS must now consider specific contexts, stakeholders and other actors, as well as the general public (Obermeyer, 1998; Sieber, 2006). PPGIS has become an upcoming practice, developing out of participatory approaches inherit to usual planning and spatial information and communication management (Rambaldi and Weiner, 2004). PPGIS means that vulnerable and disadvantaged groups in society enhance their capacity in generating, managing, analysing and communicating spatial information (Rambaldi et al., 2006).

The number of people impacted by natural hazards is showing an upward trend. More people are displaced and put into health risk from floods, earthquakes and drought. Humanitarian actors seek to reduce these risks through development strategies and community-based exercises to assess and improve the understanding of disaster risk in communities. To be able to do this, an accurate and extensive information from which communities might make decisions, and plans for, is required (Kemp, 2008). One of the best ways to do this is the use of Participatory mapping tools such as the PPGIS. PPGIS has become the most unique way to successfully incorporate local knowledge, participatory needs assessment and problem analysis, local prioritizing, and understanding responses and coping strategies (McCall, 2008). This makes it very useful tool also to understanding local dynamics with regard to the climate change studies (Pradhan, 2009).

PPGIS is a fast growing field of research that focusses on the use of GIS by the general public. PPGIS is an abbreviation which indicates that public

needs to be supported when addressing community based problems, since a variety of perspectives are common in different planning processes. PPGIS seeks to expand the use of GIS to the general public and non-governmental organizations that are not usually represented in traditional top-down GIS projects (Steinmann et al., 2004). PPGIS has been used in some communities around the world to successfully map natural disaster risk prone areas, forest mapping, customary land tenure systems, land use dynamics and community resource in many countries globally (Green, 2010; Harwell, 2000; Jordan, 1999; Kabo-bah et al., 2010; Sedogo and Groten, 2000). For instance, in Burkina Faso, PPGIS was used to enlighten competing perspectives and conflicting interests of local groups. In Ghana, PPGIS is being used to map vulnerable risk zones in Northern Ghana. In Nepal, PPGIS was developed, applied and evaluated to determine its potential to assist village communities in the management of their communal forest resource. In Indonesia, GIS was used as the medium for competing accounts of fire disasters in 1998. In Scotland, PPGIS was used to evaluate the legitimacy in decision making in public participation in coastal management and waterfront development. Few sample cases have been presented here but it is obvious that the list is not exhaustive enough to provide the wide range of acceptability and applicability of PPGIS as an innovative tool towards resource management and conflict resolution and management.

The most important aspect of PPGIS is the ability to communicate meanings about the fragile space in which people are trying to live their lives by combining complex technologies with local knowledge. Research conducted by Gonzalez (2002) reveals the impact on poor farmers to engage in knowledge interaction with others in analyzing the space. In this study, interpretation of satellite image with the workshop participants demonstrates how a 'common window' was shared in analysing the complex image pixels (Gonzalez, 2002).

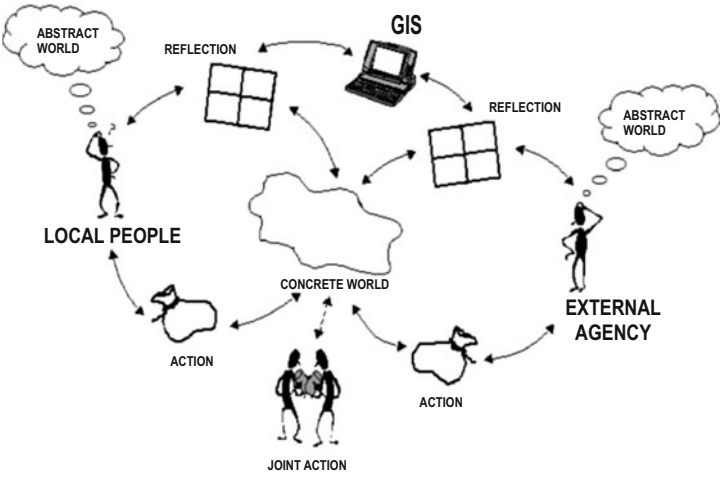


**Figure 9.** PPGIS simplified framework.
(*Source:* Gonzalez, 2002)

In this way, PPGIS has a more people-centred GIS compared to a traditional technocratic, expert-driven tool or methodology (Schlossberg and Shuford, 2005). PPGIS has a critical role in the implementation of IWRM plans, understanding climate change scenarios and better development of coping strategies for communities around the world. PPGIS has in recent past shown that it has capabilities for introducing good governance, by improving dialogue, and using local knowledge, exposing local stakeholders to geospatial analysis and empowerment by supporting community members' participation in decision making and actions and by enabling land use planning decisions (McCall and Minang, 2005).

Regardless of the theoretical feasibility and acceptance of the PPGIS globally, there are some few technical issues which make the complete realisation of the PPGIS a mirage, especially for disadvantaged communities. Most applications currently developed make use of the ArcGIS Desktop and some internet based applications. However, most disadvantaged communities do not have the financial resources and sustainable infrastructure to continuously upgrade the PPGIS products by themselves. This poses, somehow, a sustainable question for the full acceptance of PPGIS for community participation. In other cases also, it is still often quite difficult to involve all of the public in the use of GIS and this can lead to marginalisation of some groups and possibly disengagement from the process (Green, 2010). Therefore, for full realisation of PPGIS in most disadvantaged communities, experts must begin to explore low cost PPGIS techniques. This might include developing applications with more open source GIS and also helping communities to set up their own community based GIS database. This is of course a huge challenge but if vulnerable communities are to be empowered with GIS, we must begin to think of alternative solutions.

As identified by some authors, the future of PPGIS will be dependent on the development of more decision support systems such as the web-based PPGIS (Tan and Ori, 2008) and the use of low cost GIS software. There is however some concern about the integration of PPGIS applications into the Internet which raises some prospects as well as concerns for the future of PPGIS applications among disadvantaged people (Kyem, 2002). As less privileged people are also challenged for internet infrastructure, it means as PPGIS applications via the web increases, these will however have limited use for this group of people. However, as there is also increasing availability of mobile phones among the less privileged people, one option out of this foreseen challenge will be to develop more mobile-based PPGIS applications. In this way, disadvantaged communities can and will be able to benefit from PPGIS applications.

Therefore in trying daily to understand our water problems and challenges in our societies better, it is hoped that with the fast growing GIS sector, methods such as PPGIS should be upheld as one of the techniques in climbing the water ladder to reach our optimum goal of sustainable water development and management around the world. Here, we acknowledge the merits of the

methodology and trust that few case studies, especially for water resources management, will be developed in the coming years.

## Conclusion

Water continues to be a central topic in our daily lives and in our politics in the world for economic growth. With the fast growing GIS sector in most countries, it is important we realise some of the low cost GIS technologies that can upscale the works of professionals in the water sector and also increase the participation of local people in the complete decision making process. This chapter presents two of these technologies; the GEONETCast initiative via the GEONETCast toolbox supported by the 52North organisation and the PPGIS. It is believed that recognition of these tools and methods can help tremendously towards a better understanding of our water resources. With the recent outcry on climate change effects, participation from local communities is very crucial to the holistic mitigation and adaptation measures to be implemented and adopted by various countries. Therefore, the use of low cost GIS and satellite data comes in handy as an answer towards these global issues.

## References

Abu-Zeid, M. (1998). Water and sustainable development: the vision for world water, life and the environment. *Water Policy*, **1(1)**, 9–19.

Allan, J. (1998). Virtual water: A strategic resource global solutions to regional deficits. *Ground Water*, **36(4)**, 545–546.

Bojórquez-Tapia, L., Diaz-Mondragon, S. and Ezcurra, E. (2001). GIS-based approach for participatory decision making and land suitability assessment. *International Journal of Geographical Information Science*, **15(2)**, 129–151.

Bouwer, H. (2000). Integrated water management: emerging issues and challenges. *Agricultural Water Management*, **45(3)**, 217–228.

Gleick, P. (1998). The human right to water. *Water Policy*, **1(5)**, 487–503.

Gonzalez, R. (2002). Joint learning with GIS: multi-actor resource management. *Agricultural Systems*, **73(1)**, 99–111.

Gowing, J. (2003). Food security for sub-Saharan Africa: Does water scarcity limit the options? *Land Use and Water Resources Research*, **3**, 2.1–2.7.

Green, D.R. (2010). The role of Public Participatory Geographical Information Systems (PPGIS) in coastal decision-making processes: An example from Scotland, UK. *Ocean and Coastal Management*, **53(12)**, 816–821.

Harwell, E. (2000). Remote sensibilities: discourses of technology and the making of Indonesia's natural disaster. *Development and Change*, **31(1)**, 307–340.

IPCC. (2007). Climate change 2007: Impacts, adaptation and vulnerability. Contribution of the Working Group II to the Fourth Assessment report of the Intergovernmental Panel on Climate Change.

Jønch-Clausen, T. (2004). Integrated water resources management (IWRM) and water efficiency plans by 2005: Why, what and how. Integrated Water Resources Management (IWRM) and Water Efficiency Plans by 2005. Global Water Partnership.

Jordan, G. (1999). A public participation GIS for community forestry user groups in Nepal: Putting people before the technology.

Kabo-bah, A., Odoi, J. and Lis, K. (2010). Vulnerability Assessment maps for communities in Northern Ghana: Planet Action.

Kemp, R. (2008). Public participatory GIS in community-based disaster risk reduction. *tripleC – Cognition, Communication, Co-operation*, **6(2)**, 88.

Kyem, P.A.K. (2002). Public participatory GIS: A new kind of GIS Application.

Lemmens, R., Maathuis, B., Mannaerts, C., Foerster, T., Schaeffer, B. and Wytzisk, A. (2009). Web-based spatial analysis with the ILWIS open source GIS software and satellite images from GEONETCast.

Maathuis, B. and Mannaerts, C. (2009). Potentials of GEONETCast for Distance Education in EO in Africa. ISPRS TCVI Special Sessions on Education and Outreach Enschede, ITC.

Maathuis, B., Retsios, V., Lasry, F. and Schilling, M. (2006). Installation, setup and use of a low cost C-band meteosat-8 ground receiving station in Rwanda: AARSE, Cairo, Egypt.

Madon, S. and Sahay, S. (1997). Managing natural resources using GIS: Experiences in India. *Information and Management*, **32(1)**, 45–53.

Mannaerts, C., Maathuis, B., Molenaar, M. and Lemmens, R. (2009). The ITC GEONETCast Toolbox: A Geo capacity building component for education and training in Global earth observation and Geo information provision to society.

McCall, M.K. (2008). Participatory Mapping and Participatory GIS (PGIS) for DRR, Community Risk and Hazard Assessment.

McCall, M.K. and Minang, P.A. (2005). Assessing participatory GIS for community-based natural resource management: claiming community forests in Cameroon. *Geographical Journal*, **171(4)**, 340–356.

MDG (2010). Assessing Progress in Africa toward the Millennium Development Goals: ECA, AU, ADB Group and UNDP.

Mysiak, J., Giupponi, C. and Rosato, P. (2005). Towards the development of a decision support system for water resource management. *Environmental Modelling and Software*, **20(2)**, 203–214.

Obermeyer, N. (1998). PPGIS: the evolution of public participation GIS. *Cartogr. GIS*, **25**, 65–66.

Pahl-Wostl, C., Craps, M., Dewulf, A., Mostert, E., Tabara, D. and Taillieu, T. (2007). Social learning and water resources management. *Ecology and Society*, **12(2)**, 5.

Pradhan, B.M. (2009). Making GIS work in Forest management. Geoinformatics for Resource Mapping and Analysis, Pokhara, Institute of Forestry.

Rahaman, M. and Varis, O. (2005). Integrated water resources management: evolution, prospects and future challenges. *Sustainability: Science, Practice and Policy*, **1(1)**, 15–21.

Rambaldi, G., Kyem, P.A.K., McCall, M. and Weiner, D. (2006). Participatory spatial information management and communication in developing countries. *The Electronic Journal of Information Systems in Developing Countries*, **25(1)**, 1–9.

Rambaldi, G. and Weiner, D. (2004). Summary proceedings of the "Track on International PPGIS Perspectives".

Sachs, J. and McArthur, J. (2005). The millennium project: a plan for meeting the millennium development goals. *Lancet*, **365(9456)**, 347–353.

Savenije, H. and Van der Zaag, P. (2008). Integrated water resources management: Concepts and issues. *Physics and Chemistry of the Earth, Parts A/B/C*, **33(5)**, 290–297.

Schlossberg, M. and Shuford, E. (2005). Delineating 'public' and 'participation' in ppgis. *Editors and Review Board*, **16(2)**, 15.

Sedogo, L.G. and Groten, S.M.E. (2000). Definition of land management units for GIS support to participatory planning: a case study on participatory land management in Burkina Faso. *Canadian Journal of Development Studies*, **21** (Special Issue), 523–542.

Sieber, R. (2006). Public participation geographic information systems: A literature review and framework. *Annals of the Association of American Geographers*, **96(3)**, 491–507.

Steinmann, R., Krek, A. and Blaschke, T. (2004). Analysis of online public participatory GIS applications with respect to the differences between the US and Europe.

Su, B.Z. (2009). Introduction to the Surface Energy Balance System (SEBS), ITC, Enschede.

Su, Z. (2002). The Surface Energy Balance System (SEBS) for estimation of turbulent heat fluxes. *Hydrology and Earth System Sciences*, **6(1)**, 85–99.

Tan, Y. and Ori, G. (2008). Web-based public participatory GIS.

Thakur, J.K. (2010). Eco-hydrological wetland monitoring in a semi-arid region (A case study of Konya Closed Basin, Turkey). Faculty of International Institute for Geo-Information Science and Earth Observation (ITC), Universiteit Twente, Enschede, the Netherlands.

Thakur, J.K., Srivastava, P.K., Singh, S.K. and Vekerdy, Z. (2011). Ecological monitoring of wetlands in semi-arid region of Konya closed basin, Turkey. Regional Environmental Change (DOI: 10.1007/s 10113-011-0241-x).

Thakur, J.K., Thakur, R.K., Ramanathan, A., Kumar, M. and Singh, S.K. (2011). Arsenic Contamination of Groundwater in Nepal – An Overview. *Water*, **3(1)**, 1–20.

van der Kwast, J. and de Jong, S. (2004). Modelling evapotranspiration using the surface energy balance system (SEBS) and Landsat TM data (Rabat region, Morocco).

# 6

# Supraglacial Lake Classification in the Everest Region of Nepal Himalaya

**Prajjwal K. Panday, Henry Bulley[1], Umesh Haritashya[2] and Bardan Ghimire**
Clark Graduate School of Geography, Clark University
950 Main Street, Worcester, MA 01610, USA
[1]Central Connecticut State University, 1615 Stanley Street
New Britain, CT 06050, USA
[2]Department of Geology, University of Dayton, 300 College
Park Avenue, Dayton, OH 45469, USA

## Introduction

Climate change has been linked to widespread retreats and recent disappearances of small glaciers in mountainous regions such as the Patagonia, Andes, Alps and Himalaya (Dyurgerov and Meier, 2000; Fujita et al., 2006; Kargel et al., 2005; Oerlemans, 2005; Paul, Kaab et al., 2004; Racoviteanu et al., 2008; Thakur, 2010). Alpine glaciers are particularly sensitive to changes in climate due to their proximity to melting conditions, wide altitude range, and variability in debris cover (Haeberli et al., 2007; Racoviteanu et al., 2008). Alpine glacial retreat in response to climate change and recent warming trends may have severe hydroecological consequences to surrounding communities (Kehrwald et al., 2008; Milner et al., 2009). The recession of glaciers has been further linked to increases in glacier-related hazards in high mountainous areas such as avalanches, glacial lake outburst floods and debris flows which can increasingly threaten human lives, settlements, and infrastructure (Huggel et al., 2002; Quincey et al., 2005). This has necessitated the assessment and monitoring of potentially hazardous glacial lakes through the use of remote sensing, especially in high mountainous areas due to inaccessibility and lack of field surveys (Quincey et al., 2005).

There is a general pattern of glacial retreat and melting in the Nepal Himalayas leading to increased production of glacial melt water and

J.K. Thakur et al. (eds.), *Geospatial Techniques for Managing Environmental Resources*,
DOI 10.1007/978-94-007-1858-6_6, © Capital Publishing Company 2012

development of supraglacial lakes that are potentially hazardous (Fujita et al., 2006; Richardson and Reynolds, 2000; Yamada et al., 1992). An inventory of glaciers and glacial lakes in the Nepal Himalaya indicates increased frequency and magnitude of supraglacial and moraine-dammed lakes in the region (Kargel et al., 2005; Mool et al., 2001). Although remote sensing offers great opportunities in the Himalayas and in areas lacking traditional field-based glaciologic methods, there are challenges and limitations to its use in glacier studies especially in the Himalayan context. Challenges in mapping debris-covered glaciers include limited field validation data, lack of aerial photographs, lack of accurate elevation data for remote glacierized areas, lack of algorithms for automatically discerning debris-covered ice from non-ice areas with debris, and limited capability to discern changes in glacier thickness. These complexities pose several challenges in quantitative characterization of glacier surfaces, glacial lakes and mass balance (Kargel et al., 2005; Racoviteanu et al., 2008). Although aerial photographs have been primarily used for extraction of glacier parameters throughout the early 1970s, availability of aerial photographs have been either limited or restricted for certain areas such as the Himalayas (Racoviteanu et al., 2008). The classification of glaciers remains an important step for any glacier-related assessment and manual digitization remains the most common approach for glacier classification despite the abundance of multi-spectral classification methods (Raup et al., 2007).

Few studies have attempted automated classification in the Himalayan region (Bolch et al., 2008), while most studies have relied on manual digitization (Kulkarni et al., 2007; Kulkarni and Buch, 1991), band ratioing (Bolch, Buchroithner, Pieczonka, et al., 2008), and semi-automated thresholding and classification (Keshri et al., 2009; Paul, Huggel et al., 2004). Delineation of glacial lakes for identification of potentially hazardous lakes are also mostly carried out through manual digitization (Bajracharya et al., 2007) or thresholding using the normalized difference water index (NDVI) (Bolch, Buchroithner, Peters et al., 2008; Huggel et al., 2002). Supraglacial debris poses a major challenge in automatic delineation of glaciers due to the spectral similarity to the surrounding debris (Bolch et al., 2008; Bulley et al., 2011). This further confounds accurate classification of glacial lakes, particularly in the Himalayan region (Bolch et al., 2008; Bolch, Buchroithner, Pieczonka et al., 2008; Racoviteanu et al., 2008; Raup et al., 2007). Supraglacial cover mapping in the Chenab basin through the use of ratios in a systematic fashion resulted in a 91% overall accuracy (Keshri et al., 2009). Bolch et al. (2008) used a morphometry- and temperature-based glacier delineation using ASTER bands and DEM (Digital Elevation Model) in the Khumbu Glacier of Nepal that produced a discrepancy of 5% between the calculated and the manually digitized polygons. The dependence of thresholds in different sensors and seasons (Hall et al., 1995) and the possibility of underestimation or overestimation of cover classes from a slight error necessitate the selection of appropriate threshold values in supraglacial classification (Keshri et al., 2009).

A semi-automated approach to map debris-covered glaciers developed by Paul (2004a) failed when transferred to the Himalayan region (Bolch et al., 2008). It is important to develop a sequential, systematic method for glacier classification that takes spectral characteristics of supraglacial cover into account and delineates potentially hazardous glacial lakes.

Substantial effort has been focussed on the use of spatial information and recently the use of geometric attributes of features such as shape in remotely sensed imagery for improving classification (Frohn, 2006; Frohn and Hao, 2006; Zhou et al., 1995). Land use/land cover features with similar spectral responses but differing shape of spatial properties have been discriminated by the use of shape index (Zhou et al., 1995). Frohn (2006) used a perimeter-to-area shape complexity metric called the Square Pixel Metric (SqP) to differentiate lakes from rivers in Alaska and classify natural vs. anthropogenic pastures in Bolivia. The utility of landscape and shape metrics is yet to be tested in glacier classification where spectral inseparability among features has been a major problem. The SqP used by Frohn (2006) is used here to differentiate supraglacial lakes from other glacier features to improve classification.

This chapter proposes a hybrid approach of glacial lake classification using a non-parametric classification tree model combined with a squared pixel shape complexity spatial metric to differentiate supraglacial cover types and effectively discriminate supraglacial lakes. There have been recent interests in machine learning algorithms (MLA) such as classification trees and regression trees as a response to the limitations posed by multivariate classification algorithms (Hansen et al., 1996; Rogan et al., 2008; Bulley et al., 2008; Bulley et al., 2011). Classification trees involve a binary, recursive partitioning of the data and result in hierarchical trees of decision rules that can be used for classification and have proved superior to conventional classifiers in almost all cases (Rogan and Chen, 2004; Bulley et al., 2008; Bulley et al., 2011). Classification trees can further incorporate ancillary variables in the form of indices, ratios and image-based derivatives that have been used by other studies in glacier classification (Rogan et al., 2008). An initial segmentation using a classification tree is improved by the use of a spatial metric to differentiate supraglacial lakes from other supraglacial features such as shadow, ice, ice cliffs and ice-mixed debris. This chapter demonstrates the utility of this hybrid approach in producing a semi-automated and replicable technique for supraglacial characterization and delineation of glacial lakes rather than using a subjective, statistical thresholding or ratio-based glacier mapping. The value of methods presented in this chapter is demonstrated by its use on a small portion of glaciated regions in the Everest region. Continued glacier recession is expected with increased warming of the atmosphere in the future particularly in the eastern Himalaya and therefore the implication of results presented here can be crucial in terms of monitoring glacier recession and mitigation with regard to consequential increase in glacial lake development.

## Study Area

The Everest region is one of the most glaciated regions in the Nepal Himalayas and is located in the Solukhumbu district in northeastern Nepal (Fig. 1). This region has some of the world's highest peaks including Mt. Everest. Four valleys, the Dudh Kosi, the Bhote Kosi, the Imja Khola and the Lobuche Khola have large valley glaciers at their heads (Stevens, 1993). A total of 194 glaciers were recorded in the early 1970s in this region with Ngojumba, Khumbu and Bhote Kosi being the largest glaciers (Mool et al., 2001). The glaciers in this region are sensitive to summer temperatures while the area is also greatly influenced by the Indian monsoon (Bolch, Buchroithner, Peters et al., 2008). Three glacial lake outburst flood events have been reported in 1977, 1985 and 1998 within this region which have affected human lives and infrastructure (B. Bajracharya et al., 2007; S.R. Bajracharya et al., 2007). Given the reported rates of retreat of glaciers and increase in the number and size of glacial lakes within this region, mapping these for regular monitoring is crucial. In this study, we focussed on the analysis on three glaciers – Bhote Kosi, Ngojumba and Lumsamba.

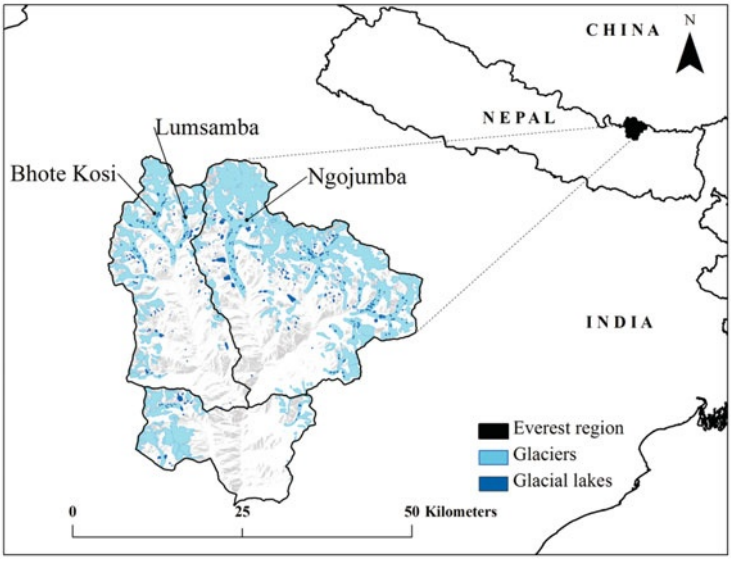


**Figure 1.** Study area showing three glaciers (Bhote Kosi, Lumsamba and Ngojumba) in the eastern Nepal Himalayas.

## Methods

### Satellite Data Processing

ASTER imagery acquired on November 10, 2004 were radiometrically and geometrically calibrated using SILCAST software to produce Level-1B

products (http://www.silc.co.jp). An orthorectified DEM of 15 m spatial resolution was also generated using 3N (nadir-viewing) and 3B (backward-viewing) spectral bands of the ASTER Level-1A VNIR data. The SWIR bands with 30 m spatial resolution were then resampled to 15 m to match the finer spatial resolution of ASTER Level-1B VNIR and DEM datasets. Glacier boundary outlines of Bhote Kosi, Ngojumba and Lumsamba glaciers were obtained from Global Land Measurements from Space (GLIMS—www.glims.org) (Armstrong et al., 2005) and used to clip the respective glaciers from the ASTER imagery to limit the area of analysis for supraglacial characterization.

## Image Derivatives

The ASTER-derived DEM was used to generate first derivatives, slope and aspect. The ASTER, VNIR and SWIR bands were used to compute image band ratios and image indices which have been used in glacier classification (Table 1). The Normalized Difference Snow Index (NDSI) utilizes the spectral properties of snow and ice which has a high reflectance in the visible region and a strong absorption in the SWIR region (Hall et al., 1995). Further, NDSI frequency distribution exhibits a bimodal distribution for a glacier with lower NDSI associated with debris and higher NDSI peak associated with snow, ice and ice-mixed debris (Keshri et al., 2009). A Normalized Difference Water Index (NDWI) was also derived using a green band, which exhibits maximum reflectance of water and near-infrared band which exhibits minimum reflectance of water (Bolch, Buchroithner, Peters et al., 2008; Huggel et al., 2002; McFeeters, 1996). A similar index to indicate the presence of water surface based on a spectral characteristic of water corresponding to stronger absorption in SWIR bands than in VNIR bands was proposed by Suzuki et al. (2007) as calculated from band 2 and band 4 of ASTER imagery. The Normalized Difference Glacier Index (NDGI), as proposed by Keshri et al. (2009), uses difference in spectral characteristics of snow/ice and ice-mixed debris in green and red bands.

## Classification Methodology

The classification tree analysis is non-parametric and structurally explicit allowing interpretations of decision rules that relate thresholds in the predictor variables with pixel classes during partitioning of remote sensing data (Friedl et al., 1999; Lawrence and Wright, 2001). As other machine learning algorithms, CTA is sensitive to quality of training data and the number of training samples per category classified (Rogan et al., 2008; Rogan et al., 2003). Given the limited ground reference data for this region, training pixels for snow, ice, ice-mixed debris, debris, and others that included shadow were selected from within the ASTER scene. Training pixels were assessed for their spectral characteristic using ERDAS Imagine and reference supraglacial cover classes

were assigned on the basis of spectral curve analysis and visual interpretation (Fig. 2). Independent variables to the classification tree were ASTER bands 1-9, band ratios, indices and environmental ancillary data (elevation, slope and aspect) (see Table 1 and Fig. 3).

CTA partitions the remotely sensed data recursively and hierarchically to form homogeneous subsets where the splitting algorithm searches for the variable that best explains the partitioning. The selection of splitting rules in CTA is not a critical factor for overall accuracy of decision-tree-based classification (Zambon et al., 2006). CTA was performed in IDRISI software using gain ratio splitting rule and the trees were pruned by removing leaves with observations less than or equal to a predetermined within class proportion of 1%. Entropy, which provides a measure of how much we know about a

**Table 1.** Input image files used for classification tree analysis

| *No.* | *Variables* | *Description* |
|---|---|---|
| 1 | Green | |
| 2 | Red | |
| 3 | Near Infrared (NIR) | |
| 4 | Shortwave Infrared 1 (SWIR1) | Also Middle Infrared (MIR) |
| 5 | SWIR2 | |
| 6 | SWIR3 | |
| 7 | SWIR4 | |
| 8 | SWIR5 | |
| 9 | SWIR6 | |
| 10 | NIR/Red | |
| 11 | MIR/Red | |
| 12 | MIR/Green | |
| 13 | MIR/NIR | |
| 14 | Normalized Difference Vegetsation Index (NDVI) | (NIR – Red/NIR + Red) |
| 15 | Normalized Difference Glacier Index (NDGI) | (Green – Red/Green + Red) (Keshri et al., 2009) |
| 16 | Normalized Difference Snow Index (NDSI) | (Green – SWIR1/Green + SWIR1) (Hall et al., 1995; Keshri et al., 2009) |
| 17 | Normalized Difference Water Index (NDWI) | (Green – NIR/Green + NIR) (Bolch, Buchroithner, Peters et al., 2008; McFeeters, 1996) |
| 18 | $NDWI_2$ | (Red – MIR/Red + MIR) (Suzuki et al., 2007) |
| 19 | Elevation (m) | |
| 20 | Aspect (degrees) | |
| 21 | Slope (degrees) | |

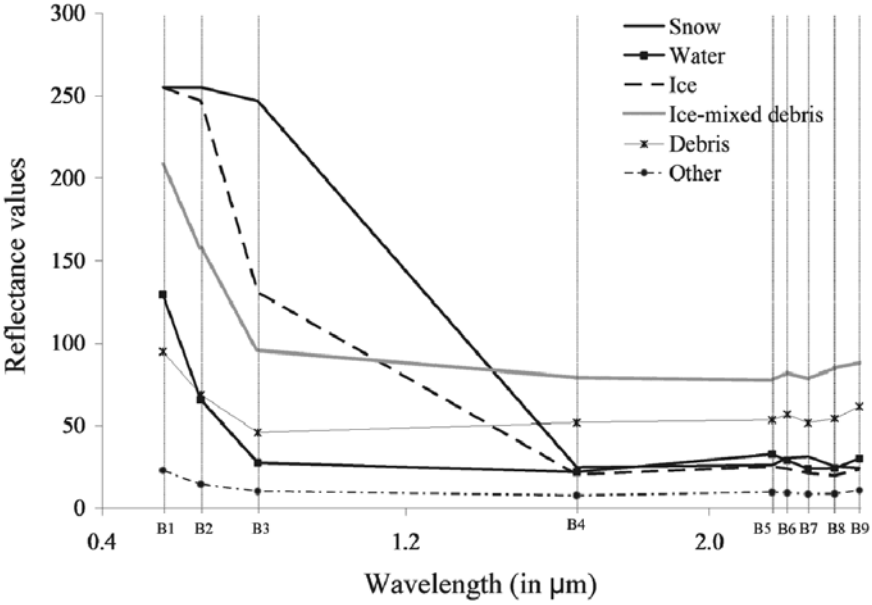


**Figure 2.** Spectral reflectance curves for supraglacial cover types obtained from ASTER data.

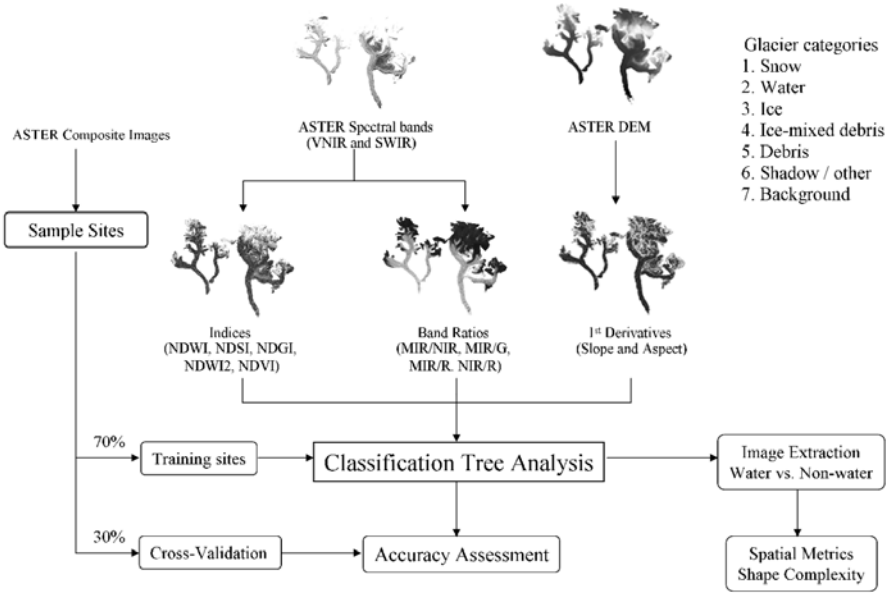


**Figure 3.** Flowchart showing classification of supraglacial cover types using ASTER data.

class, is given by equation (1) where $p_i$ is the relative frequency of class $i$ at node $T$ (Eastman, 2006; Quinlan, 1986; Zambon et al., 2006)

$$\text{Entropy } (T) = -\sum_{i} p_i \log p_i \tag{1}$$

The gain ratio algorithm attempts to overcome the potential bias from the entropy algorithm as every split can contribute to information gain (Quinlan, 1986; Zambon et al., 2006). If we define the split information of a single classification ($X$) as

$$\text{Split info } (X) = -\sum_{i=1}^{n} \frac{|S_i|}{S} \times \log 2\left(\frac{|S_i|}{|S|}\right) \tag{2}$$

Split info ($X$) represents the potential information generated by dividing $S$ (number of pixels in group $S$) into $n$ subsets. Then the information gain measures the information as:

$$\text{Gain Ratio } (X) = \frac{\text{Gain } (X)}{\text{Split info } (X)} \tag{3}$$

where gain ($X$) is defined as the entropy after classification $X$.

CTA was applied for supraglacial cover characterization of three glaciers: Bhote Kosi, Lumsamba and Ngojumba. To address the sensitivity of CTA to variations in training data, the method was conducted with ten random divisions of the reference data into calibration (70%) and validation (30%) data sets and accuracy was measured as average Kappa and overall accuracy over these ten trials. This method was also used as a validation of the CTA output due to lack of any image reference of the study area with a spatial resolution that was higher (i.e., less than) 15 m ASTER data. A statistical error matrix-based approach was used to investigate individual accuracies of each class (Congalton, 1991).

## Shape Complexity Analysis

The Square Pixel Metric (SqP) is a modified perimeter to area ratio scaled to that of a square pixel and normalized from 0-1 (Frohn, 2006).

$$SqP = 1 - (4 \times A^{1/2}/P) \tag{4}$$

where $A$ is the area of the image objects and $P$ is the perimeter of the image objects. Image pixels in the classified image output for three glaciers were clumped and aggregated into features comprising at least four adjacent pixels (900 $m^2$), which was followed by shape complexity analysis using SqP to segregate water and non-water objects. Features classified as water were examined to identify optimal SqP range to avoid confusion of water from shadow and non-water features. Lakes given their simple features tend to have low perimeter-to-area ratios and hence lower SqP values compared to features such as shadows and ice cliffs. Shape complexity analysis was also conducted for features classified as ice to identify potential lakes that may have been frozen.

## Results

ASTER red band is the first variable selected which partitions the data into pixels with low reflectance (water, ice-mixed debris, debris and shadow) and high reflectance (snow and ice) (Fig. 4). The right branch of the classification tree results in the differentiation of snow as higher reflectance and ice as lower reflectance in the NIR region. The second partitioning in the left branch of the tree indicates separation of ice-mixed debris (higher reflectance in the NIR) from lower reflectance classes (water, shadow and debris). This was followed by NDWI, elevation and NIR/Red band ratio splits for separation of water features from debris. This classification had an overall kappa value of 0.98 and overall accuracy of 99% based on the validation through 70:30 split of reference data set for calibration and validation respectively and averaged over ten trials. The error matrix indicates water pixels classified as debris or shadow and also debris confused with shadow. Water pixels have been correctly identified as water with an average accuracy of 96%, while pixels have been correctly classified as debris with an average accuracy of 93%. Most of the misclassification is due to the confusion in discriminating water, debris and shadow classes.

The SqP indicated that lake features have on an average lower SqP values than shadows, allowing water/shadow segregation. This step effectively segregated shadow features misclassified as supraglacial lake features. This step can be further used to minimize misclassification and thereby enhance glacial lake identification. SqP metric can also be potentially used to identify frozen lake surfaces and characterize these as ice features (Fig. 5). Depending on the time the image is taken, surfaces of supraglacial lakes can exist in

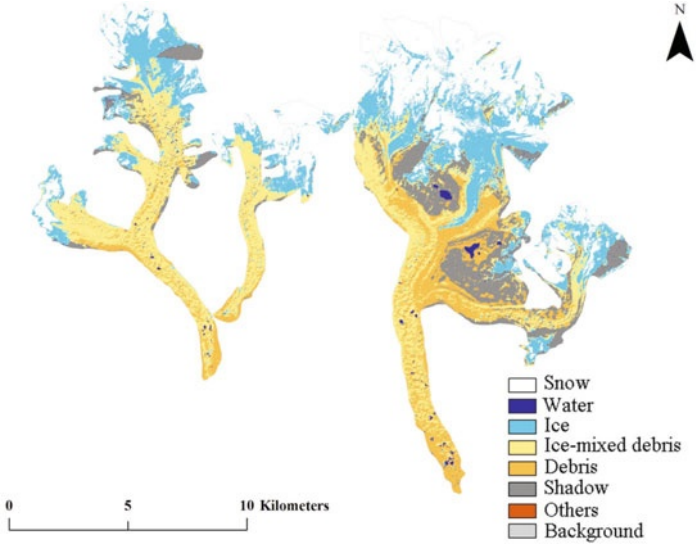


(a)

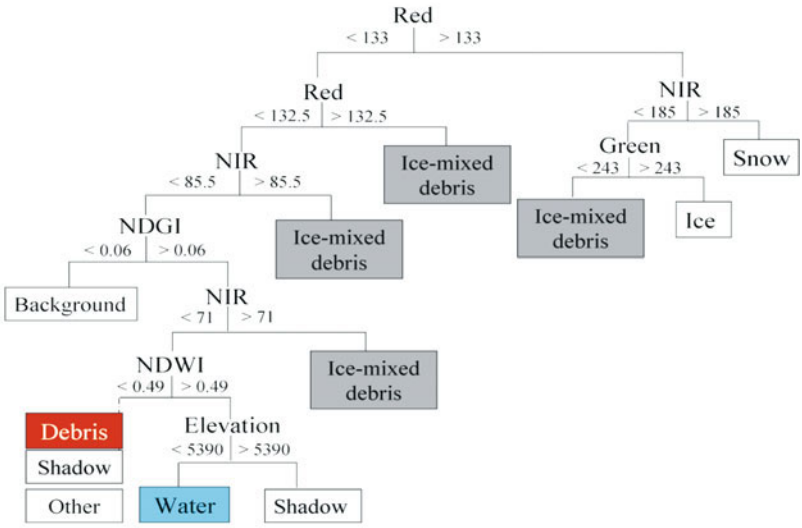


(b)

**Figure 4.** (a) Supraglacial cover type classification using CTA for three glaciers – Bhote Kosi, Lumsamba and Ngojumba and (b) classification tree decision rules of three glaciers showing classified cover types as terminal nodes (in rectangular boxes). (Dashed lines indicate nodes omitted to show the full tree structure).

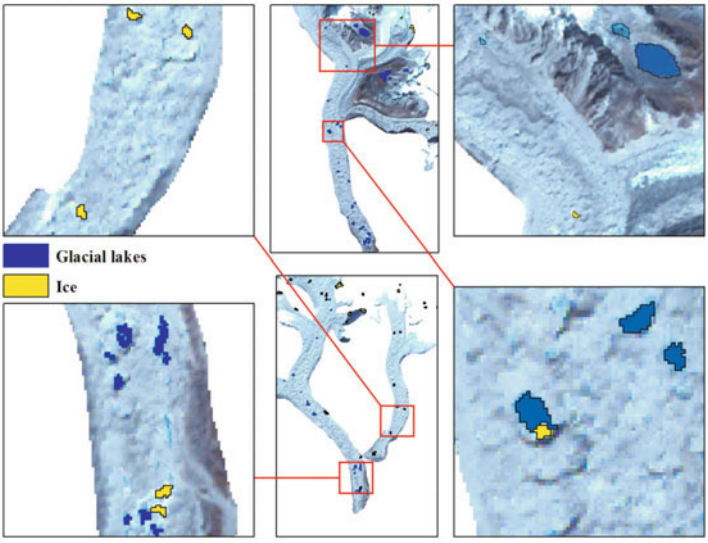


**Figure 5.** Identification of glacial lakes and ice features using shape complexity analysis.

frozen conditions. Further validation and assessment of this supraglacial classification is only possible with ground reference information or available aerial photographs.

## Discussion and Conclusion

The objective of this chapter is to utilize a hybrid approach of classification tree analysis with shape complexity metric thresholds to map supraglacial conditions in the Everest region in the eastern Nepal Himalayas. Distal parts of the debris-covered glaciers which are spectrally very similar to the surrounding environment are difficult to separate. Much of the supraglacial debris along the glacier tongues can be spectrally separated and delineated given the cooling effect from the underlying ice. Bolch et al. (2008a) has shown this to be true in the same region using a morphometric and temperature based glacier mapping method.

CTA is able to utilize ancillary variables such as image based ratios and indices effectively to facilitate classification of glaciers and snow from the surrounding environment. This method is also effective in segregating water from ice and other supraglacial features. A major advantage of classification tree is the ability of the users to investigate the linkage between the dependent variable of class membership and remote sensing data (Rogan et al., 2008). The hierarchical partitioning indicates the dominance of ASTER bands (green, red and near-infrared) in supraglacial characterization and the importance of NDWI in delineating supraglacial water bodies. Furthermore, classification tree analysis is less subjective compared to visual or statistical derivation of threshold values for glacier or supraglacial lake delineation. Rather than selecting particular indices or thresholds for classification, CTA allows the ability to include as many predictor variables to choose the one that best explains the partitioning of the data and hence allows data-derived thresholding.

The results of this study show that supraglacial lake delineation in the Everest region of the eastern Nepal Himalayas using ASTER data is promising. The study has shown that CTA is able to utilize ancillary variables such as image based ratios and indices effectively to facilitate classification of glaciers and snow from the surrounding environment. On the other hand, the shape complexity metric such as SqP was effective in reducing misclassification of glacial lakes. This chapter provides a less subjective methodology of classifying supraglacial cover types and lakes utilizing data-derived thresholds and partitioning to assign class membership. Shadows and debris-covered ice presented a majority of the classification problems in distinguishing glaciers from surrounding environment towards distal parts of the glacier tongues. Glaciers and glacial lakes are delineated using a variety of techniques as described in this chapter. While advanced techniques for better identification is certainly important, it is also essential to maintain consistency in techniques used across an image time series for conducting change analysis. The accuracy in identification of glacial retreat lies in the accuracy of glaciers/glacial lake delineation as well as use of a standardized procedure to do so. This joint approach of glacier delineation using classification tree and shape metric analysis certainly provides a first-order exploration for glacier assessment.

The applicability of proposed method needs to be tested in other glaciated areas around the world in order to extend the work for examining hazard potential of glacier lakes.

## References


Armstrong, R., Raup, B., Khalsa, S.J.S., Barry, R., Kargel, J., Helm, C. and Kieffer, H. (2005). GLIMS glacier database. from National Snow and Ice Data Center Boulder, Colorado USA.

Bajracharya, B., Shrestha, A.B. and Rajbhandari, L. (2007). Glacial lake outburst floods in the Sagarmatha region. *Mountain Research Development*, **27(4)**, 336–344.

Bajracharya, S.R., Mool, P.K. and Shrestha, B.R. (2007). *Impact of climate change on Himalayan glaciers and glacial lakes*. Kathmandu, Nepal: ICIMOD.

Bolch, T., Buchroithner, M.F., Kunert, A. and Kamp, U. (2008). *Automated delineation of debris-covered glaciers based on ASTER data*. Paper presented at the GeoInformation in Europe (=Proc. 27th EARSeL-Symposium, 4.-7.6.07, Bozen, Italy), Netherlands.

Bolch, T., Buchroithner, M.F., Peters, J., Baessler, M. and Bajracharya, S. (2008). Identification of glacier motion and potentially dangerous glacial lakes in the Mt. Everest region/Nepal using space-borne imagery. *Natural Hazards and Earth Systems Science*, **8**, 1329–1340.

Bolch, T., Buchroithner, M.F., Pieczonka, T. and Kunert, A. (2008). Planimetric and Volumetric Glacier Changes in the Khumbu Himalaya since 1962 Using Corona, Landsat TM and ASTER Data. *Journal of Glaciology*, **54(187)**, 592–600.

Bulley, H.N.N., Marx, D.B., Merchant, J.W., Holz, J.C. and Holz, A.A. (2008). A comparison of Nebraska reservoir classes estimated from watershed-based classification models and ecoregions. *Journal of Environmental Informatics,* **11(2)**, 90-102.

Bulley, H.N.N., Bishop, M.P., Shroder Jr., J.F. and Haritashya, U.K. (2011). Integration of classification tree analysis and spatial metrics to assess changes in supraglacial lakes in the Karakoram Himalaya. *International Journal of Remote Sensing* (accepted).

Congalton, R.G. (1991). A review of assessing the accuracy of classifications of remotely sensed data. *Remote Sensing of Environment*, **37**, 35–37.

Dyurgerov, M.B. and Meier, M.F. (2000). Twentieth century climate change : Evidence from small glaciers. *Proceedings of the National Academy of Sciences*, **97(4)**, 1406–1411.

Eastman, J.R. (2006). IDRISI Andes Guide to GIS and Image Processing. Worcester, MA: Clark Labs.

Friedl, M., Brodley, C.E. and Strahler, A.H. (1999). Maximizing land-cover classification accuracies produced by decision trees at continental to global scales. *IEEE Transactions of Geoscience and Remote Sensing*, **37(2)**, 969–977.

Frohn, R.C. (2006). The use of landscape pattern metrics in remote sensing image classification. *International Journal of Remote Sensing*, **27(10)**, 2025–2032.

Frohn, R.C. and Hao, Y. (2006). Landscape metric performance in analyzing two decades of deforestation in the Amazon Basin of Rondonia, Brazil. *Remote Sensing of Environment*, **100**, 237–251.

Fujita, K., Thompson, L.G., Ageta, Y., Yasunari, T., Kajikawa, Y., Sakai, A. and Takeuchi, N. (2006). Thirty-year history of glacier melting in the Nepal Himalayas. *Journal of Geophysical Research*, **111(DO3109)**, 1–6.

Haeberli, W., Hoelzle, M., Paul, F. and Zemp, M. (2007). Integrated monitoring of mountain glaciers as key indicators of global climate change: the European Alps. *Annals of Glaciology*, **46**, 150–160.

Hall, D.K., Riggs, A. and Salomonson, V.V. (1995). Development of methods for mapping global snow cover using moderate resolution imaging spectroradiometer data. *Remote Sensing of Environment*, **54**, 127–140.

Hansen, M., Dubayah, R. and Defries, R. (1996). Classification trees: an alternative to traditional land cover classifiers. *International Journal of Remote Sensing*, **17(5)**, 1075–1081.

Huggel, C., Kääb, A., Haeberli, W., Teysseire, P. and Paul, F. (2002). Remote sensing based assessment of hazards from glacier lake outbursts: a case study in the Swiss Alps. *Canadian Geotechnical Journal*, **39**, 316–330.

Kargel, J.S., Abrams, M.J., Bishop, M.P., Bush, A., Hamilton, G., Jiskoot, H., Kaab, A., Kieffer, H., Leet, E.M., Paul, F., Raup, B., Shroeder, J.F., Soltesz, D., Stainforth, D., Stearns, L. and Wessels, R. (2005). Multispectral imaging contributions to global land ice measurements from space. *Remote Sensing of Environment*, **99**, 187–219.

Kehrwald, N.M., Thompson, L.G., Tangdong, Y., Mosley-Thompson, E., Schotterer, U., Alfimov, V., Beer, J., Eikenberg, J. and Davis, M.E. (2008). Mass loss on Himalayan glacier endangers water resources. *Geophysical Research Letters*, **35(L22503)**, 1–6.

Keshri, A.K., Shukla, A. and Gupta, R.P. (2009). ASTER ratio indices for supraglacial terrain mapping. *International Journal of Remote Sensing*, **30(2)**, 519–524.

Kulkarni, A.V., Bahuguna, I.M., Rathore, B.P., Singh, S.K., Randhawa, S.S., Sood, R.K. and Dhar, S. (2007). Glacial retreat in Himalaya using Indian Remote Sensing satellite data. *Current Science*, **92(1)**, 69–74.

Kulkarni, A.V. and Buch, A.M. (1991). *Glacier atlas of the Indian Himalaya*.

Lawrence, R.L. and Wright, A. (2001). Rule-based classification systems using classification and regression tree (CART) analysis. *Photogrammetric Engineering and Remote Sensing*, **67(10)**, 1137–1142.

McFeeters, S.K. (1996). The use of the Normalized Difference Water Index (NDWI) in the delineation of open water features *International Journal of Remote Sensing*, **17(7)**, 1425–1432.

Milner, A.M., Brown, L.E. and Hannah, D.M. (2009). Hydroecological response of river systems to shrinking glaciers. *Hydrological Processes*, **23**, 62–77.

Mool, P.K., Bajracharya, S.R. and Joshi, S.P. (2001). Inventory of glaciers, glacial lakes and glacial lake outburst floods: Monitoring and Early Warning Systems in the Hindu Kush-Himalayan Region Nepal. Kathmandu, Nepal: International Centre for Integrated Mountain Development.

Oerlemans, J. (2005). Extracting a climate signal from 169 glacier records. *Science*, **308(29)**, 675–677.

Paul, F., Huggel, C. and Kaab, A. (2004). Combining satellite multispectral image data and a digital elevation model for mapping debris-covered glaciers. *Remote Sensing of Environment*, **89**, 510–518.

Paul, F., Kaab, A., Maisch, M., Kellenberger, T. and Haeberli, W. (2004). Rapid disintegration of Alpine glaciers observed with satellite data. *Geophysical Research Letters*, **31(21402)**, 1–4.

Quincey, D.J., Lucas, R.M., Richardson, S.D., Glasser, N.F., Hambrey, M.J. and Reynolds, J.M. (2005). Optical remote sensing techniques in high-mountain environments: applications to glacial hazards. *Progress in Physical Geography*, **29(4)**, 475–505.

Quinlan, J.R. (1986). Induction of decision trees. *Machine learning*, **1**, 81–106.

Racoviteanu, A.E., Williams, M.W. and Barry, R.G. (2008). Optical remote sensing of glacier characteristics: A review with focus on the Himalaya. *Sensors*, **8**, 3355–3383.

Raup, B., Kaab, A., Kargel, J.S., Bishop, M.P., Hamilton, G., Lee, E., Paul, F., Rau, F., Soltesz, D., Khalsa, S.J.S., Beedle, M. and Helm, C. (2007). Remote sensing and GIS technology in the Global Land Ice Measurements from Space (GLIMS) Project. *Computers and Geosciences*, **33**, 104–125.

Richardson, S.D. and Reynolds, J.M. (2000). An overview of glacial hazards in the Himalayas. *Quaternary International*, **65-66**, 31–47.

Rogan, J. and Chen, D.M. (2004). Remote sensing technology for mapping and monitoring land-cover and land-use change. *Progress in Planning*, **61(4)**, 301–325.

Rogan, J., Franklin, J., Stow, D., Miller, J., Roberts, D.A. and Woodcock, C. (2008). Mapping land cover modifications over large areas: A comparison of machine learning techniques. *Remote Sensing of Environment*, **112**, 2272–2283.

Rogan, J., Miller, J., Stow, D., Franklin, J., Levien, J. and Fischer, C. (2003). Land-cover change monitoring with classification trees using Landsat TM and ancillary data. *Photogrammetric Engineering and Remote Sensing*, **69**, 793–804.

Stevens, S.F. (1993). Claiming the high ground: Sherpas, subsistence, and environmental change in the highest Himalaya. Berkeley and Los Angeles: University of California Press.

Suzuki, R., Fujita, K. and Ageta, Y. (2007). Spatial distribution of thermal properties on debris-covered glaciers in the Himalayas derived from ASTER data. *Bulletin of Glaciological Research*, **24**, 13–22.

Thakur, J.K. (2010). Eco-hydrological wetland monitoring in a semi-arid region (A case study of Konya Closed Basin, Turkey). Faculty of International Institute for Geo-Information Science and Earth Observation (ITC), Universiteit Twente, Enschede, the Netherlands.

Yamada, T., Shiraiwa, T., Iida, H., Kadota, T., Watanabe, T., Rana, B., Ageta, Y. and Fushimi, H. (1992). Fluctuations of the glaciers from the 1970s to 1989 in the Khumbu, Shorong, and Langtang regions, Nepal Himalayas. *Bulletin of Glacier Research*, **10**, 11–19.

Zambon, M., Lawrence, R., Bunn, A. and Powell, S. (2006). Effect of alternative splitting rules on image processing using classification tree analysis. *Photogrammetric Engineering and Remote Sensing*, **72(1)**, 25–30.

Zhou, Y., Narumalani, S. and Jelinski, D.E. (1995). Improving remote sensing derived land use/land cover classification with the aid of spatial information. Paper presented at the ACSM/ASPRS Annual Convention and Exposition Technical Papers, Bethesda, MD.

# 7

# Towards the Improvement of Water Resource Management by Combining Technologies for Spatial Data Collection, Storage, Analysis and Dissemination

**Nafaâ Jabeur and James D. McCarthy**[1]
Computer Science Department, Dhofar University, Oman
[1]Mapping, Analysis and Design, Faculty of Environment
University of Waterloo, Canada

## Introduction

Water resource managers regularly deal with situations where timely, relevant information can be of significant benefit. One only needs to look at the extensive flooding in Australia in 2010 and 2011, and the associated loss of property and life, to discover why the desire for hydrologic monitoring tools is so great. When water resource managers deal with floods, they want to be able to monitor and predict water levels and direct emergency response efforts. However, flooding is not the only situation where water resources need to be monitored and analyzed (Thakur et al., 2011). To ensure appropriate water quality and supply for a region, these parameters must be regularly monitored, and appropriate entities must be alerted when certain warning thresholds are approached or broken. To study and preserve biodiversity, resource managers need access to long-term data about the environmental conditions in their study area, including any hydrologic factors that may have an impact on it. Several established and emerging technologies are currently providing experts with great benefit in managing environmental resources. In the hydrological domain, the use of Sensor Webs (SWs) in data collection provides decision makers with ever-growing amounts of relevant data and allows them to always be aware of conditions in their study area (Guru et al., 2008). These data can be supplemented with data collected using emerging mobile GIS technology

J.K. Thakur et al. (eds.), *Geospatial Techniques for Managing Environmental Resources*,
DOI 10.1007/978-94-007-1858-6_7, © Capital Publishing Company 2012

and applications. Currently, a multitude of mobile platforms integrating GPS technology can support data entry through generic or dedicated applications.

Once the data are collected from the field, spatial database technology and sensor network representation standards can be used to effectively make these data available to experts for analysis. To this end, information can be retrieved from the spatial databases in a format that is not only machine-readable, but also laden with information relevant to the water resource domain (McCarthy, Graniero and Rozic, 2008). Analysis methods that use these data could be supported by several tools and techniques, such as rule-based reasoning (Rozic, 2006). Web GIS and mapping technologies can make analysis results, as well as the data which spawned them, available for use by others regardless of their skills. The use of multiagent systems (Jabeur, Graniero, McCarthy and Xing, 2009) provides an interesting solution towards autonomous and intelligent use of spatial data.

The relevant technologies for spatial data collection, storage, analysis and dissemination are all rapidly growing in both numbers and functionality. However it remains to be seen what form the convergence of these technologies will take. In addition to being developed to address only one or two of these four key areas of geomatics, most of these technologies are developed by different software and hardware vendors. This results in datasets that are incompatible with analysis tools, or multiple format conversions that introduce the potential for accuracy and precision problems. For reasons such as these, there is a need for tools and techniques to handle the interchange of data between these applications and data formats in a standardized manner that interferes as little as possible with the analysis the user wishes to perform.

This chapter will examine many of the relevant technologies involved in SW design, deployment and usage, and it will explore how these technologies may be integrated into a complete framework for sensor network management. It will also highlight some applications that have been developed specifically for water resources management and how they would fit into the proposed framework.

## Spatial Data Collection Technologies

### Sensor Webs

#### *Overview of Sensor Webs*

A Sensor Web (SW) is a network consisting of large numbers of sensing platforms allowing the spatio-temporal understanding of the environment where it is deployed. This network could be compared to a sophisticated sensing tapestry draped over the environment (Delin and Small, 2009) and has the basic functionality to access data remotely. Extended and complex functionalities could generally be achieved through coordinated efforts between the deployed sensors. SWs are characterized by their multidisciplinary nature

that requires knowledge from a variety of fields such as microelectronics, mechanics, physics and computer science, and some domain knowledge of the environments being sensed. They typically face several challenges related to limited power, depletion failures, restricted resources, unstable topology, unpredictable conditions and unbounded information flow delays. These challenges are more serious when the SWs are operating unattended in hostile environments. Several initiatives have been proposed to cope with the problems facing the deployment of SWs. These initiatives span hardware (e.g. Hempstead, Tripathi, Muro, Wei and Brooks, 2005), network protocols (e.g. Intanagonwiwat, Govindan and Estrin, 2000; Jabeur and Graniero, 2007), applications (e.g. Levis et al., 2005; McCarthy et al., 2008), and operating systems (e.g. Levis et al., 2005).

Recent advances in miniaturization and wireless communications have brought a new generation of SWs comprising large numbers of cooperating small-scale sensor nodes. This cooperation allows the sensor nodes to go beyond their individual capabilities and carry out complex operations. During their interaction, the nodes have to share their collected observations and support each other in processing and routing data while taking into account their individual characteristics. To this end, they have to adapt their behaviours individually, which consequently leads to a global self-organizing behaviour allowing the SW to evolve towards a better configuration that adapts to suit the current situation (Jabeur, McCarthy and Graniero, 2008).

Thanks to their spatially distributed configurations, SWs are able to collect important spatio-temporal data for a variety of applications. These data become highly valuable when sensors are fielded in harsh environments, such as deserts, mountains and Antarctica. In addition to environmental science purposes (e.g., Heavner, Fatland, Hood and Connor, 2007), SWs have proved valuable in urban search, rescue and tracking (e.g., Howe et al., 2008), infrastructure protection (e.g., Delin and Small, 2009), hazard management (e.g., Jabeur and Haddad, 2009), and wild fire monitoring (e.g., Sahli, Jabeur and Badra, 2011). The technology is also used for controlling the environment by actuating devices (Collins, 2004). As future directions, SWs could be used to track in-field personnel during operations, protect infrastructure, decontaminate air and buildings, monitor rails and highways, and control ventilation (Delin and Small, 2009). In this chapter, we particularly focus on water resource management where SWs are being used for several purposes, such as flood monitoring, water contamination detection and agricultural development.

### *SW for Water Resource Management*

Several research works and applications have used SWs for water resource management and its related issues, such as irrigation, water contamination, water surface movement, water infiltration and flood control. In this context, the COMMONSense Net project (Jacques, Seshagiri, Prabhakar, Jean-Pierre

and Jamadagni, 2007) is an initiative that focussed on the design and implementation of a SW for agricultural management in developing countries. This project had emphasized semi-arid regions in a cluster of villages in Southern Karnataka (India). When water is polluted, for example, by industrial waste, fertilization or pesticides, SWs could be efficiently used to detect any contamination and thus prevent casualties. This is the case in Ganges delta (Bangladesh/India) where SW-based technology is being used for detecting the Arsenic pollutant in water (Zennaro, Pehrson and Bagula, 2008). Markovic, Stanimirovic and Stoimenov (2009) have developed a SW-based system called the River Water Monitoring and Alert System (RWMAS) that enables operators in crisis management centres to discover and prevent water pollution.

SWs can also facilitate the detection and monitoring of water surface movement and water infiltration in real time. This would particularly help in characterizing hydrologic phenomena (e.g. surface water movement, soil moisture and storm induced floods) and monitoring floods in real time. To work towards the elimination of the problems caused by floods, the CAVSARP (Central Avra Valley Storage and Recovery Project) (Delin and Jackson, 2003) has been proposed by the NASA Jet Propulsion Laboratory for hydrology studies located to the west of Tucson, Arizona, USA. In this location, a number of artificial recharge basins are used in a desert environment to monitor various hydrologic processes and geomorphologic features, such as wave cut terraces, polygonal patterns in soil, and ridges related to the drying of the basin floor materials. The deployed SW monitors the front movement of a potential flood and water infiltration into ground. The data are transferred to the Internet from a portal sensor pod connected to a computer. Thanks to the SW, the spatial and temporal patterns of wetting and drying of the basins that have been identified provide a hydrological model for the analysis of floods.

At a higher abstraction level, some SW-based frameworks and systems have been proposed and applied to water resource management. In this context, Xitao (2008) has proposed and designed an architectural framework to develop advanced integrated environmental monitoring systems (A-ITEMS), which feeds the requirements of complex environmental monitoring systems. In this work, an Integrated Watershed Telemetry (IWT) system has been implemented. Graniero, Weiler, Nickerson and Jabeur (2007) have presented the SWAN (Sensor Web Automation Network) project that aims at developing SW design and deployment tools that blend varied sensor and communication hardware, both mobile and stationary, into one watershed monitoring system. In a related work (Jabeur et al., 2009), we have proposed a meta-framework to guide the development of a cyberinfrastructure that can lead the way for emerging sensor infrastructures to interoperate. Without being restricted to water resource management, our meta-framework is guided by the DAST principle that summarizes the overall goal of any sensor infrastructure: acquire the right Data from the right Area using the right Sensors at the right Time.

In order to implement the DAST principle, we have proposed a Sensor Observation Service server agent that uses semantic, logical and physical connections between sensors in order to better adapt to network changes and provide adjustable services suitable for monitoring water resource conditions (Jabeur et al., 2009). In another work (Jabeur and Haddad, 2009), we have proposed to encode causality relationships about natural phenomena and their effects in time and space in order to allow the system to set up priorities between the sensor network activities and thus implement a progressive approach for the management of hazardous events, such as floods.

## GPS and Manual Data Collection

While the evolution of the Sensor Web as a macro-instrument is rapid, there will always be gaps (both physical and conceptual) that require the intervention of a domain expert in the data collection process. Some areas may be too remote or too difficult to reach to make a sensor network cost-effective. Perhaps conditions are expected to change in a study area in a way that the sensor network won't be able to capture in time, or wasn't designed to capture. Whatever the reason, supplementing sensor network data with manual measurements from the field can provide a more complete picture of conditions in a study area.

Collection can be handled with dedicated data collection applications such as Esri's ArcPad or Trimble's TerraSync. These software tools run on hardware specifically designed for data collection in the field using GPS receivers. The advantage of using these tools is that, depending on the hardware, they can accurately record a user's position in the field within a few centimetres. Since hydrologic issues are often local in scale, this repeatability and accuracy of measurement becomes very important to users looking to supplement data collected by a sensor network. These tools are also customizable so that a developer can create an application to work on the device which streamlines the data collection process so that domain experts such as hydrologists, rather than GIS/GPS experts, can spend their time in the field collecting data. This is important as they will be more qualified to judge what is important while out in the field.

This is not to say, however, that specialized devices are the only way to collect data from the field. The increasing number of applications developed for mobile devices are providing experts with valuable support in collecting data, anywhere, anytime.

From a hydrologic perspective, data collection from mobile devices could be handled in a number of ways. Expert users can enter the field equipped with specialized equipment for precisely measuring various parameters of their watershed or other study area which can then be supplied to applications either wirelessly or when the user returns from the field. Depending on the needs of the application there are other ways of handling data collection. The idea of crowd-sourcing data (encouraging the public to participate in the

collection process) has merit for certain applications as well. For example, COMAP systems (McGarry, 2008) have been successfully used in diverse areas such as heritage resource tracking, invasive species tracking and moraine analysis. In all cases, the systems are deployed with an eye towards public participation in the data collection and verification process.

### Remote Sensing and Satellite Imagery

In situations where sensor webs simply aren't feasible, or where they haven't been installed, there are still ways of gathering relevant information about a site from a distance. Satellite imagery can provide data that can act as a proxy for in situ measurements. Nakamura et al. (2005) described a process by which sea ice thickness can be measured with Synthetic Aperture Radar data. Image processing can be automated to provide information gathered by remote sensing satellites in a quantitative form to supplement sensor data. Visible satellite imagery can show the state of a study area with great accuracy. If the images are of a high enough resolution, relative measurements can be made if images are captured with any regularity and their scale is known. LIDAR data can provide extremely fine-grained measurement of physical parameters. Though not typically collected regularly like other satellite imagery, LIDAR sensors can be targeted and flown at a specific site to provide detailed information about that site. Detailed bathymetric (Irish and White, 1998), water level (Stockdon, Sallenger, List and Holman, 2002), and water quality (Barbini, Colao, Fantoni, Palucci and Ribezzo, 1995) data have all been gathered via the use of LIDAR.

## Spatial Data Storage Technologies

This section of the chapter will illustrate how varied the representation formats for spatial data have become. It begins with an examination of the most common spatial databases and then describes some of the standards being used for SW representation. A discussion of ontologies follows. This concept is referenced again later in the chapter. Finally, some strategies for dealing with the multitude of data formats in existence are suggested.

### Spatial Databases

Enterprise-level databases drive many applications on and off the web. Most of the major players in the enterprise database market have created spatially-enabled database products in recent years to keep up with the demand for geo-location and other location-based services that have exploded on the web. These spatial databases typically take one of two forms: Extensions to existing database products that enable spatial information to be stored within an existing database product, and database products specifically designed for holding spatial data.

This section will introduce the current offerings from database companies, spatial technology companies, and open source efforts. It will also look more closely at a data model designed specifically for storing hydrologic data.

### *Spatial Database Extensions*

As the demand for location-enabled data has grown, database developers have evolved their products to match. Most of these evolutions have taken the form of an extension to the existing functionality of the product rather than a separate standalone product. Database products that have followed this pattern include Oracle, MySQL, PostgreSQL, SQL Server and SQLite.

The proprietary Oracle database offers an Oracle Spatial extension which allows for the storage of spatial data according to a spatially-enabled database schema. Microsoft's SQL Server product provides similar spatial extensions to its products. MySQL provides both a proprietary and an open source version of their database product, both of which support the spatial extensions MySQL provides. Rather than provide an entire spatial database schema such as Oracle, MySQL provides a GEOMETRY column type to store geographic data.

The open source PostgreSQL database system provides spatial extensions in the form of PostGIS. Another open-source DBMS (Database Management System), SQLite, does not provide its own spatial extensions. However an independent developer has created SpatiaLite, which is one of the newer attempts to add spatial capabilities to a popular database product. One of the distinguishing features of SQLite (and thus, SpatiaLite) is that the databases themselves do not need to be stored on a persistent database server. Instead, they exist in files that can be easily managed and copied from one location to another like most other computer files.

Many of these spatial database products also provide viewer applications so that users can view the data in their database in a more familiar GIS context. All of these products are supported at some level by GIS applications, though which applications support which products varies from product to product and application to application. All of the databases mentioned in this section support the Open Geospatial Consortium's Simple Features Specification (Herring, 2010) and/or the Simple Features Specification for SQL (Herring, 2010). This is important for two key reasons. The first is that it assures that interchange is possible between formats as they are all adhering to a specific standard, even if their implementations of that standard differ. Secondly, supporting this specification means that these formats must support many common spatial analysis tasks such as comparing feature geometry, measurements, overlays, selections, and queries. Currently, support for raster data in the specification is under development and only some of these products support raster data.

### *Esri Geodatabases*

Esri provides their own geodatabase formats that are used for a variety of purposes. They are broken down into two main types, each with their own

subtypes. The two main types are Single-user and Multiuser geodatabases. Single-user geodatabases can be either File or Personal geodatabases, and Multiuser geodatabases can be Enterprise, Workgroup, and Desktop geodatabases. The choice of database type is typically made based on the type(s) of users and products that will consume it. A small number of users with only one editor can use a File Geodatabase, whereas a database that is being edited by multiple people and accessed via multiple web applications would be more suited to one of the multi-user variations. Feature geometries are stored internally in the database and so are not as easily accessed as some of the other spatial database types mentioned here. However, the specification has been made available so that non-Esri applications can access features stored in Esri geodatabase formats.

#### *ArcHydro*

ArcHydro is a data model designed specifically for water resources, implemented in an Esri geodatabase. ArcHydro is one of the most complete systems available for managing and analyzing hydrologically-themed spatial data. Because of the explicitness and level of detail in the model, sophisticated analysis tools can be built to take advantage of the information stored in the data model (more on this later in the chapter).

ArcHydro models water resources from the watershed level down to the stream level while also maintaining a network of the features involved in the watershed. Hydrologic features are modeled in four groups: Hydrography features (dams, waterbodies, monitoring points, etc.), Network features (edges and junctions of hydrologic features), Drainage features (catchments, watersheds, basins, etc.), and Channel features (cross-sections and profiles). The geodatabase also provides support for time series data and built-in layer types such as terrain and streams. The level of detail provided by ArcHydro makes for a relatively complex geodatabase with many tables, feature classes and relationships. However it is this level of detail that makes the ArcHydro tools extremely useful.

### GML

The Geography Markup Language (GML) is an XML-based OGC specification intended for representing geographic features, geometries, spatial reference systems, and other spatial primitives. GML provides the basis for representing features in many of the Sensor Web Enablement specifications the OGC maintains.

### SensorML and O&M

Encodings and representations of sensor descriptions and sensor measurements have been created to facilitate the discovery and interpretation of data provided by sensor networks. The OGC's Sensor Web Enablement working group has

created an entire suite of standards related to sensor networks. The two that will be focussed on in this chapter are SensorML and O&M. SensorML is an XML schema that describes sensors and sensor platforms and their parameters. These parameters can include hardware-specific information such as measurement accuracy and calibration information, as well as site- and application-specific information like sampling rates. While much of this information can be read from manuals or site descriptions, encoding it directly into an XML document makes it feasible for software to have access to this information when needed.

O&M (Observations and Measurements) is an XML schema which complements SensorML. It describes measurements made by sensors and can provide insight into the significance of a measurement. When combined with SensorML and other representations, applications and expert users can have a complete view of the state of a sensor network in the field.

## SOS

A Sensor Observation Service (SOS) makes use of SensorML and O&M to provide an interactive, useful view of current and historical conditions at a site. More specifically, it stores, manages and organizes sensor data as well as sensor descriptions. If made public, these data can be queried and discovered by other users, which aids in collaboration. The service can respond to queries from an application or an expert user and provide current or historical data that are relevant to the user's needs.

## Ontologies

This chapter has shown that sensor measurements are most useful when they have context that gives them meaning. This meaning can be encoded in the form of an ontology. Ontologies can be made machine-readable through the use of various ontology representation formats. This section will examine two of those representation formats: OWL and CLIPS. In order to compare these two formats, however, a basic understanding of ontologies is necessary and is provided here.

Ontologies are a means of explicitly describing a particular area of interest. The term 'area of interest' is used in a broad context here and could refer to an application domain or more general concepts. An ontology is generally composed of the facts, objects, rules and relationships that make up an application domain. It can look similar to an object model or a database model, and this is something that can be leveraged when trying to integrate ontologies into applications. The ArcHydro data model provides an excellent, detailed basis on which an ontology could be formed. The additional information provided by an ontology can be used by an application to better interpret or apply meaning from simple data. For example knowing that a certain stream is flowing at 2000 $m^3$/sec can be useful, but knowing precisely

where on the stream the measurement was taken, by what type of instrument, what that instrument's typical accuracy is, and what other instruments are nearby, can provide an expert user with far more information in a more upfront fashion. This enables the user to make more informed decisions.

OWL (Web Ontology Language) and CLIPS are two ontology representation approaches that have proven to have particular utility in enhancing the information that can be gained from a hydrologic sensor network. OWL is a W3C endorsed, XML-based specification for representing ontological information. It is one of the most commonly used ontology specification formats. OWL is reasonably human-readable while being machine-readable. In OWL, concepts are broken down into Instances, Classes, Properties and Operators. These concepts could be further subcategorized in the OWL specification when necessary. CLIPS is not by its nature an ontology definition language, but rather a rule-based programming language. In this language, concepts of a domain can be represented as facts and rules, and as in most rule-based programming languages, these facts and rules are what govern the execution of the program, not a sequence of pre-programmed steps. This allows a language such as CLIPS to react dynamically to changing conditions, and to have a current snapshot of the conditions of the program at any time.

## Strategies for Negotiating between Data Formats

With the plethora of data formats available to use, the decision about what format to use is often not under the user's control. When the user wishes to use data from one application in another application, ideally the data is already in a format supported by both applications. Practically, however, this is often not the case. Therefore a conversion is needed to make the data usable in the new application. Two approaches to conversion are discussed here.

### *FME*

FME is a commercial product created by Safe Software which has the primary goal of allowing users to convert their data from one spatial format to another. While the list of spatial data formats that is supported is quite exhaustive, FME also provides tools to process the data as well. These tools allow the user to automate data manipulation and processing within the FME environment in order to streamline data processing tasks.

### *GDAL/OGR*

GDAL (Geospatial Data Abstraction Library) and the OGR Simple Features Library are part of the GDAL library which is a C++ library used primarily to convert data between different geospatial formats. GDAL provides many command line tools to achieve these conversions, and because it is an open source library its functionality is built into many free and open source GIS desktop packages.

## Spatial Data Analysis Technologies

### Rule-based Systems

Rule-based systems such as CLIPS are based on a defined set of facts and rules which make up a body of knowledge. Rather than executing sequentially like a more common procedural analysis, a rule-based analysis reacts to changing conditions. When the facts of a situation change, the rules of the system are re-evaluated and new outcomes are decided. In situations such as water resource management where conditions are changing rapidly and unpredictably, a rule-based system is able to be more responsive and is more likely to be capable of handling an unforeseen situation. McCarthy et al. (2008) describe how a rule-based analysis system integrated into ArcGIS is able to track the movement of sensors embedded in a hillslide. Rules are defined that classify what the risk characteristics are for slope failure and at every time step the facts of the situation are evaluated against these rules. The facts in the system in this case are the measurements being made by two types of sensors: inclinometers to measure the movement of the slope material, and piezometers to track the water level. The system also understands the makeup of slope material and how susceptible the different materials are to sliding. These facts are evaluated against the rule base which includes rules about acceptable movement for that particular slope and the interaction between the water table and the elastic portion of the slope. According to these rules, a risk level is determined based on a decision tree and the map is symbolized accordingly. If a high risk level is indicated, an alert could be sounded. The described system was designed to be portable to other domains (Rozic and Graniero, 2005), and so could be applied to the monitoring of a watershed.

### ArcHydro and HEC

Earlier in the chapter was a discussion on the ArcHydro data model and how it represents hydrologic features. This representation scheme enables powerful analysis tools within the ArcGIS environment. In addition to tools that help users bring their existing hydrologic data into the ArcHydro environment, ArcHydro provides tools for examining terrain, watersheds, stream networks, flow rates, time series analysis, watershed delineation, and several other common water resource based tasks.

An alternative to the ArcHydro environment for hydrologic analysis is the suite of tools provided by the U.S. Army Corps of Engineers Hydrologic Engineering Center (HEC). Many of the tools are provided for a specific purpose, such as river analysis, hydrologic modelling and ecosystem study. The tool that is most relevant to this chapter is the Corps Water Management System (CWMS). It attempts to provide a suite of water resource management and spatial-decisions support tools, and integrates both incoming sensor data and modelled or simulated data to supplement analysis.

## Spatial Data Dissemination Technologies

### Web Applications

A variety of options exist for disseminating analysis results and raw sensor data via the Internet. For raw data, most spatial databases can be made available to be queried over the web either through direct queries or web applications. There are also several web-GIS platforms that can be tied into existing spatial database products, such as ArcGIS Server, Map Server and Open Layers. The different platforms provide a variety of support for data formats and differ widely in how they serve data over the web.

In the hydrological domain, applications such as the South Esk Hydrological Sensor Web (Guru et al., 2008) show how data collected in the field can be displayed simply by overlaying points onto a relevant basemap. Now, even if a user doesn't have direct access to an SOS or some other sensor-based measurement database they can still view the conditions in a study area from anywhere with an internet connection.

### Open Data Initiatives

Many organizations are moving much of their spatial data online for use by the broader community. While in the early days of data collection this information may have been hidden behind paywalls and licensing agreements, there has been a shift in thinking towards the idea that making the data available to anyone willing to accept it as is will provide more benefit to the community. Ultimately the decision of whether or not to make data available freely must be made by organizations that hold data, and this decision will often come down to striking a balance between serving the greater good and making a profit.

However the Open Data movement is indeed growing, driven largely by municipalities. In Canada, many of the largest municipalities (such as Toronto and Vancouver) are making much of their data available through Open Data Initiatives. These initiatives are often driven by a desire for transparency in governance. The technologies used to disseminate these data vary from simple websites that provide static files for download to dynamic, map-based applications that allow users to browse through the data in a spatial context before downloading it.

## Towards the Improvement of Water Resource Management

The data collected by the sensors are concretely valuable once this data is appropriately analyzed and presented to end-users. For the sake of increasing the benefits from this data and making it available for real-time applications, the chain of processing including data collection, storing, analysis and

dissemination must be coordinated in order to allow a smooth data flow between the different processing steps. To achieve this goal, a variety of technological tools could be necessary and the intervention of experts would be inevitable. Thus, our idea is not limited to combining a package of technologies. It is rather an attempt to make automatic the entire process starting from the field until the data are accessible to the end user.

## Combining Data Collection, Storage, Analysis and Dissemination

In Fig. 1, we present a high-level framework that aims at combining data collection, storage, analysis and dissemination within one single system for sensor network management. This framework could be used for spatio-temporal applications, including water resource management. We guide our framework

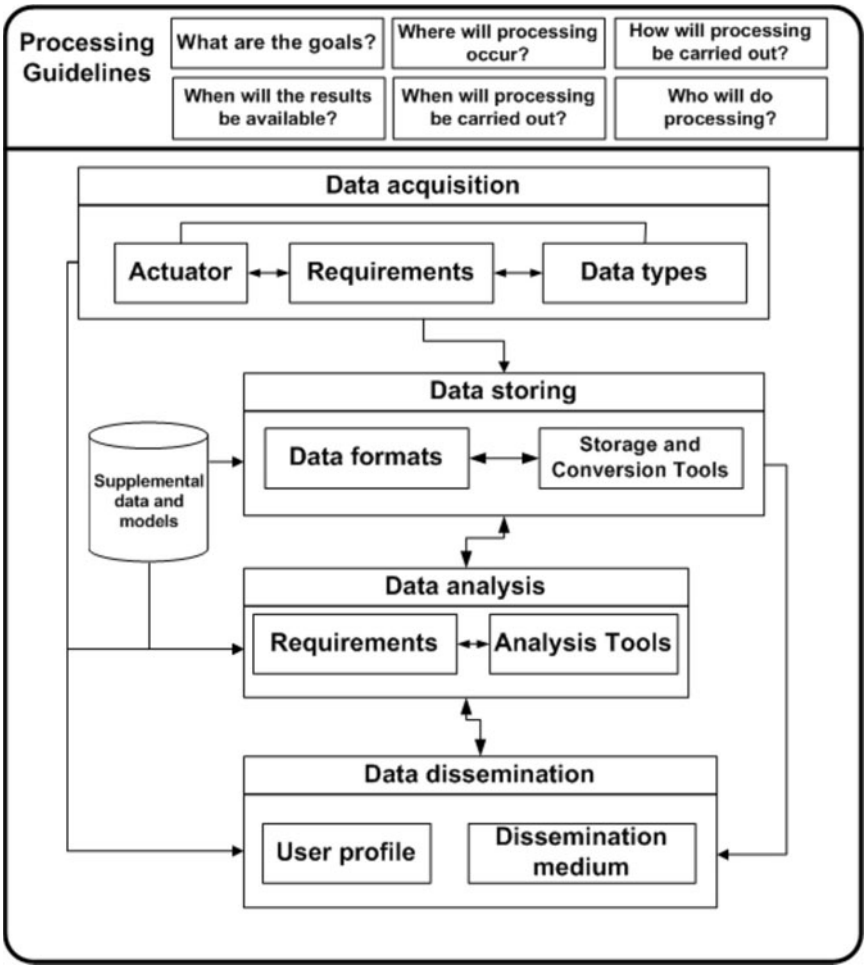


**Figure 1.** High-level framework combining data collection, storage, analysis and dissemination.

with a set of rules related to the answers to six questions: What are the goals of the processing request? Where will the processing occur? How will the processing be carried out? When will the processing take place? Who will do the processing? And, when will the results be provided? In these questions, the term *processing* refers to any activity carried out by the proposed system.

The data acquisition component includes the actuators (e.g., sensors, GPS, Radars, Satellites, etc.) that will be used in order to collect the requested data. The data are identified based upon specified requirements and some processing guidelines. The data collected are sent to the other components of the system in one or more relevant formats depending on the requirements as well as the components and technologies used in a particular sensor network installation. When data are to be stored, processing must take into account the format that suits the anticipated use of the data, the tools used for data storage, the processing guidelines, and some additional data models. Examples of additional data models would concern the geographic space and the model of phenomena that would be of interest for the application. To achieve this, the data storage component must have access to data conversion and storage tools and an understanding of which data formats suit which type of requirement.

The data analysis component carries out the necessary processing with respect to the current requirements and the available tools. Data that has been analyzed would be stored and/or sent to the data dissemination component. In this component, data is provided to end-users depending on the user's profile and the medium used for data dissemination.

In what follows, we present our scenario for water resource management. Then, we adapt this proposed framework to this scenario, showing where different components described in this chapter would fit in an implemented system. The resulting system architecture is based upon the use of software agents for the sake of an automatic and autonomous data flow between the different processing stages.

## Water Resource Management Scenario

Our scenario comprises several management goals and complex challenges. It can be described as follows: Sensors take their measurements and forward them to the application user according to a predefined schedule which may depend on the sensitivity of their positions. Due to flood risks in rough conditions and soil contamination, we need a SW that supervises the flow and level of water in sensitive places (e.g. A, B and C in Fig. 2) and adapts to changes on the basis of collected data. For example, MA2 is sleeping most of the time and triggered when water flow in its location is extreme. According to the activity of the factory, MA1 increases the frequency of its measurements in order to monitor the water quality in the soil which may be polluted by the factory's waste. When rain falls in abundance motes MA10, MA4, MA11 and MA12 must speed up their measurements, assess the level of water in the big lake, and notify the authority of any likely inundation.


**Figure 2.** Water resource monitoring scenario.

## Multiagent-based System for Water Resource Management

SW solutions need to foresee the development of the situation, adjust the priorities of their processing, and allow sensors to change their behaviours according to their current situations. To this end, they have to be sufficiently autonomous. This autonomy can be found in the concept of multiagent systems where several software agents, with partial views of the environment, would collaborate and self-organize in order to achieve common goals beyond their individual capabilities.

Our agent-based solution is depicted in Fig. 3. In this solution, the processing components are integrated by using various standards and technologies. In concrete terms, we propose to use several models related to SW, geographic space, requirements, natural phenomena and results. The geographic space can be represented using GML and/or GIS data. SWs can be represented using SensorML and controlled through the Sensor Web Language (Nickerson, Sun and Arp, 2005). In our phenomena model, events can be described using XML descriptions or database models (e.g. ArcHydro) while interaction can be handled using the Web Notification Service (Simonis and Etcherhoff, 2007) or any suitable communication languages between the actors of the system (e.g. FIPA ACL for communication between software agents).

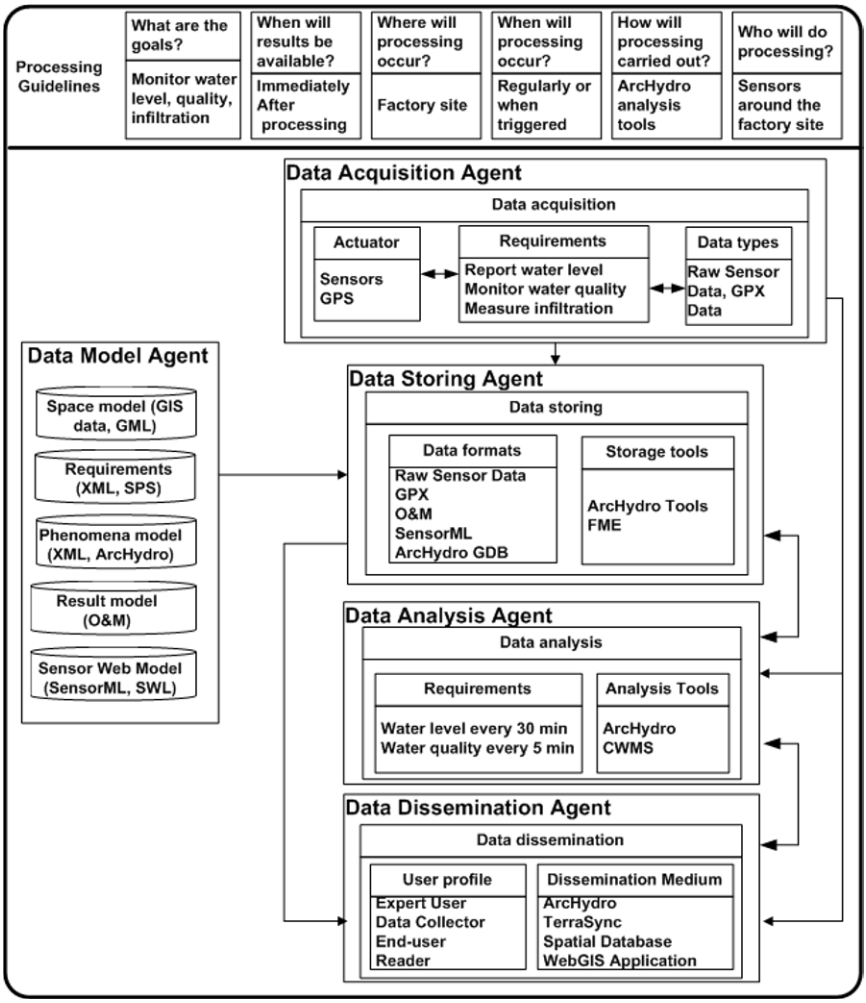


**Figure 3.** Our agent-based solution for water resource management.

Measurements and results can be described using Observations and Measurements (O&M). Requirements may be handled through the Sensor Planning Service (Simonis, 2005). For the sake of integration, databases using the ArcHydro model provide GIS data organized in a way that enables domain-specific tools to be used for analysis of hydrologic phenomena. Many of the OGC representations can be easily integrated as well. A system such as FME or ENGINE (McCarthy et al., 2008) can be used to mediate the conversion between different data formats.

In order to integrate the different components of our system, we propose to wrap them with software agents. In this case, a Data Model Agent (DMA) maintains update information about the geographic space, the SW, the natural phenomena and the results. A Data Acquisition Agent (DAA) is responsible

for the monitoring of the data acquisition component. It receives the requirements of the user and returns the measurements to the other components depending on the need. A Data Storing Agent (DSA) controls the storing of data in the right format. A Data Analysis Agent (DAA) is responsible for the analysis of data. A Data Dissemination Agent (DDA) is responsible for disseminating the requested data to the right user using the right medium. Our software can be built using any existing multiagent-system platform, such as Jade, Jack, Beegent and AgentBuilder. They may coordinate their processing by exchanging FIPA ACL messages.

## Future Research and Conclusions

Moving forward policy makers will continue to demand tools that provide them with meaningful information as opposed to raw data with little semantic value. Ideally these tools and their associated data will be made available to the public so they can contribute to, and remain informed about, the management of the hydrologic resources that impact their daily lives. Much of the development in the water resource management sector will revolve around the integration of the technologies mentioned throughout this chapter, as well as technologies that have yet to emerge. This integration will also need to become more seamless to both the domain expert and the end-user. Having a guiding framework to facilitate this integration will be very important to avoid fragmentation in the market that will result in systems that are harder for domain experts such as hydrologists to use. Data models, analysis methods and sensor hardware will always need to be designed to match the requirements of the specific application domain they are being deployed in, but the tools for dissemination and management should develop in a way that is domain-agnostic whenever possible to reduce duplication of effort.

This chapter focussed on and explored some existing technologies related to four main aspects of geomatics: collecting, storing, analyzing and disseminating data. It thoroughly studied the interoperability between these technologies and proposed a high-level framework allowing for their approachable and collaborative use. It also serves as a guideline for the integration of components provided by a variety of vendors and organizations with different goals. It may also be used by those developing new tools as a means of guiding their development in a way that promotes integration of components. This framework could be applied to a variety of application domains, and was illustrated with examples that would be used in an agent-based hydrologic monitoring and analysis system. In addition to making this management seamless to researchers and end-users, agents provide our solution with flexibility, autonomy and intelligence that would be very helpful in integrating new components relevant to data collection, storing, analysis or dissemination.

## References

Barbini, R., Colao, F., Fantoni, R., Palucci, A. and Ribezzo, S. (1995). Remote sea-water quality monitoring by means of a lidar fluorosensor. Global Process Monitoring and Remote Sensing of the Ocean and Sea Ice. Volume 2586. pp 46–55.

Colllins, J. (2004). NASA creates thinking RF sensors. *RFID Journal*, Retrieved January 20, 2011 from http://www.rfidjournal.com/article/articleview/1146/1/47/

Delin, K. and Small, E. (2009). The Sensor Web: Advanced Technology for Situational Awareness. Wiley Handbook of Science and Technology for Homeland Security. John Wiley and Sons.

Delin, K.A. and Jackson, S.P. (2003). The Sensor Web: A New Instrument Concept. SPIE Symposium on Integrated Optics, San Jose, CA.

Graniero, P.A., Weiler, M., Nickerson, B.G., Arp, P.A. and Jabeur, N. (2007). An integrated sensor web design and deployment infrastructure for watershed monitoring. Retrieved February 5, 2011 from http://matrix.memf.uwindsor.ca/publications/posters/SWAN-GranieroEtAl-SWANOverview-GEOIDE2007.pdf

Guru, S.M., Taylor, P., Neuhaus, H., Shu, Y., Smith, D. and Terhorst, A. (2008). Hydrological Sensor Web for the South Esk Catchment in the Tasmanian state of Australia. *In:* IEEE 4th International Conference on eScience, **7(12)**, 432–433.

Heavner, M.J., Fatland, D.R., Hood, E. and Connor, C. (2007). SEAMONSTER: A Sensor Web Technology Implementation and Testbed in Southeast Alaska. Paper presented at NASA Science and Technology Conference, College Park, MD.

Hempstead, M., Tripathi, N., Mauro, P., Wei, G-Y. and Brooks, D. (2005). An ultra low power system architecture for sensor network applications. *Proceedings of SIGARCH Computational Architecture*, **33**, 208–219.

Herring, J.R. (2010). OpenGIS Implementation Standard for Geographic information – Simple feature access – Part 1: Common architecture. Open Geospatial Consortium. 93 pp. Retreived February 15, 2011 from http://www.opengeospatial.org/standards/sfa

Howe, B.M., Parrish, N., Tracy, L., Gray, A., Chao, Y., McGinnis, T., Arabshahi, P. and Roy, S. (2008). A Smart Sensor Web for Ocean Observation: Integrated Acoustics, Satellite Networking, and Predictive Modeling. *In:* Proceedings of NASA Science Technology Conference (NSTC2008), University of Maryland.

Intanagonwiwat, C., Govindan, R. and Estrin, D. (2000). Directed diffusion: a scalable and robust communication paradigm for sensor networks. *In:* Proceedings of International conference on Mobile Computing and Networking.

Irish, J.L. and White, T.E. (1998). Coastal engineering applications of high-resolution lidar bathymetry. *Proceedings of Coastal Engineering,* **35(1)**, 47–71.

Jabeur N. and Haddad, H. (2009). Using Causality Relationships for a Progressive Management of Hazardous Phenomena with Sensor Networks. *In:* Proceedings of the International Conference on Computational Science and Applications (ICCSA'09), Yongin, Korea, pp. 1–16

Jabeur, N. and Graniero, P. (2007). A Hybrid Location-Semantic Approach to Routing Assisted by Agents in a Virtual Network. *In:* Frontiers of High Performance Computing and Networking. ISPA 2007 Workshops, pp. 523–533.

Jabeur, N., Graniero, P., McCarthy, J. and Xing, X. (2009). A Knowledge-Oriented Meta-Framework for Integrating Sensor Network Infrastructures. *International Journal of Computers and Geosciences*, **35**, 1–14.

Jabeur, N., McCarthy, J.D. and Graniero, P. (2008). Improving Wireless Sensor Network Efficiency and Adaptability through an SOS Server Agent. *In:* Proceeding of the 1st IEEE International Workshop on the Applications of Digital Information and Web Technologies (ICADIWT 2008), Ostrava, Czech Republic, pp. 409–414.

Jacques, P., Seshagiri, R., Prabhakar, T.V., Jean-Pierre, H. and Jamadagni, H.S. (2007). COMMONSense Net: A Wireless Sensor Network for Resource-Poor Agriculture in the Semiarid Areas of Developing Countries. *Journal of Information Technologies and International Development*, **4(1)**, 51–67.

Levis, Ph., Gay, D., Handziski, V., Hauer, J.H., Greenstein, B., Turon, M., Huio, J., Klues, K., Sharp, C., Szewczyk, R., Polastre, J., Buonadonnao, Ph., Nachman, L., Tolleo, G., Cullero, D. and Wolisz, A. (2005). T2: A Second Generation OS for Embedded Sensor Networks. Technical Reports Series, (Ed.) Dr.-Ing. Adam Wolisz.

Markovic, N., Stanimirovic, A. and Stoimenov, L. (2009). Sensor Web for River Water Pollution Monitoring and Alert System. *In:* Proceedings of 12th AGILE International Conference on Geographic Information Science Advances in GIScience, Germany. ISSN 2073–8013.

McCarthy, J.D., Graniero, P.A. and Rozic, S.M. (2008). An Integrated GIS-expert system framework for live hazard monitoring and detection. *Sensors International Journal*, **8**, 830–846.

McGarry, F. (2008). Collaborative Geomatics for Social Innovation in Environmental Practice. Presented at the First Nations GIS Workshop. Retrieved February 10, 2011 from http://www.comap.ca/index.php?MenuItemID=7

Nakamura, K., Wakabayashi, H., Naoki, K., Nishio, F., Moriyama, T. and Uratsuka, S. (2005). Observation of sea-ice thickness in the sea of Okhotsk by using dual-frequency and fully polarimetric airborne SAR (pi-SAR) data. *IEEE Transactions in Geoscience and Remote Sensing*, **43 (11)**, 2460-2469.

Nickerson, B.G., Sun, Z. and Arp, J. (2005). A sensor web language for mesh architectures. Proceedings of the 3rd Annual Communication Networks and Services Research Conference (CNSR'05), Halifax, NS, Canada. IEEE Computer Society, pp. 269–274.

Rozic, S.M. and Graniero, P.A. (2005). Representing domain and spatial knowledge with ontologies in a spatial decision support framework. *In:* Proceedings of GeoComputation 2005, Ann Arbor, MI. 15 (CD-ROM).

Sahli, N., Jabeur, N. and Badra, M. 2011. Agent-Based Approach to Plan Sensors Relocation in a Virtual Geographic Environment. *In:* Proceeding of International Conference on New Technologies, Mobility and Security (NTMS'2011).

Stockdon, H.F., Sallenger, Jr., A.H., List, J.H. and Holman, R.A. (2002). Estimation of Shoreline Position and Change using Airborne Topographic Lidar Data. *Journal of Coastal Research*, **18(3)**, 502–513.

Thakur, J.K., Thakur, R.K., Ramanathan, A., Kumar, M. and Singh, S.K. (2011). Arsenic Contamination of Groundwater in Nepal – An Overview. *Water,* **3(1)**, 1–20.

Xing, X. (2008). An architectural framework for developing advanced integrated environmental monitoring systems. Unpublished MSc thesis, Department of Earth and Environmental Sciences, University of Windsor.

Zennaro, M., Pehrson, B. and Bagula, A. (2008). Wireless Sensor Networks: a great opportunity for researchers in Developing Countries. *In:* Proceedings of 2nd IFIP International Symposium on Wireless Communications and Information Technology in Developing Countries (South Africa).

# 8

# Geomorphologic Risk Modelling of the Sibiu Depression Using Geospatial Surface Analyses

**Marioara Costea, Roxana Giusca[1] and Rodica Ciobanu[2]**
"Lucian Blaga" University of Sibiu, Faculty of Sciences, Department of Ecology and Environment Protection, Sibiu, Romania
[1]American Sentinel University, Aurora, Colorado, USA
[2]National Brukenthal Museum, Sibiu, Romania

## Introduction

Extreme events in general, and the geomorphologic ones in particular, are highly topical problems. There were addresses by many researchers in the field of geology and physical geography (more specific by the climatologists and geomorphologists), but also by biologists, chemists, ecologists, etc. These are studied through the analysis of some types of processes and production mechanisms, and secondly by the effects they create on other environmental subsystems.

Triggering causes and mechanisms of geomorphologic processes are known. Nevertheless they constitute a threat by their magnitude that occur in some areas and which have a negative impact on short and long term, as well. Among these are: changes in the landscape, land degradation and loss of soil fertility, sometimes irreversible, damage to transport infrastructure, economic losses and even social effects, etc.

Although geomorphologic processes are natural phenomena, man is no stranger to them. He is an integral part in this chain of causes-mechanisms-effects, involving all the chain links. In the context of demographic explosion, industrialization and urban explosion, man has had an impact on the environment, and especially on the landscape through land use, resource management, industry, agriculture and habitat—putting unprecedented pressure on it. Changes of these components can be caused directly or indirectly by human activities resulting in transformations in modelling conditions and in the action mechanisms of the external agents. Avoiding such situations and

J.K. Thakur et al. (eds.), *Geospatial Techniques for Managing Environmental Resources*,
DOI 10.1007/978-94-007-1858-6_8, © Capital Publishing Company 2012

reducing the damage to property or others is possible through a better understanding of the environmental relationships, through continuous monitoring of geomorphologic phenomena and through identifying changes in trends. In this context, a new research direction emerged in recent decades, namely the study of risk (Varnes, 1984).

The risk equation operates with three terms, many times used ambiguously, to define what most people simply call: danger. The risk depends directly on the hazard and vulnerability. The speciality literature is pretty rich in definition and explanations of the concepts (Panizza, 1996; Cannon, 1993; Alcantara-Ayala, 2002).

Panizza (1986) introduced the evaluation of the geomorphologic risk as the amount of the geomorphologic hazard, susceptibility and geomorphologic vulnerability. This study presents these concepts applied to the Sibiu Depression area and different geospatial analyses methods used to estimate the geomorphologic dimension of the risk (Fig. 1). From these concepts we can extrapolate to the geomorphologic risk zoning as function of the environmental components at risk, their distribution in space, evolution in time and probability to occur.

The susceptibility of the Sibiu Depression means the ability to suffer (being affected by) some geomorphologic processes under the influence of internal or external factors (Soeters van Vesten, 1996). The mention of the degree of susceptibility to different geomorphologic processes requires an assessment of local conditions in which they occur. Probability of occurrence of these phenomena is greatest where the potential risk factors accumulate (Zêzere, 2002), and increases the incidence of these phenomena where areas are already affected by earlier geomorphic processes and conditions. When the geomorphological processes risk will occur they will be similar to those which led to their development in the past (Neaupane and Piantanakulchai, 2006).

The vulnerability is quantifiable and South Pacific Applied Geosciences Commission (SOPAC) recommended, in 2005, the Environmental Vulnerability Index (EVI) to be used from an economic perspective. From the environmental point of view, there is the geomorphologic vulnerability which measures the damages within a geomorphologic system as a result of the hazard presence. The hazard can be represented by extreme values or extreme actions of the natural factors, of the human activity or of their combination. The geomorphologic hazards have, as a background, the geologic support over which are added the natural and the anthropic (modified by human) features. Where the vulnerable components or components exposed to the geomorphologic hazard don't exist, the risk is negligible (Alkema and Cavalin, 2001, cited by Giusca, 2006). The same authors highlighted the role of the geomorphologic processes in change of the environmental conditions. They concluded that there is a direct risk as well as an indirect risk.

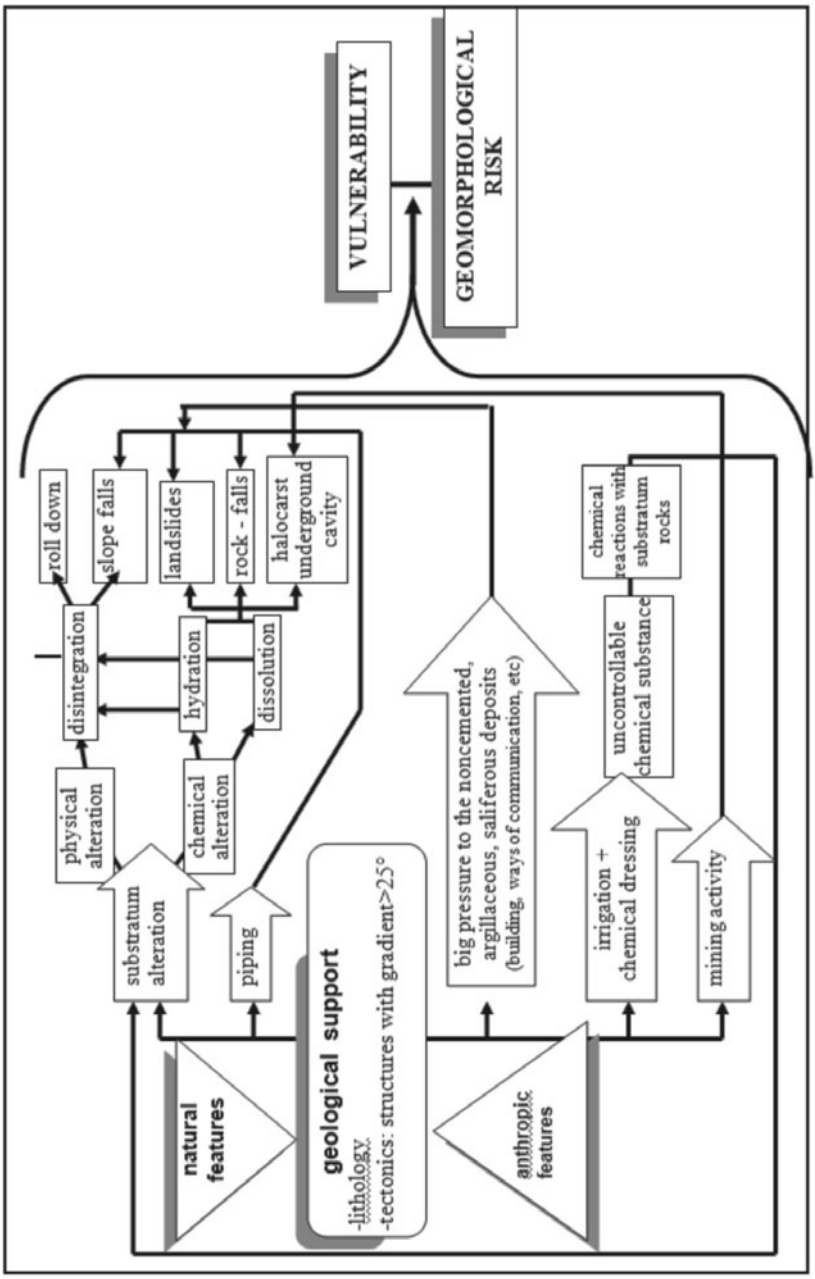


**Figure 1.** The interaction relations among the geologic substratum and the geomorphologic risk phenomenon.
*Source:* Ciobanu R (2007).

Vulnerability assessment is however a more complex and difficult process, involving quantification of social-demographic and economic indicators and assessment of potential losses arising from the nature of geomorphologic processes with risk character. At this point we do not have such data, which makes our research focussed on susceptibility to different geomorphologic hazards. The main data we have are: direct field observations, laboratory processing, data derived from digital terrain model and morphometric maps, from topographic maps, geologic and soil maps.

Today, when the development of information technology and the volume have increased substantially in all of economic and scientific areas, the relief analysis and geomorphologic risks relies increasingly on computer technology with fast processing and modern methods of analysis achieved through complex specialized software, more efficient and effective. Besides, its capability to locate and to show the spatial distribution and extension of the geomorphologic processes, the Geographical Information Systems (GIS) software contains a tremendous collection of tools which can be successfully used to identify and analyze the environmental components. The monitoring of the geomorphologic components as part of the environment and their susceptibility to risk as well as their level of risk can be accomplished using the geospatial techniques, dedicated algorithms or customized scripts/tools.

Therefore, in what follows, we will focus on analyzing the main components of the environment which contribute to the production of the geomorphological phenomena. The aim is to identify key factors and their role in triggering the nature of risk processes.

## The Role of the Environmental Components in Defining the Level of the Geomorphologic Risk

The Sibiu Depression is located in the central part of Romania (Fig. 2), south of the Transylvanian Depression. It is part of the longitudinal and of the sub-


**Figure 2.** The position of the Sibiu Depression within Romania. (*Source* of basis maps www.google.com)

mountainous lane of Fagaras Sibiu-Saliste-Apold, extended between the Olt valley (at east) and Mures and Sebes valleys (at west) (Tufescu, 1966). The Sibiu Depression has a surface of 333 square kilometres and it is drained by the Cibin River and its tributaries from the inferior basin.

The genesis of Sibiu Depression and its asymmetric development could be explained by the transposition in landforms of some particularities resulted from the:

- tectonic contact between two major structuro-genetic units: Southern Carpathians and Transylvanian basin;
- lithological contact between the metamorphic rocks of the southern mountains with the sediments from the plateau region (Ciupagea, Pauca and Ichim, 1970);
- morphological contact clear between the depression area and the Cindrel and Lotru Mountains (in south) and the Transylvanian Plateau (in north) (Posea, 2002);
- evolution of the hydrographical network, the development of the convergent areas situated almost central of the depression area and the fluvial modelling of the Cibin River and its tributaries, which assign the erosion-accumulation to the depression area; and
- relief configuration as a result of the Pliocene-Quaternary evolution in this area; the asymmetric aspect of the depression as a consequence of the decreasing elevation of the landforms from south-south-west to north-north-east: edge-mountainous hills, piedmonts and glacis, the terraces and the river bed of the Cibin River.

The morphological and structural differences are accentuated by the limits between the Sibiu Depression and its neighbours, which increase both the geomorphologic individuality (Sandu, 1998) and risk potential of this depression space. The morphogenetic processes which take place in this area give it a low to moderate dynamic in most of the space (about 75% of surface), except on the areas characterized by a moderate dynamic (15%) and active (almost 10% of surface). Such areas at geomorphologic risk are located at the contact with the surrounding units in high piedmont area, foreheads of terraces and, local in the river beds of Cibin and its tributaries. A variety of geomorphologic processes with risk attributes and with forms of degradation exists in these areas, relatively small compared with the depression surface. Their frequency and intensity depend on the slopes, slope orientation, relief energy and fragmentation level of the versants. They are sustained by geological base which has a high potential of degradation on the alignments fault, on the monoclinal structure of the layers heads or unconsolidated or poorly cemented rocks (marl, clay, sand, gravel, conglomerates) that come in direct contact with the crystalline. The degradation of the versants is also accentuated by the human intervention in the landscape in the area of the Sibiu Depression limits. The dynamic topography and the occurrence of the active forms of degradation

are explained by the accumulation in this small space of propitious natural factors such as lithology, structure, climate and relief morphometry associated with land use (Fig. 3).

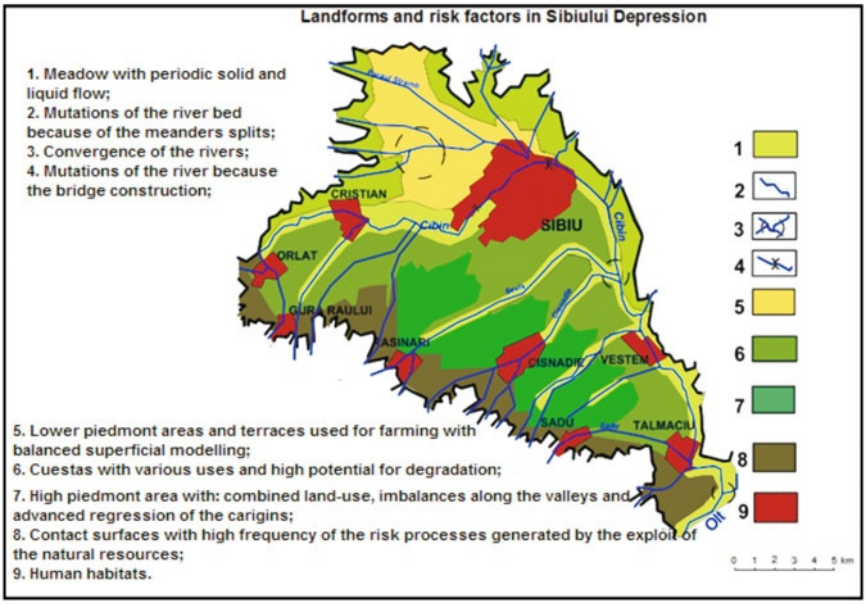


**Figure 3.** Landforms and risk factors in Sibiu Depression.

The inventory of the environmental components, focussed on recording and analysis of the causes of the geomorphologic risk processes, reveals several key issues, namely:

- The accentuated oscillation of level and the convergence of the hydrographic network to the bottom of the depression generate a sum and a transfer of matter and energy that is mirrored in the morphology of the relief, specially of the bounds.
- The lithology and structure, as passive factors condition the selective dynamic of the landforms, and implicitly of landscape, by different mechanical and chemical behaviour of rocks and deposits and by their spatial arrangement. The versants mobility is more pronounced in the contact zone of the studied area with the plateau area, where clay deposits (monoclinal structure) alternate with sand deposits, and in the contact area: Cindrel mountains – Sibiu Depression, where the sedimentary deposits cover the crystalline, which has the function of a bed slip (Ciobanu, 2007).
- Thermal stress is an active factor through: deviation (till +1.5 ºC, or till –1.5 ºC) from the multiannual average of temperature (8.7 ºC), inversions (3-5 ºC and >5 ºC) and their duration (2-20 days) on the depression bottom, diurnal temperature variation and sunstroke on Cuesta Hartibaciu Plateau

and low temperatures on the shadow slopes at the contact mountain-depression; heat waves, as well as the freezing prepare and favour the action of the gravitational or of the run-off processes.

- Mechanical action of the precipitation is favoured by strong heatstroke of the southern slopes of south-western exhibition (Hartibaciu Cuesta, forehead of the rivers terraces), structural steep of the plateau; kinetic energy of rainfall is responsible for ravening and gullying associated to the raindrops impact and rill erosion; this action is amplified by variability of rainfall which fall into depression (precipitation average is 650-700 mm/year), the alternating periods of wet (10-320 mm in excess respect multiannual average) and dry (deficit between 8 and 280 mm) and their torrential character in spring and autumn (the average yearly rainfall in the period from September to November being 30-50 mm).
- The hydrological factors, as a consequence of climatic factors, support the geomorphological risk in riverbeds by the oscillations of flows and levels and their deviations from the normal values of flow (4.72 $m^3$/s at Sibiu; 14.3 $m^3$/s at Talmaciu). Maximum flow is not a risk at Sibiu, because the Cibin River is arranged as hydropower, but downstream to the confluence with Hartibaci River, Cisnadia, and with Talmacel stream it does exists flooding risk due to the confluences in series and due to the progressive contribution of the local tributaries from the plateau or depression.
- One explanation for the degradation of the versants in Sibiu Depression is the deforestation of oak forests in ancient time and changes of the land use. The forest area in the early nineteenth century is still preserved today only about 20%, dispersed in territory.
- The anthropogenic intervention in Sibiu Depression changed the conditions and mechanisms for production of geomorphological processes, leading to vulnerability of the geomorphological system, determining the increasing of climatic and hydrological action. The actual morphodynamic is accelerated by the land use of space by agricultural practices, by the mechanic stress generated by the traffic and heavy constructions on the terraces and glacis and by the clay mine pits on the structural steep of the plateau. However, they represent the nucleus of the intensive degradation of the terraces forehead and versants by undermining and new plans of "attack" for the run-off, gullying, sliding and collapse processes. The impact of the exploits is also due to the drainage, uncover of the soil on the cuesta, and the lack of the fixing work of the deposits and the lack of the ecological rehabilitation.

The combination of the potential factors mentioned above, the alternation and the coincidence of the manifestation of these in time and space assign an active, morpho-dynamic and high degradation potential for some sectors of the Sibiu Depression versants. The geomorphologic processes which lead to the terrain degradation in these areas don't act isolated, they act associated in morphogenetic systems (Ielenicz, 2004). The conditions discussed above interact with each other and cause potential instability of geomorphological

system in Sibiu Depression. We must understand that cascaded relationship of these conditions (factors) can affect the geomorphologic system and they can trigger geomorphological processes with risk character. Therefore, it is necessary to raise awareness of the danger that could be generated by these processes and a constant monitoring of the environmental conditions (of the active factors, in particular) (Thakur et al., 2011) and a correct forecast of weather-climatic and hydrological phenomena. The scratchy geological substrate, the high drainage of the landforms in the contact sector between the depression and the neighbour units, the tilt and the differentiated exhibit of the versants determine the variation of the spatial distribution of the actual geomorphologic processes and their grouping by representative zones. These types of grouping will be analysed in three case studies that have different positions within the Sibiu Depression. Delimitation and practical analysis of these areas are subject to the following case studies.

## The Evaluation of the Morphological Parameters Using the Surface Analysis Techniques: Case Studies

Since, as we stated earlier, geomorphologic hazard occurs where repeated events occurred and where it is recorded a combination of morphological factors, the analysis of the modelling conditions must be accompanied by an analysis of morphometric parameters. Comparative analysis of geological map, of the direct observations on the land use and of the spontaneous distribution of the vegetation and the morphometric analysis of maps produced for depression based on GIS methods and techniques, coupled with hydro-climatic conditions, have enabled us to identify areas susceptible to the production of the geomorphologic risk.

To analyse, quantify and estimate the contribution of the environmental components to the geomorphologic risk, we used the surface analyses tools. Using tabular and raster data, we have processed and obtained vectorial data and other raster formats as output. Some of the surface analyses algorithms used to generate the maps are: Slope, Aspect, Curvature, Hillshade etc. These maps were generated for the case studies presented below and offered as the great opportunity to compare the results from one area to another area.

As techniques we also used the Overlay between different maps, such as: topographic map on top of the Digital Elevation Model, slope map combined with the hypsometric maps, stream flow map on top of the topographic map or Digital Elevation Model etc. The overlay provided us the chance to correlate different values of the components, such as elevation with slope, stream order with the slope, aspect etc.

Having the maps in the digital format represents a huge advantage in the process of estimating the geomorphologic risk because there can be run queries, calculate predictions, generate hot-spot maps etc. The quantification of the parameters of various components was critical and GIS algorithms and software

were used to obtain the values of some index. Few of the indices we have calculated were inserted below as parts of the case studies. These processes occur in some areas where they act more intensive and most of the time combined. The areas presented as case studies definitely prove these aspects.

## Cibin River Confluence with Sadu River

One of the major confluence areas, it is represented by the Cibin River with one of its main tributaries, Sadu River.

In this sector, the asymmetry of the Cibin Valley is obvious. On the right side the elevation of the relief decreases in stairs: the Sadu piedmont, Sadu and Cibin terraces and the common meadow of both the rivers; on the left side the contact with the Hartibaciu cuesta is steep (at over 500 m altitude). The overlay of the Slope map, Aspect map, Stream Order map, Elevation Model etc. was very helpful in the process of extraction of some values of interest and to realize the correlation between the analysed parameters (Fig. 4).

Thus, the Slope and Aspect map of this confluence area shows the high values of the slope on the south-east of the confluence. This is the result of the lithology of the versant. The same map contains a dejection cone created by the Sadu River. While the most part of its stream is on the mountain area, after

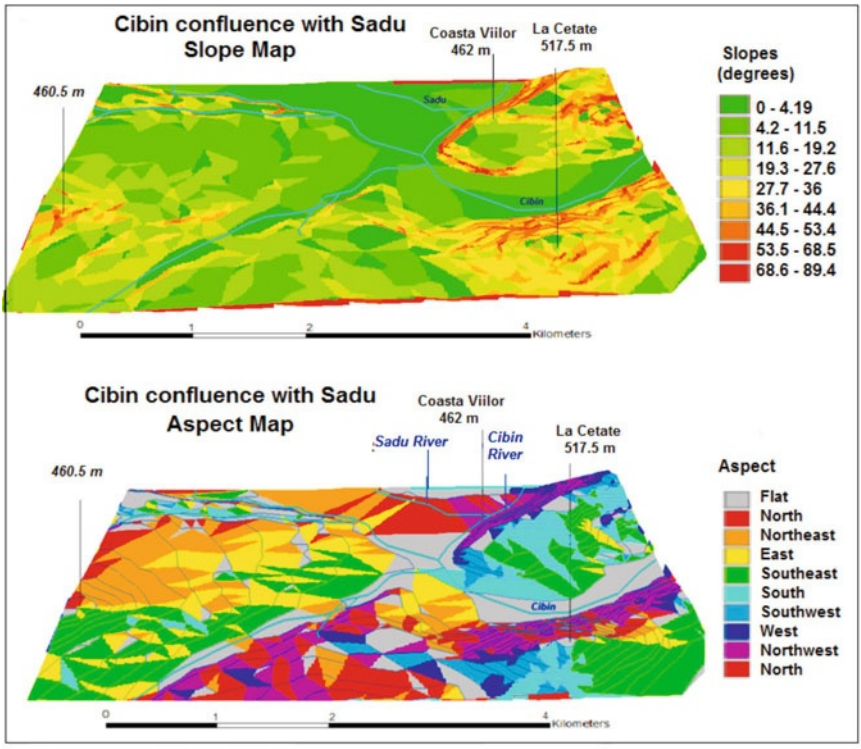


**Figure 4.** Cibin confluence with Sadu – Slope and Aspect map.

it gets to the low area of the Sibiu Depression, the slope decreases and favours the accumulation of the alluvium transported from mountains. The high values of the slope declivity correspond to the north sides of the hills, where the erosion occurred and had broken the equilibrium of the versant. The causes can be identified in the lithology, lack of vegetation and human intervention.

The sedimentary rocks where these two rivers have dug their beds have different facies: sandy-marl, marl-tuff and conglomerates deposited in different conditions of the bathymetry of the Transylvanian basin. Polygenic conglomerates deposited over marl, lead in certain environmental conditions, to risk phenomena-imbalances in the slopes. Conglomerate elements, different in terms of petrographic, react differently to mechanical stress, variations in environmental factors, and most unstable by altering chemical and physical processes which have led to the disintegration of rocks. The marls also favour the passage of water to basis of the versant, increasing slope instability through the processes of alteration and conversion of geologically stable rocks to the unstable rocks. Even more, the marls have thin intercalation of sands, which in turn increases the degree of instability. The values of the slopes varies between zero and 12º in the major river bed and increase to almost 90 º there where the parts of the slopes have broken and have collapsed as a result of the drops of the rain impact and of the surface erosion. The left side of the Cibin Valley in the sector of Talmaciu the valley has an exhibition south-south-west, relief energy ranging between 100-140 m and a fragmentation of 1-2 km/sq km. Together with the declivity, these morphometric parameters increase the slope instability in terms of geological substrate which consists of highly altered polygenic conglomerates. Slope exposition promotes strong heatstroke and by evapotranspiration volume changes contribute to loss of balance and trigger crashes by the processes of evaporative rocks and volume changes. The relief dynamic is accelerated by the improper use of space. In this area the slope base is undermined by human excavation for the removal of rubble, and the surface slope is modified by cutting a road of local importance (for access to a landfill).

The high values of the declivity match the sectors where the Terrain Ruggedness Index has values between 8 and 11 (Fig. 5). This index provides the measure of the terrain heterogeneity and terrain ruggedness affects snow melting patterns and water drainage, which are major factors determining nutrient availability, plant phenology and biomass (Murray and Miller, 1982; Matthes-Sears et al., 1988; Nelleman and Fry, 1995). The Terrain Ruggedness Index is defined as the mean difference between a central pixel and its surrounding cells (Wilson et al., 2007). The units used to evaluate the Terrain Ruggedness Index (TRI) are the same with the ones used to estimate the differences in elevation, which in our case are metres. This index is available as algorithm and tool in several software applications and represents a great opportunity to the users, otherwise being so difficult, almost to calculate it for large areas and to refer its values to the elevation and slope as we did using the GIS software.

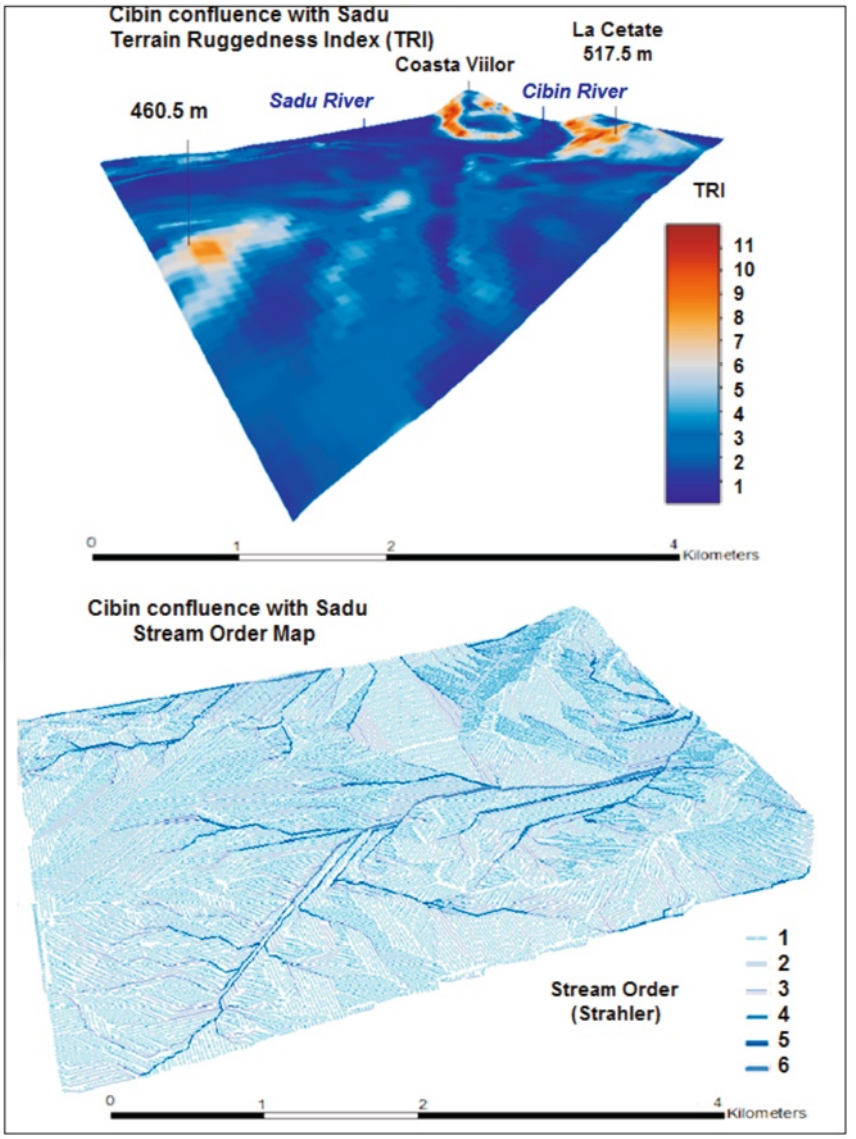


**Figure 5.** Cibin confluence with Sadu – TRI and Stream Order map.

The areas drained by the first and second stream order are ones where the slope corresponds to the unstable surfaces. The Cibin River has the sixth stream order, while Sadu River has fifth stream river order. When it is raining the first two orders of tributaries are receiving water. They cause the erosion on the concave slopes and also depose the silt and alluvium on the convex slopes. When they are dry, they are still representing nuclei of instability. The current solid flow (3, 20 kg/s at Talmaciu) is the result of the solid sediments which were provided by the tributaries downstream of Sibiu, especially by

those that are native to the plateau or to the depression. It is also the result of the erosion of the riverbanks and of erosion of the riverbed bottom of Cibin in depression.

## The Interfluve Sevis-Cisnadie Valley

Gulling, surface run-off and the erosion processes are typical for this area. These processes are installed on the connecting surfaces of the mountainous hills reaching down to the terrace about 500 m altitude and 3rd of Cibin of 450-475 m absolute altitude. Fragmentation is performed by a network of elementary talweg (I, II) with a temporary drain in the hills with their source, tributary of the right of the Sevis or left side of Cisnadie Valley.

The difference in elevation is over 142 metres (Fig. 6).

The consequence of this elevation for such a short distance is the high values of the declivity, as they result from the Slope map (Fig. 7). These morphometric conditions and the lack of forest in this area lead to an accentuated and regressive erosion and also increase the chances of the rills to extend their depth and surface. The sources of the two torrential bodies pass beyond 500 m altitude and catchment boundaries coincide with the line of detachment of landslides of the average depth (2.5-5 m). These processes occur in badenian formations, where specific conglomerates are replaced by sandstones and marl clays.

The deluvio-colluvial glacis with widths of 10-50 m and thickness of about 5-6 m are the junction between the edge-mountainous hills and the third terrace of the Cibin on the south meadow of the Cisnadie River or north to the Sevis. Their formation is related to the withdrawal of the soft rock versants and climatic conditions of the Holocene; the process is active today. The aspect map contains a variety of nuances because of the fragmentation of the terrain and because of the different tilts of this glacis (2-15$^{o}$). It has the look of a terrace inclined towards the axis of the valleys (more suggestive on the Cisnadiei Valley) and its fragmentation was possible due to the high brittleness of the rocks. We signal the presence of the rills and gully length of 3 to 5-10 m and depths of 1.5-2.5 m, which is active nuclei decay.

The terrace deposits through their low consolidation, the layered arrangement and by structure help shallow landslides and gullying processes. They are present on the forehead of the 3rd terrace which is the connection with gravel beds to north and south, or with the 2nd terrace to the east. Terrace deposits are composed of a succession of layers: thick horizon of small gravels embedded in a clay-sandy mass that develops over a horizon from 0.5 to 1 m thick horizon of sandy clay covered by the soil. Clayey-clay component embedded gravel terrace favours the accumulation of large reserves of ground water in the form of lenses. Their depth varies from 2-3 m to 15-16 m. On contact meadow – terrace, or the top of the third terrace, these groundwaters

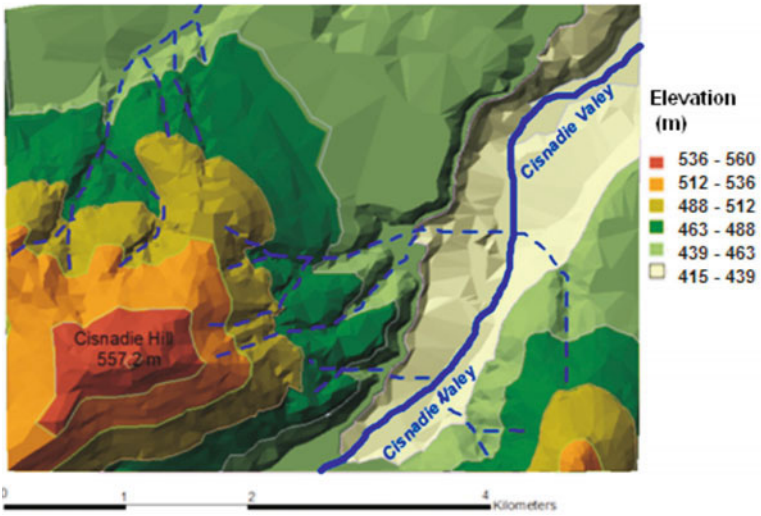


**Figure 6.** Sector of the Cisnadie Valley – Hypsometric-Overlay map.

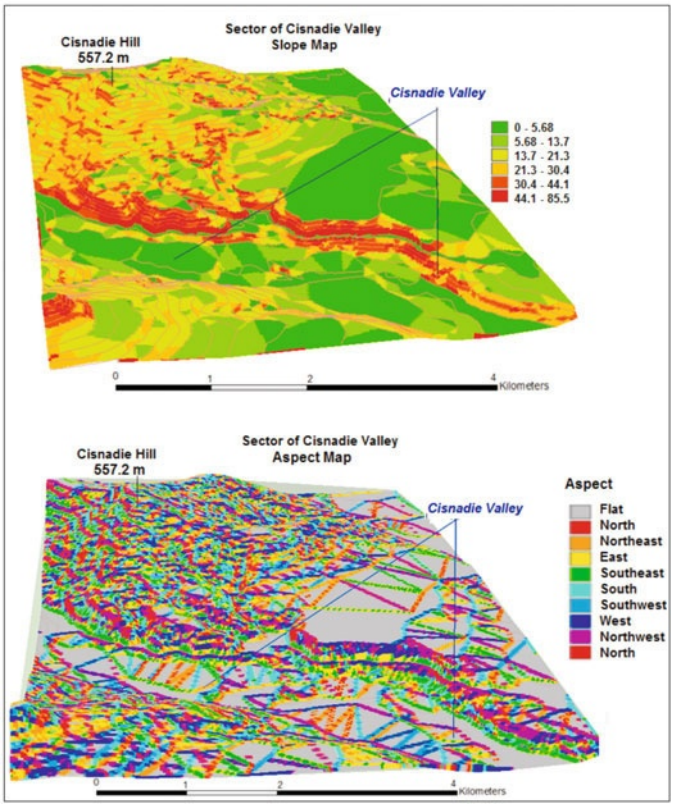


**Figure 7.** Sector of the Cisnadie Valley – Slope and Aspect maps.

affect surface as springs or maintaining wetlands. Thirty years ago, in order to eliminate excess water and for the agricultural land use, land reclamation and drainage works were made. Unfortunately, these arrangements have been neglected over time and drainage channels were clogged and gradually returned to a land use predominantly in the form of pasture and meadow.

The riverbed is also very clearly delineated by the forehead of terrace because of the lateral erosion produced by the river under the condition of rich debits (melt of snow or torrential rains). The Cisnadie River has developed a pretty large meadow and its base level is lower (416 m) than the Sevis level (450 m).

The meadow in this sector is bilateral but asymmetrical, its width varying from 250 m to 1 km. The mobility of the talweg by meanders and splitting is accentuated by the decrease of the slope, and due to the action of the streams which come from the left side of the Cisnadie valley. The meadow landscape is represented by meanders and holms. The sinuosity of Cisnadiei riverbed varies between 1.0 and 1.5 and increases significantly to downstream in terms of a solid carrier composed predominantly of fine sediments (shores, sand) and small gravel, becoming even stronger meandering riverbed downstream to Cisnadie and until the confluence with Cibin river. Some of the sinuosity values presented in this chapter were obtained by using the formula after doing the measurements based on aerial photographs and some are the result of using the Fractal dimension algorithm, which can be finding as tool of some of the GIS software.

## Gusterita Hill

Gusterita Hill lies north and east of the city of Sibiu and it is part of the contact between the depression area and Hartibaciu plateau, marking the alignment cuesta relief units located in the north-west of the county of Sibiu. This area contains elements of the combined action of natural factors as triggers of the geomorphologic processes and of the human action.

In the Gusterita area, geomorphologic risk phenomena are intensified by the rock lithology. Geological deposits of the area include marl and clay at the base, and sand and gravel at the top. Intercalation sand (unconsolidated rock) increased the instability of the stack of rocks on the slopes. Clays, under conditions of high rainfall, retain water, their volume is increasing, they are becoming plastic and cause “flow” along the slopes. Marls also let the water from rainfall to pass, leading to the base of the slope – at the clay level – phenomena of undermining of slope.

The morphometric characteristics have an important role in the morpho-dynamic of this sector. The isometric line of 400 m separates Cibin meadow in this sector and it insinuates to the base of the steep of the plateau structure. The amplitude of the elevation varies from 400 m (on valley) to 598 metres on Padurii Hill (Fig. 8). Besides the valleys, the Wetness Index has high

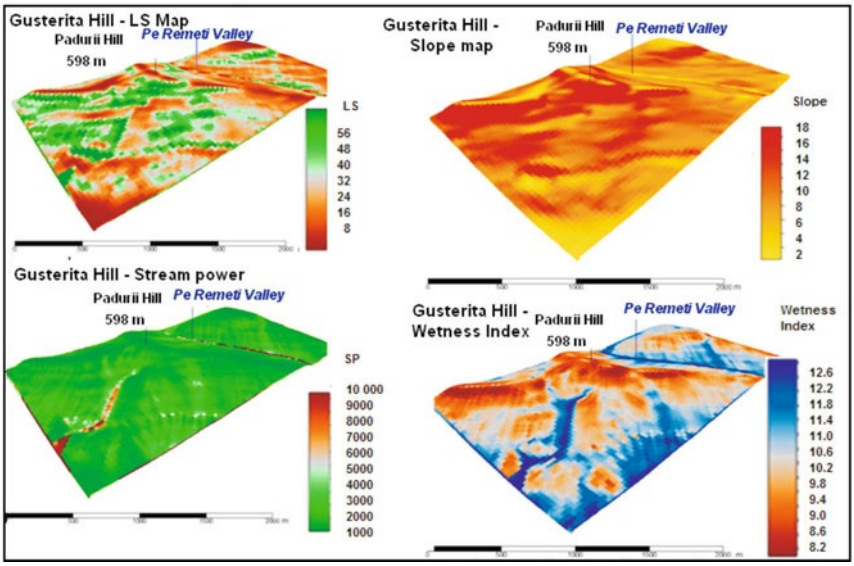


**Figure 8.** Gusterita Hill.

values on the slopes and even higher on the interfluves. Fragmentation of the relief is different depending on the landform. The sliding glacis of Cibin and alluvial plain have a density of fragmentation of 0-0.5 km/sq km and the energy relief of 0-10 m. The forehead of cuesta is fragmented by a temporary and short network, which belongs to the plateau and generates a fragmentation density of 2 to 2.5 km/sq km; the relief energy also varies, the highest recorded values in this sector being 80-140 m. The slopes have differentiated values: minimum of 0-5° on the major riverbed of Cibin and its tributaries, to major values of 10-35°.

The interfluves characterized by very low values of the declivity retain the water because there is no declivity to help the flow. Also the water from rain and snow is not absorbed in totality by the soil due to the clay component of it and due to increased impermeability from clay. The highest values of the slope are concentrated around the Padurii Hill and they have low values on the interfluves and on the convex slopes. The highest frequency of the slopes belongs to the range 10-12 degrees, followed by 8-10 degrees (Toderas and Giusca, 2004). The Slope map presents the cuts on the slope because of the exploitation and also because of the collapse from natural causes.

A mixture of geomorphologic processes, such as landslides, gullying and gravitational collapse process, individualize this area as one with a high geomorphologic risk, compared to the rest of Sibiu Depression. The run-off and piping are also parts of this mixture as a result of the exploitation of marls and clays.

The dynamic of the relief is accelerated by the industrial exploitation with mechanical shocks in clay pit and by the creation of new surfaces with different

slopes and slope differential suitability for processes. The mining terraces (lower slopes) are subject to compaction and suffusion, while operating slopes (greater slopes, even 90º) are subject to sheet erosion, rill erosion and the collapses. Deluvial contribution due to the run-off and gravitational processes also determine the remodelling of the waste dumps stored at the base of the exploits on Gusterita Hill. The intensive exploitation of clay explains the contribution of the coluvio-proluvial deposits to the riverbeds of the creeks. These creeks have an independent character by the monoclinale structure of the layers and they fragment the cuesta Hartibaciu Plateau in this sector (Farmandoala Valley, Pe Remeti Valley).

As we have mentioned, the erosion is present on the concave banks, while the accumulation is representative for the convex banks. To present this process together with the prognosis of their future evolution and to evaluate the potential of the erosion caused by the water streams, we have created and analysed the Stream Power (SP) Index map. This is a function of the surface of the basin and of the slope gradient. Its values for the Gusterita Hill vary within a range between 1000 and 10000. The lowest numbers belong to the interfluves and the highest to the creeks. There are also intermediate values which correspond to ravines and to the rills created on the slopes exploited for clay. An important role is played by the lack of the forest. The vegetation is only represented by the meadow and several sporadic trees, far from enough to retain part of the water which flows on the slopes. An overlay of the maps: Wetness Index, Stream Power Index and Length of Slope, together with the NDVI map (Normalized Difference Vegetation Index), geological, soil and stream order helps to identify the zones with the highest susceptibility at geomorphologic risk.

## The Comparative Analysis

The comparative analysis of case studies allowed us to establish direct, indirect, strong or weak connections between morphology, morphometric parameters, conditions and geomorphological processes with the character of risk on the four areas representative of Sibiu Depression. Links are positive when morphometric parameters and conditions determined an increase of geomorphological phenomena and they are negative when the factors taken into account lower the geomorphological processes with risk character. Conclusive analysis reveals the following aspects:

a. *Direct, strong and positive* connection between:

- high values of the fragmentation, the geologic support composited by unconsolidated and low cemented deposits and the extensions of the gullying and torrentiality on the forehead of Cibin's terraces, the deluvial glacis at Gusterita and at the base of the interfluve Sevis-Cisnadie;
- the values of the slopes, density of the fragmentation, the rain wash processes, gullying and torrentiality are favoured and amplified by the land use as pasture and hay field;

- the fragmentation indexes and the human pressure developed in time by clearing, fallowing, shepherded, agricultural practices of ploughing along the slope;
- the geologic base (clay deposits laminated, clayey sands), the energy of relief, steep slopes (head of cuesta), the land use (slope excavation and exploitation materials) and gravitational processes (collapses, deep landslides) at Gusterita and Talmaciu; a triggering factor is represented by the mechanical shock on the physical and chemical behaviour of rocks and preparatory factors (meteorization); and
- low slopes on the top of terraces or waterside terraces, the terrace or alluvial deposits with high porosity and un-cemented, the density of the communication ways and of buildings and the compaction process (Cibin meadow and terraces).

b. *Direct, strong and negative* connection between the use of forestry and of the orchards and current geomorphologic processes under conditions of low to moderate slope, due to the stability and due to the protection they provide to the land and geological substrate (the forest area of Gusterita Hill and the forest and fruit trees areas in Cisnadie); that use also is involved in regulating of the flow through rainfall interception.

c. *Indirect, weak and positive* connection between the density of fragmentation, slope index, forest plantations on small areas and the torrentiality and gullying; this was demonstrated in the resurgence of the phenomenon in Gusterita Hill because of land reclamation through afforestation measures only in the drains of the torrents zone and not in the catchment, which didn't have the desired effect.

d. *Indirect, strong and positive* connection between:

- the morphological sloping surfaces and their division into small areas (lots) and the rain wash and gullying processes which increases the drainage density on the border between the lots boundaries (Gusterita Hill, foreheads of terraces, Cisnadie Hill); and
- from the sloping surface morphology, the land use, drainage channel processes and river bed processes. Cibin and Cisnadie river's beds stand by the recrudescence of riverbed erosion processes during wet and dry storage periods. This oscillation is subject to vulnerability of climatic and hydrological conditions, and watershed management related areas (Costea, 2006).

Reports identified above are valid for the whole depression area, but at a different scale of intensity. They are driven primarily by slope, relief intensity and density of fragmentation and anthropogenic climate conditions listed above. Given that, the largest area of central depression located almost in middle (about 230 sq km, i.e. 69%) has slopes ranging from 0-5°, fragmentation between 0 and 0.75 km/sq km and energy of relief 0-40 m/sq km, is to be emphasized that the stability of the landscape and geomorphological processes

are reduced in the centre and steep at the periphery (where the relief varies from 50 to 150 m/sq km, drainage density is 2-5 km/sq km and slopes vary up to 45°).

In this context, the results of the quantification of the susceptibility of geomorphologic risk for the entire surface of the Sibiu Depression (333 sq km) shows that: 54.41% doesn't present the risk of producing actual geomorphologic processes, 9.23% are settlements (covered with infrastructure), and the rest of 36.36% present different levels of risk: 5.38% high risk, 21.41% average risk and 9.57% low risk. The case studies presented by us belong to the high and moderate geomorphologic risk.

While most of the indexes and the values of the parameters presented in this chapter were calculated and plotted using GIS techniques and models, the data is stored and it consists in a database which is very valuable to the decision makers from the local administration, transportation, real-estate etc. Other advantages consist in following the temporal evolution of the data and the environmental monitoring in space.

## Conclusions

Geomorphologic risk assessment must be made by reference to natural and the anthropic factor. The study conducted for the Sibiu Depression, based on the weight analysis of morphological parameters, the identification of critical thresholds in the evolution of geomorphologic processes and selective areas of GIS methods, made possible identifying some risk areas.

*Moderate risk area* includes a low floodplain area of Cibin River downstream Sibiu, lower meadows of the tributaries, terraced overheads and sliding glacis at the base of cuesta. Land use is diverse (grassland, pastures, farms and industrial). As risk factors we include: the direct influence of rivers by floods, moisture excess due to the presence of the groundwater near the surface and due to the sources. The channel processes are predominant: accumulation, meandering, lateral erosion, undermining and collapse of banks. On slopes with low-moderate inclination on glacis and top of terraces the predominant processes are: splash and sheet erosion, rill erosion and gullying, associated with superficial and small depth landslides.

*High risk area* covering the entire surface of the western slope of the Hartibaci Plateau between Sibiu and Talmaciu, with a reduced stability induced by high levels of declivity and relief energy. The very active morphodynamic processes is due to mass movement (landslides deep collapse), and due to the gullying and torentiality. Reactivation potential is high due to high rainfall and the presence of coastal springs. We note the presence of very high-risk nuclei caused by human activity as exploits of clay in the industrial system. Most of the classification criteria and of the typologies presented in this chapter can be inserted to the GIS software as algorithms to enable the specialists to realize selective analyses of the geomorphologic risk. To extract

the indices which concur to the geomorphologic risk study, these analyses could be realised using the overlay technique. Even more, the data from the geomorphologic studies can be overlaid to the demographical data (plotted from the statistics) to show the impact of the geomorphologic processes with different levels of risk to the human habitats. That will ease the assessment of the risk. To ensure the accuracy and the precision of the data, Global Position (GPS) receivers with under-metre accuracy can be used. This high accuracy is necessary to evaluate the dynamic of the landslides, gullying and other current processes and the data is easy to be made accessible to the GIS.

In conclusion, the technology we have used in the monitoring activity had started since the phase of planning, have continued with the data acquisition process, analyses algorithms and it ended with the interpretation of the results and their storage to a database. We have also used Remote Sensing data such as aerial images to follow the meanders and other changes occurred to the environment. These images, integrated to GIS offer valued information about the evolution, which may be positive or negative of the components of the geomorphologic system.

The research we have done using the geospatial techniques can be the scientifically based startup to establish the specific strategies and objectives of the management to reduce, prevent and protect against the geomorphologic processes with risk character. We refer to the interventions which interest the durable development of the space by the control of the building development areas, land reclamation, works to improve the degradation and ecological restoration of degraded areas. Local government involvement is imperative in the development of risk maps and action plans that will lead to a better space management. This can be accomplished with the participation of the geologists, geomorphologists and of the advanced techniques to process the data in regional and local planning projects.

## References

Alcantara-Ayala, I. (2002). Geomorphology, natural hazards, vulnerability and prevention of natural disasters in developing countries. *Geomorphology*, **47**, 107–124, Amsterdam, Elsevier.

Alkema, D. and Cavallin, A. (2001). Geomorphologic Risk Assessment for EIA, Studi Trontini, di Scienze Natureli. *Acta Geologica*, **78**, 139–145.

Cannon, T. (1993). A hazard need not a disaster make: vulnerability and the causes of natural disasters. *In:* Merriman, P.A., Browitt, C.W.A. (Eds.), Natural Disasters: Protecting Vulnerable Communities (pp. 92– 105). Thomas Telford, London.

Ciobanu, R. (2007). The implications of the geological support in the geographical risk phenomena: the Sibiu County case. *Brukenthal. Acta Musei*, Sibiu, **II(3)**, 19–29.

Ciupangea, D., Pauca, M. and Ichim, Tr. (1970). Geologia Depresiunii Transilvaniei. Bucuresti, Editura Academiei.

Costea, M. (2006). Riscul la inundatii. Impactul in peisaj. *In:* Stef, V. and Costea, M. (Eds.), Hidrologie aplicata (pp. 205–240). Sibiu, Editura Universitatii "Lucian Blaga".

Giusca, R. (2006). Modele ale degradarilor de teren din Muntii Sureanu, Muntii Cindrel si Depresiunea Sibiului. Sibiu, Editura Universitatii "Lucian Blaga".

Ielenicz, M. (2004). Geomorfologie, Editura Universitatii, Bucuresti.

Matthes-Sears, U., Matthes-Sears, W.C., Hastings, J.C. and Oechel, W.C. (1988). The effects of topography and nutrient status on the biomass, vegetative characteristics, and gas exchange of two deciduous shrubs on an arctic tundra slope. *Arctic and Alpine Research*, **20**, 342–351.

Murray, C. and Miller, P.C. (1982). Phenological observations of major plant growth forms and species in montane and Eriophorum vaginatum tussock tundra in central Alaska. *Holarctic Ecology*, **5**, 109–116.

Neaupane, K.M. and Piantanakulchai, M. (2006). Analytic network process model for landslide hazard zonation. *Engeneering Geology*, **85**, 281–294.

Nellemand, C. and Fry, G. (1995). Quantitative Analysis of Terrain Ruggedness in Reindeer Winter Grounds. *Arctic*, **48(2)**, 172–176.

Panizza, M. (1986). The geomorphological hazard assessment and the analysis of geomorphological risk. *In:* V. Gardiner (ed.). *International Geomorphology*. Wiley, Chichester, 225–229.

Panizza, M. (1996). Environmental Geomorphology in Developments. Earth Surface Processes 4, Elsevier, Amsterdam.

Posea, Gr. (2002). Geomorfologia Romaniei. Bucuresti, Editura Fundatiei "Romania de Maine".

Sandu, M. (1998). Culoarul depresionar Sibiu – Apold. Studiu geomorfologic. Bucuresti, Editura Academiei.

Soeters, R. and van Westen, C.J. (1996). Slope instability recognition, analysis and zonation. *In:* Turner, A.K. and Schuster, R.L. (Eds.), Landslides. Investigation, Mitigation, Transportation Research Board (pp. 129–177). Special Report 247, National Academy Press, Washington D.C.

Thakur, J.K., Srivastava, P.K., Singh, S.K. and Vekerdy, Z. (2011). Ecological monitoring of wetlands in semi-arid region of Konya closed basin, Turkey. Regional Environmental Change (DOI: 10.1007/s10113-011-0241-x).

Toderas, T. and Giusca, R. (2004). Aplicarea noilor tehnici GIS in evaluarea reliefului din Depresiunea Sibiului. *Revista Geografica*, Bucuresti, 68–72.

Tufescu, V. (1966). Subcarpatii si Depresiunile marginale ale Transilvaniei, Bucuresti, Editura Stiintifica.

Varnes, D.J. (1984). Landslide hazard zonation: A review of principles and practice. United Nations International, Paris.

Wilson, M.F.J. et al. (2007). Multiscale terrain analysis of multibeam bathymetry data for habitat mapping on the continental slope. *Marine Geodesy*, **30**, 3–35.

Zêzere, J.L. (2002). Landslide susceptibility assessment considering landslide typology. A case study in the north Lisbon (Portugal). *Natural Hazards and Earth System Sciences*, EGU. **2**, 73–82.

http://www.vulnerabilityindex.net/evi_2005.htm

# 9

# Geospatial Technique to Study Forest Cover Using ALOS/PALSAR Data

**Ram Avtar, Jay Krishna Thakur[1], Amit Kumar Mishra[2] and Pankaj Kumar[3]**

Institute of Industrial Science, The University of Tokyo, 4-6-1 Komaba Meguro-Ku, Tokyo-153-8505, Japan

[1]Department Hydrogeology and Environmental Geology, Institute of Geosciences, Martin Luther University, Halle (Saale), Germany

[2]Graduate School of Environmental Studies, Nagoya University Nagoya 464-8601, Japan

[3]Graduate School of Life and Environmental Sciences University of Tsukuba, Tsukuba, Japan

## Introduction

Forests are one of the most crucial life supporting system that provide range of economic, social and environmental benefits, including essential ecosystem services such as climate change mitigation and adaptation. Forest plays an important role in maintaining ecological balance and homeostatic in the environment (Wulder and Franklin, 2003). Forest cover mapping is necessary for sustainable management and utilization of forest resources. Forest cover monitoring based on geospatial data can significantly contribute in future forest management plans for reducing deforestation and implementation of climate change mitigation policies. Establishing a reliable baseline of forest cover and monitoring forest cover change in the tropical countries become essential (FAO, 2001; REDD, 2010). Recent report of FRA (2010) shows the global change in forest area is about –5.2 million hectares per year during 2001-2010.

Forest cover mapping through ground surveys is labour intensive, time consuming, relatively infrequent and very expensive and these maps become easily outdated. Geospatial techniques like remote sensing and geographical information system (GIS) become useful for forest cover monitoring in a cost and time effective way (Williams et al., 2006). In tropical countries the frequent

J.K. Thakur et al. (eds.), *Geospatial Techniques for Managing Environmental Resources*, DOI 10.1007/978-94-007-1858-6_9, © Capital Publishing Company 2012

cloud cover often restrains the acquisition of optical remote sensing data. Radar data become feasible way of acquiring remotely sensed data within a given time frame because radar system can collect data in all weather conditions. Due to this unique feature, radar data have been used extensively in many fields, including forest cover identification and mapping (Lu, 2006).

In January, 2006, Japan Aerospace Exploration Agency (JAXA) launched the Advanced Land Observation Satellite (ALOS) with Phased Array type L-band Synthetic Aperture Radar (PALSAR) sensor. PALSAR provides L-band synthetic aperture radar (SAR) data, which is quite useful for forest cover and deforestation monitoring because, it has the higher penetration to the vegetative areas (Rosenqvist, 2007). It has quad polarization (HH, HV, VH and VV) mode, which characterize various targets on the basis of physical, dielectric and geometric properties. The ability of PALSAR data to retrieve more information about physical properties of the targets has led to wide range of its applications; for example in crop monitoring, hydrological modelling, soil moisture, forest monitoring, disaster monitoring, ocean and coastal monitoring etc. (Mcnairn et al., 2009; Entekhabi et al., 2010; Mitnik, 2008).

This study demonstrates the application of full polarimetric PALSAR data for forest cover classification. Full polarimetric PALSAR data determines the types of interaction with different types of forest cover based on their biophysical parameters (tree height, crown diameter, diameter at breast height, biomass, tree density, etc.). Co-polarized signal interact with similar orientation, so vertical stalks interact strongly with VV polarization. Horizontal branches and soil surface interact strongly with HH polarization and cross-polarized signal HV is related to volume scattering (Rignot et al., 1995). On the basis of interaction between various polarization and targets; surface, volume and double-bounce scattering occurs from the scatterers. There are basically two decomposition techniques: (a) coherent decomposition (pure targets) and (b) incoherent decomposition (distributed targets). In this study we have demonstrated the application of eigen vector based Cloude-Pottier decomposition. Cloude-Pottier decomposition for polarimetric classification is based on eigen value and eigen vector calculation of the coherency matrix of quad polarization PALSAR data. This decomposition is useful for extracting the information about polarimetric scattering of various features (Cloude and Pottier, 1996, 1997). Classification based on different polarimetric decomposition entropy ($H$), alpha ($\alpha$) and anisotropy ($A$) is used to understand polarimetric response of SAR data to study purity of target, mean scattering mechanism and number of scattering mechanism involved for each targets (Patel et al., 2009).We used Wishart unsupervised classification method, which classify the image automatically by finding the cluster based on certain criterion (Singh et al., 2008).

The important role of forest in global carbon cycle was pointed out in many previous studies (Brown, 2002; Houghton, 2005; IPCC, 2007; Thakur et al., 2010; Thakur et al., 2011, Avtar et al., 2011). Therefore, it becomes

necessary to effectively monitor forest covers and their changes (deforestation and forest degradation) for effective implementation of REDD policies in a post Kyoto protocol climate change regime. For the REDD policies implementation, it is necessary to monitor forest on a spatial and temporal scale and the results should be reproducible, to provide consistent results, to meet standards for mapping accuracy, and it can be implemented at the national level (Defries, 2007). This study represents the utilization of quad polarimetric PALSAR data for forest cover mapping in a part of Cambodia based on Cloude-Pottier target decomposition theorem. The selection of best SAR based forest classification is highly desirable to get more accuracy and consistency in the results.

## Study Area

Cambodia has an area of 181,035 square kilometers and situated in the southwest corner of Indochina peninsula, bordered by Thailand to the west, Lao P.D.R. to the north, Vietnam to the east and Gulf of Thailand to the south. Cambodia's average temperature ranges from 21° to 35°C. The country experiences the rainy season during May to October and a dry season during November to April. The mean annual precipitation is 150 to 180 cm; more precipitation occurs in mountainous regions. Cambodia has highest rate of deforestation in Indochina countries (Table 1) (FRA, 2010). Between 2000 and 2005 Cambodia had lost 29% of its primary forests (FRA, 2005). Various logging activities, combined with rapid development, population growth, urbanization and agricultural expansion have been the primary reason for Cambodia's forest loss (Gaughan et al., 2009). Cambodia has signed for the REDD policies in 2009 and study of forest cover is necessary for the REDD policies implementation. The study area is situated in part of Stung treng and Kratie province of northern Cambodia and has an area of about 1877.5 $km^2$ (Fig. 1). We visited this study area in December, 2009 and November, 2010 for the ground truth data collection and validation of results.

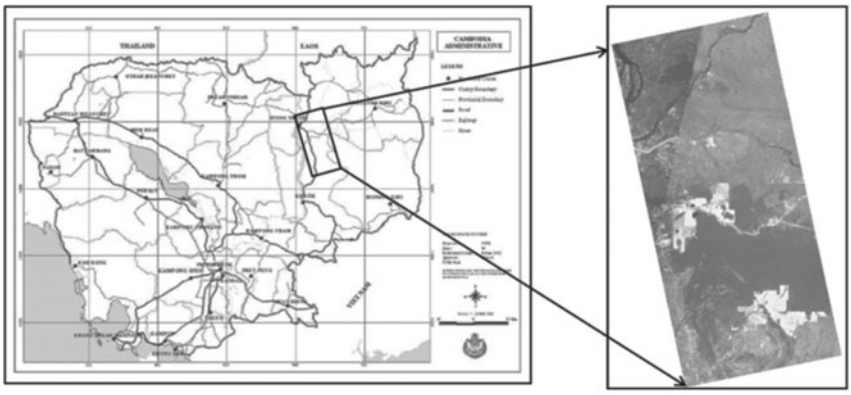


**Figure 1.** Location map of the study area.

**Table 1:** Forest covers change in Indochina countries (FRA, 2010)

| | *Forest area* | | | | *Annual change rate* | | | | | |
|---|---|---|---|---|---|---|---|---|---|---|
| | 1990 | 2000 | 2005 | 2010 | 1990-2000 | | 2000-2005 | | 2005-2010 | |
| Country/area | 1000 ha | 1000 ha | 1000 ha | 1000 ha | 1000 ha/yr | % | 1000 ha/yr | % | 1000 ha/yr | % |
| Cambodia | 12,944 | 11,546 | 10,731 | 10,094 | -140 | -1.1 | -163 | -1.4 | -127 | -1.2 |
| Lao PDR | 17,314 | 16,532 | 16,142 | 15,751 | -78 | -0.5 | -78 | -0.5 | -78 | -0.5 |
| Myanmar | 39,218 | 34,868 | 32,321 | 31,773 | -435 | -1.2 | -309 | -0.9 | -310 | -0.9 |
| Thailand | 19,549 | 19,004 | 18,898 | 18,972 | -55 | -0.3 | -21 | -0.1 | 15 | 0.08 |
| Vietnam | 9,363 | 11,725 | 13,077 | 13,797 | 236 | 2.3 | 270 | 2.2 | 144 | 1.08 |

## Forest Cover Map of the Study Area

Forests are valued for their high biodiversity and commercial importance and play an important role in social, economic and cultural development of rural areas (Kummer and Turner, 1994). Forest cover map (Fig. 2) was generated using the maximum likelihood classification techniques. ASTER data acquired in 2005 was used to generate forest cover map of the area supported with ground truth data. The study area was classified into various forest cover classes such as deciduous forest, evergreen forest, mixed forest, agricultural land, water and other classes. Most of the area is covered by deciduous forest followed by evergreen forest. Table 2 shows percentage of area covered by various forest cover classes.

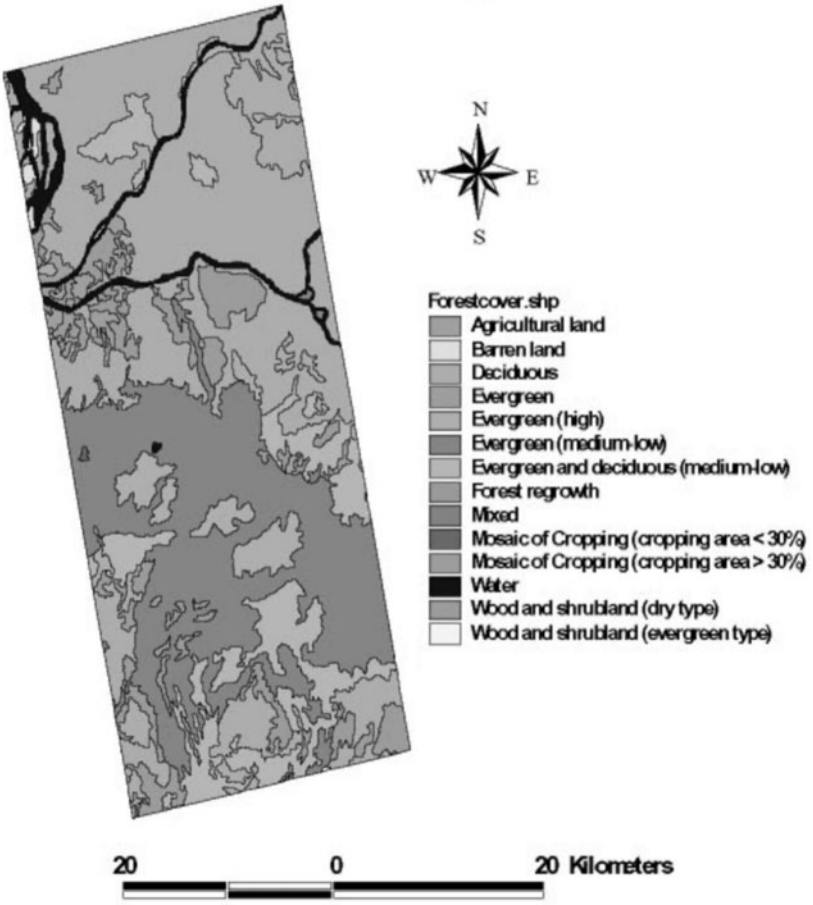


**Figure 2.** Forest cover map of the area.

**Table 2:** Percentage of different types of forest cover of study area

| *Land use classes* | *Area ($km^2$)* | *% of land cover* |
|---|---|---|
| Evergreen | 0.88 | 0.05% |
| Agricultural land | 33.36 | 1.78% |
| Barren land | 7.02 | 0.37% |
| Deciduous | 809.05 | 43.09% |
| Evergreen (high) | 55.02 | 2.93% |
| Evergreen (medium-low) | 520.21 | 27.71% |
| Evergreen and deciduous (medium-low) | 222.50 | 11.85% |
| Forest regrowth | 1.56 | 0.08% |
| Mixed | 1.16 | 0.06% |
| Mosaic of Cropping (cropping area < 30%) | 0.76 | 0.04% |
| Mosaic of Cropping (cropping area > 30%) | 9.92 | 0.53% |
| Water | 58.28 | 3.10% |
| Wood and shrubland (dry type) | 157.35 | 8.38% |
| Wood and shrubland (evergreen type) | 0.40 | 0.02% |
| Total area | 1877.47 | 100.00% |

## Methodology

We used PALSAR 1.1 level full polarimetric single look complex (SLC) data acquired on 6th April, 2009 with 21.5° look angle. For data processing we used the PolSARpro4.03 software (Pottier, 2008). The detailed methodology is shown in the flow chart (Fig. 3). Most of the objects in the study area are natural vegetation, therefore Cloude-Pottier incoherent target decomposition model has been used in this study.

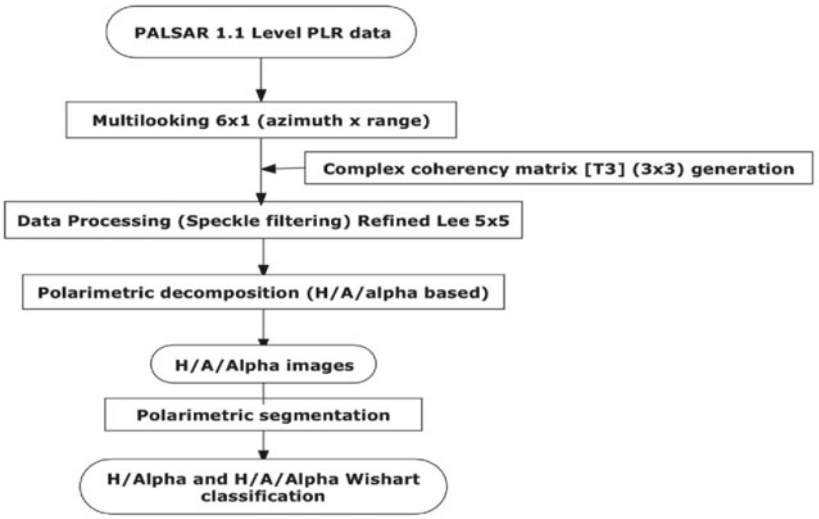


**Figure 3.** Flow chart of the methodology adopted for polarimetric classification.

## Cloude-Pottier Decomposition

Polarimetric decomposition is used to understand the physical characteristics of various scatterers. Cloude and Pottier proposed a method of extraction of mean diffusion based on eigen values/eigen vectors decomposition of coherence matrix (Cloude and Pottier, 1997). A target coherence matrix [*T*] can be expressed as

$$[T] = [U][\Lambda][U]^{-1} \tag{1}$$

where [Λ] is a diagonal matrix with non negative real element and [*U*] is a unitary matrix.

The real nonnegative diagonal matrix [Λ] of eigen value of coherency matrix is defined by

$$[\Lambda] = \begin{bmatrix} \lambda_1 & 0 & 0 \\ 0 & \lambda_2 & 0 \\ 0 & 0 & \lambda_3 \end{bmatrix} \tag{2}$$

If only one eigen value is non zero then the scattering can be related to pure target. If all eigen values are non zero and identical then the average coherency matrix represents a completely decorrelated, unpolarized random scattering target. In between these two cases, scattering matrix represents the distributed or partially polarized scatterers.

The 3 × 3 unitary matrix [*U*] of the three eigen vectors of coherency matrix is

$$[U] = [u_1\, u_2\, u_3] \tag{3}$$

where $u_1$, $u_2$ and $u_3$ are the three unit orthogonal eigen vectors. The eigen vector can be expressed as

$$u_i = \begin{bmatrix} & \cos\alpha_i & \\ \sin\alpha_i & \cos\beta_i & e^{-j\delta i} \\ \sin\alpha_i & \cos\beta_i & e^{-j\gamma i} \end{bmatrix} \tag{4}$$

where $i$ = 1, 2 and 3.

Equation (4) can be expressed as

$$[T] = \sum_{i,j=1}^{3} \lambda u_i u_i^{*T} \tag{5}$$

Based on this eigen value decomposition three secondary parameters viz., entropy, anisotropy and alpha can be defined as function of the eigen values

of the coherency matrix. Entropy, α angle and anisotropy are polarimetric features derived from eigen values and eigen vectors (Lee and Pottier, 2009). *H*/α/*A* is used to interpret target scattering properties. Entropy (*H*) indicates the randomness of the scatterers. *H* equals to 0 for the pure targets, whereas 1 for the distributed target (no dominant scatterers).

$$H = \sum_{i=1}^{3} -P_i \log_3 P_i \tag{6}$$

$$0 \le P_i = \frac{\lambda_i}{\sum_{i=1}^{3} \lambda_i} \le 1 \tag{7}$$

where $P_i$ is pseudo-probabilities, which can be obtained from the eigen values, $\lambda_i$ represents relative intensity of the *i*-th scattering process.

The alpha (α) angle is acquired from $\alpha_i$ angle of each of the eigen vectors as follows

$$\bar{\alpha} = \sum_{i=1}^{3} P_i \alpha_i \tag{8}$$

α measures the dominant scattering mechanism within a specified target. It varies between 0° to 90°. α = 0° represents odd-bounce scattering from flat surfaces, α = 45° represents dipole or volume scattering, while α = 90° represents a double bounce scatterer or dipole scattering.

In case of more than one dominant scatterer ($H > 0.7$), anisotropy (*A*) is introduced because the second and third eigenvalues are highly affected by noise for low entropies. *A* is acquired from the second and third eigen values as

$$A = \frac{\lambda_2 - \lambda_3}{\lambda_2 + \lambda_3} \tag{9}$$

where $\lambda_2$ and $\lambda_3$ are smaller eigen values. Anisotropy measures the relative importance of the second and third eigenvalues of the eigen decomposition. If $A = 1$, the second scattering process is fairly important and could be employed in discriminating similar surface characteristics (Trisasongko, 2010).

## Classification Technique

*H*/Alpha and *H*/*A*/Alpha Wishart classification approaches have been attempted for the classification of PALSAR image. The Wishart distribution can be expressed by:

$$P\left(\langle T\rangle / T_m\right) = \frac{L_n^{L_n P}\left|\langle T\rangle\right|^{L_n - N} e^{-L_n Tr\left([T_m]^{-1}\langle T\rangle\right)}}{\pi^{\frac{N(N-1)}{2}}\Gamma(L_n - N + 1)[T_m]} \quad (10)$$

where $L_n$ is number of looks and $N$ is polarimetric dimension. Using the complex Wishart distribution of the coherency matrix [$T$], an appropriate distance measure, "$d$", can be calculated according to Bayes maximum likelihood classification as

$$d_m\left(\langle T\rangle\right) = L_n Tr\left([T_m]^{-1}\langle T\rangle\right) + L_n \ln\left([T_m]\right) - \ln\left(P\left([T_m]\right)\right) + K \quad (11)$$

thus leading to a minimum distance classification independent of the number of looks used to form the multi-looked coherency matrix [$T$]:

$$\langle [T]\rangle \in [T_m] \text{ if } d_m\left(\langle [T]\rangle\right) < d_j\left(\langle [T]\rangle\right) \forall j \neq m \quad (12)$$

## Results and Discussion

We used the ASTER generated forest cover map as a reference map (Fig. 2). The polarimetric decomposition was applied on the PALSAR data of April 06, 2009. The Entropy ($H$), Alpha ($\alpha$) and Anisotropy ($A$) of the PALSAR data has been generated from eigen values based target decomposition (Figs 4a, b, c). The entropy value of evergreen forest is higher than deciduous forest. This indicates more statistical disorder (randomness) in evergreen forest as compared to deciduous forest. Forests show a high value of entropy because of distributed targets, which causes depolarization effects due to the volume scattering from the vegetation. The entropy value becomes less for deforested area because most of the deforested area shows the pure target properties (Guerra et al., 2008). This decrease in entropy value is related to identification of deforestation and forest degradation which, can be confirmed by using optical and SAR data supported with ground truth data. The value of alpha shows spatial variation however, most of the area shows value of alpha ranges from 40° to 50° because these regions are covered by forest. Volume scattering is the property of forest, which shows value ranges from 40° to 50°. In case of deforested area the value of alpha decreases (10-20°) because deforested area shows surface scattering (Lee and Pottier, 2009).

Cloude and Pottier has proposed an algorithm to identify unsupervised way of polarimetric scattering mechanisms in the H-alpha plane. The H-alpha classification plane is sub-divided into nine basic zones based on characteristics of different scattering behaviours. The result of this classification is given in Figs 5a and 5b. Figure 5b represents the efficiency of this algorithm in the discrimination of various scattering characteristics. Every zone is used as identification of information associated with particular types of land cover class. It has been observed that most of the pixels fall in random anisotropic scatterers (zone 1), anistropic particle (zone 5), random surface (zone 6) and

bragg surface (zone 9) of the H-alpha plane. Volume scattering and surface scattering are the dominant scattering from the targets. Only very few pixels show double bounce scattering. It might be because of the interaction of the SAR signal with the tree trunk and the ground surface.

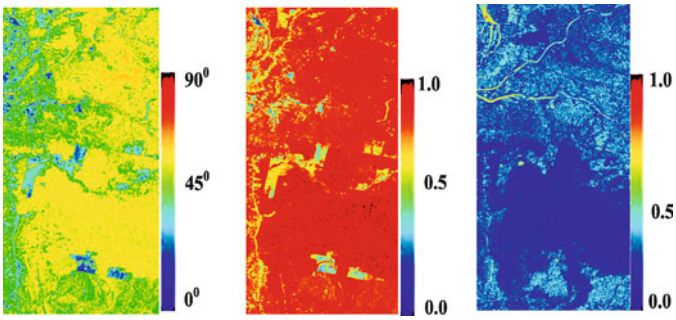


**Figure 4.** (a) Alpha, (b) Entropy and (c) Anisotropy image of PALSAR data.

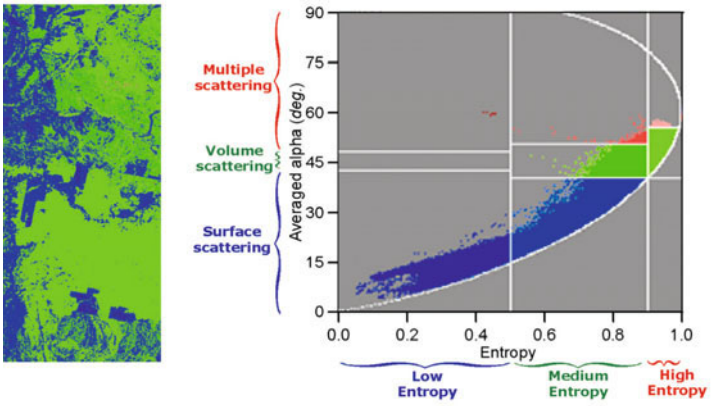


**Figure 5.** (a) H/Alpha segmentation image and (b) H/Alpha segmentation plane.

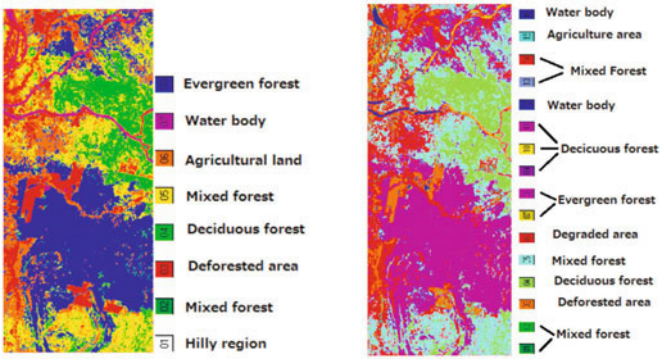


**Figure 6.** (a) H/Alpha (b) H/A/Alpha Wishart unsupervised classified image.

Wishart unsupervised H/Alpha and *H*/*A*/Alpha classification is based upon polarimetric decomposition classification parameters i.e. *H, A*, alpha. The *H*/Alpha Wishart classifier group the total image into eight different classes (Fig. 6a). After introducing anisotropy (*A*), the classifier identifies sixteen different classes (Fig. 6b). Anisotropy (*A*) is useful to discriminate scattering mechanism with different eigen value distribution but with similar intermediate entropy values. The anisotropy image (Fig. 4c) shows most of the area having low value of A which corresponds to dominant first scattering and low secondary scattering mechanism. ASTER based classification and field data has been used to add legends in the image. H/A/Alpha technique classify image into 16 classes therefore we can discriminate different types of forest on the basis of types and density. In Fig. 6b deciduous forest has been divided into three classes and evergreen into two classes as compared to Fig. 6a. These three classes of deciduous forests represents dense deciduous, sparsely deciduous and medium deciduous forest whereas, two classes of evergreen forest represents medium evergreen and medium-low evergreen forest. H/A/Alpha Wishart classification is better than H/Alpha classification. We find some misclassification between deforested area and agricultural area because both the classes show same types of surface scattering properties. If agricultural area has some crops then it might be easy to distinguish from the deforested area as such crops vary in scattering characteristics.

## Conclusion

This study shows use of full polarimetric L-band PALSAR data for forest cover classification. H-alpha plane showed most of the pixels fall in random anisotropic scatterers (zone 1), anistropic particle (zone 5), random surface (zone 6) and bragg surface (zone 9) to discriminate different types of scattering behaviours of targets. Wishart unsupervised classification is useful for forest cover classification. Results show that use of full polarimetric data improves the detection of structural differences between forest canopies, thus helping in better forest type mapping and provide additional information for forest management practices. Based on the experiment, it was concluded that Cloude-Pottier based classification is useful for forest cover mapping. However, further studies should concentrate on the capability of other target decomposition theorems such as Freeman-Durden three component (1998) and Yamaguchi four component decomposition (2006) and their applicability in forestry area is needed to be explored. The new generation of geospatial techniques with full polarimetric SAR data could help to study various biophysical parameters of forest for better implementation of REDD policies.

## Acknowledgements

The authors are highly thankful to the Monbukagakusho (MEXT) Japanese Government fellowship which helped to pursue research. Authors also want

to put on record contribution of Institute of Industrial Science, The University of Tokyo for facilitating data analysis in its labs and also to the Department of Civil Engineering, The University of Tokyo for providing fund during the field visit.

## References

Avtar, R., Singh, C.K., Shashtri, S. and Mukherjee, S. (2011). Identification of erosional and inundation hazard zones in Ken-Betwa River Linking Area, India using remote sensing and GIS. *Environmental Monitoring and Assessment*, doi.org/10.1007/s10661-011-1880-6.

Brown, S. (2002). Measuring carbon in forests: Current status and future challenges. *Environ. Pollut*., **116**, 363–372.

Cloude, S.R. and Pottier, E. (1996). A review of target decomposition theorms in radar polarimetry. *IEEE transactions on Geoscience and Remote Sensing*, **34(2)**, 498–518.

Cloude, S.R. and Pottier, E. (1997). An entropy based classification scheme for land applications of polarimetric SAR. *IEEE Transaction on Geoscience and Remote Sensing*, **35**, 68–78.

Defries, R., Achard, F., Brown, S., Herold, M., Murdiyarso, D., Schlamadinger, B. and De Souza Jr C. (2007). Earth observations for estimating greenhouse gas emissions from deforestation in developing countries. *Environmental Science and Policy*, **10**, 385–394.

Entekhabi, D., Njoku, E.G., O'Neill, P.E., Kellogg, K.H., Crow, W.T., Ed e lstein, W.N., Entin, J.K., Goodman, S.D., Jackson, T.J., Johnson, J., Kimball, J., Piepmeier, J.R., Koster, R.D., Martin, N., McDonald, K.C., Moghaddam, M., Moran, S., Reichle, R., Shi, J.C., Spencer, M.W., Thurman, S.W., Tsang, L. and Van Zyl, J. (2010). The soil moisture active passive (SMAP) mission. *Proceedings of the IEEE*, **98(5)**, 704–716.

FAO (2001). State of the World's forests. Food and Agriculture Organisation of the United Nations, Rome.

FRA (2005). Global Forest Resources Assessment. Food and Agriculture Organisation of the United Nations, Rome.

FRA (2010). Global Forest Resources Assessment. Food and Agriculture Organisation of the United Nations, Rome.

Freeman, A. and Durden, S.L. (1998). A three-component scattering model for polarimetric SAR data. *IEEE transactions on Geoscience and Remote Sensing*, **36**, 963–973.

Gaughan, A.E., Binford, M.W. and Southworth, J. (2009). Tourism, forest conversion, and land transformations in the Angkor basin, Cambodia, *Applied Geography*, **29**, 212–223.

Guerra, J.B., Freitas, C.D.C. and Mura, J.C. (2008). Evaluating potential of band polar data to discrimination increment areas in Amazon rain forest. Proceedings of IEEE IGARSS08.

Houghton, R.A. (2005). Aboveground forest biomass and the global carbon balance. *Global Change Biology*, **11**, 945–958.

IPCC (2007), Climate Change 2007: Fourth Assessment Report of the Intergovernmental Panel on Climate Change, edited by S. Solomon et al. Cambridge Univ. Press, Cambridge, U.K.

Kummer, D.M. and Turner, B.L. (1994). The human causes of deforestation in Southeast Asia. *Bioscience*, **44(5)**, 323–326.

Lee, J.S. and Pottier, E. (2009). Polarimetric radar imaging: From basics to application, CRC Press, Taylor and Francis Group, Boca Raton.

Lu, D. (2006). The potential and challenge of remote sensing-based biomass estimation. *International Journal of Remote Sensing*, **27(7)**, 1297–1328.

McNairn, H., Shang, J., Jiao, X. and Champagne, C. (2009). The contribution of ALOS PALSAR multipolarization and polarimetric data to crop classification. *IEEE Transactions on Geoscience and Remote Sensing*, **47(12)**, 3981–3992.

Mitnil, L.M. (2008). Advanced land observing satellite PALSAR observations of the oceanic dynamic phenomena in the coastal zone. IEEE, IGARSS 2008.

Patel, P., Srivastava, H.S. and Navalgund, R.R. (2009). Use of synthetic aperture radar polarimetry to characterize wetland targets of Keoladeo National Park, Bharatpur, India. *Current Science*, **97(4)**, 25, 529–537.

Pottier, E., Ferro-Famil and Lee, J.S. (2008). POLSARPRO V4.0 – lecture notes: Advanced concepts. Available at: http://earth.esa.int/polsarpro/.

REDD (2010). Resource book, GOFC-GOLD.

Rignot, E., Zimmermann, R. and Zyl, van J. (1995). Spaceborne applications of P band imaging radars for measuring forest biomass. *IEEE Transactions on Geoscience and Remote Sensing*, **33(5)**, 1162–1165.

Rosenqvist, A. et al. (2007). ALOS PALSAR: A Pathfinder Mission for Global-Scale Monitoring of the Environment, *IEEE Transactions on Geoscience and Remote Sensing,* **45(11)**, 3307–3316.

Singh, G., Venkataraman, G., Kumar, V., Rao, Y.S. and Snehmani (2008). The H/A/Alpha polarimetric decomposition theorem and complex wishart distribution for snow cover monitoring. Presented in IGARSS'08 at Boston, USA.

Thakur, J.K., Srivastava, P.K., Singh, S.K. and Vekerdy, Z. (2011). Ecological monitoring of wetlands in semi-arid region of Konya closed Basin, Turkey. Regional Environmental Change (DOI: 10.1007/s10113-011-0241-x).

Thakur, J.K. and Singh, S.K. (2010). Eco-hydrological monitoring of wetlands in a semi-arid region using remote sensing, GIS, GPS and various data sets: A case study of Konya closed basin, Turkey IAH 2010, Krakow, Poland.

Trisasongko, B.H. (2010). The use of polarimetric SAR data for forest disturbance monitoring. *Sens Imaging*, **11**, 1–13.

Williams, K., Sader, S.A., Pryor, C. and Reed, F. (2006). Application of geospatial technology to monitor legacy conservation easements. *Journal of Forestry*, **104**, 89–93.

Wulder, M.A. and Franklin, S.E. (2003). Remote sensing of forest environments concepts and case studies. Kluwer Academic Publishers, London.

Yamaguchi, Y., Yajima, Y. and Yamada, H. (2006). A four-component decomposition of POLSAR images based on the coherency matrix. *IEEE Geoscience and Remote Sensing Letter*, **3**, 292–296.

# 10

# Assessment of Land Use/Land Cover Using Geospatial Techniques in a Semi-arid Region of Madhya Pradesh, India

**Prafull Singh, Jay Krishna Thakur[1], Suyash Kumar[2] and U.C. Singh[3]**
Dept. of Civil Engineering, SAMCET, Bhopal, Madhya Pradesh, India
[1]Dept. Hydrogeology and Environmental Geology, Institute of Geosciences, Martin Luther University, Halle, Germany
[2]Department of Geology, Govt. PG Science College, Gwalior, India
[3]School of Studies in Earth Science, Jiwaji University, Gwalior, India

## Introduction

The Earth's land cover characteristics and its use are key variables in global change. The society today is already in the mainstream of another revolution – the information revolution. This brings enormous changes to life and living, providing new approaches: how to advance the frontiers of previous revolutions particularly those of earth resources mapping and monitoring. Over the last few decades, there has been a significant change on land use and land cover (LULC) across the globe due to the climatic changes and over demand of the growing inhabitants. Semi-arid regions are undergoing severe stresses due to the combined effects of growing population and climate change (Mukherjee et al., 2009). In the last three decades, the technologies and methods of remote sensing have progressed significantly. Now a days remote sensing data, along with increased resolution from satellite platforms, makes these technology appear poised to make better impact on land resource management initiatives involved in monitoring LULC mapping and change detection at varying spatial ranges (Singh et al., 2010; Thakur, 2010). Remote sensing technology offers collection and analysis of data from ground-based, space and Earth-orbiting platforms, with linkages to Global Positioning System (GPS) and geographic

J.K. Thakur et al. (eds.), *Geospatial Techniques for Managing Environmental Resources*,
DOI 10.1007/978-94-007-1858-6_10, 

information system (GIS) data with promising modelling capabilities (Franklin, 2001; Thakur et al., 2010). This has made remote sensing valuable for land cover and land use information.

As the demand for quantity and quality of information and technology continues to improve, remote sensing is becoming more significant for the future. Therefore, the chapter focuses on the issues and challenges associated with monitoring LULC mapping in semi-arid region. For example, at the rural-urban fringe, large tracts of undeveloped rural land are rapidly converted to urban land use. To maintain up-to-date land-cover and land use information, where typical updating processes are on an interval scale of five years, is difficult task for planners (Chen et al., 2002). The full potential of geospatial technology for change detection applications still has to be realized for planners at local, regional, and international levels. In the near future, the field of remote sensing will change dramatically with the projected increase in number of satellites of all types (Glackin, 1998). In order to have better understanding of the rapid advancements in geospatial technology, we provide a brief history of the advances in geospatial technology.

In developing countries like India, efforts are being made for the sustainable land resource planning and management with reliable and updated geoinformation, which is pre-requisite for land use planning. Such information could only be obtained through the modern techniques and equipment for research and mapping. Since land use and land cover changes are active features over space and time, it is difficult to obtain real time information through conventional resources and these methods are time consuming, laborious, high cost and work force oriented. Spatial variation of LULC creates doubt about the point data collected by conventional methods. In modern times, satellite based remote sensing technology has been developed, which are of immense value for preparing LULC map and their monitoring at regular periodic intervals of time (Kumar et al., 2004).

As such, spatial repetitive and synoptic coverage from satellites collected over a wide range of electromagnetic spectrum admirably suit the requirement of LULC mapping and monitoring. These spatial data indicates the distribution of various LULC categories in an area. Due to the availability of repetitive data, it is possible to update existing database for various land use planning and design making. Therefore, with the use of geospatial technology (remote sensing, GIS, GPS and computational techniques) it is evident that these could be used effectively to prepare LULC mapping (Tejaswini, 2005; Rao et al., 1996, Mukherjee et al., 2009; Srivastava et al., 2010). Geospatial technology guarantees the availability and quick access of real time data, geospatial information for resource mapping.

LULC relates to the observable earth surface expressions, such as vegetation, geology, water resources and anthropogenic features which describes the Earth's physical condition in terms of the natural environment with man-made structures.

In India, spatial accounting and monitoring have been carried out at a national level on 1:250,000 scale, using multi-temporal Indian Remote Sensing (IRS) satellites to address the spatial and temporal variability in landuse patterns (NRSA, 1989). In the absence of basic information about the current land use pattern, it would be difficult to determine future improvements and their deterioration. Therefore, it is necessary to provide up-to-date information about earth resources that helps planners in decision-making for sustainable development and utilization of the earth resources. The use of geospatial information establishes a discussion between science, and national development strategies.

## Background

The relative evaluation of land for various uses is an urgent issue in the semi-arid regions. Industrial and recreational park, and nature preserves versus diverse agricultural and pastoral uses of the land should be evaluated. Options for gathering the problems, though limited, are based on the ecology of the specific local area or region (Dhinva et al., 1992).

Application of remote sensing technology for LULC change analysis has been carried out in semi-arid region of Madhya Pradesh and found that the use of remote sensing along with Survey of India toposheets could be used appropriately for LULC mapping of semi-arid area (Jaiswal et al., 1999).

The semi-arid regions are characterized by erratic rainfall and high rate of vegetation dynamics. The dynamics of plant species over time is mainly due to continuous and complex interactions of the plant communities with their environment. The human interferences and climatic variations are common driving forces in bringing changes to the environment (Shetty et al., 2005). The increasing biotic pressure together with increasing human demands exerts pressure on the available land resources all over the region. Therefore, in order to have best possible use of land, it is not only necessary to have the information on the existing LULC, but also to monitor the dynamic land use resulting because of increasing demands aroused from the growing population (Raghavswamy et al., 2005). Continuous overexploitation of natural resources like land, water, and forest has caused serious threat to the local population of the semi-arid region (Rao et al., 2006). This causes problems like little scope for soil moisture storage, high rate of soil erosion, declining groundwater level and shortage of drinking water. In a semi-arid area, there will be less vegetation so the diverse classes of vegetation will not be clearly recognized; and are the major problem of LULC mapping (Chaudhary et al., 2008).

It has extreme importance to the planners and decision makers for formulating the long-term plans for land resources development and management to improve the quality of habitat in semi-arid regions. In general, the study area has limited rainfall and, subject to prolonged droughts as well

as anthropogenic activities, reduces the natural vegetal cover and soil loss due to high erosion and environmental degradation (Singh, 2009). As per the regional status of the area some work has been reported such as LULC mapping of Kanera watershed of Madhya Pradesh is carried out through the use of remote sensing data for groundwater exploration purpose and observed that satellite data are very useful for land evaluation of semi-arid region (Akarm et al., 2009; Singh et al., 2011).

The study area presented in this chapter is located in the Gwalior district (latitude 26° 5′-26° 25′ N and longitude 78° 10′-78° 25′ E), of about 405 sq km, in the northern part of Madhya Pradesh, India in the Indo-Gangetic Plain (Fig. 1). The Gwalior city consists of three distinct urban areas: old Gwalior in the north, Laskar to the southwest and Morar towards the east. This region is dominated by semi-arid climate marked by extreme temperatures and erratic rainfall patterns. Geologically, Gwalior group of lithounits rest unconformably over Bundelkhand granite and comprises basal arenaceous Par formation which

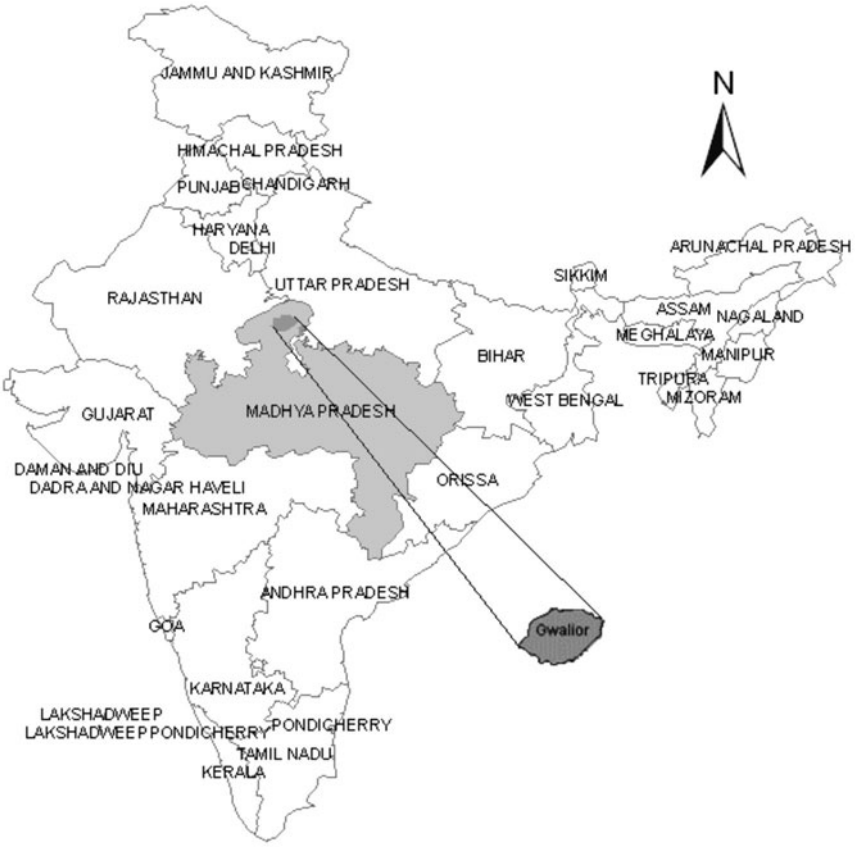


**Figure 1.** Location map of the Gwalior district, Madhya Pradesh, India.

are overlain by volcano-sedimentary sequences of Morar formation consisting of ferruginous shale with bands of chert-jasper.

The main objective of this chapter is to explore the role of geospatial technologies for land use mapping of one of the drought prone city of Madhya Pradesh, India and to examine the present status of LULC within the basin using satellite data for sustainable utilization of resources and their development.

## Data Used and Methodology

National LULC classification system using remote sensing data for mapping has been attempted by National Remote Sensing Agency (NRSA, 1995) of the country to understand and manage country's natural resources. Thereafter further efforts to map on 1:50,000 scales followed certain standards that required modifications in the current day's context. To this extent, an exhaustive LULC classification was evolved to facilitate an in-depth assessment of all the LULC categories (NRSA, 2005). The benefits of adopting a classification are tending to persuade for evolving a standard classification system that is guided by practical experience and continuous observation over the past many years and above all that meet the user requirements. The remotely sensed data, thematic maps and ground truth data used are in Table 1.

**Table 1:** Remote sensing and other data used in the study

| *S.No.* | *Data* | *Sources* |
|---|---|---|
| 1. | IRS ID LISS III image and PAN image | National Remote Sensing Agency (NRSA), Hyderabad, India |
| 2. | Survey of India Topographic Map (Sheet numbers 54 J/3, J/4, J/7 and J/8 on 1:50,000 scale) | Survey of India |
| 3. | Field data on land use/land cover | Ground truth collection during field survey and district revenue department |

Image interpretation has been carried out in two most popular ways e.g. digital analysis and visual interpretation. In the digital classification process, training areas for different classes were defined for the satellite imagery on spectral response pattern in different spectral bands generated. Based on these training areas, satellite imagery was classified into different classes using parametric or non-parametric classifiers (Lu et al., 2007). Following image processing steps were involved in image classification starting from processing of IRS LISS III Image to correct for atmospheric errors, registration of LISS III and Pan images with reference to toposheets from Survey of India (SOI), generation of other secondary data, image classification and accuracy assessment. The information provided by the satellites in combination with other sources to quantify the various parameters for efficient mapping of land

use of the basin was evaluated by applying various image processing steps using ERDAS Imagine and ArcGIS 9.3.

## Preprocessing

Accurate registrations of satellite images are essential for analyzing LULC conditions of a particular geographic position. The atmospheric scattering is common in remote sensing images, which are more pronounced in the shorter wavelength regions, and they cause some additional contribution to spectral reflectance. In the present study, satellite data was geometrically corrected for the distortions and degradations caused by the errors due to variation in altitude, velocity of the sensor platform, earth curvature and relief displacement.

The images of IRS ID and PAN (Path 97 and Row 53) were geometrically corrected and geocoded to the Universal Transverse Mercator (UTM) coordinate system by using a reference image of SOI toposheets. A minimum of 45 regularly distributed ground control points were selected from the images. The registration was performed using first order polynominal transformation, resampling using a nearest neighbour algorithm. The transformation with a Root Mean Square (RMS) error is 0.643. Image enhancement, contrast stretching and false colour composites were worked out.

## Image Classification

Supervised classification was performed to produce land cover map from the IRS satellite data. Defining of the training sites, extraction of signatures from the image and then classification of the image was done. Training data extraction was a critical step in supervised classification; these must be selected from the regions representative of the land cover classes under consideration. Thus, data were collected from relatively homogeneous areas consisting of those classes. The collection of training data was time consuming and tedious process, as it involved laborious field surveys and accumulation of reference data from various sources. The features of training sites were digitized. Three training sites were selected for this purpose. This procedure assures both the accuracy of classification and the true interpretation of the results. After the training site areas digitization, the statistical characterizations of the information were created. These were called signatures. Finally, the classification methods were applied. All the classification techniques like the maximum likelihood classification (MLC), parallelepiped and minimum distance to mean classification were applied for the images and the best classification technique was then chosen. It was observed that Maximum Likelihood Classification (MLC) gave good results as compared to the other two techniques. To determine the accuracy of classification, a simple testing pixel was selected on the ground trothed reference data. In thematic mapping from remotely sensed data, the accuracy, and the degree of 'correctness' of a map or classification was calculated.

## Result and Discussions

Land is one of the most important natural resources. The landuse pattern and its spatial distribution are the prime requisites for the preparation of an effective landuse policy needed for the proper planning and management of any area. The land use map prepared using above methodology has been shown in Fig. 2 and their spatial distributions are given in Table 2. The various LULC classes delineated from the available data include built-up, agriculture,

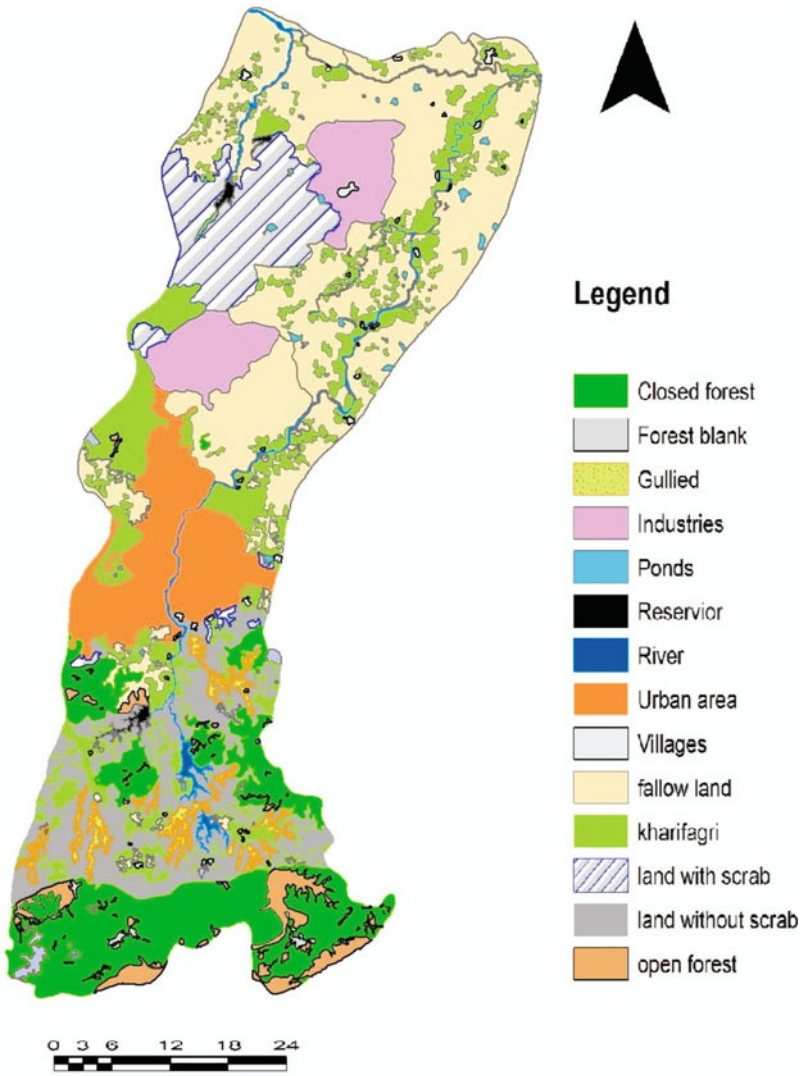


**Figure 2.** Land Use/Land Cover map of the Morar River Basin Madhya Pradesh, India.

wasteland, forest and water bodies. Three types of built-up lands were delineated: urban settlement, rural settlement and industrial complex. On satellite images these structures look as block-like appearance and show bluish tone on the image and on the PAN data they look typically blocky appearance with light tone.

The urban settlements are widely spread in central part of the basin. It covers an area of about 31.87 sq km. About 20 villages are identified from satellite image, covering an area of about 5.82 sq km. Within the basin, one of the important industrial complexes is named as Malanpur Industrial Complex covering an area of about 20.95 sq km. The total area covered by settlements in the basin constitutes 58.64 sq km (16.23%) respectively.

Forest is discerned by their red to dark red tone and varying in sizes. They show irregular shape and smooth texture. These forest areas are found on lower side of the basin. Based on the tonal and textual variations, the forests of the basin are divided into three categories as dense, open and forest blank. Dense forests are found in lower and central side of the area at upland topography. Approximately such dense forests cover an area of about 50.76 sq km. Open forests cover an area of about 11.74 sq km. Forest blank appears in light yellow to light brown tone generally small and most of these forests are found on hilltops and slopes. Forest blanks account very small having an area of about 1.85 sq km. These forests cover an area of about 19.05%. Agricultural land is shown in pink colour with smooth appearance on pan data and dark patches with step-like arrangement and agricultural land without crops is shown in bluish/greenish grey with smooth texture. In the present study, such cropped areas were found mostly in the northeastern portion and some amount in southwestern portion. Such cropped areas cover approximately 61.51 sq km (16.71%). Fallow lands were identified by their dark greenish tone, smaller size, regular shape and medium texture. Such fallow lands are found well distributed in the central and northeastern portion of the basin, which occupies 110.53 sq km (29.33%).

Due to non-availability of satellite data of Kharif season, some agricultural land is marked as fallow land in the basin as they were verified during field survey. Three categories of wasteland are identified such as land with scrub, land without scrub and gullied/ravenous land from satellite image and they cover approximately 83.34 sq km (20.61%). Land without scrub is in the lower part of the basin. Gullies are formed because of localized surface run-off affecting the unconsolidated material resulting in the formation of perceptible channels causing undulating terrain. They are mostly associated with stream courses and sloping grounds with good rainfall and entrenched drainage. Number of surface water bodies such as ponds, one reservoir named Ramaua with one perennial and one seasonal river are delineated from the satellite image and they cover 9.10 sq km (2.48%).

**Table 2:** Areas under different classes of Land Use/Land Cover

| *S.No.* | *Land use/Land cover* | *Area (in sq km)* | *Area (in %)* |
|---|---|---|---|
| 1 | Urban settlement | 31.87 | 8.87 |
| 2 | Rural settlement | 5.82 | 1.44 |
| 3 | Industrial complex | 20.95 | 5.92 |
| 4 | Dense forest | 50.76 | 14.04 |
| 5 | Open forest | 11.74 | 2.90 |
| 6 | Forest blank | 1.85 | 2.11 |
| 7 | Agricultural land | 61.51 | 16.71 |
| 8 | Fallow land | 110.53 | 29.33 |
| 9 | Land with scrub | 31.25 | 7.73 |
| 10 | Land without scrub | 46.04 | 11.39 |
| 11 | Gullied/ravenous land | 5.05 | 1.49 |
| 12 | Reservoir | 1.40 | 0.34 |
| 13 | River | 6.08 | 1.50 |
| 14 | Ponds | 1.62 | 0.64 |

## Conclusion and Recommendation

The present research work demonstrates the capability of geospatial techniques to capture the land use categories in a semi-arid region of Madhya Pradesh, India, which are necessary for optimum and sustainable utilization of land resources and prevention of further undesirable deterioration in land use. Analysis shows the agricultural area mostly found in the northern portion whereas southern portion of the basin is occupied by the forest cover over the denudational hills. The observation also shows major portion of the basin affected by severe soil erosion due to the occurrence of shales and steep slope. Therefore, the present work suggested that area urgently needs to minimize soil erosion by applying various techniques of soil conservation and large-scale aforestation.

Wastelands must be converted into cultivable land through massive programmes of afforestation, plantation or pasture development to increase food, fodder and fuel production. Land with and without scrub can be utilized for growing plants, which need soil cover. These plants are a source of fuel wood whereas some of them are of medicinal and economic importance. Check bunds should be constructed with waste-weirs wherever necessary to control soil erosion in the gullied/ravenous land. These bunds allow retention of water and soil whereby lands can be reclaimed and brought under cultivation.

To ensure planned development and monitor the land utilization pattern, preparation of LULC maps is necessary in the area. Scientists should use geospatial as reliable mapping and monitoring tool for new research and planning applications. It is expected that this trend will have dramatic implications in the field of geoinformatics for the natural resource mapping, monitoring and modelling over the next decade.

## References

Balak, Ram and Kolarkar, A.S. (1993). Remote sensing application in monitoring land use changes in arid region of Rajasthan. *International Journal of Remote Sensing*, **14(17)**, 3191–3200.

Chaudhary, B.S., Saroha, G.P. and Yadav, Manoj (2008). Human induced land use/land cover changes in Northern part of Gurgaon district, Haryana, India. *Journal of Human Ecology*, **23(3)**, 243–252.

Chaurasia, R. and Sharma, P.K. (1999). Land Use/Land Cover Mapping and Change Detection using Satellite Data—A Case Study of Dehlon Block, District Ludhiana, Punjab. *Journal of Indian Society of Remote Sensing*, **27(2)**, 115–121.

Chen, D. and Stow, D. (2002). The effect of training strategies on supervised classification at different spatial resolutions. *Photogrammetric Engineering and Remote Sensing*, **68**, 1155–1161.

Cihlar (2000). Land cover mapping of large areas from satellites: status and research priorities. *International Journal of Remote Sensing*, **21(6&7)**, 1093–1114.

Dhinwa, P.S., Pathak, S.K., Sastry, S.V.C., Rao, M., Majumdar, K.L., Chotani, M.L., Singh, P.J. and Sinha, R.L.P. (1992). Land use change analysis of Bharatpur District using GIS. *Journal of the Indian Society of Remote Sensing*, **20(4)**, 237–250.

Diouf, A. and Lambin, E.F. (2001). Monitoring land-cover changes in semi-arid regions: remote sensing data and field observations in the Ferlo, Senegal. *Journal of Arid Environments*, **48(2)**, 129–148.

Foody, M.G. (2002). Status of land cover classification accuracy assessment. *Remote Sensing of Environment*, **8**, 185–201.

Franklin, S.E. (2001). Remote Sensing for Sustainable Forest Management. Lewis Publishers, Boca Raton, FL.

Gautam, N.C. and Channiah, C.H. (1985). Land use and land cover mapping and change detection in Tripura using satellite Landsat data. *Journal of the Indian Society of Remote Sensing*, **6(3&4)**, 517–528.

Glackin, D.L. (1998). International space-based remote sensing overview: 1980–2007. *Canadian Journal of Remote Sensing*, **24**, 307–314.

Jaiswal, R.K., Saxena, R. and Mukherjee, S. (1999). Application of remote sensing technology for landuse/landcover change analysis. *Journal of the Indian Society of Remote Sensing*, **27**, 123–128.

Javed, Akram, Khanday, M.Y. and Ahmed, Rizwan (2009). Prioritization of sub-watersheds based on morphometric and land use analysis using remote sensing and GIS techniques. *Journal of the Indian Society of Remote Sensing*, **37(2)**, 261–274.

Jensen, J.R. (1996). Introductory Digital Image Processing, Second Edition. Prentice-hall Press, New Jersey.

Jensen, J.R. and Cowen, D.J. (1999). Remote sensing of urban/suburban infrastructure and socio-economic attributes. *Photogrammetric Engineering and Remote Sensing*, **65**, 611–622.

Kumar, Vijay, Rai, S.P. and Rathore, D.S. (2004). Land use mapping of Kandi Belts of Jammu Region. *Journal of Indian Society of Remote*, **32(4)**, 323–328.

Kunwar, P., Kachhwaha, T.S., Kumar, Anil, Agrawal, A.K., Singh, A.N. and Mendiratta, Nisha (2010). Use of high-resolution IKONOS data and GIS technique for transformation of landuse/landcover for sustainable development. *Current Science*, **98(2)**, 204–212.

Lillesand, T.M., Kiefer, R.W. and Chipman, J.W. (2008). Remote sensing and image interpretation. John Wiley & Sons, Inc., New York.

Lu, D. and Weng, Q. (2007). A survey of image classification methods and techniques for improving classification performance. *International Journal of Remote Sensing*, **28(5)**, 823–870.

Merem, E.C. and Twumasi, Y.A. (2008). Using Geospatial Information Technology in Natural Resources Management: The Case of Urban Land Management in West Africa. *Sensors*, **8**, 607–619.

Mukherjee, S., Shashtri, S., Singh, C., Srivastava, P. and Gupta, M. (2009). Effect of canal on land use/land cover using remote sensing and GIS. *Journal of the Indian Society of Remote Sensing*, **37(3)**, 527–537.

National Remote Sensing Agency (1989). Manual of Nation wide Land use/Land cover Mapping using satellite imagery, Part I. NRSA, Hyderabad.

National Remote Sensing Agency (1995). IMSD Technical Guidelines. National Remote Sensing.

NRSA (2005). Integrated Mission for Sustainable Development. Technical Guidelines, Hyderabad.

Palaniswami, C., Upadhyay, A.K. and Maheswarappa, H.P. (2006). Spectral Mixture Analysis for sub pixel classification of coconut. *Current Science*, **91(12)**, 1706–1711.

Raghavswamy, V., Pathan, S.K., Ram, Mohan, P., Bhanderi, R.J., Padma, Priya (2005). IRS-IC applications for urban planning and development. *Current Science*, **70**, 582–588.

Ranjeet, J., Jiquan, Chen, Nan, Lu, Ke, Guo, Cunzhu, Liang, Yafen, Wei et al. (2008). Predicting plant diversity based on remote sensing products in the semi-arid region of Inner Mongolia. *Remote Sensing of Environment*, **112(5)**, 2018–2032.

Rao, D.P., Gautam, N.C., Nagaraja, R. and Ram, M.P. (1996). IRS-1C applications in land use mapping and planning. *Current Science*. **70(7)**, 575–581.

Rao, K.N. and Narendra, K. (2006). Mapping and evaluation of urban sprawling in the Mehadrigedda watershed in Visakhapatnam metropolitan region using remote sensing and GIS. *Current Science*, **91(11)**, 1552 –1557.

Rogana, John and Chen, D.M. (2004). Remote sensing technology for mapping and monitoring land-cover and land-use change. *Progress in Planning*, **61**, 301–325.

Saha, A.K., Arora, M.K., Csaplovics, E. and Gupta, P.K. (2005). Land cover classification using IRS LISS III image and DEM in a rugged terrain: A case study in Himalayas. *Geocarto International*, **20(2)**, 33–40.

Shetty, Amba, Lakshman, N., Sangeeta, T. and Rajesh, M.V.S. (2005). Land use-land cover mapping using satellite data for a forested watershed, Udipi district, Karnataka state, India. *J. Indian Soc. Remote Sensing*, **33**, 233–238.

Singh, Praful, Kumar Suyash and Singh, U.C. (2011). Groundwater resource evaluation in the Gwalior area, India, using satellite data: an integrated geomorphological and geophysical approach. *Hydrogeology Journal*, (DOI:10.1007/s10040.011-0758-6).

Singh, P.K. (2009). Remote sensing and GIS based hydrogeological study of Morar Watershed, District Gwalior (M.P) India. Unpublished Ph.D. thesis, Faculty of Science, Jiwaji University, Gwalior, M.P., India.

Singh, A. (1989). Digital change detection technique using remote sensing data. *International Journal of Remote Sensing*, **26**, 1–6.

Singh, P.K. and Singh, U.C. (2009). Water resource evaluation and management for Morar River basin, Gwalior District, Madhya Pradesh, using GIS. *E-journal of Earth Science India*, **2(3)**, 174–186.

Singh, S.K., Thakur, J.K. and Singh, U.K. (2010). Environmental monitoring of land cover/land use changes in Siwalik Hills, Rupnagar district of Punjab, India using remote sensing and ancillary data. Paper presented at the International Conference on Global Climate Change.

Srivastava, P., Mukherjee, S. and Gupta, M. (2010). Impact of Urbanization on Land Use/Land Cover Change using Remote Sensing and GIS: A Case Study. *Journal of Ecological Economics and Statistics*, **18**, 106–117.

Tapiador, F. and Casanova, J.L. (2003). Land use mapping methodology using remote sensing for the regional planning directives in Segovia, Spain.

Tejaswini, N.B. (2005). Land use/Land cover mapping in the coastal area of North Karnataka using remote sensing data. *Journal of the Indian Society of Remote Sensing*, **33(2)**, 253–257.

Thakur, J.K. (2010). Eco-hydrological wetland monitoring in a semi-arid region (A case study of Konya Closed Basin, Turkey). Faculty of International Institute for Geo-Information Science and Earth Observation (ITC), Universiteit Twente, Enschede, the Netherlands.

Thakur, J.K. and Singh, S.K. (2010). Eco-hydrological monitoring of wetlands in a semi-arid region using remote sensing, GIS, GPS and various data sets: A case study of Konya closed basin, Turkey. Paper presented at the IAH 2010.

# 11

# The Environmental Calculator: A Tool for the Efficient Assessment of Environmental Services Loss due to Deforestation

**Miguel Martínez Tapia, Xanat Antonio Némiga and José Isabel Juan Pérez**
Autonomous University of the State of Mexico, Mexico

## Introduction: Why an Environmental Calculator?

Forest ecosystems contribute to protect soils from erosion and to regulate watersheds and local hydrological systems by reducing variation in water flows. They also provide local and global climate regulation, carbon storage as well as air and water purification. Forests contain the largest assortment of species found in any terrestrial ecosystem and supply numerous social and cultural services. They are also part of our cultural and historical heritage (Stenger et al., 2009). Information about forest values might be needed for legal processes of damage compensation, but also for cost-benefit analyses, for the establishment of governmental regulations, for "environmental pricing" or simply for general information (Elsasser et al., 2009). The unavailability of cartographical values, representing differential prices for the economical value of environmental services which forest provides, make it difficult to use such resources on a sustainable basis. One major threat to forest sustainability is deforestation. Deforestation has several side effects on the ecosystem services of a site. As runoff and erosion increase, they modify soil structure, which in turn reduces water infiltration and reservoirs recharge. The associated functions that a forest cover usually plays are also affected: thermal regulation, biodiversity support, and carbon sequestration, among others.

Forest resources at the Biosphere Reserve of Monarch Butterfly have historically been under heavy pressure. Therefore, deforestation at this zone has been documented, along with ecosystem deterioration and depletion of wooden resources (PROFEPA, 2001). For such reason, the tool here presented attempts to economically calculate the losses on ecosystem services that

J.K. Thakur et al. (eds.), *Geospatial Techniques for Managing Environmental Resources*,
DOI 10.1007/978-94-007-1858-6_11, © Capital Publishing Company 2012

are associated to deforestation, to suggest an adequate fine. It integrates methods for soil erosion assessment (Domínguez-Cortazar et al., 2001; Cortés T. et al., 1991; Sanaphre-Villanueva et al., 2003), for water infiltration estimation (Hernández-Valdez, 2005; Mobayed, 2001); and carbon sequestration calculation. Once modelled, its outcome is linked to one platform that allows entering the site coordinates and returns the estimated value of such loss. To develop it, Geographic Information Systems (GIS) technology was used to visualize, analyze and correlate said environmental variables. This tool is based on the theory of value and that of environmental economy (Martínez-Alier et al., 2001; Pearce et al., 1995) and integrates territory values as currency to make them comparable in time and space (Gómez-Jiménez et al., 2007).

## Background

Ecosystem services are the processes of ecosystems that support human well-being. Common forest ecosystem services are timber, non-timber forest products, wildlife habitat, water quantity and quality, carbon sequestration and storage, and recreation opportunities (Patterson and Coehlo, 2009). Not all forests provide the same ecosystem services: the structure, composition and location have a key role in the determination of the services that a forest can offer and whom those services can be offered to (Baskin, 1997; Myers, 1997; Roper and Park, 1999; Schmidt et al., 1999; Sharma, 1992). The importance of these functions is strictly linked to the socio-economic and environmental context of which the forest is a part (Goio et al., 2008). Since 2000, a growing number of researches related to the economic evaluation of the ecosystem services that forests provide can be found worldwide, especially on the valuation of non-market environmental goods and services (McComba et al., 2006). This is because it is widely accepted that an improved understanding of the value of forests can be useful to determine their optimal use among competing users, often providing a strong economic argument for forest conservation, or at least lessening the incentive for deforestation (Lange, 2004). These methods are being increasingly used and applied to conduct cost-benefit analysis of environmental regulations, to value environmental services and raise awareness on its linkages to economy, and to aid in the development of green national accounts (McComba et al., 2006); a thorough revision of the methods applied for non-timber forest benefits valuation is provided by Lindhjema (2007). Tools to economically valuate the environmental services consider direct use value, indirect use value, option value, and intrinsic value in terms of capital (natural, human and technological). The total economic value is the sum of all these values (Leff, 2004). A sound description of the total economic value (TEV) framework and related concepts can be found at Croitoru (2007).

The economical and environmental valuation of the space implies the allocation of the natural loss of goods and environmental services and their prices in a given time lag (Gómez-Jiménez et al., 2007). In Mexico, several

studies have economically valuated the loss of these environmental services, but often separately, and without considering the spatial perspective (Angulo-Carrera et al., 1996; Martínez-Tapia, 2003; WWF, 2004). A revision of articles in *Science Direct* database revealed that integrative and spatial studies of the value of the environmental services that forests provide are certainly an emerging research line. In this regard, the studies by Sherrouse et al., *(*2010), Troy and Wilson (2006) and Nengwang et al. (2009) are remarkable. Pressure from publications to create novel methods or formulations has resulted in an abundance of studies that are distant from the day-to-day needs of policy makers for cost-benefit analysis or improved understanding of the economy of water and air quality, and climate change (McComba et al., 2006). That was a reason in this exercise to implement well-known techniques and software (cityGreen, ArcView, ArcGIS), and to adapt the methods that Mexican legislation usually recognizes (technical norms of the Federation).

### The Biosphere Reserve of Monarch Butterfly

The Chincua-Cerro Pelón corridor selected for this study is located within the biosphere reserve; its coordinates are between 19° 44′ 27″ and 19° 18′ 32″ of North Latitude and between 100° 22′ 26″and 100° 09′ 07″ of West Longitude (Fig. 1). Administratively, it comprises several municipalities of the State of Mexico (such as Temascalcingo, San Felipe del Progreso, Donato Guerra and Villa de Allende) and the State of Michoacan (Contepec, Senguio, Angangueo, Ocampo, Zitácuaro and Aporo). According to Cornejo et al. (2003), it is located at the Trans-Mexican Volcanic Axis, whose volcanic structures belong to the early and medium Cenozoic Period and are dominated by hills and hillocks with few inter-mountainous plates. Andosols are the predominant soils. Lerma, Santiago and Balsas river basins coexist at this reserve, which is considered part of the floristic province, called Mesoamerican Mountain Region. Forest at this reserve are communities from 20 to 40 metres in height often dominated by *Abies religiosa*, *Arbutus xalapensis*, *Cupresus lussitanica*, *Pinus hartwegii*, *Pinus pseudostrobus* and *Quercus laurina*. The total surface of the study area is 1858 kilometres.

## Method

This study aims to calculate the economic value of the loss of environmental services caused by illegal deforestation. The models used to generate the basic information needed to determine said loss of environmental services are developed on a GIS environment, considering expected scenarios of change of land use, under which it is possible to calculate the increment of soil erosion (tonnes/ha/year), the reductions of water infiltration (volume expressed in $m^3$ per hectare) and reductions of carbon sequestration (tonnes/ha). The processes considered to build this tool include a method for the assessment of hydrological balance, as described by the Mexican official norm *NOM-011-CNA-2000*; the Universal Soil Loss Equation, and the process of Carbon

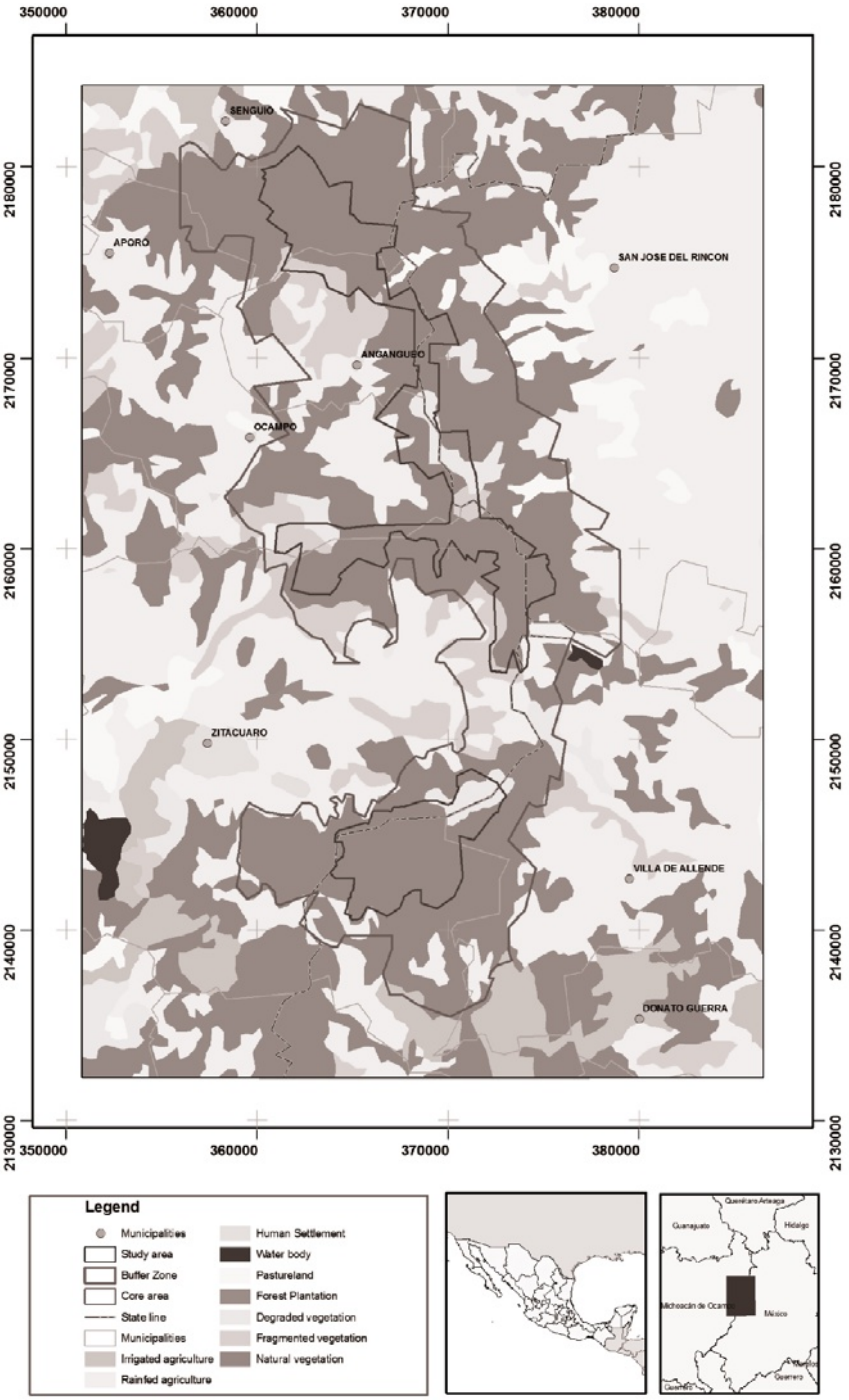


**Figure 1.** Study area location and land use types.

Sequestration Assessment included in City Green software. Several data sources are needed to run these processes. These were obtained from diverse documents and databases, specifically on climate and forest cover. Besides, the cartography of vegetation and land use types, soils and topography are also needed. These data are processed as maps and tables that work as inputs for the spatial analysis that ArcGIS 9.3, ArcView 3.2 and City Green perform (see Figs 2 and 3). The environmental calculator has a model structured by compounds that integrate the evaluation of environmental services loss. It shows the methodological process followed to organize, analyze and generate new thematic information for the calculation of each compound of the tool, when the graphic and alphanumeric information is available to be entered into a GIS. The logical model of the environmental calculator is based on the models for infiltration, soil erosion caused by water, and carbon sequestration (Fig. 2).

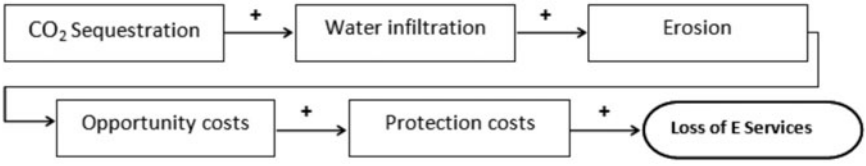


**Figure 2.** Logical model of the environmental calculator.

Data inputs, transformation and process for these models are shown below (Figs 3a to 3e).

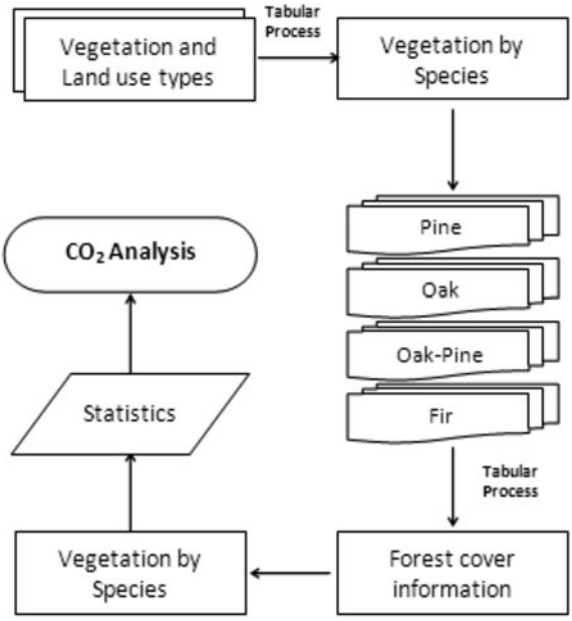


**Figure 3a.** Model used for the evaluation of carbon sequestration.

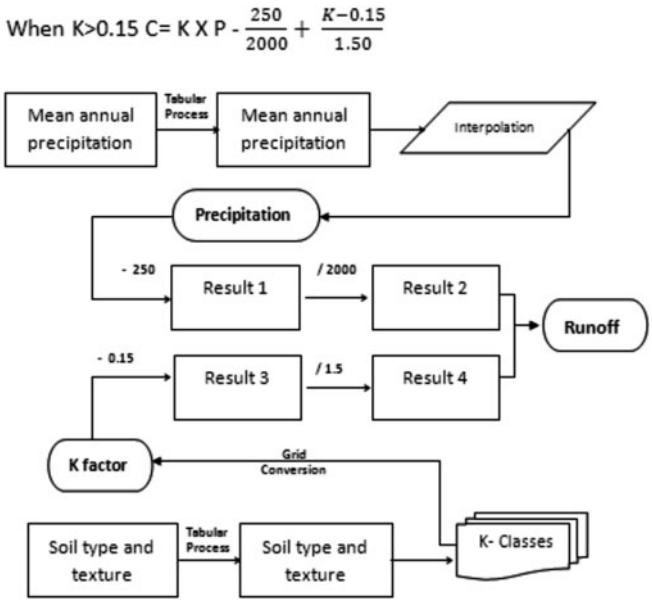


**Figure 3b.** Model used for the calculation of the runoff coefficient.

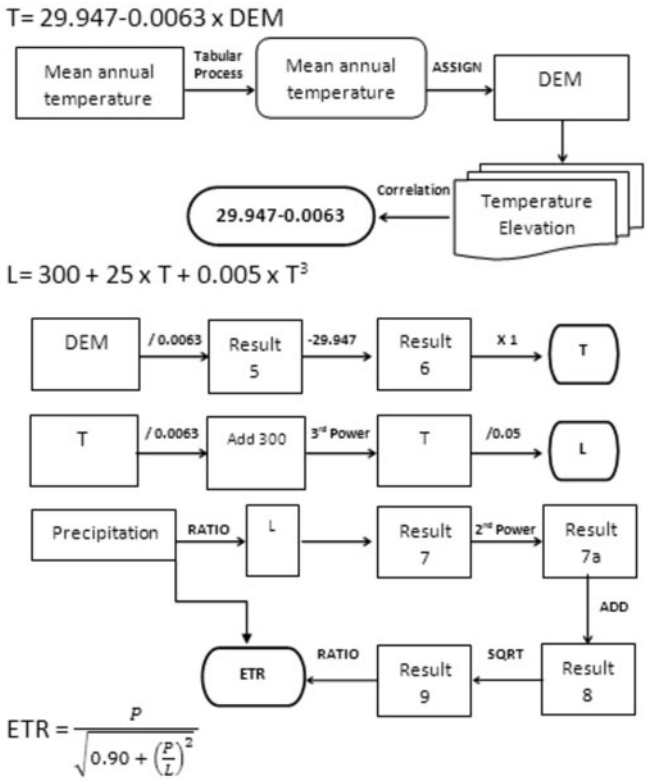


**Figure 3c.** Model used to calculate the potential evapotranspiration.

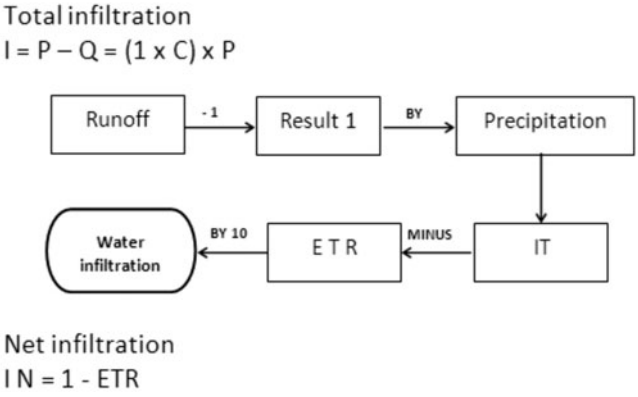


**Figure 3d.** Model used to calculate total infiltration.

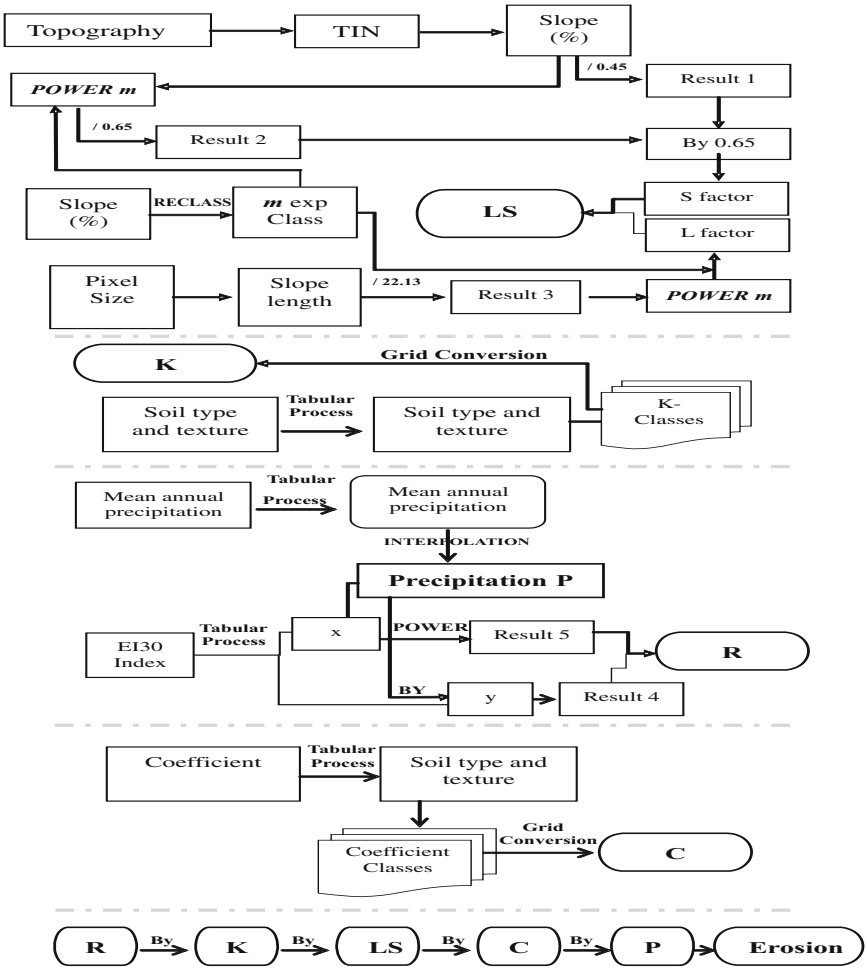


**Figure 3e.** Structure of the model used to calculate soil erosion caused by water.

## Partial Results According to the Method

### *Carbon Sequestration Model*

Data process was carried coupling ArcView version 3.2 with the City Green application. It allows the spatial analysis of vegetation and of the amount of carbon that a forest captures. To do so, data regarding tree diameter, tree height, health of the forest, and vegetal species used is needed and it returns the tonnes of carbon sequestered per year and the average of the potential carbon sequestration in tonnes/year. Models and coefficients used to convert biomass to sequestered carbon are species-sensitive, thus its variations are minimal from place to place. Temperate forest cover facilitates applying this tool; further refinements may be needed to adapt it to tropical environments. The national forest inventory carried out by the Secretariat of Natural Resources was used as an input (SEMARNAT, 2000). The following land use types are recognized: irrigated agriculture (5%), non-irrigated agriculture (38%), human settlements (1%), water bodies (0.4%), grassland (4%), natural vegetation (39%), degraded vegetation (2%), fragmented vegetation (6%), and reforestation (0.2%). With this information, forest stands were delineated and data regarding tree diameter, height and health recorded. Such data was obtained from institutional records and field sampling performed at the study area. With this information, the following values of carbon sequestration for each forest type were obtained (Table 1).

**Table 1:** Carbon sequestration for each forest type

| *Parameter* | *Pine* | *Fir* | *Oak* |
|---|---|---|---|
| Tonnes of $CO_2$ fixed per year | 12,814.958 | 3,636.165 | 3,825.059 |
| Total surface covered | 67,351.034 | 19,110.438 | 2,129.225 |
| Carbon sequestration (tonnes/ha/year) | 0.190 | 0.190 | 1.796 |

### *Infiltration Model*

An indirect method was used following the norm by National Commission of Water, "NOM-011-CNA-2000", which defines how to calculate the mean annual availability of national waters. It was implemented in a GIS environment through the calculations described below.

*Runoff Coefficient: K* values are obtained by cross-relation with soil permeability and land use type. Soil types and their permeability values were obtained from the soil charts by INEGI (National Institute of Statistics and Geography). Permeability is grouped as: (a) pervious soil; (b) semi-pervious soil; and (c) almost pervious soil. A raster map of *K* values for soil permeability class within the land use types was built. The average annual precipitation value, *P*, was obtained from the records of the meteorological stations around the study area and interpolated to a continuous raster map.

With *K* and *P* values in a continuous raster map, the following calculation was performed:

$$\text{when } K > 0.15 \quad C = K \times P - \frac{250}{2000} + \frac{K - 0.15}{1.50}$$

where $C$ is the runoff coefficient; $P$—mean annual precipitation in mm; and $K$ is land use and soil permeability related parameter.

*Potential Evapotranspiration:* Turc formula of potential evapotranspiration was applied; it is described as:

$$ET = \frac{P}{\sqrt{0.90 + \left(\frac{P}{L}\right)^2}}$$

where $L$ is $300 + 25 \times T + 0.05 \times T^3$; $P$ is the mean annual precipitation expressed in mm/year, and $T$ the mean annual temperature in °C. $T$ was obtained from a linear relationship between the average annual temperature and the altitude at the meteorological station where such temperature is registered according to the following expression: $T = X - Y \times Alt$, being $T$ temperature and $Alt$ terrain elevation, based on the digital elevation model (DEM). Once the constants $L$ and $P$ were in a raster format, the potential evapotranspiration was calculated applying the formula described above. Knowing the potential evapotranspiration and the runoff coefficient, it is possible to calculate total infiltration and net infiltration.

*Total Infiltration $I_T$:* Total infiltration can be obtained from $I_T = P_a - Q_a = (1 - C) \times P_a$. It means that this is a function of the runoff coefficient and the mean annual precipitation. To calculate it, the maps of runoff coefficient and mean annual precipitation were related to the following:

$$(1 - [C]) \times [P]$$

*Net Infiltration $I_N$:* Net infiltration is the water volume that is infiltrated in this region, expressed in millimetres. These values should be converted to cubic metres in order to understand the reduction of infiltrated water volume in the study area. With the real evapotranspiration ETR value, the net infiltration can be obtained by: $I_N = P_a - Q_a - ETR$. The maximum value of net infiltration in this area is 6053 $m^3$, while the minimum is 800 $m^3$.

## Modelling Soil Erosion Caused by Water

The Universal Soil Loss Equation (Wischmeier and Smith, 1979) was used. It estimates the tonnes of soil that a place would lose in a year having no protection or forest cover and being on a steep slope (exposed to rain erosive action). It represents susceptibility to erosion and is expressed as:

$$A = R.\ K.\ S.\ L.\ C.\ P$$

where $A$ is soil loss per surface unit (tonnes/ha.year); $R$ is the rain erosive factor (in MJ.mm/ha h); $K$ is soil erodibility (tn.ha.h/ha.MJ.mm); $L$ is the slope length (non-dimensional); $S$ is the slope (non-dimensional); $C$ is a

cultivation and territorial ordination factor and *P* is a factor related to cultivation practices. These *R*, *K*, *LS* and *C* factors were calculated with ArcGis 9.3 software, using the procedures described below.

*Rain Erosive Factor R:* Usually *R* is calculated using the Wischmeier index. However in order to calculate it, rain intensity values and rain graphic records are needed. Being such data unavailable, the mapping developed by Cortés (1991) was used instead. According to this author, the study area belongs to the region *V*. The equation used is then $Y = 3.4880\ X + 0.000188\ X^2$. *Y* is the annual index of rain erosive factor expressed in MJ mm/ha h and *X* is the mean annual precipitation expressed in mm.

*K Factor Determination:* This factor represents the susceptibility of soils to soil erosion caused by water. Its value depends on the content of organic matter, soil superficial texture, soil structure, and permeability. Again, the alternative method provided by Cortés (1991), which includes the soil type unit and its superficial texture, was used. FAO soil classes and the records of soil superficial texture provided by the soil chart were considered to assign the *K* value for each soil and texture combination.

*LS Factor Determination:* To determine the *LS* factor the following equation was used: $LS = (\lambda/22.13) \times (0.065 + 0.045.\ S + 0.0065\ S^2)$, where λ is the slope length expressed in metres; (*S*) is the slope expressed as percentage, and *m* an exponent directly related to slope. Its values range between 0.2 and 0.5. To assign this value Table 2 was used.

**Table 2.** Values assigned to *m* exponent

| *Slope (%)* | *M* |
|---|---|
| Above 5% | 0.5 |
| 3% to 5% | 0.4 |
| 1% to 3% | 0.3 |
| Below 1% | 0.2 |

Then, the LS factor was obtained typing on the map calculator of ArcGis the expression:

([slope_s] × .045 + .065 + .006541 × [slope_s] × [slope_s])
× pow ((50/22.1), [m])

*C Factor:* To calculate the maximum potential erosion in theory, it is assumed that there is no vegetation cover ($C = 1$), that the soil is on a steep slope and there are not implemented practices of soil conservation ($P = 1$). *C* factor was determined using the table of *C* factor values proposed and described by Ramos-Taipe (2001). With the previously calculated values *R*, *K*, *LS* and *C*, soil erosion in the study area was calculated. At the reserve, the maximum value of soil erosion caused by water was 5109 tonnes/ha a year, while the minimum was 0.002 tonnes/ha a year.

## Economic Valuation of Environmental Services

Two scenarios were considered to economically calculate the environmental services loss caused by the illegal activity of deforestation. The first scenario attempts to evaluate the hectares of soils that may be lost to deforestation. It was defined considering the forest cover, comparing the current conditions of the forest against the conditions that would result with the change of use of the forest terrain due to illegal activities (Table 3). The forest cover defined under this scenario is used to calculate *C* value, and with it, the soil erosion caused by deforestation is estimated.

**Table 3:** Forest cover conditions considered to determine *C* value

| *Current condition* | *Scenario of change of land use* |
|---|---|
| Natural forests | Fragmented forests |
| Fragmented forests | Degraded forests |
| Degraded forests | Non-irrigated agriculture |

These scenarios were designed considering the documented patterns of change of land use in the study area (PROFEPA, 2001).

The second scenario considers the forest current structure in order to determine the *K* value, which is used to establish the runoff coefficient that in turn is needed to evaluate total and net infiltration at a given place. For this scenario, the condition of the forest cover was determined under the following feasible percentages of forest cover change due to illegal activities (Table 4).

**Table 4.** Forest cover conditions to determine *K* value

| *Current condition* | *Condition on the land use change scenery* |
|---|---|
| Closed forest canopy | Forest canopy from 25 to 50% of density |
| Fragmented forest canopy | Forest canopy with less than 25% of density |
| Degraded forest | Non irrigated agriculture with annual species |

*C* and *K* factors calculated under these two scenarios were then used to calculate the amount of soil and the volume of water which can be lost due to deforestation.

The economic value of the loss of environmental services in the study area was calculated using the following formula:

$$PCN = CO + EH + DI + DCCO_2$$

In said formula *PCN* is the economic value of the loss of environmental services; *CO* is the opportunity cost; *EH* is the economic value of soil erosion caused by water, *DI* are reductions of water infiltration and $DCCO_2$ are reductions of carbon sequestration.

## Economic Value of Soil Erosion Caused by Water

Total soil lost *PS* was calculated by subtracting the current soil erosion value *ESA* to soil erosion under *ESE* scenario, according to $PS = ESE - ESA$. Figure 4 shows: (A) a fragmented forest (SEMARNAT, 2000); (B) current soil loss

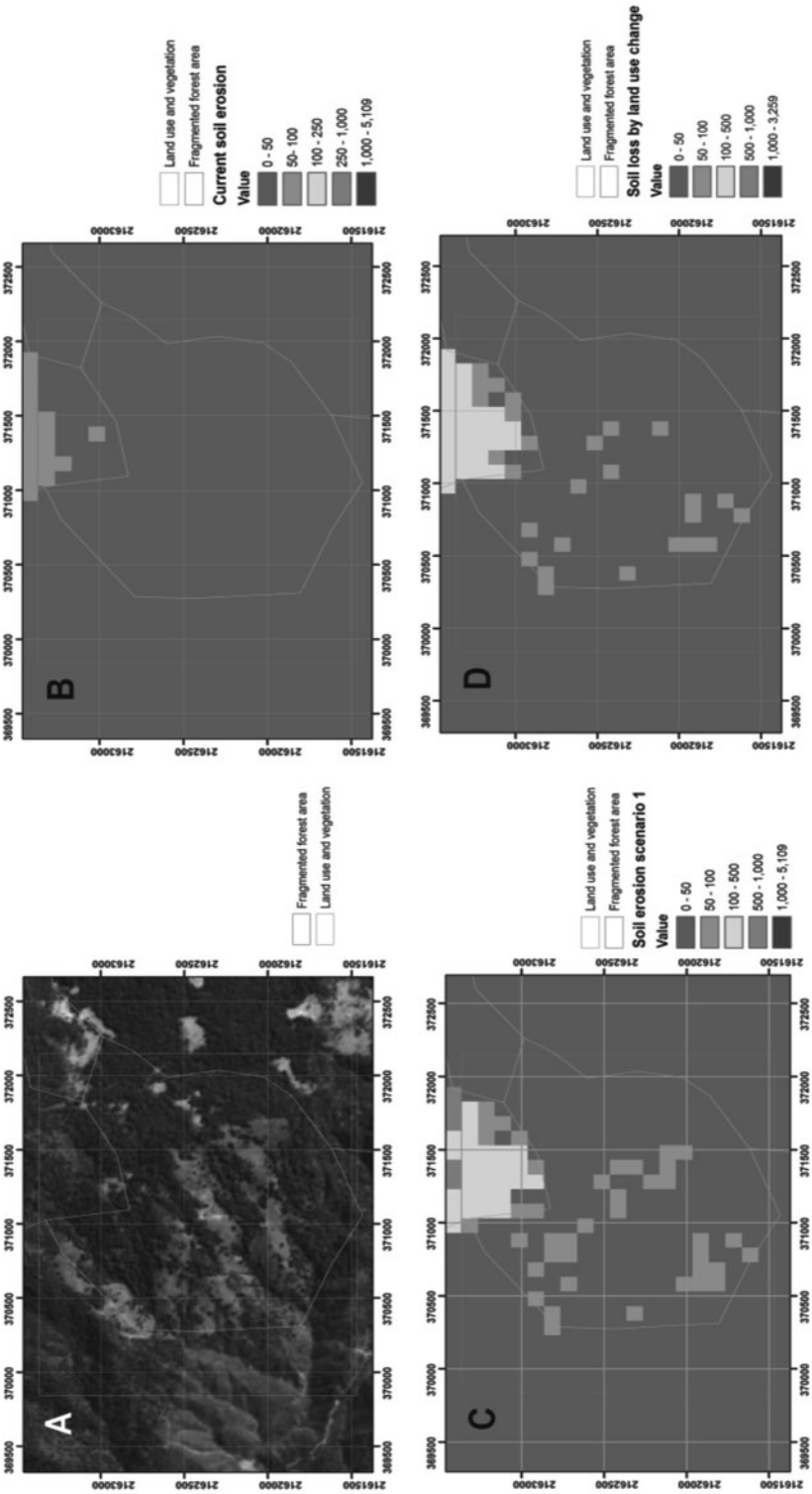


**Figure 4.** Increase of soil erosion caused by water, caused by the transition from fragmented forest to agriculture.

value calculated with USLE equation; (C) soil erosion caused by the transition from fragmented forest to agriculture; and, (D) soil lost that can occur by the transition at C. Due to this transition, an area previously considered with light erosion turns into an area where erosion is moderate, reaching more than 10 tonnes/ha/year (Fig. 5). It proves the increase of soil erosion due to forest cover loss.

The direct costs of soil erosion CEH are calculated multiplying the price of soil nutrients lost per hectare *PN*, by the total lost soil *PS* expressed in tonnes/ha/year using $CEH = (PN \times PS)$.

Soil erosion caused by water is a selective process that removes the smallest particles where most organic matter in the soil is, thereby, the most fertile soils. A moderate erosion level of 30 tonnes/hectare/year can cause losses from 16 to 34 kg of nitrogen (34 to 72 kg of urea); 3 to 5.5 kg of phosphorous, 16 to 34 kg of potassium and 23 to 45 kg of calcium every year. The first upper millimetres of soil are the richest in humus and nutrients and also the first to be lost by accelerated erosion (Rivera-Ruiz, 2005). Therefore, to evaluate the costs of soil lost nutrients, the outcome of USLE equation, which was given in tonnes/hectare/year, was translated into costs using current costs of soil nutrients (Table 5).

**Table 5.** Costs of soil nutrient loss at the reserve area

| *Minimal cost of* | *Unit* | *I* | *II* | *Unit cost* | *Required cost* |
|---|---|---|---|---|---|
| Nitrogen | Kg | 16 | 0.53 | $ 3.50 | 1.87 |
| Phosphorous | Kg | 3 | 0.10 | $ 3.50 | 0.35 |
| Potassium | Kg | 16 | 0.53 | $ 3.50 | 1.87 |
| Calcium | Kg | 23 | 0.77 | $ 3.50 | 2.68 |
| Cost of soil nutrients lost by hectare | | | | | **4.08** |

The final economic cost of soil erosion *EH* is the sum of restoration costs *CR* and the costs directly caused by erosion itself, using: *CEH*: $EH = CR + CEH$. Such costs were estimated considering that many of the raw materials, from fires, cuts and dead wood, which are required to build the infrastructure for soil retention, are already available. Therefore, to build one of the artisanal dams to preserve soil, commonly of two metres long and one metre deep, the costs are approximately $255 Mexican pesos (MXN). Such costs are due to the following concepts: material collection and transportation, surface cleaning and alignment, cornerstone establishment, and installation of galvanic wires of 14″. In surfaces of one hectare, ten of such dams would be required to stop soil loss due to water erosive effect, which would cost 2550 MXN. The final economic value of soil erosion caused by water reaches a maximum value of 15,849.5 MXN, and a minimum value of 2550 MXN per hectare. Since the

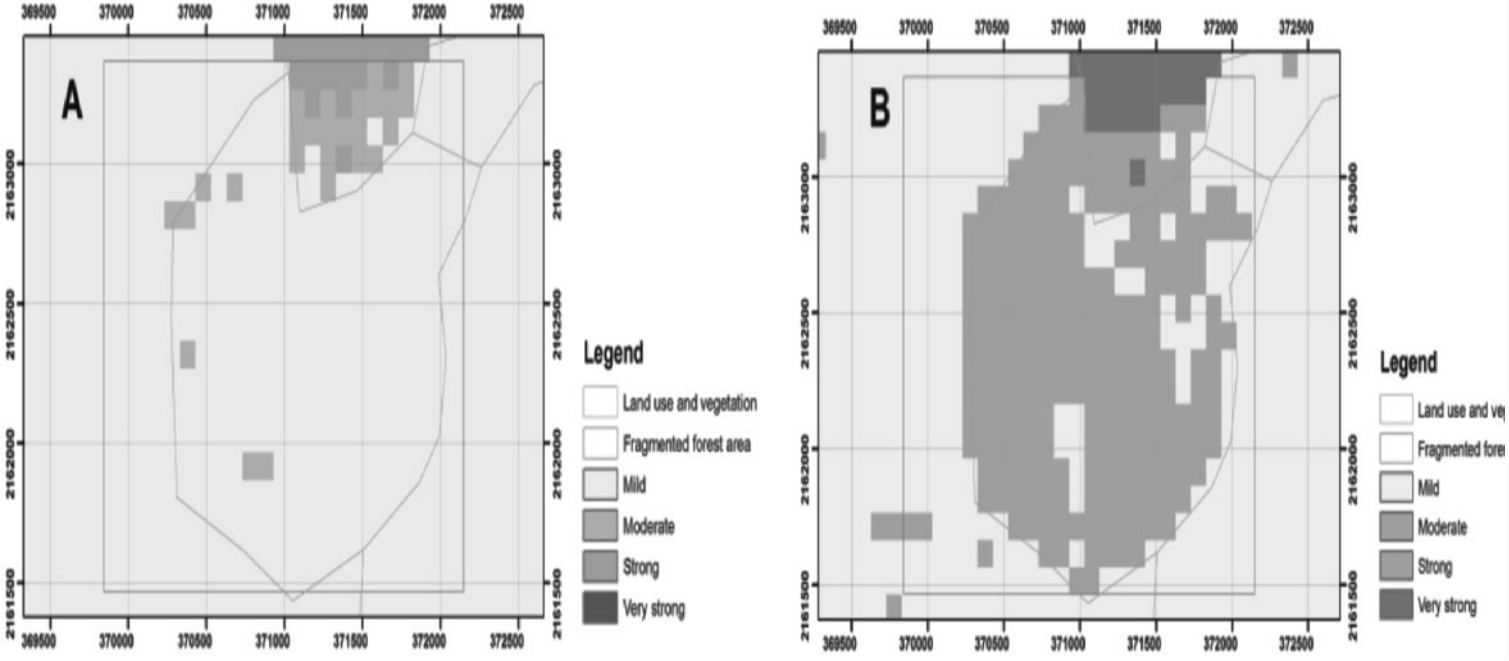


**Figure 5.** Current (A) and projected (B) soil erosion evaluated for a transitional region.

spatial analysis is performed in raster format at pixel level, it allows the calculation of differentiated prices for soil loss of environmental services.

## Economic Value of Changes in Infiltration

The economic evaluation of infiltration also followed three steps. First, an assessment of the amount of water infiltrated under two scenarios is performed; then the costs of that infiltrated water is estimated; and finally, the economic value of the reduction of water infiltration is evaluated by adding the costs of water to the costs of reforestation. In order to estimate the volume of water that is infiltrated by hectare, the procedure for hydraulic balance, which has been described under the technical norm NOM-011-CNA-2000 of the National Commission of Water, was followed. Infiltration capacity depends on the forested surface, forest condition, rain availability and soil characteristics. Cartographical records from the National Forest Inventory (SEMARNAT, 2000) were used, as well as the records for the annual total precipitation from 1950 to 2000 (García-Reyna et al., 2010). To evaluate the differences on net infiltration due to deforestation, *K* values of the second scenario were used to calculate the runoff coefficient. Figure 6 shows how net infiltration is reduced: (A) a fragmented forest; (B) net infiltration ($m^3$); (C) infiltration considering land use change; and (D) volume that would be lost by the removal of forest cover. This was calculated using the formula:

$$DCI\ ha = INA - INE$$

where *DCI ha* are differences in cubic metres that are infiltrated in a hectare; *INA* are Net Infiltration under current conditions, expressed in $m^3$ and *INE* is the net infiltration under the evaluated scenario, expressed in $m^3$.

The loss of capacity for water infiltration in a forest of the extension of 1858 sq. km that has lost nearly 75% of its tree cover could be around 1400.00 $m^3$ of water. This estimated reduction of water infiltration capacity *DCI ha* is used for the economic valuation of infiltration reduction. The amount of non-infiltrated water is multiplied by the prices that Mexican government defines considering both the aggregated value of water, and its availability. To do so, Mexico has been divided into regions, and on each one a price has been given to a cubic metre of water. The regions belonging to zone 1 are labelled as low availability or high demand, whereas the $9^{th}$ zone represents the opposite conditions. Considering that this area belongs to zone 5, the cost for a cubic meter of water is 5.5053 MXN, according to the equation

$$CAI = PM \times DCI\ ha$$

where *CAI* are the costs of infiltrated water, *PM* is the price for a cubic metre of water, and *DCI ha* are differences in cubic metres infiltrated in a hectare. These costs are added to the costs of reforestation in order to obtain total costs

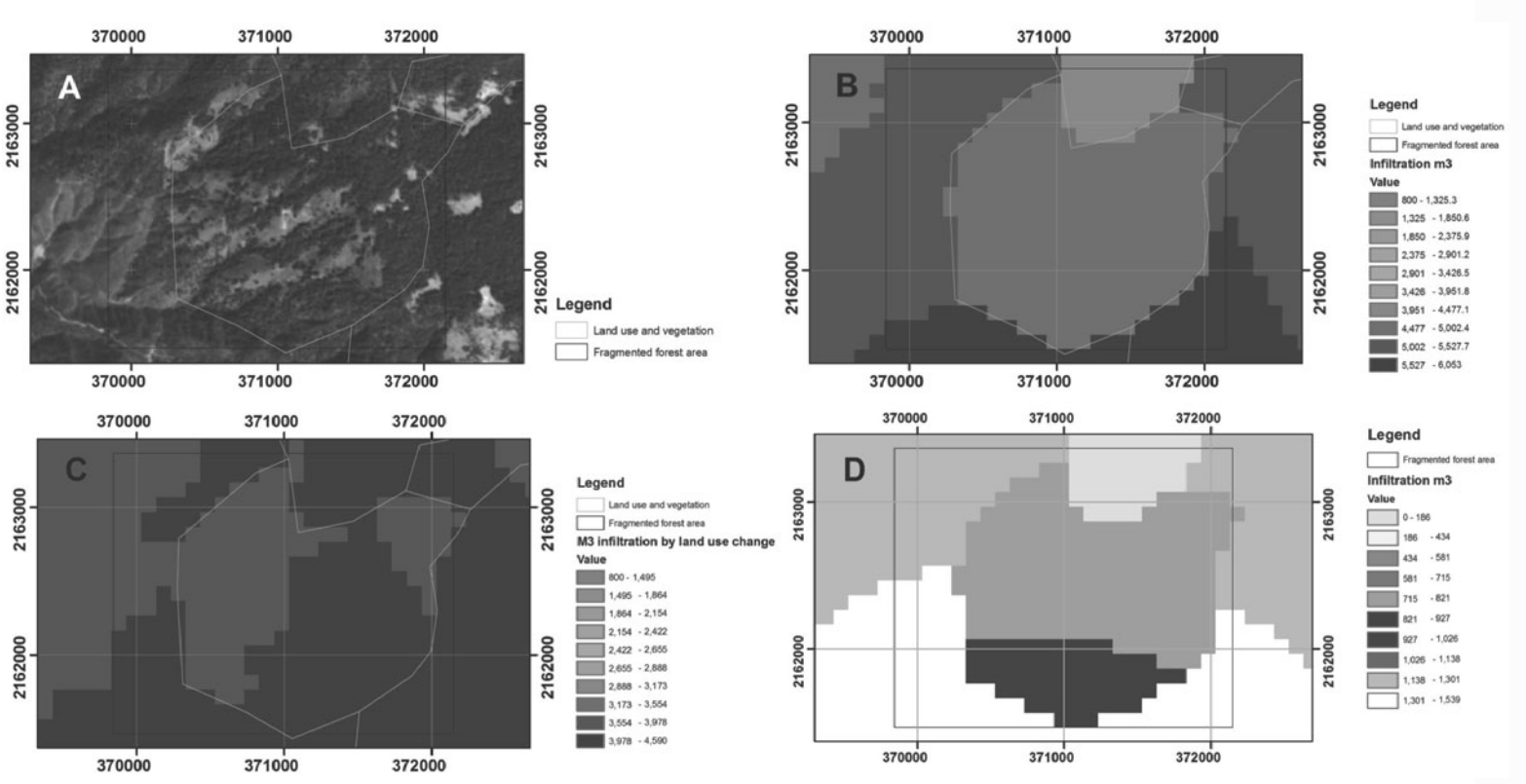


**Figure 6.** Reductions of water infiltration due to forest cover loss.

of the reductions in water infiltration. Reforestation costs were estimated by hectare and the concepts for cleaning, digging, distribution of materials, seedling costs, and transportation were taken into account. In the region, these costs reach the amount of 1360.00 MXN. Such costs are included in the formula

$$DI = CR + CAI$$

where *DI* stands for reductions on infiltration, *CR* are reforestation costs, and *CAI* the costs of infiltrated water. The maximum cost for loss of water infiltration that can be obtained in this region is 9829.85 MXN per hectare, while the minimum cost is 1360.00 MXN per hectare. It is also feasible to obtain differentiated values for the economic value associated to loss of water infiltration.

## Economic Valuation of the Variations of Carbon Sequestration

The amount of carbon that can be sequestrated was calculated using the carbon sequestration model under the current condition and the land use change scenario (Table 4). Prospective carbon sequestration was subtracted of the current carbon sequestration, and the following formula applied

$$DCCO_2 = (CP + PICO_2)$$

where $DCCO_2$ are reductions of the amount of $CO_2$ that is sequestrated; *CP* protection costs, and $PICO_2$ international price for carbon sequestration. The cost of protection was considered to be equal to the amount that local authority spends on forest vigilance to protect the study area, where only one Forest Guard has been paid for 144 days, at a price of 60 MXN a day, which means that the Local Authority has invested 8640 MXN. The international price of carbon sequestration $PICO_2$ is estimated on a surface basis. The cost is given per hectare considering the potential for carbon sequestration of a specific site. In this study area, according to the models of carbon sequestration and the forest cover density and preservation, the cost was estimated to be 14 USD per hectare, as

$$PICO_2 = (CT \times PS/Ha)$$

where $PICO_2$ is international price of carbon sequestration, *Ct* is the international price per ton, and *Ps/ha* is the total amount of carbon that can be potentially sequestrated by the forest surface (ha). With these considerations, the maximum cost by the reduction of carbon sequestration is 8966.85 MXN, and the minimal cost is 8640 MXN per hectare.

## Economic Value of the Loss of Environmental Services

Having estimated the environmental value of increased erosion, decreased water infiltration and decreased carbon sequestration that are associated to

deforestation, the economic value of the loss of environmental services was estimated using

$$PCN = CO + CEH + DI + DCCO_2$$

The previously calculated costs were added to the opportunity cost *CO*. This opportunity cost was estimated considering the market prices, as an alternative to obtain the minimum value for a product or service. For example, the minimal value for a natural park was estimated based on the market price for the products and services that are not directly used, such as wood, minerals, and pastures (Jäger M. et al., 2001). In this area, the opportunity cost was estimated to be 500.00 MXN per hectare, which is the amount of money paid by the programme for environmental services of the Government of the State of Mexico.

## Results

Carbon sequestration calculated by CityGreen in the forest of the Reserve Biosphere of Monarch Butterfly is estimated to be of 12,814 tonnes per year at the pine forest, 3636 tonnes per year at the fir forest, and 3825 tonnes per year at the oak forest. In this area, the maximum value for net infiltration, calculated with the technical norm NOM-011-CNA-2000, is 6053 $m^3$, while the minimum value is 800 $m^3$. Applying the USLE method to the particular environmental conditions of this area, the maximum value of soil erosion caused by water is 5109 tonnes/ha per year, and the minimum 0.002 tonnes/ha per year. The final economic value of soil erosion caused by water in this region reaches a maximum value of 15,849.5 MXN, and a minimum value of 2550 MXN for each hectare. The loss of capacity of water infiltration on a forest of the extension of 1858 sq. km that has lost nearly 75% of its tree cover could be 1400.00 $m^3$ of water. The cost of loss of water infiltration can be as high as 9829.85 MXN per hectare, while the minimum cost is of 1360 MXN per hectare. With the scenarios of carbon sequestration reduction, the maximum cost of this reduction is 8966.85 MXN and the minimal cost is 8640 MXN per hectare. As a result from this integration of spatial analysis and models, the maximum value that has resulted from this integration of spatial analysis and models yields a maximum value for the loss of environmental services of 29,475 MXN. The fine that should be charged for the removal of tree cover at the Biosphere Reserve of Monarch Butterfly ranges between 15,000 and 20,000 MXN (Fig. 7).

A query menu was designed to recover the value of loss of environmental services at a specific site. This menu allows introducing the coordinates of a place where an affectation over forest cover has occurred, and provides differentiated and specific prices for forests lost, as a result of the integration of the models simulating the decrease on water infiltration, growing soil erosion, and carbon sequestration loss (Fig. 8).

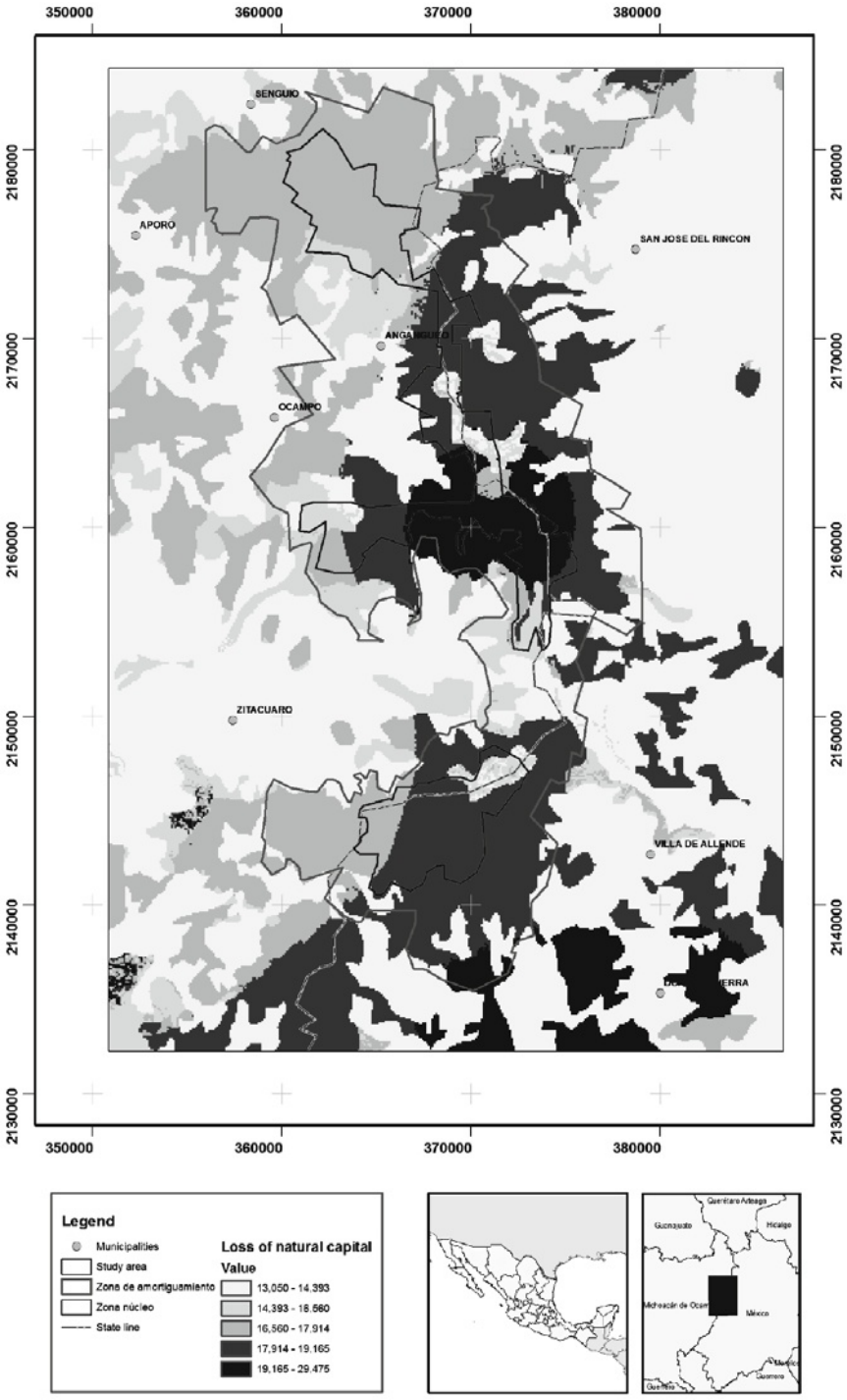


**Figure 7.** Economic value of loss of environmental services.

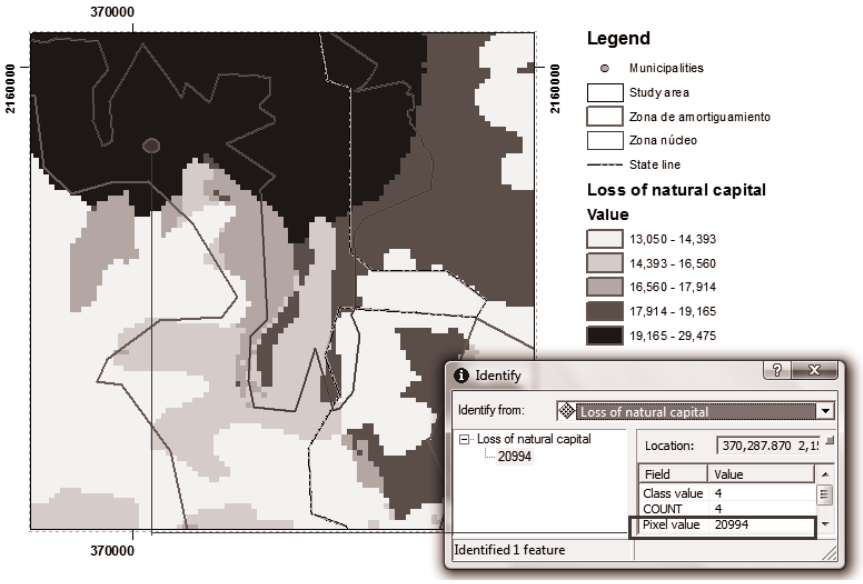


**Figure 8.** Querying the fine to be applied at the specific site where an illicit occurs.

## Discussion and Recommendations

This tool is a first attempt to economically value the damage that a person or a group of people causes to forests. It does not try to present a price, but rather giving indicators of the monetary value of forests lost. It is proposed as a tool for the authorities involved in the punishment of illegal deforestation, aiming to increase their efficiency and to improve the administration of environmental justice. However, it could also be used to calculate the payment of environmental services for those persons living near well-preserved forests. Since having an economical value of reference could work as a dissuasive tool to reduce illicit activities. The fine that should be charged for deforestation at the Biosphere Reserve of Monarch Butterfly ranges between 15,000 and 20,000 MXN per hectare (around 1245 and 1660 USD). This is low considering that it would be a single payment. As a remote framework of comparison Bernard et al. (2009) have valued on 42.9 USD/ha the annual cost for maintenance of biodiversity, water supply and recreation and tourism at the Tapantí Protected area in Costa Rica.

The Mexican Legislation has the legal framework for the application of environmental fines, as it states "Those who damage the environment, make an irresponsible use of its resources or alter ecosystems shall assume the inherent costs" (LGEEPA, article 21, section III). This could become part of the administrative procedure that is usually carried out at PROFEPA (Council for Environmental Protection), allowing the presentation of a technical declaration of the affectation caused by an illegal activity at a Public Prosecutor

Office, including affectations to forests, soil and water. Thus, the environmental fine is a mechanism of value transference for the regeneration of natural resources that are affected by an environmental irregularity. To effectively operate, a mechanism to carry out a follow-up of the money received through the fine and an effective application of such resources for the protection and restoration of the reserve shall be operated by PROFEPA. Properly instrumented, this mechanism would imply an improvement of forest conditions by the generation of a fund to finance the activities of vigilance, reforestation, and soil restoration, among others. The application into other countries would require the proper legal framework and institutional infrastructure. In this specific case the feasibility to implement this tool is high due to the fact that this reserve has a huge biological importance (for the presence of Monarch Butterfly), but also a key role as income generator through ecotourism. The main author of this work has been working on this tool diffusion and acceptation.

## Conclusions

Geographic information technologies can be successfully adapted to the legal and policy framework and procedures for the economic evaluation of loss of environmental services. This could ultimately aid in the process of forest vigilance and restoration at the Biosphere Reserve of Monarch Butterfly, through the calculation of an appropriate fine for deforestation, considering the associated loss of environmental services. Indeed, it could be established in other natural protected areas of Mexico. The unavailability of cartographical values representing differential prices of the economic value of environmental services that forest provides makes it difficult to use said resources on a sustainable basis; therefore detailed, integrative and spatially focussed studies on the value of environmental services which forests provide are required. These should take advantage of the emerging technologies of geographic information to collect and process data regarding the state, processes and values of environmental services, and also must incorporate the social, economical and institutional framework to generate sound initiatives for the peculiarities of each country and region. Increasing and improving the strategies to preserve our remaining forests using the best of our knowledge and technologies is still a priority for our world management agenda.

## References

Angulo-Carrera, A., De Jesús-Apolinar B., Duran-Gálvez B., González-Jácome, O., Leyva-López J.A., Martínez-Tapia M., Moreno-Cárdenas G. and Valdés-Muciño, I. (1997). *Cuenta patrimonial del recurso suelo en la reserva de la biósfera mariposa monarca*. Centro de Monitoreo y Evaluación de Daños a los Recursos Naturales. Internal document SEMARNAP-PROFEPA.

Baskin, Y. (1997). The Work Of Nature: How The Diversity Of Life Sustains Us. Washington: Island Press.

Bernard, F., De Groot, R. and Campos J.J. (2009) Valuation of tropical forest services and mechanisms to finance their conservation and sustainable use: A case study of Tapantí National Park, Costa Rica. *Forest Policy and Economics*, **11**, 174–183.

Comisión Nacional de Áreas Naturales Protegidas. (2001). Programa de Manejo de la Reserva de la Biosfera Mariposa Monarca. CONABIO. Mexico 139 pp.

Cornejo, T., Casas, G.A., Farfán, B., Villaseñor, J. and Ibarra G. (2003). Flora y Vegetación de la zona núcleo de la Reserva de la Biosfera de la Mariposa Monarca. *Bol. Soc. Bot. Mex*, **73**, 43–62.

Cortés, T. H. (1991). Caracterización de la erosividad de la lluvia en México utilizando métodos multivariados. Master degree thesis. Colegio de Postgraduados, Montecillos, Mexico. 168 pp.

Croitoru, L. (2007). How much are Mediterranean forests worth? *Forest Policy and Economics*, **9**, 536–545.

Diario Oficial de la Federación (2000). *NORMA OFICIAL MEXICANA NOM-011-CNA-2000, Conservación del Recurso Agua que Establece las Especificaciones y el Método para determinar la Disponibilidad Media Anual de las Aguas Nacionales*. Gobierno Constitucional de los Estados Unidos Mexicanos. April 7th 2002. Mexico.

Diario Oficial de la Federación (2000). *Decreto de la Reserva de la Biosfera Mariposa Monarca*. Gobierno Constitucional de los Estados Unidos Mexicanos. November 10th 2000. Mexico.

Domínguez-Cortazar, M.A. and Ventura-Ramos E. (2001). *Evaluación del riesgo de erosión hídrica en el estado de Querétaro*. Informe Técnico para la Secretaria del Medio Ambiente y Recursos Naturales, Delegación Querétaro. Facultad de Ingeniería, División de Estudios de Posgrado, Universidad Autónoma de Querétaro.

Elsasser, P., Meyerhoff, J., Montagne, C. and Stenger, A. (2009). A bibliography and database on forest benefit valuation studies from Austria, France, Germany and Switzerland – A possible base for a concerted European approach. *Journal of Forest Economics*, **15**, 93–107.

García-Reyna, M.E. and Martínez-Ramón, O. (2010). *Temperatura y Precipitación media anual, Sistema de Consulta a la Base de Datos del Servicio Meteorológico Nacional*. Tesis de Licenciatura. Facultad de Geografía, Universidad Autónoma del Estado de México. Toluca, Mexico. 100 p.

Goio, I., Gios, G. and Pollini C. (2008). The development of forest accounting in the province of Trento (Italy). *Journal of Forest Economics*, **14**, 177–196.

Gómez-Jiménez, I., Martínez de Anguita P. and Romero-Calcerrada, R. (2008). *Evaluación de la viabilidad del uso de los métodos de valoración económico-ambiental en un contexto espacial*. UNED. Espacio, Tiempo y Forma. Serie VI. No. 1.

Jäger M., García-Fernández, J., Cajal, J., Burkart, R. and Riegelhaupt, E. (2001). *Valoración económica de los bosques Revisión, evaluación, propuestas*. Fundación para la Conservación de las Especies y el Medio Ambiente, FUCEMA. Informe Final para la Unión Mundial para la Naturaleza, UICN Oficina Regional para América del Sur.

Lange, G.-M. (2004). Manual for Environmental and Economic Account for forestry: a tool for crosssectoral policy analysis. Working Paper, FAO, Forestry Department, Rome.

Leff E. (2004). *Racionalidad ambiental, La reapropiación social de la naturaleza, La teoría objetiva del valor, la revolución científico-tecnológica y las fuerzas productivas de la naturaleza*. Siglo XXI Editores, S.A de C.V. Mexico, D. F. 1-43 p.

Lindhjema, H. (2007). 20 years of stated preference valuation of non-timber benefits from Fennoscandian forests: A meta-analysis. *Journal of Forest Economics*, **12**, 251–277.

Martínez-Alier, J. and Roca-Jusmet, J. (2006). *Economía Ecológica y Política Ambiental*. Colección Economía, 2ª edición, Mexico. 489 p.

Martínez-Tapia M. (2003). *Pago de servicios ambientales en el estado de Querétaro.* Internal document. SEMARNAT, Querétaro. Mexico. 110 p.

McComba, G., Lantz, V., Nash K. and Rittmaster, R. (2006). International valuation databases: Overview, methods and operational issues. *Ecological Economic*, **60**, 461–472.

Mobayed, K.N. and Soto-Ávila, A. (2002). *Sistema Hidro-fisiográfico del estado de Guanajuato.* Seminario "intercambio del conocimiento y experiencias en el manejo del recurso hídrico. Guanajuato, Mexico. Retrieved May 2010 http://seia.guanajuato.gob.mx/panel/document/vinculos/doc1870/A20207.pdf.

Myers, N. (1997). The World's Forests and Their Ecosystem Services. En: G. Daily (ed.). Nature's Services: Societal Dependence on Natural Ecosystems. Island Press, Washington.

Nengwang, Ch., Huancheng, L., Lihong, W.(2009). A GIS-based approach for mapping direct use value of ecosystem services at a county scale: Management implications. *Ecological Economics*, **68**, 2768–2776.

Patterson, T. and Coelho, D. (2009). Ecosystem services: Foundations, opportunities, and challenges for the forest products sector. *Forest Ecology and Management*, **257**, 1637–1646.

Pearce, D.W. and Turner, K.H. (1995). *Economía de los Recursos Naturales y del Medio Ambiente*. Celeste, Madrid.

PROFEPA (2001). *Informe Final del Operativo Mariposa Monarca.* (Documento interno). Procuraduría Federal de Protección al Ambiente. México. 15 p.

Ramos-Taipe, C. L. (2001). *Modelamiento Ambiental para análisis de susceptibilidad erosiva en la cuecna media y alta del Río Cañete y Determinación del Mapa de Erosión. Universidad Nacional Agraria Molina.* Retrieved September 2009 http://tarwi.lamolina.edu.pe/~cramostMODELO%20DE%20EROSION% 20HIDRICA%20-%20SIG.pdf.

Rivera, Ruiz (2005). *Curso-Taller-Práctico para formar promotores técnicos en "Diseño y establecimiento de prácticas conservacionistas para la cuenca Villa Victoria*". Comisión Nacional del Agua, Gerencia Regional de Aguas del Valle de México y Sistema Cutzamala, Gerencia de Organismos del Agua.

Roper, C.S. and Park, A. (Editors) (1999). The Living Forest: Non-Market Benefits of Forestry. Proceedings of an International Symposium. Edinburgh 24-28 June 1996, Forestry Commission. London: HMSO.

Sanaphre-Villanueva, L. and Ventura-Ramos, J. (2003). *Evaluación de la erosión hídrica en la microcuenca San Pedro (Huimilpan, Querétaro) y selección multicriterio de especies de vegetación nativa para su control*. Universidad Autónoma de Querétaro. Retrieved October 2009: http://www.ine.gob.mx/descargas/cuencas/cong_nal_06/tema_03/19_lucia_sanaphre.pdf.

Schmidt, R., Berry, J.K. and Gordon, J.C. (Editors) (1999). Forests to Fight Poverty: Creating National Strategies. Yale University Press, New Haven.

Sharma, N.P. (ed.) (1992). Managing the World's Forests: Looking for Balance Between Conservation and Development. Ames: Kendall/Hunt Publishing Company.

Sherrouse, B., Clement J.M. and Semmens, J.D. (2010). A GIS application for assessing, mapping, and quantifying the social values of ecosystem services. *Applied Geography*, **1**, 13. In press.

Stenger, A., Haroub, P. and Navrud, S. (2009). Valuing environmental goods and services derived from the forests. *Journal of Forest Economics*, **15**, 1–14.

Troy, A. and Wilson, M. (2006). Mapping ecosystem services: Practical challenges and opportunities in linking GIS and value transfer. *Ecological Economics*, **60**, 435–449.

WWF. Programa México (2004). *La tala ilegal y su impacto en la Reserva de la biosfera Mariposa monarca*. Report. WWF-Programa México. Retrieved August 2006 http://eco-index.org/search/pdfs/363report_2.pdf

**Cartography**

- SEMARNAT (2000). National Forest Inventory. Scale 1:250,000. Secretaría de Medio Ambiente y Recursos Naturales, Mexico.
- INEGI (1980). Soil chart. Scale 1:250,000. Instituto Nacional de Estadística y Geografía. Aguascalientes, Mexico.
- INEGI (1976). *Topographical map*. Scale 1: 50000. Charts: E14a15, E14a16, E14a25, E14a26, E14a35, E14a36. Instituto Nacional de Estadística y Geografía. Aguascalientes, Mexico.
- Secretaría de Marina. *SPOT 4 Satellite Imagery.* HERMEX, Mexico. February 2006.

**Software used:** ArcView 3.3 ™ by ESRI., City green ™ by American Forester Org., and ArcMap 9.3 ™ by ESRI.

# 12

# Urban Tree Detection Using Mobile Laser Scanning Data

**Arun Kumar Pratihast and Jay Krishna Thakur**[1]
ITT, Cologne University of Applied Science, Cologne, Germany; and
Center for Geo-information, Wageningen University
Wageningen, The Netherlands
[1]Department of Hydrogeology and Environmental Geology, Institute of Geosciences, Martin Luther University, Halle, Germany

## Introduction

Nearly half of the world's population (47 per cent) lives in urban areas and is expected to grow by two per cent per year during 2000-15 (UN, 2001). Urban trees are essential data sets for studies on urban biomass, ecological function, water budgets and radiation transfer in an urban system. Furthermore, it is also useful for 3D cadastre and 3D city models used by planners and environmentalists for planning, modelling and ecological assessments of the city.

Traditionally, optical remote sensing methods have been used for acquisition of urban data sets. These data sets have been extensively used for tree identification, 3D modelling, and biomass estimation. An advantage of these methods is that the data is being collected for a large area in a single attempt. Whereas the disadvantages of these methods include comparatively coarse resolutions and some shadow effect on all the optical images. Therefore, it is complicated to identify the single tree pixel and also two-dimensional measurements is not sufficient to determine canopy structure.

Nowadays, laser scanning is a well-established technology to acquire the three dimensional data. Several experiments have been carried to detect the tree and estimation of tree geometry parameters such as canopy height, crown width and foliage for the forest monitoring applications and modelling of 3D tree using airborne as well as terrestrial laser scanning (TLS) data (Bucksch and Lindenbergh, 2008; Mallet and Bretar, 2009; Rosell et al., 2009; Vauhkonen et al., 2009).

J.K. Thakur et al. (eds.), *Geospatial Techniques for Managing Environmental Resources*,
DOI 10.1007/978-94-007-1858-6_12, © Capital Publishing Company 2012

Mobile laser scanning (MLS), an extension of Terrestrial Laser Scanning (TLS) technique, is emerging nowadays. This technique captures highly dense 3D point cloud of larger urban areas in a rapid and cost effective way (Norbert et al., 2008). The point density of these MLS data depends upon speed of the vehicles, sensor configuration and season of the acquisition. Limited research has been done to extract the information and model the tree from these data sets (Pratihast, 2010; M. Rutzinger et al., 2010; Ussyshkin, 2009). In this context, taking account of the problems and suggestions given by previous researches and taking the advantages of MLS data, the aim of this chapter is to describe an automatic method that can detect the tree in urban areas.

## Laser Scanning

Laser scanning is an active remote sensing technology used for mapping topography, vegetation, urban areas, ice and infrastructures. The scanner used is an active sensor that measures the distance from the sensor to the ground on which the laser beam is reflected. It uses the time of flight measurement principle to capture the three dimensional structure of the earth surface. The main working principle in this scanning is range measurement. The approaches to measure distance with lasers range finding are time-of-flight and triangulation. In time of flight measurement, time elapsed between the emitted laser pulse and reflected pulse back to the photosensitive sensor is measured. If $t$ is the amount of time taken by laser pulse to travel and return back to sensor and $c$ is the speed of light, then $d$ is the distance of object, which is approximately half the distance travelled by the laser pulse. Following mathematical relation is being used to calculate the $d$:

$$d = c \times t/2 \tag{1}$$

Precision in distance measurement is improved by applying phase shift measurement. The phase shift between transmitted and received signal is calculated by:

$$r = \Delta\Phi/(2\Pi) \times \gamma/2 + \gamma/2 \times n \tag{2}$$

where $\Delta\Phi$ is the phase difference measured in radian, $\gamma$ is the wavelength measured in metre and $n$ is number of full waveform between the sensor and object surface. Range is determined via angle measurement instead of direct measurement to have higher precision with laser scanning. Two laser beams produced by either separate laser or formed by splitting of the single laser beam is used for triangulation. Based on the source position, the angle of intersection between two laser beams is measured and finally the distance to target object is calculated. Collected data of laser scanning, called point

cloud, contains three dimensional information (X, Y, Z) and reflection intensity value.

The first air-borne platforms for terrain measurement using laser scanning had been done in the early 1965 (Miller, 1965). Air-borne laser scanning combining with GPS and inertial navigation system were started in 1988 (Lindenberger, 1989). With the advancement in the development of sensors in the recent years, collection of multiple echo and full waveform of reflected rays is easier and accurate. The accuracy of ALS increases up to a few centimetres (Mallet and Bretar, 2009). Terrestrial laser scanning (TLS) was started in late 1990's as an alternative way of laser scanning which is used to capture the 3D information of complex surfaces in high speed and often in accessible environment. Based on the sensor movement, there are two types of terrestrial laser scanning techniques namely static and mobile laser scanning.

### *Static Terrestrial Laser Scanning*

The static terrestrial laser scanning is used for the measurement of buildings, bridges and tunnel facilities and energy infrastructures development. The scanners used in this type of laser scanning are fully integrated with high quality digital cameras. Obtained point clouds are highly dense and accurate. Scanning is independent of weather conditions.

### *Mobile Laser Scanning*

Mobile laser scanning (MLS) is a dynamic means of terrestrial laser scanning used to capture highly accurate and high resolution dynamic 3-dimensional spatial data at normal traffic speeds. One or several scanners mounted on a mobile platform are used to acquire the point cloud. These mobile platforms might be car, train or vessel. Shan and Toth (2008) published a comprehensive study on current devices and specification of mobile platform. During the scanning, a rotating mirror (scanner) deflects the laser beam across the driving direction and the swath terrain along the driven direction is recorded. Runtime measurement is conducted for the calculation of distance to the surface. Figure 1 shows the field of view of MLS sensors. The recorded point cloud is highly dense and complete georeferenced which has high potential in the corridor mapping (Barber et al., 2008) and 3D modelling of urban environment like tree, building and poles (N. Haala et al., 2008; Ussyshkin, 2009). The vehicle-based MLS used for the data acquisition in this research is shown in Fig. 1. The main elements of mobile laser scanning are Differential GPS, Inertial measurement unit (IMU), Distance measurement instrument (DMI) as Odometer, Software and hardware for registering and processing data, laser scanner(s) and/or digital camera(s) and/or video camera(s).

**Figure 1.** Vehicle-based mobile laser scanning (Optech, 2008).

## Segmentation and Filtering Techniques

Extraction of tree points from a dense point cloud in an urban environment is still a challenging task. Efficient segmentation and filtering techniques are essential to extract these features from high amount of data set.

### *Surface Growing Segmentation*

A comprehensive review of various segmentation techniques is done by Vosselman et al. (2004). Among them, the relevant surface growing segmentation in point cloud data is discussed in this Section. Surface growing segmentation in point clouds works similarly to the region growing segmentation in image. It is mainly the culturing of the surface points having similar properties. The process is carried out in two steps. First step includes the identification of seed surface and second is the growing of seed surface.

**Identification of Seed Surface:** Selection of seed surface is performed by fitting the plane to the group of points and analysing the residual values of each of them. The point belonging to a plane having residuals less than some threshold is considered as seed surface. In the presence of outlier, more robust methods like the least square or the Hough transformation methods are used to fit the plane.

**Growing of Seed Surface:** Once the seed surface is identified, the growing of the seed surface towards the neighbourhood points is done based on the proximity, global planarity and smooth normal vector field.

*Proximity of points:* The points, which are within a certain distance from the selected seed surface, are added to the surface. 2.5 D and TIN data structures are used to identify the points on the surface.

*Locally planar:* For this, first the equation of enclosed plane through all the surface points within the radius is determined. A candidate point is selected from surface points. The selection criterion is based on the orthogonal distance of a point to the plane. The point within this distance is selected if all the neighbouring points in a plane are below some threshold value.

*Smooth normal vector field:* To implement these criteria, local surface normal for each point in the point cloud is calculated. A candidate point is chosen if the angle between the normal of growing surface and local normal of point is below some threshold value.

Rabbani et al. (2006) presents the smoothness constraint to segment the unstructured point cloud of industrial scene. The method is based on two steps, local surface estimation and surface growing. Local surface normal is estimated by fitting the plane to neighbourhood points based on the k-nearest neighbourhood (KNN) or the fixed distance neighbourhood (FDN). KNN uses K-D tree data structure to create adjacency information of points by maintaining a list of indices for each neighbourhood points. FDN considers a given fixed Area of Interest (AOI), and selection is done within the area for each query point. The surface growing of segment is performed based on the calculated norms and its residuals. In this phase, additional points are added to the segment based on the proximity and smoothness criteria of the surface.

### *Filtering Ground Points*

Different approaches for identification and filtering ground and no ground points in ALS datasets are proposed in different literatures. Vosselman (2000) proposed a slope based filtering method for the identification of ground points by comparing slopes between the laser point and its neighbours. The working principle of this algorithm is closely related to the erosion operator used in mathematical morphology. A point is classified as a ground if the calculated slopes value between a point and its neighbourhood point is less than a predefined threshold. The critical step in this method is setting of slope threshold, by using prior knowledge of the terrain, which is somewhat subjective. The improvement is done by using progressive morphological filter (Zhang et al., 2003). The method utilizes different windows size for the identification of ground and no ground surface from laser scanning data. The filtering results are satisfactory in both the urban and mountainous areas; however selection of windows size is a difficult task.

Several attempts have been made for the improvement of slope-based filter. Slope adaptive neighbourhood method was proposed as a modification

of the slope-based filter to correct the problem regarding the steep sloped terrain (Filin and Pfeifer, 2006). Cluster-based segmentation approach is used for computing the features like normal vector and the classification of surface based on the similar orientation. It has improvement over the feature quality so the segment tends to be greater with respect to triangulation-based segmentation. A slope-based planar-fitting filtering algorithm for data filtering and feature extraction in urban area is presented by Qihong (2008). Their methods analyse the spatial distribution of laser point cloud. This study uses a plane fitting algorithm. It fits the horizontal planes for filtering the ground points and vertical planes for the building walls in the urban areas. Meng, Wang et al. (2009) explore the Multi-directional ground filtering (MGF) algorithm which is sensitive to detect steep slopes as it integrates the advantages of neighbourhood-based and directional scanning approaches. The major limitation of these algorithms is on the assumption of slope difference. Most of these slope-based algorithms assume that the slope difference between the ground point to another neighbouring point are gradual. However, these are abrupt in reality. The scan line directly produces an elevation or slope profile for each scan line. An adaptive filtering technique for identification of ground points by utilizing the slope threshold of a profiler has been proposed in Sithole and Vosselman (2001). The scan line technique produce a slope profile for each scan line, which is useful for the identifications of ground points along the profiles. Elevation differences along scan lines are used by Sithole and Vosselman (2005) for the identification of ground and non-ground points along the scan lines. The major drawback of these approaches is that the result is highly influenced by the choice of filtering direction.

### *Urban Tree Point Cloud Detection*

An urban area is a heterogeneous composition of objects like tree, building, poles, vehicles etc. Several researches have been done for the detection and filtering of these objects. Haala and Brenner (1999) proposed an integrated classification approach from the multi spectral images and laser altimetry data for the extraction of urban objects like building, tree and grass covered area. The algorithm requires normalised DSM derived from laser data to get the height information of each image pixel. The morphological filtering operation to detect and filter urban objects was used by Chen et al. (2007). Their method performed well even in many complicated objects such as large buildings, steep slopes, bridges, ramps and vegetation on steep slopes. However, the main limitation of this method is every data sets, parameters should be specified on trial and error basis, which leads to more manual iteration.

Normalized difference vegetation index (NDVI) is a numerical indicator, used by researchers to detect the vegetation in urban environment. Lovan et al. (2007) detect the urban vegetation by combining NDVI and saturation index (SI) from a high resolution aerial image and a DSM with 20 cm resolution in an automatic way. Tao and Yasuoka (2002) used high resolution satellite

imagery and ALS data for the detection of urban tree. The methods use digital elevation model (DEM) derived from ALS data. There is a limitation in the calculation of NDVI value due to a number of perturbing factors including spectral effects, atmospheric effects, clouds, soil effects etc.

Derivative approach was used to separate building and tree by Morgan and Tempfli (2000). The main concept behind this algorithm was: canopy structure of tree was irregular whereas roof surface of buildings were considered as planer. The first and second derivatives of an irregular surface should be variable whereas the first derivatives planar surfaces were either zero in flat roof case or constant in sloped roof case, and the second derivatives of a sloped planar surface were zero. These methods are not free from limitations because of the small features such as chimneys or water tanks that introduce the discontinuity in the measurement and finally lead to abnormal derivatives value.

Laser scanning systems have the capability to record the multiple reflections caused by the objects on the earth's surface. Alharthy and Bethel (2002) used the difference between the first and last echo to separate building and tree. Tovari and Vogtle (2004) had implemented a fuzzy logic approach based on first and last echo differences to classify vegetation. The difference is generally larger for tree and close to zero for building measurements. However, their method does not work well for dense trees area where laser pulses cannot penetrate.

Object-based point cloud analysis (OBPA) was used for the detection of urban vegetation by M. Rutzinger et al. (2007). The presented algorithm used surface roughness, the ratio between 3D and 2D point density and the statistics on first and last echo occurrence within the segments for the extraction of objects. The main advantage of this method is that it does not require DTM calculation. Their algorithm has limitations over heterogeneous distribution of point cloud.

## Data Sets and Test Site

Implementation of developed algorithm was done on two data sets having different point density. Data set contains both deciduous and coniferous species of tree. The following sub section explains the details of both data sets.

### *Data Set and Test Site I*

The first data set was acquired with a LYNX Mobile Mapper V100 system (Optech, 2008) by surveying eight kilometre long track city of Enschede, The Netherlands in 2008. The scanning system consists of two 360° rotating laser sensors mounted at the backside of the vehicle orientated diagonal to each other. The sensor setup is proven to be minimal shadow effects and safer to use. The manufactory information of the sensor is shown in Table 1.

**Table 1.** Manufacturer specifications of LYNX system (Optech, 2008)

| | |
|---|---|
| Date | 2008 |
| Maximum range | 100 m (at 20% reflectivity target) |
| Range precision | 0.7 cm (1 sigma) |
| Absolute accuracy (GPS) | 5.0 cm (at 100 km/h) |
| Scan angle | 360 degree |
| Scan rate | 150 Hz (9000 rpm) |
| Measurement rate | 100,000 pulses/sec per sensor |
| Echo per pulse | 4 echoes |

### *Data Set and Test Site II*

EuroSDR (Kukko et al., 2007) data set of test site Espoonlahti was used as the second data set. The City Espoonlahti is located in Espoo, about 15 km west of Helsinki, Finland. ROAMER-mobile laser scanning system was used to acquire this data along the 1.7 km of road environment. The sensor setup consists of frequency 48 Hz and having rotation of both clockwise and counter clock wise. Scanning system details are summarised in Table 2.

**Table 2.** ROAMER data of Espoonlahti (Kukko et al., 2007)

| | |
|---|---|
| Date | 2009 |
| Laser scanner | Faro Photon™ 80 |
| Laser point measuring frequency | 120 kHz |
| IMU frequency | 100 kHz |
| GPS frequency | 1 Hz |
| Driving speed | 30 km/h |

## Methodology

Urban areas are the dense mixture of objects such as traffic poles and signs, electric masks, buildings and trees. Modular approach is used to detect the tree point cloud from dense mixture of urban objects. The details of step are shown in Fig. 2.

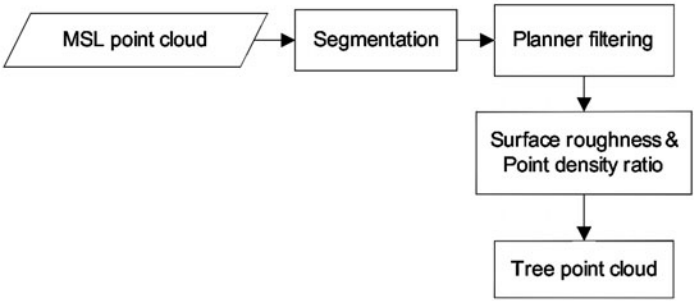


**Figure 2:** Workflow for tree detection (Adopted from Pratihast, 2010).

The workflow started with mobile laser scanning point cloud as input data set. From MLS point clouds, only 3D positional information i.e. (X, Y, Z) coordinate, was used for further processing.

Segmentation is considered as one of the most important processes for automatic process of MLS point cloud. The process of segmentation starts with the establishment of neighbourhood relationship among the points. Most common data structures available for this neighbourhood relationship are Delaunay triangulation, Octree and kd-tree. In this work, surface growing segmentation technique was used to segment the point clouds. In this segmentation, 3D kd-tree was used to establish the neighbourhood relationship among the points. 3D Hough transformation was used to generate seed surfaces. The surface growing parameters such as surface growing radius, maximum distance to the surface and the minimum distance to the recomputed local plane which guide the extension of seed to the neighbourhood point was defined by users.

After the surface growing segmentation, the larger planer area was removed by using the horizontal plane fitting algorithm (Qihong, 2008). The remaining point clouds contain traffic poles and signs, electric masks, buildings, vertical walls and trees. Connected component analysis was applied on these points. This analysis is simplified version of clustering algorithm (Barbakh et al., 2009). The implementation of algorithm starts with the selection of seed point. The set of points connected to each seed point with distance smaller than some threshold were labelled as connected one. This analysis comprises better results for relatively dense and well separated objects.

Once the objects were connected, the trees and non-tree objects are separated by calculating surface roughness and point density ratio. Point density ratio (modified after Rutzinger et al., 2007; Höfle et al., 2009) to a given height threshold was estimated using following mathematical relation:

$$DR = \frac{N_{\text{Totl}}}{N_{\text{Hth}}} \tag{3}$$

where $DR$ is point density ratio, $N_{\text{Totl}}$ is total number of points and $N_{\text{Hth}}$ is number of points present in certain height threshold.

Height threshold of 0.5 m was considered. The idea behind applying this threshold value is to remove features like small cars, thinner walls, and pedestrian and at the same time keep tree points. Further improvement in filtering was done by calculating surface roughness of each segment. It was implemented by calculating standard deviation (SD) of height (Z coordinate) of plane fitting residuals.

## Results

The developed algorithm was implemented in C++ as a programing language. First, a surface growing segmentation was performed in input dataset. Figure

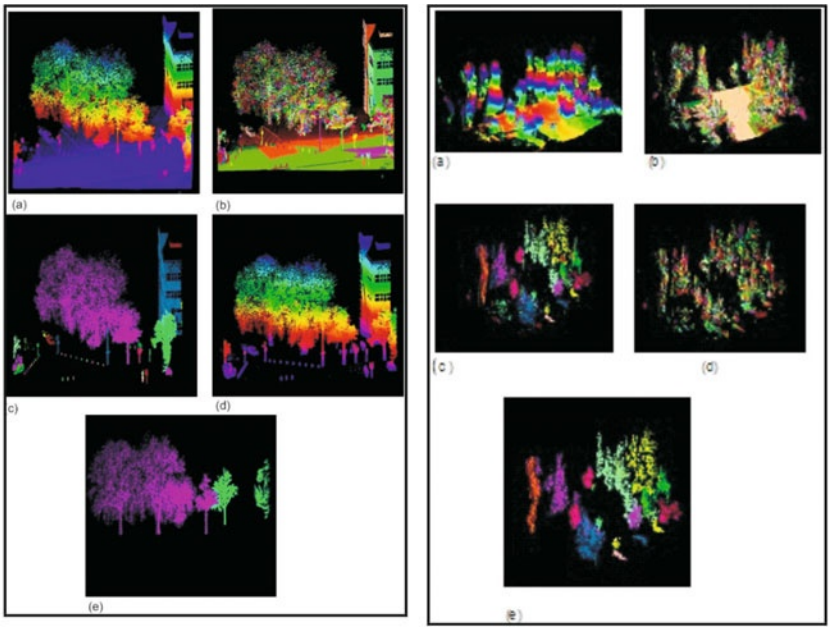

**Figure 3.** Left: Enschede data set I (Adopted from Pratihast, 2010), Right: EuroSDR data set II (a. Input data, b. Segmented point clouds, c. Removal of planer surface, d. Connected component analysis, e. Tree point clouds).

3(a) is the visual representation of input data sets. The parameters of the segmentation were obtained by trial and error basis to obtain larger planner ground segment area. Table 3 shows the parameters for surface growing segmentation.

**Table 3.** Surface growing segmentation parameters used in point cloud mapper

| Surface growing parameters | Value |
|---|---|
| Surface model | Planer |
| Surface growing neighbourhood definition | Direct neighbours |
| Surface growing radius | 0.6 m |
| Maximum distance to surface | 0.3 m |
| Minimum distance to recomputed location | 0.15 m |

The result of surface growing segmentation is shown in Fig. 3(b). It can be clearly identified that the larger segmented area is a planer region. The larger planer regions were filtered by fitting the horizontal plane to each segment. Threshold of Angle 10 ° and area 100 m² was used to fit the plane.

Figure 3(c) represents the dataset after removing planer segments. Connected component analysis was performed on remaining data sets. The parameters used for this analysis are listed in Table 4.

**Table 4.** Parameters for connected component used in point cloud

| Connected component parameters | Value |
|---|---|
| Maximum distance between the points | 1.5 m |
| Minimum number of points | 10 |

The result after application of connected component analysis is shown in Fig. 3(d). Each unique colour represents each connected segments. Further improvement in filtering was done by using surface roughness and point cloud density ratio value. The threshold of surface roughness of greater than 0.85 and point density ratio larger than 2 was used to select the trees. The final output is shown in Fig. 3(e). From the final output, it is clear that the datasets contains only the tree point clouds.

## Conclusions

It is noticeable that the mobile laser scanning has provided the opportunity to be of use for larger scale mapping. The developed algorithm has shown potential to detect the trees inventories in larger data sets. The overall accuracy of the detected trees in both data sets is 78% and 85%. What our study has shown is that surface roughness and point density ratio are significant features to separate the tree and non-tree objects. The detected point clouds are highly suitable for 3D tree modelling (Pratihast, 2010; M. Rutzinger et al., 2010; Martin Rutzinger et al., 2011) and urban biomass estimations. More testing of methods is required in forest data sets. Further development is required in differentiating bushes and small trees.

## Acknowledgement

We would like to thank Optech and EuroSDR for providing data for this research. The authors are also thankful to Faculty of Geo-information Science and Earth Observation (ITC), Universiteit Twente, Enschede, The Netherlands, especially Geoinformatics department, for overall research arrangements and valuable advice during the study.

## References

Alharthy, A. and Bethel, J. (2002). Heuristic filtering and 3D feature extraction from LIDAR data. *International Archives of Photogrammetry Remote Sensing and Spatial Information Science*, **34(3/A)**, 29–34.

Barbakh, W., Wu, Y. and Fyfe, C. (2009). Review of Clustering Algorithms. Non-Standard Parameter Adaptation for Exploratory Data Analysis (pp. 7–28).

Barber, D., Mills, J. and Smith-Voysey, S. (2008). Geometric validation of a ground-based mobile laser scanning system. *ISPRS Journal of Photogrammetry and Remote Sensing*, **63(1)**, 128–141.

Bucksch, A. and Lindenbergh, R. (2008). CAMPINO – A skeletonization method for point cloud processing. *ISPRS Journal of Photogrammetry and Remote Sensing*, **63(1)**, 115–127.

Chen, Q., Gong, P., Baldocchi, D. and Xie, G. (2007). Filtering airborne laser scanning data with morphological methods. *Photogrammetric Engineering and Remote Sensing*, **73(2)**, 175.

Filin, S. and Pfeifer, N. (2006). Segmentation of airborne laser scanning data using a slope adaptive neighborhood. *ISPRS Journal of Photogrammetry and Remote Sensing*, **60(2)**, 71–80.

Haala, N. and Brenner, C. (1999). Extraction of buildings and trees in urban environments. *ISPRS Journal of Photogrammetry and Remote Sensing*, **54(2–3)**, 130–137.

Haala, N., Peter, M., Cefalu, A. and Kremer, J. (2008). Mobile lidar mapping for urban data capture. Paper presented at the Conference on Virtual Systems and MultiMedia Dedicated to Digital Heritage, Limassol, Cyprus.

Iovan, C., Boldo, D. and Cord, M. (2007). Automatic extraction of urban vegetation structures from high resolution imagery and digital elevation model. *Urban Remote Sensing Joint Event*, 2007, 1–5.

Kukko, A., Andrei, C., Salminen, V., Kaartinen, H., Chen, Y., Rönnholm, P. et al. (2007). Road Environment Mapping System of the Finnish Geodetic Institute–FGI Roamer. Paper presented at the International Archives of Photogrammetry, Remote Sensing and Spatial Information Sciences.

Lindenberger, J. (1989). Test Results of Laser Profiling for Topographic Terrain Survey. *Schriftenreihe des Instituts für Photogrammetrie der Universität Stuttgart*, **13**, 25–39.

Mallet, C. and Bretar, F. (2009). Full-waveform topographic lidar: State-of-the-art. *ISPRS Journal of Photogrammetry and Remote Sensing*, **64(1)**, 1–16.

Meng, X., Wang, L., Silvun-Curdenas, J.L. and Currit, N. (2009). A multi-directional ground filtering algorithm for airborne LIDAR. *ISPRS Journal of Photogrammetry and Remote Sensing*, **64(1)**, 117–124.

Morgan, M. and Tempfli, K. (2000). Automatic building extraction from airborne laser scanning data. *International Archives of Photogrammetry and Remote Sensing*, **33(B3/2; Part 3)**, 616–623.

Norbert, H., Michael, P., Alessandro, C. and Jens, K. (2008). Mobile Lidar Mapping For Urban Data Capture. Digital Heritage – Proceedings of the 14th International Conference on Virtual Systems and Multimedia, VSMM, 95–100.

Optech (2008). LYNX Mobile Mapper Data Sheet. http://www.optech.ca/pdf/LynxDataSheet.pdf, accessed on 2-10-2009.

Pratihast, A.K. (2010). 3d tree modelling using mobile laser scanning data. University of Twente, Faculty of Geo-Information and Earth Observation ITC, Enschede.

Qihong, Z. (2008). Data filtering and feature extraction of urban typical objects from airborne lidar point cloud. The International Archives of the Photogrammetry, Remote Sensing and Spatial Information Science, 37 (Part B3b).

Rabbani, T., van den Heuvel, F. and Vosselmann, G. (2006). Segmentation of point clouds using smoothness constraint. *International Archives of Photogrammetry, Remote Sensing and Spatial Information Sciences*, **36(5)**, 248–253.

Rosell, J.R., Llorens, J., Sanz, R., Arnó, J., Ribes-Dasi, M., Masip, J., Escolà, A., Camp, F., Solanelles, F., Gracia, F., Gil, E., Val, L., Planas, S. and Palacin, J. (2009). Obtaining the three-dimensional structure of tree orchards from remote 2D terrestrial LIDAR scanning. *Agricultural and Forest Meteorology*, **149**, 1505–1515.

Rutzinger, M., Hofle, B. and Pfeifer, N. (2007). Detection of high urban vegetation with airborne laser scanning data. Proceedings Forestat, Montpellier, France.

Rutzinger, M., Pratihast, A.K., Oude Elberink, S.J. and Vosselman, G. (2010). Detection and modelling of 3D trees from mobile laser scanning data. *In:* Proceedings of the ISPRS Commission V mid - term symposium : Close Range Image Measurement Techniques, 21-24 June 2010, Newcastle, UK/ed. by J.P. Mills et al. *The International Archives of the Photogrammetry, Remote Sensing and Spatial Information Sciences (ISPRS)*, **38(part 5)**, 520–525.

Rutzinger, M., Pratihast, A.K., Oude Elberink, S.J. and Vosselman, G. (2011). Tree modelling from mobile laser scanning data-sets. *The Photogrammetric Record*, (10.1111/j.1477-9730.2011.00635.x).

Shan, J. and Toth, C. (2008). Topographic Laser Ranging and Scanning: Principles and Processing. Taylor and Francis Group.

Sithole, G. and Vosselman, G. (2001). Filtering of laser altimetry data using a slope adaptive filter. *International Archives of Photogrammetry and Remote Sensing*, **34(3/W4)**, 203–210.

Sithole, G. and Vosselman, G. (2005). Filtering of airborne laser scanner data based on segmented point clouds. *International Archives of Photogrammetry, Remote Sensing and Spatial Information Sciences*, **36(part 3)**, 12–14.

Tao, G. and Yasuoka, Y. (2002). Combining high resolution satellite imagery and airborne laser scanning data for generating bareland DEM in urban areas. *International Archives of the Photogrammetry, Remote Sensing and Spatial Information Sciences*, **30**.

Tovari, D. and Vogtle, T. (2004). Classification methods for 3D objects in laser-scanning data. *Int. Archives of Photogrammetry and Remote Sensing*, 1682–1750.

UN (2001). World urbanization prospects: the 1999 revision – Key findings. Retrieved 25.05.2011, from http://www.un.org/esa/population/publications/wup1999/urbanization.pdf

Ussyshkin, V. (2009). Mobile Laser Scanning Technology for Surveying Application: From Data Collection to End-Products. Paper presented at the FIG Working Week, Surveyors Key Role in Accelerated Development Eilat, Israel, 3–8 May 2009.

Vauhkonen, J., Tokola, T., Packal, N.P. and Maltamo, M. (2009). Identification of Scandinavian Commercial Species of Individual Trees from Airborne Laser Scanning Data Using Alpha Shape Metrics. *Forest Science*, **55(1)**, 37–47.

Vosselman, G. (2000). Slope based filtering of laser altimetry data. *International Archives of Photogrammetry and Remote Sensing*, **33(B3/2; Part 3)**, 935–942.

Vosselman, G., Gorte, B., Sithole, G. and Rabbani, T. (2004). Recognising structure in laser scanner point clouds. *International Archives of Photogrammetry, Remote Sensing and Spatial Information Sciences*, **46(Part 8)**, 4–6.

Zhang, K., Chen, S., Whitman, D., Shyu, M., Yan, J. and Zhang, C. (2003). A progressive morphological filter for removing nonground measurements from airborne LIDAR data. *IEEE Transactions on Geoscience and Remote Sensing*, **41(4)**, 872–882.

# 13

# Multisensor Fusion of Remote Sensing Data for Crop Disease Detection

**Dimitrios Moshou, Ioannis Gravalos[1], Dimitrios Kateris Cedric Bravo[2], Roberto Oberti[3], Jon S. West[4] and Herman Ramon[2]**

Department of Hydraulics, Soil Science and Agricultural Engineering, School of Agriculture, Aristotle University Thessaloniki 54124, Greece

[1]Technological Educational Institute of Larissa, School of Agricultural Technology, Department of Biosystems Engineering 41110 Larissa, Greece

[2]Division of Mechatronics, Biostatistics and Sensors Department of Biosystems, K.U. Leuven, Belgium

[3]Istituto Di Ingegneria Agraria, Universita Degli Studi di Milano, Italy

[4]Plant Pathology and Microbiology Department, Rothamsted Research Harpenden AL5 2JQ, UK

## Introduction

There is an increasing pressure to reduce use of pesticides in modern crop production in order to decrease the environmental impact of current practice and to lower the cost of production. It is therefore important that spraying of chemicals only takes place when and where it is really needed. Since disease appearance in fields is frequently patchy, sprays may be applied unnecessarily to disease-free areas. The control of disease could be more efficient if disease patches within fields could first be identified and then phytosanitary chemicals are applied only to the infected areas. Recent developments in optical sensor technology and control systems provide the potential to enable direct detection of foliar diseases under field conditions and subsequent precise application of chemicals through targeted spraying.

With mechanisation and intensification of agriculture in Europe, fields and farms are becoming larger. However, currently inputs (fertilizer, pesticides,

J.K. Thakur et al. (eds.), *Geospatial Techniques for Managing Environmental Resources*,
DOI 10.1007/978-94-007-1858-6_13, © Capital Publishing Company 2012

fungicides) are applied uniformly despite substantial variability in soil type, crop density or disease pressure. Recent developments in agricultural automation have made it possible to spatially adjust farm application of phytosanitary chemicals. New technologies such as the global positioning system (GPS) and variable rate spraying systems allow the prospect of Precision Pest Management (PPM), which aims to target phytosanitary chemicals where and when needed and at an appropriate dose. PPM could make an important contribution by assisting farmers in the reduction of inputs and it could also significantly reduce both residues in produce and environmental contamination. Patchiness can pose a problem to the accurate assessment of disease, which could influence the decision to spray and the dose to apply. Methods for assessing the spatial distribution of disease in fields would greatly assist both spray decision making and spray application. Disease can cause changes in transpiration rate, leaf colour, morphology and crop density, which in turn affect, to a certain extent, the optical properties of the canopy. Indeed, changes in optical properties have been used to assess visually the risk of disease for many years, but such assessments by the farmer or the extension worker are time consuming and can be relatively inaccurate. Recent progress in sensor technology (Moshou, Bravo, West, McCartney and Ramon, 2004) has made possible the differentiation of diseased and healthy areas of the crop, and thus the prospect of automatically measuring the spatial distribution of crop diseases.

In the current work, data fusion has been used to improve crop disease detection in the field. The data fusion was performed using a Support Vector Machine (SVM) neural network which decreased the error to 1%. The SVM-based disease classifier can be implemented in on-line field disease detection.

## Background

### Sensing for Disease Detection

There are strong indicators that crop diseases can be detected automatically (Moshou et al., 2004). The carriers of information for detection considered in this work are electromagnetic waves. The working hypothesis is that healthy plants interact (absorb, reflect, emit, transmit or fluoresce) with electromagnetic radiation in a different way compared to infected plants. Plants show different optical properties. Some of these differences can be spotted by the naked eye, others are revealed by using advanced equipment. According to Lee et al. (2010), at the earliest infection stages fluorescence is the most appropriate technique for fungal disease detection since it samples the health status in terms of photosynthetic efficiency. However, fluorescence alone cannot provide a clear indication of specific stress factors, having only medium detection accuracy, while accuracy is sensitive to light intensity.

Following initial metabolic changes, the fungus spreads radially around its infection point. The initial infection area necroses: it loses pigmentation, the photosynthetic apparatus is disassembled and the cell walls collapse. At this moment infection patterns become visible. According to Lee et al. (2010), analysis of the light reflection can help in detecting infection from this stage onwards. Pathogen propagules can be detected in the visible spectrum (400-700 nm) depending on the pathogen; chlorophyll degradation in the visible spectrum and red-edge; senescence in the visible spectrum and short-wave near-infrared (680-800 nm) due to browning and near-infrared (1400-1600 nm and 1900-2100 nm) due to dryness and variations in canopy density and leaf area in the short-wave near-infrared.

The disease will gradually take control over the entire plant, which will show a global stress leading to general closure of the stomata, in order to reduce water losses. This change in transpiration can be monitored by thermographic sensors. However, the overall leaf temperatures change rapidly, and are heavily dependent upon ambient temperature, illumination and wind. Therefore, due to changing environmental factors, thermography gives poor results when used on proximal sensing platforms.

Previous work on wheat yellow rust detection has been based on single sensors or fusion of sensor data. Examples include the work of Zhang and Dickinson (2001), where fluorescence is used to assess the dynamics of fungal growth in wheat. Another approach presented by Bravo, Moshou, West, McCartney and Ramon (2003) concerns the detection of yellow rust in wheat by using spectral information from a spectrograph. This approach was extended to include the use of neural networks in order to increase detection performance (Moshou et al., 2004). The advantage of using sensor fusion of spectral and fluorescence imaging features has been shown by Moshou et al. (2005). Image processing methods to detect soybean rust from multispectral images under laboratory conditions have been presented by Cui, Zhang, Li, Hartman and Zhao (2010).

### *Remote Sensing for Crop Disease Detection*

Remote sensing either by using satellites, aerial or ground-based platforms has been used extensively for the detection of crop diseases. Myers (1983) reviewed studies on the use of aerial photography for detecting potato late blight, clitocybe root rot of pecans, bunch disease of pecans, phony disease of peaches, corn leaf blight, bacterial blights and root rot in beans, and root rot in cotton and alfalfa fields. Ryerson, Curran and Stevens (1997) reviewed more aerial photographic studies grouped by four major types of crop diseases: air-borne, seed-borne, insect-borne, and soil-borne. In addition to the above mentioned diseases, they reported that aerial photography has been successfully used to detect the following diseases: yellow rust of wheat, stem canker in rape, leaf spot and rust of the sugar-bearing crops of beet and cane, mould and dwarf-mosaic virus in corn, virus yellows in sugar beet, barley yellow dwarf

virus in winter wheat, barley yellow mosaic virus, take-all in winter wheat, and docking disorder root infection in sugar crops. Johnson, Alldredge, Hamm and Frazier (2003) investigated the spatial and temporal dynamics of late blight from colour-infrared (CIR) aerial photographs of five commercial potato fields and they concluded that aerial photography coupled with spatial analysis was an effective technique to quantitatively assess disease patterns in relatively large fields and was useful in quantifying an intensification of aggregation during the epidemic process on a large scale. Although aerial photography has been the primary remote sensing technique used for study of crop diseases, multispectral and hyperspectral electronic imaging systems have also been used for this purpose.

Apan, Held, Phinn and Markley (2004) demonstrated that Hyperion satellite hyperspectral imagery can be used to detect the orange rust disease in sugarcane. Du, French, Skaria, Yang, and Everitt (2004) evaluated the potential of air-borne multispectral and hyperspectral imagery for detecting citrus greasy spot. Franke and Menz (2007) evaluated high resolution QuickBird satellite multispectral imagery and air-borne HyMap hyperspectral imagery for detecting powdery mildew and leaf rust in winter wheat and their results showed that high enough classification accuracies were achieved only when the infection was severe at the late crop growth stages.

Pre-mapping of diseases and stresses could also be achieved using air-borne systems. Spatial resolutions down to a few metres are possible from satellites and to below 1 m from aircraft (Blakeman, Bryson and Dampney, 2000). Current commercial satellite sensing is probably not suitable for early disease detection (even if the wavelengths at which data are collected were suitable) because of limitations in spatial resolution. At best, satellite images can be useful by highlighting relatively large areas of disease or other stresses in a crop, which can then be checked by the farmer. In addition, revisit time and variability in cloud cover could mean that even this simple information may not be available when required. Aircraft-mounted systems do not have these constraints and could be used when required. However, data acquisition equipment would likely have to be faster, more sophisticated, and more expensive than for terrestrial vehicle-mounted systems. Disease maps, whether produced by tractor-, aircraft-, or satellite-mounted detection systems, could be used to control spray equipment, positioned using GPS or a local reference system.

As far as we are aware, practical disease-mapping/spray application systems based on remote sensing are not yet available for any crop/disease system. Cropforecaster™, a service of Infoterra and ZedX (http://www.cropforecaster.com/) offers a comprehensive set of online products including maps and summary statistics of crop status. Products include information on crop stage, acreage, condition and expected yields. This information is updated on a daily basis thereby quantifying the impacts of each day's weather observations and forecasts.

### *Fusion-based Classifiers in Remote Sensing*

Some studies employ SVM classifiers in remote sensing tasks. In some cases, the performance of SVM-based classification is improved through data fusion. Zhang, Huang, Huang and Li (2006) proposed a pixel shape index describing contextual information of nearby pixels and evaluated its usability for land cover classification using QuickBird data based on SVMs. Pixel shape indices were combined with transformed spectral bands such as principal component analysis or independent component analysis. They found that fusion of spectral and shape features as well as transformed spectral components in an SVM were able to improve the accuracy of classification. Mitra, Shankar and Pal (2004) proposed an active learning-based approach to reduce the selected support vectors. Their semi-supervised method gradually created clusters based on user input. Their method yielded better results than a typical SVM; however the authors cautioned on the sensitivity of the algorithm regarding user-provided erroneous labelling. Zhang and Ma (2008) proposed an SVM variant, the Potential SVM as an alternative for multispectral image classification. The Potential SVM is an attractive variant due to its ability to handle non-Mercer kernels and its mathematical formulation that addresses SVM scalability issues. A fusion approach to classification using extended morphological profiles was proposed in Fauvel, Benediktsson, Chanussot and Sveinsson (2008). They evaluated the approach using high spatial/spectral resolution ROSIS data in urban areas based on SVM classification. Ensemble methods for multiple SVM integration were evaluated by Pal (2008).

## Multisensor Fusion for Crop Disease Detection

### Fields, Plants and Material

Yellow rust patches were established in six plots of winter wheat, 10 × 9 m in size and surrounded by 3 m wide guard rows, and located on IACR-Rothamsted's experimental farm. Pots (10 cm diameter) containing six winter wheat plants (cv. Madrigal) at the second leaf stage (GS 12) and growing in potting compost, were dusted with uredospores of pathogen *Puccinia striiformis* (which causes yellow rust), mixed with 10 parts talcum powder. The plants were then covered with transparent plastic cloches to maintain a high humidity and were kept at 10 °C. The cloches were removed after two days and the plants were transferred to a glasshouse (14–20 °C). The procedure was repeated seven days after the first inoculation to ensure that all plants would be well colonized. Chlorosis was visible 15 days after the first inoculation (sporulation after about two weeks). One pot of infected plants was planted at the centre of each of the six field-plots, approximately three weeks after the first inoculation. Similar uninoculated plots were used as a control. Forty days later, the inoculated plots had clearly visible patches (plants with over 5% disease severity) of yellow rust approximately 2–3 m in diameter. This was the stage of yellow rust development at which the decision to use pesticides had to be

made. Measurements of plants infected with yellow rust and healthy plants were obtained using spectrographic and fluorescence equipment in plots of winter wheat. So, a disease spread simulating realistic situation has been reproduced and examined by experts visually to provide reference data for the automated classification. The classification accuracy of the automated classification has been tested against expert visual inspection.

## Spectral Equipment and Data Acquisition

The spectral equipment used during the experiments consisted of a JAI CV-M300 digital visual monochromatic camera on which a V9 Specim spectrograph (Herrala, Okkonen, Hyvarinen, Aikio and Lammasniemi, 1994) was mounted. The spectrograph measured a line on the canopy. The length of the measured line was 0.5 m and its width was 4 mm. For every single area of 0.65 mm by 4 mm along this line the spectrograph projected a spectrum (between 460-900 nm) onto the camera. The projections from all these small areas created a spectral image, with spectral and spatial axes. Light was directed through a Canon 13 mm 1:1.5 C-mount objective into the spectrograph. An irradiation reference of 50% reflectance (Spectralon SRS 50-010, 1.25″ diameter, constant 50% reflectance over the 300-2500 nm band) was placed at a constant vertical distance of 70 cm from the objective. It had a flat surface and was positioned horizontally. The equipment was fixed on a buggy, and it was possible to maintain a constant distance between objectives and canopy. Measurements were made in plots of winter wheat under ambient conditions. The objectives were positioned at spray boom height (approx. 1 m). After data acquisition, the images were stored as 8-bit matrices with a spectral and a spatial dimension. An example of how the images were stored is shown in Fig. 1.

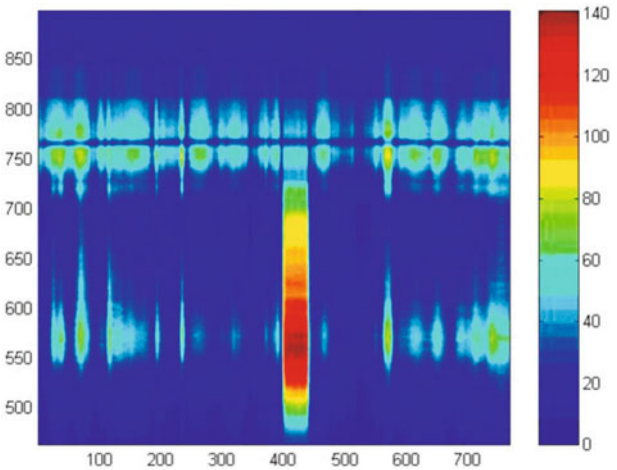


**Figure 1.** A spectral image as it was stored. Numbers on the vertical axis correspond with wavebands in nm, the horizontal axis represents the spatial dimension in camera pixel units.

## Waveband Selection

The spectral resolution of the spectrograph was 20 nm. As a first step, in the spectral axis, every 25 pixels were fused into larger bands of 20 nm using uniform averaging. In order to find the best discriminating wavebands between diseased and healthy spectra, wavebands were selected through a stepwise variable selection procedure. The procedure was based on the following: a waveband was only selected when its addition to the existing set of selected wavebands significantly increased the discriminating power of the new set of wavebands as determined by an F-test; and before a new waveband was chosen, the already chosen wavebands were investigated for the significance of their presence in the selected set. The ultimate selection was then used to build the discrimination model. The waveband selection leads to the advantage that only three wavebands were needed to be processed from each image which reduces substantially the computational burden and can be implemented in real-time.

## Support Vector Machines

SVMs (Vapnik, 1998) correspond to a relatively new computational intelligence technique, related to the machine learning concept. SVMs are used in pattern recognition as well as in regression estimation and linear operator inversion. SVMs have interesting attributes, different than other computational intelligence techniques, such as neural network training algorithms and more specifically algorithms used for training multilayer perceptrons. In contrast to many classical neural network training algorithms which exhibit many local minima, SVMs are always able to find a global minimum and they have a simple geometric interpretation. More specifically, in order to estimate a classification function such as:

$$f: \mathbf{x} \rightarrow \{\pm 1\} \tag{1}$$

The most important is to select an estimate $f$ from a well restricted so-called *capacity* of the learning machine. Small capacities may not be sufficient to approximate complex functions, while large capacities may fail to generalize, which is the effect of what is called "overfitting".

In the case of neural networks two major techniques are used to avoid overfitting. One is "early stopping" while the other technique is based on the regularization or smoothing of the error function and it aims at limiting the complexity of the neural network model. In the case of support vector machines, regularization is also used to avoid overfitting. However, overfitting in SVMs is limited according to the statistical theory of learning from small samples (Vapnik, 1998). The simpler decision functions are the linear functions. In case of SVM, the implementation of linear functions corresponds to finding a large margin of separation between two classes. This margin corresponds to

the minimum distance of the training data points from the separating surface. The procedure that is followed in order to find the maximum margin of separation is formulated as a convex quadratic problem (Vapnik, 1999). An additional parameter enables the SVM to misclassify some outlying training data in exchange for obtaining a larger margin between the rest of the training data, without however affecting the optimization of the quadratic problem.

The input data are projected into a feature space $F$ using a map such as:

$$\phi : \mathbf{x} \rightarrow F \tag{2}$$

Then a linear learning machine can be extended to a non-linear one. In SVMs the latter procedure is applied implicitly. What has to be supplied is a dot product of pairs of data points $\phi(\mathbf{x}_i) \cdot \phi(\mathbf{x}_j) \in F$ in the feature space. Thus, in order to compute these dot products, one has to supply the kernel functions that define the feature space via:

$$K(\mathbf{x}_i, \mathbf{x}_j) = \phi(x_i) \cdot \phi(x_j) \tag{3}$$

It is not necessary to know the mapping $\phi$ since it is performed implicitly. SVMs can also learn which of the features implied by the kernel are distinctive for the two classes. The selection of an appropriate kernel function may boost the learning process.

## Sensor Fusion

### *Introduction*

Multi-sensor data fusion systems (Hall, 1992) combine data from multiple sensors to perform inferences that may not be possible from a single sensor alone. Applications span military problems (target identification, threat assessment), remote sensing problems (location of mineral resources), medical diagnosis, control of complex machinery and automated manufacturing. Data fusion is analogous to the ongoing cognitive process used by humans to integrate data continually from their senses to make inferences about the external world.

Development issues for data fusion systems depend on the phenomena that are observed, the type of sensors utilised, and the inferences sought. These inferences in turn determine the type of techniques required. Generally applications aimed at higher-level inferences require techniques from the artificial intelligence domain such as expert systems, template matching, neural networks and fuzzy logic. The relative advantages and disadvantages of the different sensing techniques lead to consideration of a combination of spectral techniques with fluorescence imaging as clearly advantageous due to higher recognition accuracy and less sensitivity to environmental factors. So there is a need to employ sensor fusion.

*Generic Scheme for Sensor Combination*

A generic scheme for sensor fusion has to include a number of steps to assure that the handling of the data doesn't result in loss of information critical for the classification. Also due to the typically small datasets that are available the method that is used should be able to handle missing or sparse data. From this point of view a network like the SVM is preferable in the case of small and sparse datasets. The feedforward neural networks also known as multilayer perceptrons (MLP) typically need a large supply of data to be able to produce an accurate mapping. Therefore in the case of small datasets the MLP is not recommended. Independent of the type of neural network in use, the proposed scheme is shown in Fig. 2.

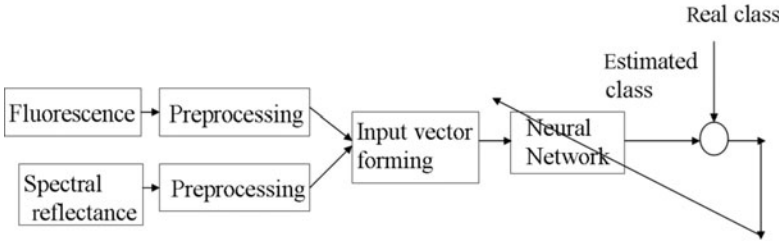


**Figure 2.** Schematic representation of a conceptual sensor fusion system based on Neural Networks (either SVM or MLP).

In practice a situation can arise where a failure of one or more of the sensors can actually jeopardise the successful operation of the whole fusion-based disease detection system. In such a case a modular decision architecture that is based on the remaining sensors must be in place ready to switch into action or operate in parallel and provide a decision in parallel to the fusion system. A generic modular scheme for sensor fusion (conceptual design shown in Fig. 3) has to include a number of steps to assure that the handling of the

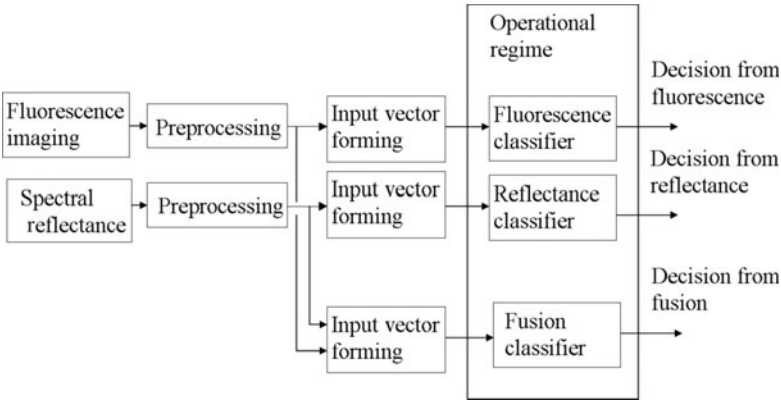


**Figure 3.** Schematic of a modular sensor fusion system based on neural networks.

data doesn't result in loss of information critical for the classification. Also due to the typically small datasets that are available the method that is used should be able to handle missing or sparse data.

## Quadratic Discriminant Analysis (QDA)

Once the most discriminating set of wavebands was selected, a simple discrimination rule was defined. This criterion, called the quadratic classification rule, was based on the Mahalanobis distance of a single observation (average of normalized spectra over a fixed window) to the class means (healthy or diseased). An observation was then classified according to the smallest Mahalanobis distance to a class mean. The overall spectral dataset consisted of 9800 spectra from healthy plants and 15700 spectra from diseased plants. The criterion was trained on 75% of the data. The discrimination models were thereafter validated by a test dataset using the other 25% of all data. Results of using QDA are shown in Table 1.

**Table 1.** Different classification results for spectrographic data. Results obtained using QDA

| *Status* | *Classified healthy* | *Classified diseased* | *Total* |
|---|---|---|---|
| Healthy | 90.24% (2211 of 2450 spectra) | 9.76% | 100% |
| Diseased | 12.74% | 87.26% (3425 of 3925 spectra) | 100% |

Observations expressed in % classified into each category.

## Imaging Fluorescence Disease Detection

The multispectral fluorescence imaging system (MFIS) was based on a 10-bit CCD camera with a digital output and a resolution of 1300′1000 pixels, linked with a four-band optical beam splitter. This optical device allowed to split the current field of view of the camera in four identical sub-images, each one independently filtered with pass-band filters (450 nm, 550 nm, 690 nm, 740 nm, all with a full width at half maximum FWHM of 10 nm). Chlorophyll fluorescence was excited by a continuous emission xenon arc lamp (ILC Technology LX175 with a power of 175 Watt) equipped with an IR cut-off filter and a low pass filter with a threshold at 420 nm, limiting its emission to the spectral range 350-420 nm. The lamp was controlled via a TTL trigger signal by a portable PC, which acquired and stored the images. As the intensity of the fluorescence signal is extremely weak, representing a few percent of the xenon lamp light absorbed, compared to the reflected environmental light, background disturbance was reduced by means of an opaque shield, which covered the sampled canopy as well as the instrumentation.

During the initial field experiments, for each measurement, two consecutive images were acquired: first, a background image with the xenon lamp off and immediately after, a second image when the sample was illuminated by both the environmental and the xenon lamp light. However, having as target the real-time use of the MFIS, only a fluorescence image recorded at the fluorescence peak was used, thus avoiding the waiting time of one second between image recordings. All subsequent processing was based on the image obtained at the fluorescence peak. The fluorescence image was acquired at exactly one second from the start of the excitation by the xenon light in order to coincide with the fluorescence peak using an exposure time of 10 msec.

The MFIS was mounted on a mobile platform (buggy) and operated from a distance of about 0.8 m from the canopy and the area excited to fluorescence by the xenon lamp light had a typical diameter of 0.5-0.6 m. Fluorescence images at 450 nm, 550 nm, 690 nm and 740 nm were obtained for canopy areas of about 0.2 m diameter, situated in the middle of the illuminated region, resulting in a typical resolution of about 0.3 mm/pixel. The obtained fluorescence images showed typical disease patches (Fig. 4). It was observed that disease lesions are characterised by a high emission at 550 nm and a low emission at 690 nm, where for a healthy region the fluorescence intensity was quite uniform in the two bands.

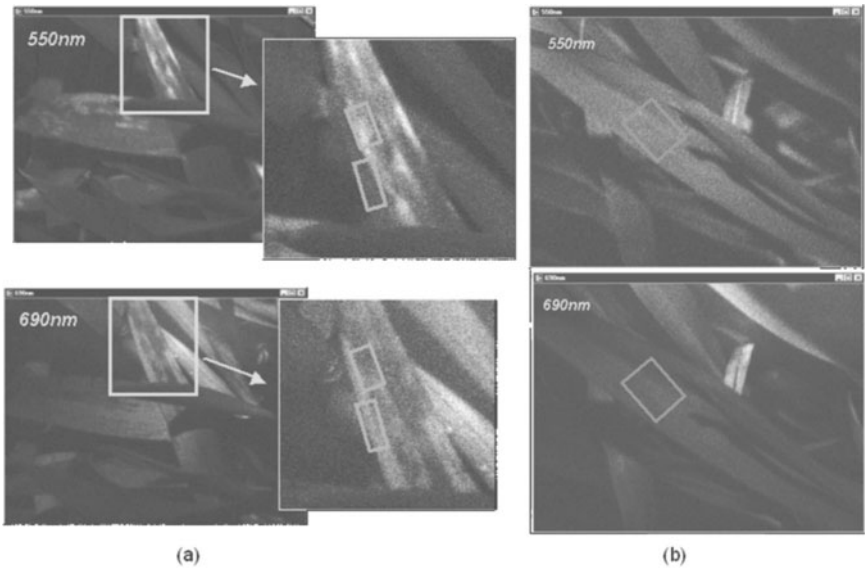


**Figure 4.** Night field fluorescence images obtained at 550 nm and 690 nm of an infection patch (4a) and of a healthy leaf (4b). On infected regions two typical properties can be observed: (i) a high emission at 550 nm and a low emission at 690 nm associated with the lesion (orange frame); (ii) a low emission at 550 nm and high at 690 nm in the surrounding area (green frame). Healthy regions (blue frame) characterised by a more uniform emission in the two bands.

Based on this, just the images in the two fluorescence bands 550 nm and 690 nm were used and a disease index for each pixel was defined as the relative intensity in the two bands, $f_G$ (equation 4).

$$f_G = \frac{I_{550\text{nm}}}{I_{550\text{nm}} + I_{690\text{nm}}} \tag{4}$$

In bi-spectral (550 and 690 nm) fluorescence images, an infected region in a healthy plant appeared as a spatial discontinuity of the ratio $f_G$, which looked like a "patch", on an approximately uniform background. Numerically, this means that $f_G$ related to a disease patch diverged from a value of 0.5, which was typical for healthy regions, to higher values for lesions ($f_G \approx 0.7$) or to lower value for surrounding halos ($f_G \approx 0.3$).

A fluorescence image based disease detection algorithm has been presented in Moshou et al. (2005). A brief description is given here:

1. An adaptive thresholding procedure was applied to the image at 690 nm in order to segment the image in well illuminated canopy regions and background (including soil, dead leaves, shadow etc.). The segmentation is based on a grey level threshold automatically calculated by an iterative histogram analysis.
2. The retained regions were then spatially filtered by using morphological filtering in order to eliminate spots pertaining to noise and to fill possible "holes" in closed areas in order to obtain the vegetation region to be inspected.
3. Equation (4) was applied pixel by pixel to the regions retained after step 2, in order to calculate for each point the function $f_G$ and to obtain a spatial map of $f_G$ values. The pixels characterised by $f_G > 0.65$ were classified as suspect lesion area *SLA*; finally the ratio of *SLA* on the total investigated pixels was considered as an estimate of the disease severity degree in the imaged sample.

For classification purposes a pixel was assumed to be "diseased" when $f_G$ exceeded 0.65. A lesion index (LI), defined as the fraction of the analyzed pixels that were "diseased" ($f_G > 0.65$), and representing the suspected diseased area, was calculated for each image. Only well illuminated vegetation pixels, determined by an adaptive threshold were included in the analysis. For all measurements LI values were determined and saved in appropriate format to be fused with spectral measurements for the same measured field areas. Typical values obtained were: LI = 0 – 0.07 for a healthy canopy; LI = 0.05 – 0.20 for a slightly infected canopy; LI = 0.35–0.60 for a disease focus. QDA results from LI are shown in Table 2.

**Table 2.** Disease classification results for fluorescence imaging. Results obtained using QDA

| *Status* | *Classified healthy* | *Classified diseased* | *Total* |
|---|---|---|---|
| Healthy | 71.43% (1750 of 2450 spectra) | 28.57% | 100% |
| Diseased | 4.35% | 95.64% (3754 of 3925 spectra) | 100% |

Observations expressed in % classified into each category.

## Sensor Fusion Results for Disease Detection

In order to design a practical optical sensing system that can detect healthy and diseased canopies it is important to reduce the number of selected wavebands to a minimum, while still maintaining satisfactory discrimination performance. QDA was used for disease detection based on the features identified from the F-test waveband selection. Three 20 nm wide wavebands (680, 725, 750 nm) that gave the best discrimination performance were selected. A total of four fusion features were used: three spectral reflectance values and the fluorescence parameter, LI. The two 20 nm wide wavebands (750 nm and 680 nm) were also used for leaf detection by NDVI. Disease discrimination results derived from a fusion of these measurements are presented in Table 3.

**Table 3.** Disease classification results derived from the fusion of sensor measurements made in the field. Results obtained from the test dataset using QDA.

| *Status* | *Classified healthy* | *Classified diseased* | *Total* |
|---|---|---|---|
| Healthy | 97.75% (2395 of 2450 spectra) | 2.22% | 100% |
| Diseased | 8.87% | 91.13% (3577 of 3925 spectra) | 100% |

Observations expressed in % classified into each category.

The SVM described in the previous section was also tested in the same testing set as the proposed technique. The kernel that gave the best results was a radial basis function, spread ($\sigma$) of 7.07 as this was able to provide the best result.

The preprocessing steps were exactly the same as those followed for the QDA. The two wavebands used for leaf detection by NDVI (750 +/– 10 nm and 680 +/– 10 nm) should always be considered for discrimination purposes. Diseases could successfully be discriminated by using the following three wavebands: 680, 725, 750 +/– 10 nm (ordered as 725 – 750 – 680 nm in the feature vector). Results of sensor fusion based on the SVM are shown in Table 4.

**Table 4.** Results of field experiments: sensor fusion (SVM)

| *Status* | *Classified healthy* | *Classified diseased* | *Total* |
|---|---|---|---|
| Healthy fusion | 98.78% (2420 of 2450 spectra) | 1.22% | 100% |
| Diseased fusion | 0.66% | 99.34% (3899 of 3925 spectra) | 100% |

Observations expressed in % classified into each category.

### Discussion

Optical sensing and mapping with the proposed system is most likely to assist the optimization of fungicide applications against fungal foliar diseases. Optical disease detection systems are unlikely to be able to detect nonsymptomatic infections in field conditions (although this can be possible with individual leaves under laboratory conditions), and even may only be able to detect disease at relatively high severity thresholds. It is therefore likely that optically derived disease maps will underestimate disease patch sizes. Even if low disease thresholds were detectable, for polycyclic pathogens, new (secondary) areas of infection would probably be incubating outside detected areas as zones of asymptomatic latent infections. Reduction in inoculum early in an epidemic, for example by spraying a visible disease patch, would delay an epidemic by the time period taken for the disease to return to the level prior to treatment (Vanderplanck, 1984). This could be enough for the crop to escape any economic yield effects but when the growth rate of an epidemic is high, the effect of decreasing initial inoculum is reduced and the need to eliminate all of the disease in and around a focus increases. Spraying the original patch at an early stage with an eradicant-type fungicide may be effective but only if the epidemic rate of the disease is low. It may be possible to treat latent infections around the visible disease patch by predicting the area of incubating infections using disease-spread models. In practical systems, it would therefore be necessary to modify initial disease maps to account for undetected disease or latent infections around detected disease patches. The modified maps would then form the basis for spatial spray application using a curative fungicide.

## Future Research Directions

The results of the experiments presented in this work clearly demonstrate that techniques based on the fusion of measurements from different optical sensors have great potential for developing tractor-based (or mobile or autonomous platform) systems for disease detection in the field. It is shown that the SVM-based disease classifier can be implemented in on-line field disease detection. With the proposed adaptations the whole disease detection system shows

clear potential for real-time field based disease detection. Some of the challenges in these techniques are: (i) the effect of background data in the resulting profile or data, (ii) optimization of the technique for a specific plant/tree and disease, and (iii) automation of the technique for continuous automated monitoring of plant diseases under real world field conditions.

Future investigations could encompass comparisons of the accuracy of data obtained from satellite, air-borne and ground data on the same fields where crop diseases have appeared. An interesting approach would be to combine data at different scales through data fusion techniques.

One particular emerging issue is the sensor-web or sensor networks. Earth environments are exceptionally dynamic and interrelated through a number of systems. To understand Earth systems and dynamics, significant improvements in spatial and temporal observations are required. The consensus is that fusion of data from multiple sensor systems is currently one of the optimal solutions. However, increasingly inexpensive, yet sophisticated, chips for the computer and telecommunication industries provide an unique opportunity to develop a distributed, heterogeneous, and adaptive observing system or sensor web in the future. Such sensor networks can enable the continuous monitoring of vast areas of cultivated land and issue warnings over early symptoms of pathogen attacks on crops.

Kung, Hua and Chen (2006) described a Drought Forecast and Alert System (DFAS), which is a four-tier system framework composed of mobile users, ecology monitoring sensors, integrated service server, and intelligent drought decision system. DFAS combines wireless sensor networks, embedded multimedia communications, and neural network decision technologies to effectively achieve the forecast and alert of the drought. Emphasis is on multi-sensor fusion of large arrays of local sensors, joined with other assets, to provide real-time imagery, weather, targeting information, mission planning, and simulations for military operations on land, sea and air. A similar forecast and alert system might benefit the early detection of the onset of disease epidemics.

Machine learning techniques, such as artificial neural networks (ANN), support vector machines and regression trees, have been widely used in many applications. However, they are often considered to be "black-box" approaches that do not reflect the physics of the modelled process in remote sensing (Krasnopolsky and Schiller, 2003; Loyola, 2006). With the rapid development of these techniques, their potential needs further exploration. For example, neural networks have been combined into hierarchical or multi-neural systems with either redundant or modular elements. The combination of neural networks solves complex tasks more effectively and can furthermore result in dramatic performance improvement. It fully exploits the advantages of neural methods and expands the range of applicability. An important drawback of many ANNs is their lack of explanation capability. It is increasingly apparent that, without some form of explanation capability, the full potential of trained ANNs may

not be realized. Many studies have focussed on mechanisms, procedures and algorithms designed to insert knowledge into ANNs (knowledge initialization), extract rules from trained ANNs (rule extraction) and utilize ANNs to refine existing rule bases (rule refinement) (Andrews, Diederich and Tickle, 1995; Ding and Xin, 2006; Lofstrom, Johansson and Niklasson, 2004; Nunez, Angulo and Catala, 2006; Saad and Wunsch, 2007). The land remote sensing community should pay close attention to these developments. These approaches can result in highly performant adaptive intelligent systems for prediction of disease epidemics through extraction of early stress indicators and better decision support regarding treatment strategy development.

Air-borne, space-borne and ground-based imagery has been used successfully to detect and map a large number of crop diseases, but early detection remains difficult and in some cases even impossible. In most cases, by the time disease symptoms can be detected on the remote sensing imagery, damage has already been done to the crop. For some diseases, this may be early enough to take control measures in order to minimize damage; for others, it may be too late to correct the problem within the growing season. In fact, remote sensing imagery has been primarily used to assess the extent and intensity of the damage caused by disease. In this regard, remote sensing is a very cost-effective tool. Moreover, remote sensing image data obtained in the current growing season can be useful for the management of reoccurring diseases, such as soil-borne fungi, in the following seasons.

As remote sensing imagery is becoming more available and less expensive, it will present a great opportunity for both growers and researchers to use more effectively this data source for the detection of crop diseases. Many crop diseases have been identified as good candidates for remote sensing, but practical procedures for farming operations are still lacking. Efforts need to be devoted to the development of operational methodologies for detecting and mapping these candidate diseases. Meanwhile, more research is needed to evaluate more advanced imaging systems and image processing techniques for distinguishing diseases that are difficult to detect or occur with other stresses.

## Conclusion

Previous laboratory studies have shown that optical sensing techniques have the potential to discriminate between diseased and healthy plants. The work that is reported here demonstrates the feasibility of using such methods for disease detection under field conditions. Two separate approaches were used: one based on spectral reflectance measurements and one based on fluorescence imaging. A spectral reflection method, based on only three wavebands, was developed that could discriminate disease from healthy winter wheat crops. The method based on fluorescence was less accurate (overall discrimination error of about 16.5%), although it used only two fluorescence wavebands.

However, fusing the measurements from the two approaches together allowed overall disease from healthy discrimination of 94.5% by using QDA (discrimination error of 5.5%). Further, by using SVM for the fusion classifier, increased the overall discrimination performance to around 99%. More significantly, while the advantage of SVM over QDA in healthy plant detection was marginal (only 1% improvement), the improvement in diseased plant detection increased over 8%. The results of these experiments clearly demonstrate that techniques based on the fusion of measurements from different optical sensors have great potential for developing tractor-based systems for disease detection in the field. It is shown that the SVM-based disease classifier can be implemented in field disease detection. The results suggest that these methods of disease detection show a good potential with an ability to detect plant diseases accurately. The spectrographic and fluorescence imaging technology could be integrated in a fusion prototype carried by a vehicle or a robotic platform for reliable and real-time plant disease detection in order to achieve superior plant disease control and management.

## References

Andrews, R., Diederich, J. and Tickle, A.B. (1995). Survey and critique of techniques for extracting rules from trained artificial neural networks. *Knowledge-Based Systems*, **8(6)**, 373–389.

Apan, A., Held, A., Phinn, S. and Markley, J. (2004). Detecting sugarcane orange rust disease using EO-1 Hyperion hyperspectral imagery. *International Journal of Remote Sensing*, **25(2)**, 489–498.

Blakeman, R.H., Bryson, R.J. and Dampney, P. (2000). Assessing crop condition in real time using high resolution satellite imagery. *In:* Aspects of Applied Biology 60, Remote Sensing in Agriculture (pp. 163–171). The Association of Applied Biologists, Wellesbourne, UK.

Bravo, C., Moshou, D., West, J., McCartney, A. and Ramon, H. (2003). Detailed Spectral Reflection Information for Early Disease Detection in Wheat Fields. *Biosystems Engineering*, **84(2)**, 137–145.

Bravo, C., Moshou, D., Oberti, R., West, J., McCartney, A., Bodria, L. and Ramon, H. (2004, December). Foliar disease detection in the field using optical sensor fusion. International Commission of Agricultural Engineering (CIGR, Commission Internationale du Genie Rural) E-Journal, Manuscript FP 04 008, 6. Retrieved April 7, 2011, from http://www.cigrjournal.org/index.php/Ejournal/article/view/537/531.

Cui, D., Zhang, Q., Li, M. Hartman, G.L. and Zhao, Y. (2010). Image processing methods for quantitatively detecting soybean rust from multispectral images. *Biosystems Engineering*, **107(3)**, 186–193.

Ding, X.Q. and Xin, S. (2006). Application research on extraction of rule from artificial neural networks for nonlinear regression. *Dynamics of Continuous, Discrete and Impulsive Systems. Series A: Mathematical Analysis*, **13**, 565–568.

Du, Q., French, J.V., Skaria, M., Yang, C. and Everitt, J.H. (2004). Citrus pest stress monitoring using airborne hyperspectral imagery. *In:* Conference Proceedings of the International Geoscience and Remote Sensing Symposia Vol. VI (pp. 3981–3984). Piscataway, New Jersey, IEEE.

Fauvel, M., Benediktsson, J.A., Chanussot, J. and Sveinsson, J.R. (2008). Spectral and spatial classification of hyperspectral data using SVMs and morphological profiles. *IEEE Transactions on Geoscience and Remote Sensing*, **46(11)**, 3804–3814.

Franke, J. and Menz, G. (2007). Multi-temporal wheat disease detection by multi-spectral remote sensing. *Precision Agriculture*, **8**, 161–172.

Hall, D.L. (1992). Mathematical Techniques in Multisensor Data Fusion. Artech House, Boston/London, UK.

Herrala, E., Okkonen, J., Hyvarinen, T., Aikio, M. and Lammasniemi, J. (1994). Imaging spectrometer for process industry applications. Paper presented at Optical Measurements and Sensors for the Process Industries, Frankfurt, Germany.

Johnson, D.A., Alldredge, J.R., Hamm, P.B. and Frazier, B.E. (2003). Aerial photography used for spatial pattern analysis of late blight infection in irrigated potato circles. *Phytopathology*, **93(7)**, 805–812.

Krasnopolsky, V.M. and Schiller, H. (2003). Some neural network applications in environmental sciences. Part I: Forward and inverse problems in geophysical remote measurements. *Neural Networks*, **16(3–4)**, 321–334.

Kung, H.Y., Hua, J.S. and Chen, C.T. (2006). Drought forecast model and framework using wireless sensor networks. *Journal of Information Science and Engineering*, **22(4)**, 751–769.

Lee, W.S., Alchanatis, V., Yang, C., Hirafuji, M., Moshou, D. and Li, C. (2010). Sensing technologies for precision specialty crop production. *Computers and Electronics in Agriculture*, **74(1)**, 2–33.

Lofstrom, T., Johansson, U. and Niklasson, L. (2004). Rule extraction by seeing through the model. *In:* N.R. Pal et al. (Eds.), Lecture Notes in Computer Science 3316: Neural Information Processing (pp. 555–560). Springer, Berlin-Heidelberg, Germany.

Loyola, R.D.G. (2006). Applications of neural network methods to the processing of Earth observation satellite data. *Neural Networks*, **19(2)**, 168–177.

Mitra, P., Shankar, B.U. and Pal, S. (2004). Segmentation of multispectral remote sensing images using active support vector machines. *Pattern Recognition Letters*, **25(9)**, 1067–1074.

Moshou, D., Bravo, C., West, J., McCartney, A. and Ramon, H. (2004). Automatic detection of yellow rust in wheat using reflectance measurements and neural networks. *Computers and Electronics in Agriculture*, **44(3)**, 173–188.

Moshou, D., Bravo, C., Oberti, R., West, J., Bodria, L., McCartney, A. and Ramon, H. (2005). Plant disease detection based on data fusion of hyper-spectral and multi-spectral fluorescence imaging using Kohonen maps. *Real-Time Imaging*, **11(2)**, 75–83.

Myers, V.I. (1983). Remote sensing applications in agriculture. *In:* R.N. Colwell (Ed.), Manual of Remote Sensing (pp. 2111–2228). American Society of Photogrammetry, Falls Church, VA.

Nunez, H., Angulo, C. and Catala, A. (2006). Rule-based learning systems for support vector machines. *Neural Processing Letters*, **24(1)**, 1–18.

Pal, M. (2008). Ensemble of support vector machines for land cover classification. *International Journal of Remote Sensing*, **29(10)**, 3043–3049.

Ryerson, R.A., Curran, P.J. and Stephens, P.R. (1997). Applications: agriculture. *In:* W.R. Philipson (Ed.), Manual of Photographic Interpretation (pp. 365–397). American Society for Photogrammetry and Remote Sensing, Bethesda, MD.

Saad, E.W. and Wunsch, D.C. (2007). Neural network explanation using inversion. *Neural Networks*, **20(1)**, 78–93.

Vanderplank, J.E. (1984). Disease Resistance in Plants. Academic, New York/London, UK.

Vapnik, V.N. (1998). Statistical Learning Theory. Wiley Interscience, New York.

Vapnik, V.N. (1999). The Nature of Statistical Learning Theory. Springer-Verlag, New York.

Zhang, L. and Dickinson, M. (2001). Fluorescence from rust fungi: a simple and effective method to monitor the dynamics of fungal growth in planta. *Physiological and Molecular Plant Pathology*, **59(3)**, 137–141.

Zhang, L., Huang, X., Huang, B. and Li, P. (2006). A pixel shape index coupled with spectral information for classification of high spatial resolution remotely sensed imagery. *IEEE Transactions on Geoscience and Remote Sensing*, **44(10)**, 2950–2961.

Zhang, R. and Ma, J. (2008). An improved SVM method P-SVM for classification of remotely sensed data. *International Journal of Remote Sensing*, **29(20)**, 6029–6036.

# 14

# Geospatial Analysis of Cancer Cases in the Eastern Black Sea Region of Turkey

**Ebru H. Colak and Tahsin Yomralioglu[1]**
Karadeniz Technical University, Dept. of Surveying Engineering
GISLab, Trabzon, Turkey
[1]Istanbul Technical University, Dept. of Geomatics Engineering
Istanbul, Turkey

## Introduction

Cancer has remained an important health issue in recent years. Examining variations of cancer cases temporally and spatially is necessary to develop strategies to combat its occurrence and to put cancer control programmes into practice. Creating cancer maps is necessary for obtaining information such as the location and frequency of cancer cases, the geographic distribution of cancer types and the location of the highest densities of cases. Consequently, creating more reliable and precise data infrastructures will increase the number of accurate decision making options available and aid in determining how and where to implement control strategies.

Numerous studies have been conducted on cancer epidemiology, the majority of which are thematic mapping studies including the observation of spatial distribution of cancer (Pickle et al., 2007; Kulldorff et al., 2006; Brewer, 2006; Morra et al., 2006; Jacquez, 2004; Berke, 2004; Vieira et al., 2002). In addition, more specific cancer studies exist in which advanced statistical analyses are performed (Yomralioglu et al., 2009; Draper et al., 2005; Greiling et al., 2005; Oliver et al., 2005; Flinton and Walters, 2004; Diggle, 2000).

In Turkey, the number of studies on cancer epidemiology remains insufficient. Although control policies were developed and employed against cancer by the Turkish Ministry of Health (2004), comprehensive cancer-mapping for the whole country are not yet available. The studies conducted are mostly regional and oriented toward a specific feature of cancer due to the

J.K. Thakur et al. (eds.), *Geospatial Techniques for Managing Environmental Resources*,
DOI 10.1007/978-94-007-1858-6_14, © Capital Publishing Company 2012

problems regarding reliable cancer statistics for all of Turkey. In line with the current cancer policies, the importance of a cancer registry has gradually increased in recent years. Some regions and cities have initiated pilot schemes for a cancer registry, including the cancer registry centre in the city of Trabzon, located in the Eastern Black Sea region of Turkey.

Spatial epidemiology studies aim to investigate the relationships between important health and environmental factors. Information about the causal factor of the disease is vital for the investigation of the relationship between the geography and the disease. For the spatial relationships among health issues to be explored, information about the disease and the environmental factors that influence it should first be collected and then be analyzed using statistical methods in line with the requirements. Such analyses can be performed effectively using GIS, which can evaluate spatial information, information related to health issues and information related to environmental factors together.

In this study, cancer density maps were produced using GIS techniques for an area that comprises seven cities in Turkey. A model proposal was developed through which statistical studies could be performed about whether carcinogenic environmental factors affect the cases in the defined cancer density areas. Mapping cancer cases enables the consideration of the cancer densities within each administrative unit by also considering the population sizes of these administrative units and the demonstration of an integrated approach to addressing carcinogenic environmental factors. Several studies oriented toward cancer mapping and defining cancer cluster areas exist. Studies that investigate the impacts of environmental factors on cancer focus primarily on more specific issues, including examinations of the relationships between a specific type of cancer and a specific carcinogenic factor. Studies that examine all of these factors in an integrated framework are needed. This study proposes a higher-scale integrated approach that could guide studies on cancer and this proposal promotes the simultaneous operation of the desired specific studies and the consideration of other factors. Different thematic cancer maps have been created using GIS for more detailed studies in the region in epidemiological topics. Consequently, the results of this study would help develop and apply cancer control programmes in the country.

## Background and Context

Cancer incidence has been increasing worldwide and specifically in developing countries. In Turkey, the cancer incidence is calculated as 180-200 per 100,000 people, a rate half that of the European Union countries; this difference is due in part to the age distribution of the population of each region. Turkey expects 144,000 new cancer cases among its population of 72 million and current cancer incidence of 200 per 100,000 (Tuncer, 2009).

The mapping of cancer incidence has enabled the development of important hypotheses about the carcinogenic factors. Due to suitable statistical map presentation techniques, the spatial representation of the density of cancer is made possible by the simultaneous examination of population and cases (Thomas, 1990).

Health geography is a discipline that examines how diseases and health services are distributed across the globe. Scientists have investigated the relationship between health and geography for centuries. Today, the powerful tool used in these studies is GIS technologies (Lang, 2000). The use of GIS in the public health increases the efficiency of spatial analyses and enhances the developments of statistical methods in epidemiology.

GIS is used in community health programmes to monitor developmental and spreading stages of diseases, to assess environmental risks, to develop control strategies related to health issues and to examine issues such as the management and planning of health services. Due to developments in GIS technologies and statistical methods, health and population data in a specified geographical area can be addressed together. Especially in small areas, the investigation of the logical spatial variations or relationships in disease risks becomes possible. Spatial epidemiology is related to both definition and comprehension of such variations. The use of GIS in public health renders the more efficient use of spatial analyses and the development of statistical methods in epidemiology.

## Data and Procedures

### Methodology

Using GIS technologies, this study aims to produce cancer maps for the Eastern Black Sea region of Turkey and to prepare the ground for studies investigating whether the carcinogenic environmental factors are related to the cases in the defined cancer density areas.

For this purpose, the geodatabase has been built with the use of GIS techniques for examining the distribution of cancer cases in the region and thematic maps relating to cancer cases in allocation units was created. Cancer density maps were produced in digital format to examine cancer cases and geographical locations of database content. Geo-statistical analysis was also conducted in a spatial environment.

The presence of data appropriate for the objectives of a study will guide the planned execution of the study. In that case, the existing cancer records limit the accuracy of the descriptive statistical cancer data and analyses for the administrative units.

Figure 1 shows the main methodological structure planned in this study, but general technical methods and steps for developing other similar studies include the following:

- Researching the current literature about health GIS, cancer maps and geostatistics
- Designing and establishing a geospatial database for cancer oriented GIS
- Obtaining cancer statistics for cancer mapping and controlling the address data of cancer cases
- Determining and providing spatial and non-spatial data for the designed cancer based geospatial database and integrating these data into the geodatabase

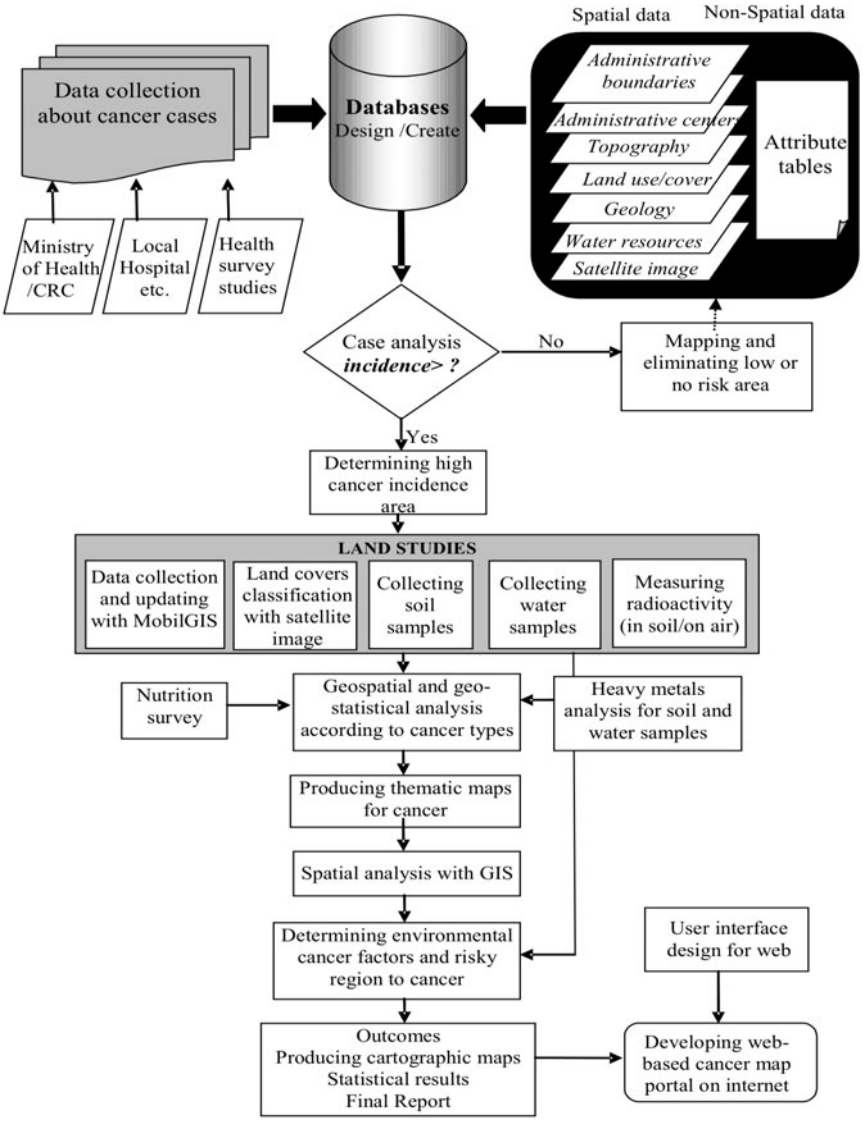


**Figure 1.** A methodological framework of geospatial analysis of cancer cases and associated environmental features.

- Establishing the geo-relationship of cancer cases on the base maps and mapping the spatial distribution of cancer cases
- Performing population-based studies on cancer statistics (incidence, mortality, morbidity, age-standardized cancer incidence rate, etc.)
- Calculating and analyzing the cancer incidence rate for each administrative unit
- Verifying statistical rates associated with cancer risk by cancer types, sex and age groups and integrating these rates into GIS
- Mapping the cancer density maps using geostatistic methods and determining the high cancer density regions
- Applying spatial analysis to the data by cancer types and geostatistic methods
- Determining cancer cluster areas and generating a cancer clustering map
- Examining the relationship between cancer data and geographic features using statistical methods and geostatistics
- Using advanced statistical methods for cancer risk areas
- Identifying high risk areas associated with cancer and environmental exposure
- Representing the final products as thematic maps and other cartography products
- Producing final reports and GIS-based thematic maps

## Cancer-based GIS

Designing the database that enabled the management of the cancer case data and produced spatial statistical data in the GIS environment enabled future studies to use the produced data. The geodatabase managed the data obtained from different sources through different methods by categorizing them in the geospatial data groups of Health (HE), Administrative Unit (AU), Topography (TO), Land Cover (LC) and Geophysics/Environment (GE). In the Cancer-Based Geospatial database shown in Figure 2, each geospatial data group consists of interoperable feature classes.

## Data Inputs

### *Administrative Units and Demographic Data*

The correlation of health events with the geography of residential units was based on administrative units, depending on the scope of the research. The Eastern Black Sea region of Turkey was selected as a case study (Fig. 3), including a total of seven cities (Trabzon, Rize, Artvin, Giresun, Ordu, Bayburt and Gumushane) in the region. Based on this, geospatial data about the administrative centres and boundaries of provinces, counties, districts and villages were collected.

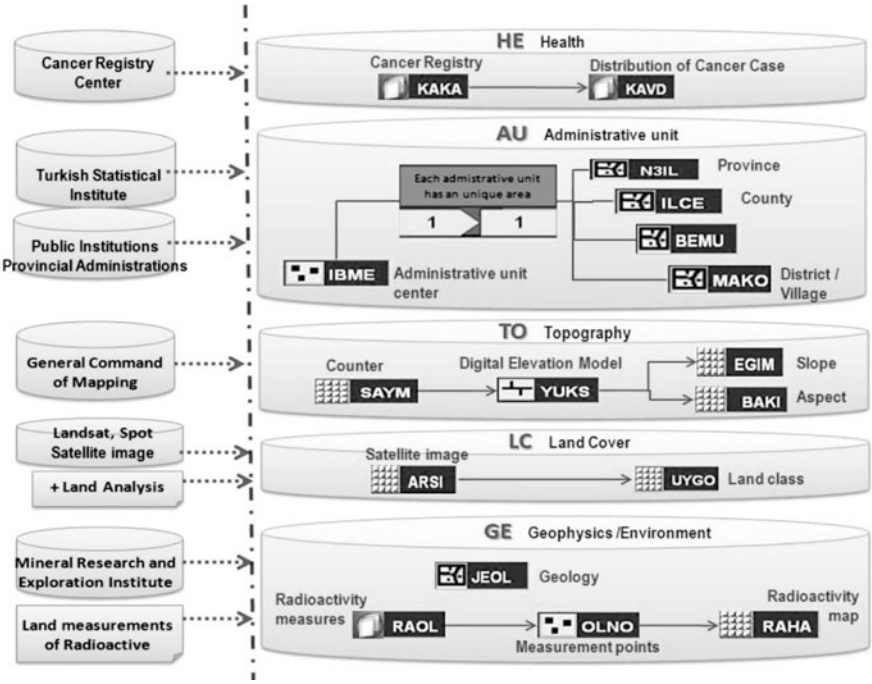


**Figure 2.** Designing the cancer-based geospatial database.

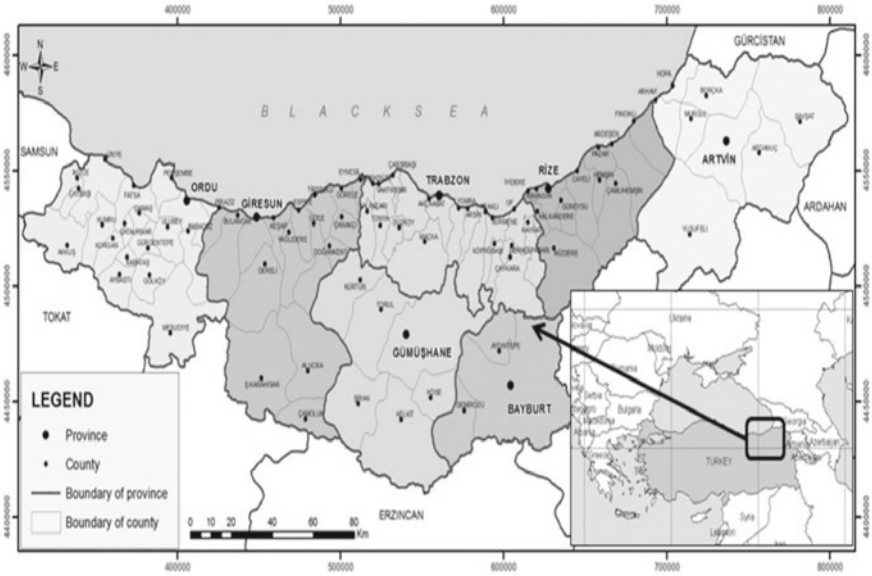


**Figure 3.** Study area: The Eastern Black Sea region of Turkey.

In the Administrative Units data group, provinces, counties and districts/villages are defined in the GIS "polygon" feature class and the centres of administrative units are defined in the "point" feature class. The Administrative Unit Code (AUC) was used to establish an effective relationship between the databases that represent administrative units and statistical health data. The spatial relationship was established by geocoding according to the AUC defined for each administrative unit.

Demographic data regarding the administrative units were gathered from the Turkish Statistical Institute (TURKSTAT). Demographic information on spatial locations was added to the database containing administrative unit data. Demographic data were further classified according to gender. The demographic data used in calculating cancer density rates in the administrative units were important, and the comparison of the number of cancer cases with the population ensured the accurate interpretation of cancer frequency.

### *Cancer Data*

Address specifications were of the utmost importance for the spatial distributions of cancer cases. Statistical cancer data were obtained from the Provincial Directorates of Health with the permission of the Ministry of Health and consisted of information such as the patient's age, gender, address, diagnosis, the disease's ICD code, topology and the diagnosis date.

Cancer statistics from between 2000 and 2007 were obtained from the Cancer Registry Centres (CRC) in the seven provinces included in the scope of this study in the Eastern Black Sea region of Turkey. In total, 15,299 cancer cases were obtained from these CRCs and included in the cancer database, of which 9,520 were males and 5,779 were females.

To place each case in the cancer database on the map, the Administrative Unit Code was added to the designed database according to the address data of the cases. The relationship between the database that includes cancer cases and the database that includes administrative units was formed through the AUC, enabling the transfer of the cancer database to the designed geographical information system. In addition, with the help of geocoding, each cancer case was identified as a point on the map according to its address information.

### *Topographic and Land Use Data*

Geospatial data that represent height describe Earth's topography and are used in base maps and many other mapping practices. In this study, expressing the relationship of cancer cases to height required contour data. Relevant institutions provided 286 pieces of 1/25,000 scale digital maps of the study area that were obtained through the digitizing of contour lines and formed the base data of this study. Using the Spatial Analysis function, a Digital Elevation Model of the area was produced and converted into grid representation.

The land cover map of the Eastern Black Sea region of Turkey was produced using satellite images, including Landsat ETM+ satellite images from 2000. A total of four satellite images in an East-West orientation cover

this area, and correcting the satellite images geometrically concluded the image classification. In the classification of the satellite images, two main methods were used: controlled and uncontrolled classification. While ISODATA algorithm was used in the uncontrolled classification, the Maximum Likelihood algorithm was used in the controlled classification. Extract more information from the existing satellite image, the image enhancement techniques of spectral rationing and principal component transformations were also utilized.

### *Geological Data*

The base map depicting the region's geological structure was another important data layer, with data obtained from the Mineral Research and Exploration Institute. These maps were produced by digitizing 1/100,000 scale analog maps. The produced geological polygon data were incorporated with the geological data and added to the geodatabase. The prepared geology data layer was then subjected to spatial analysis with the cancer data layer, and the data layer produced with the results of the soil test of the region. The region's rock structure was evaluated under seven groups: sedimentary, volcanic, granitoid, alluvial, metamorphic/ophiolithic and other rock types. Figure 4 shows the Geologic Map that represents the region's main geological structure.

### *Radioactivity Data*

Natural radiation originates in space and in elements in the Earth's crust, including uranium-238, thorium-232, radium-226, radon-222 and potassium-40. Analyzing the natural radiation level of a region requires the radiological analysis of that area and involves analyzing its soil, water and air (UNSCEAR, 2000). The area's geological structure also significantly influences its radioactivity level.

To create the radioactivity map of the Eastern Black Sea region of Turkey, radiation levels in the area were measured. The radiation levels measured were the terrestrial outdoor gamma dose rate and the occurrence of radioactive elements, such as uranium, thorium, potassium and cesium, in the soil samples extracted from each test site. Radioactive analyses on the collected soil samples were later analyzed and assessed in the laboratory setting and used to define the locations where radioactivity values would be measured on the map, starting with the prioritized areas. The locations where radioactivity values would be measured were marked according to the cancer density values and proximity to town centres and central transportation lines. Care was taken to distribute the locations homogeneously throughout the region.

After the measurements for radioactivity values were completed, the values from the collected soil samples were analyzed in the laboratory setting. The analysis results were arranged in a table database linked to the geodatabase and designed according to the location coordinates where radioactivity values were measured. Raster surfaces were formed to produce the area's radioactive value maps from the locations with vector data structures. The raster structure was produced using the kriging spatial analysis method, a geostatistical method.

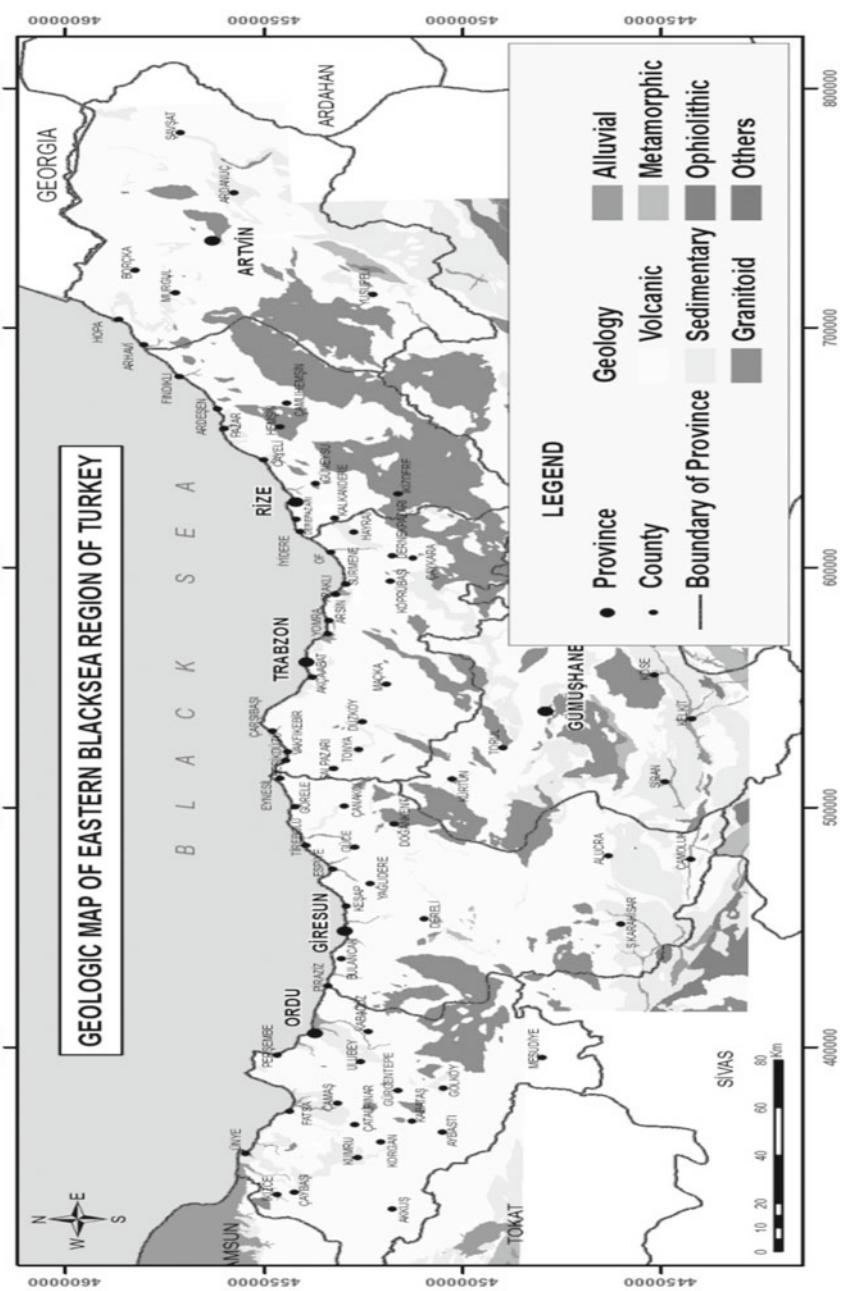


**Figure 4.** Geologic map of Eastern Black Sea region of Turkey.

Figure 5 demonstrates the radioactive value maps of gamma dose, uranium (U-238), thorium (Th-232) and cesium (Cs-137), each produced through the kriging method.

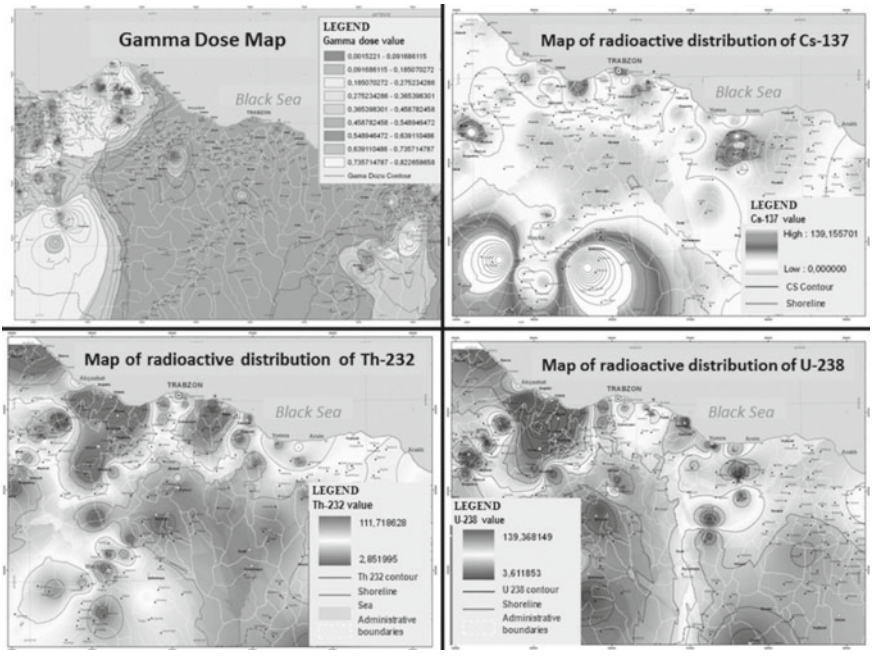


**Figure 5.** Maps of radioactivity in Trabzon Province of Turkey.

*Water Analysis Data*

Water samples were taken from the water supply networks fed by different sources in the area and subjected to necessary chemical analyses to create the water assessment map of the Eastern Black Sea region of Turkey. Preliminary examinations were performed to identify the carcinogenic elements, such as As, Sb, Be, Cd, Co, Cr, Hg, Ni, Pb, Ve, Se, Te, Tl, V, Ba, Sr, Cu, Bi and Mo (Dissanayake and Changrajith, 1999), and sample collection stations were identified. In total, 574 water samples, defined with a 95% confidence level and 10% limit of error, were collected from the region, thereby enabling the investigation of a correlation between heavy metal data and cancer cases.

Relevant chemical analyses were performed on the collected water samples. In the evaluation of the analysis results, the international water quality standards defined by the World Health Organization (WHO) were used. Analysis results were added to the database, and the locations of the samples were represented on the map. This database was then integrated with the cancer-based geospatial database. Heavy metal analysis maps were produced with these results using spatial analyses and statistical map presentation techniques. These maps enabled the statistical examination of the correlation between all heavy metal data and cancer incidence in the administrative units.

## Integration of Spatial Data

All of the spatially-oriented maps and relevant databases produced throughout the study were integrated in the common geographical reference system using a geodatabase created in a GIS environment, and all spatial and geostatistical analyses were performed on this geodatabase.

To ensure more flexible management of the data that form the basis for spatial analysis, grid representations with dimensions of 100 × 100 m were produced for common use throughout the region. Previously created geospatial data layers were overlaid with these grid areas, guaranteeing the uniform use of pixels in this unique system. Figure 6 demonstrates spatially the most general version of the geospatial data layers produced and used in the study. In conclusion, all geospatial data layers were combined in a geodatabase, and the required spatial analyses were conducted using the integrated approach.

One of the important problems encountered in the analysis of GIS-based cancer cases is that the total number of cases, rather than their point-source distribution, was considered for each administrative unit centre because the cases were not fully attached to a meaningful address. Each case was represented as a point on the administrative unit centre, according to the specified administrative unit code, but for most spatial overlay analysis, a polygon-based data layer was needed, rather than a point-based one. To eliminate this problem, by considering the population data of the administrative

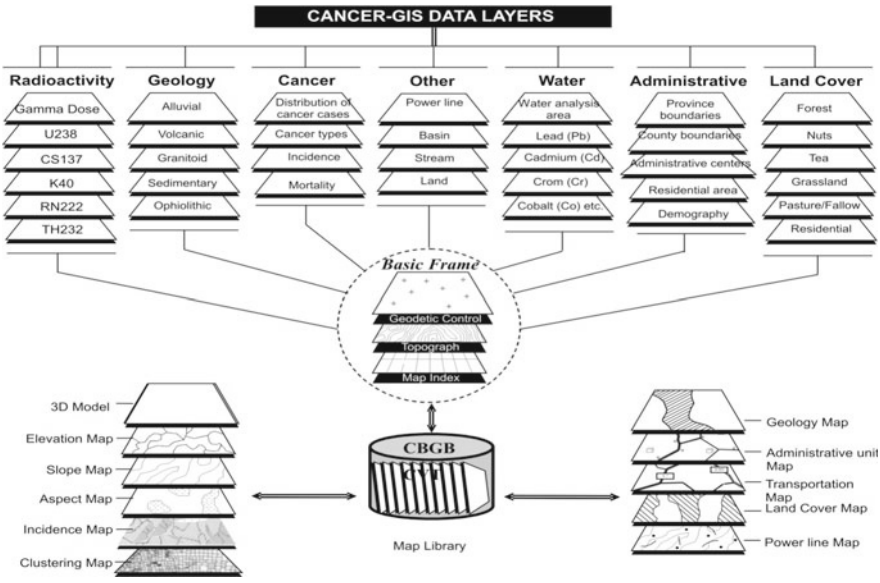


**Figure 6.** Integration of geospatial data layers for a cancer-based GIS.

centres, a polygon-based data layer including detailed data about cancer cases was produced through the application of "buffer" analysis for the spatial representation of administrative units. Most spatial overlay activities were performed with this data layer. This approach prevented unnecessary processes and time loss in GIS.

## Mapping Process for Cancer Cases

The cancer datasets collected in the study and all other required spatial data were incorporated into the geodatabases. Then, various thematic maps were produced through the data presentation opportunities provided by GIS in the scope of the cancer-based Geospatial Database (GDB).

In this study, the spatial distribution of the cancer cases observed in the Eastern Black Sea region of Turkey between 2000 and 2007 was integrated in a geodatabase and shown on base maps using GIS technologies. The cases were represented as points on the administrative units on the map according to the address data obtained. After the cancer cases distribution map was created, incidence rates and the cancer density criteria in each administrative units were calculated and added to the database. Various cancer density maps that depict the cancer densities in the administrative units in the region were produced drawing on the incidence rate data.

In the production of cancer maps, incidence rates indicated the density of cancer in administrative units. The map of distribution of cancer cases observed in the Eastern Black Sea region between 2000 and 2007 was produced in the form of a thematic map presentation, and the map of incidence rates in administrative units was produced using the proportional symbol mapping techniques. In these maps, the representations of cancer density were symbolized by scaling proportional symbols calculated by the incidence values. This chapter includes only one sample map depicting cancer densities in the administrative units produced using the geostatistical method. This cancer density map, shown in Fig. 7, was produced using the kriging interpolation method based on the cancer incidence values.

## Statistical Methods

Although the cancer density rates in administrative units were assessed statistically, only the cancer incidence rate, standardized cancer incidence rate or specific cancer incidence rate was used.

Incidence is defined as the number of new cases of a disease or a health event that occur in a specified time period (Stewart, 2002). Incidence rate indicates the number of new cases within a given time period (i.e. in a year), in a society, the rate of which is known.

Standardization is necessary when comparing two or more societies or communities, the differing basic characteristics (e.g., age, race and socio-economic status) of which influence their respective risks of disease (Esteve

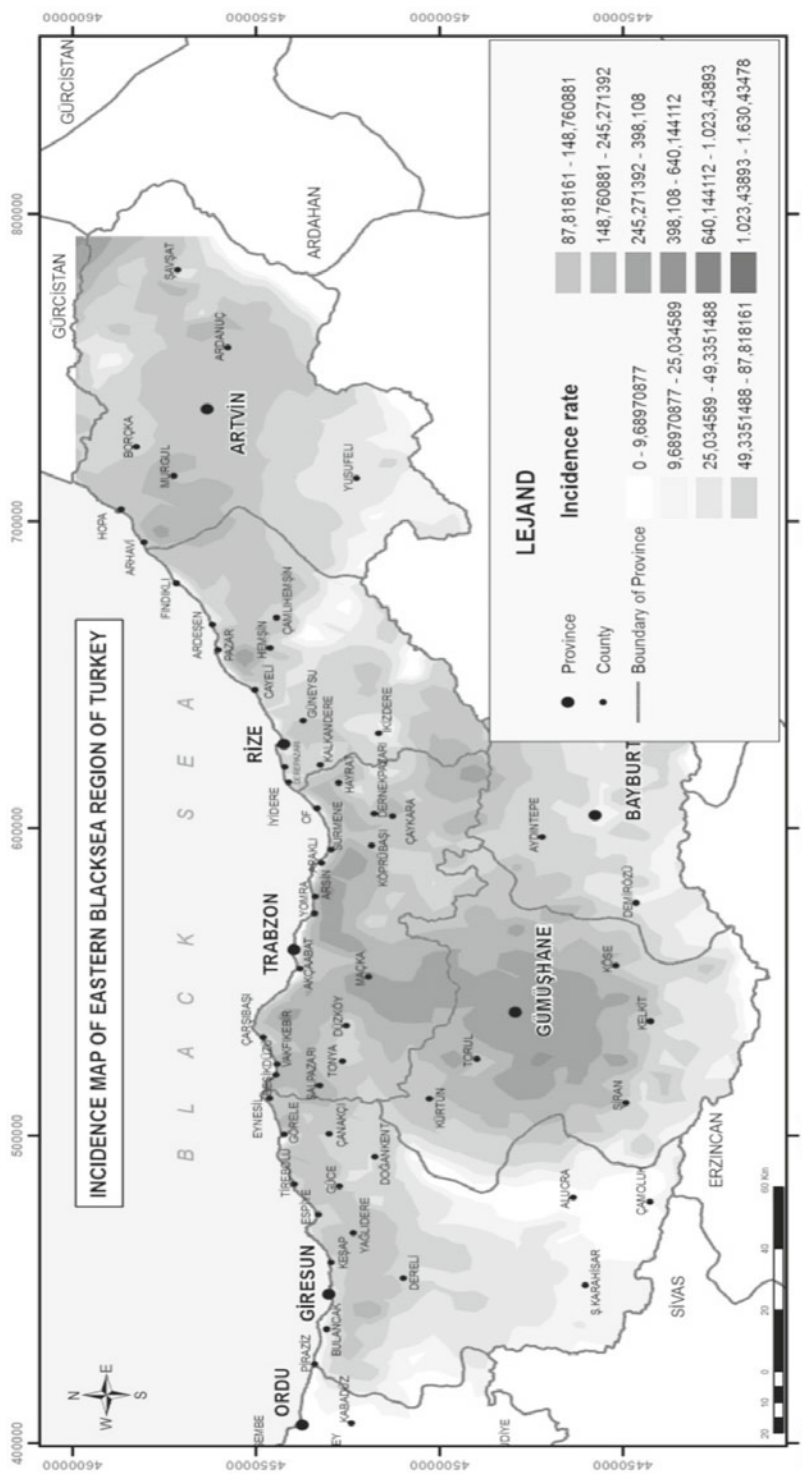


**Figure 7.** The incidence distribution map of Eastern Black Sea region of Turkey.

et al., 1994). The standardized cancer incidence rate refers to the application of common or homogenous characteristics such as age, gender or disease group among different cancer incidence data to enable comparison.

After the incidence densities in the administrative units were calculated, kriging geostatistical analysis method was used to map these densities on geography. In this study, cancer densities were shown on the map of the region in the raster format, using the kriging method. Cancer cluster areas were defined through the Kernel density analysis.

To examine the correlations between cancer frequency and density in the administrative units and the environmental carcinogenic factors, all data were assessed in an integrated style in the GIS environment through spatial analysis and investigations. Relationships between the possible carcinogenic factor targets for investigation and the cancer frequency in residential areas were assessed using the necessary statistical analyses. The Pearson chi-square statistical analysis was used to investigate one-to-one or one-to-many correlations, and other statistical analysis methods, such as the Independent Samples t-test and linear regression, were used in the hypothesis test of bilateral correlations and the analysis of correlations between multifactor environmental causes and cancer frequency, respectively. Statistical methods differed with respect to the content of the hypothesis constructed between each environmental factor and cancer frequencies.

## Examining the Association between Environmental Factors and Cancer

To explore the cancer cases and environmental carcinogenic factors, various spatially based examinations were performed, based on the cancer-based GDB. The cancer data were subjected to overlay analyses in either separate or integrated ways with layers including regional environmental data such as topography, geological structure, water, land cover and radioactivity. The results were then analyzed statistically.

The spatial and statistical analyses in this study tested whether a correlation exists between cancer types and aspect, land cover, geological structure and radioactivity. The chemical analysis results of the heavy metals found in the water samples collected from the administrative units in the region were assessed and represented on maps, and their relationships with the cancer frequencies were tested through geostatistical analyses.

Correlations between cancer cases observed in administrative units or cancer frequency and the environmental factors were considered separately and assessed both geospatially and statistically.

This model allows the examination and statistical assessment of numerous hypotheses regarding environmental factors. However, this book chapter focussed on only one case study. To explore its uses, a sample hypothesis was

developed to examine the correlation between the geological structure and the types of cancer, and the necessary spatial examinations and statistical evaluations were carried out.

### Examination of the Correlation between the Geological Structure and Types of Cancer

To examine the correlation between the region's geological structure and types of cancer, spatially-based statistical analyses were performed. With the help of the spatial examinations carried out using the Eastern Black Sea region geological map and the map of the point distribution of the administrative units, the number of cancer cases encountered depending on the geological structure were categorized by cancer type. The Pearson chi-square test was used to identify any correlation between the land's geological structure and types of cancer. The data were classified and arranged for assessment by statistical software.

Pearson chi-square test was employed through a statistics software in order to statistically examine whether there exists a correlation between types of cancer and the land's geological structure. The statistical analysis used classes of seven rock types and ten types of cancer (lung/bronchial/larynx, skin, leukemia, breast, stomach, colon/rectum, bladder, prostate, thyroid and other types of cancer). The impact of elevation on cancer types was significant according to the results of the Pearson chi-square test ($\chi^2 = 82.378$, SD = 45, $p = 0.001$). According to the results of the statistical analyses, 10.3% of 15,223 cancer cases were observed in sedimentary rock type, 83.1% in volcanic, 2.7% in granitoid, 2.3% in alluvial, 0.1% in metamorphic and ophiolitic mixture and 1.4% in other rock types.

In determining the correlation between types of cancer and rock types, examining the environments that cause this correlation is necessary. Adjusted residuals were used for this purpose. An adjusted residual greater or equal to two is significant for the correlation between two categories of data (rock type and type of cancer). Based on the results of the statistical analysis, stomach and breast cancers were encountered more in areas where the rock type is volcanic, and stomach cancer was observed more in areas where the rock type is granitoid (adjusted $R^2 \geq |2|$).

## Conclusion

Accurately analyzing diseases that threaten public health is necessary to determine prevention and control strategies. To this end, the spatial distribution of the disease, its density areas and relevant statistical dimensions should be examined. Obtaining patient address information and medical history enables the investigation of the health-location relationship. Today, the monitoring of the spatial distribution of diseases uses GIS to produce information systems

based on location and to conduct various spatial and statistical examinations. These systems allow for the simultaneous consideration of health and location, and these systems increase the flexibility and comprehensiveness to demonstrate the regional differences in terms of health and the correlation between a disease and its spatial distribution, land cover, land use, geological structure and elevation.

The frequency of cancer cases in administrative units was spatially compared with population, and its various relationships with environmental factors were investigated through geospatial analyses and statistical examinations. The study aimed to bring together the variety of studies oriented toward cancer epidemiology and address them with an integrated approach. Regions and locations in need of more detailed studies can be determined, and more specifically, environmental exposure studies focussing on a certain type of cancer can utilize these locations. In conclusion, GIS enabled the simultaneous consideration of many environmental factors and played a significant role in this research.

This study demonstrated the effective use of GIS in cancer prevention and control programmes through the spatial representation of cancer case distributions. Performing numerous epidemiological statistical analyses and examinations using the digital cancer maps was enabled by GIS. Visual representation of cancer incidence became possible through these maps, and the important data became available for decision-makers and public health researchers.

The use of GIS in public health management and practice has provided a descriptive and analytic tool that increases the understanding of geographic patterns, spatial relationships and related phenomena. GIS can also utilize mathematical modelling to predict spatial trends and future occurrences (Thrall, 1999). Recent studies have been more concerned with the production of cancer atlases, and studies investigating the relationship between environmental health risks and cancer have covered smaller areas. Future studies on cancer mapping may demonstrate the differences between countries or even continents rather than small areas, and more sophisticated mathematical and statistical algorithms will enable the modelling of the complex relationship between the environmental exposures and human health.

All environmental exposures including pollution discharge sites, underground storage tanks, hazardous waste sites, water discharge pipes and plumes, radioactive elements and others, can also be monitored and analyzed using GIS, and the relationship between human health and these environmental exposures can be examined. GIS will also enable researchers to share the latest analyzed data. The ability to publish results immediately with the statistical outputs in GIS will strengthen health research and enhance information sharing.

## Acknowledgements

The authors would like to acknowledge the support of the Scientific and Technical Research Council of Turkey (TUBITAK) for the research grant that enabled this study (Project ID: 105Y308).

## References

Berke, O. (2004). Exploratory disease mapping: kriging the spatial risk function from regional count data. *International Journal of Health Geographics*, **3**, 18.

Brewer, C.A. (2006). Basic Mapping Principles for Visualizing Cancer Data Using Geographic Information Systems (GIS). *American Journal of Preventive Medicine*, **30(2)**, 25–36.

Diggle, P.J. (2000). Overview of statistical methods for disease mapping and its relationship to cluster detection. *In:* Elliot, P., Wakefield, J.C., Best, N.G. and Briggs, D.J. (Eds.), Spatial Epidemiology: Methods and Applications (pp. 87–104). Oxford University Press, New York.

Dissanayake, C.B. and Changrajith, R. (1999). Medical geochemistry of tropical environments. *Earth Science Reviews*, **47**, 219–258.

Drapper, G., Vincent, T., Kroll, M.E. and Swanson, J. (2005). Childhood cancer in relation to distance from high voltage power lines in England and Wales: a case-control study. *BMJ*, **330**, 1290.

Esteve, J., Benhamou, E. and Raymond, L. (1994). Statistical Methods in Cancer Research, Vol. IV: Descriptive Epidemiology (Pub. No. 128). IARC Scientific Publications, Lyon.

Flinton, D.M. and Walters, N.J. (2004). Occupational activity and risk of prostate cancer in Ireland. *Journal of Radiotherapy in Practice*, **4**, 102–106.

Greiling, D.A., Jacquez, G.M., Kauföamm, A.M. and Rommel, R.G. (2005). Space-time visualization and analysis in the Cancer Atlas Viewer. *Journal of Geographical System*, **7**, 67–84.

Jacquez, G.M. (2004). Current practices in the spatial analysis of cancer: flies in the ointment. *International Journal of Health Geographics*, **3**, 22.

Kulldorff, M., Song, C., Gregorio, D., Samociuk, H. and DeChello L. (2006). Cancer Map Patterns: Are They Random or Not?. *American Jorunal of Preventive Medicine*, **30(2)**, 37–49.

Lang, L. (2000). GIS for Health Organisation. ESRI Press, California, USA.

Morra, P., Bagli, S. and Spadoni, G. (2006). The analysis of human health risk with a detailed procedure operating in a GIS environment. *Environment International*, **32**, 444–454.

Oliver, M.N., Matthews, K.A., Siadaty, M., Hauck,F.R. and Pickle, L.W. (2005). Geographic bias related to geocoding in epidemiologic studies. *International Journal of Health Geographics*, **4**, 29.

Pickle, L.W., Hao, Y., Jemal, A., Zou, Z., Tiwari, R.C., Ward, E., Hachey, M., Howe, H.L. and Feuer, Ej.J. (2007). A New Method of Estimating United States and State-level Cancer Incidence Counts for the Current Calendar Year. *CA Cancer Journal of Clinicians*, **57**, 30–42.

Stewart, A. (2002). Basic Statistics and Epidemiology: A practical guide. The Redcliffe Medical Press, Oxford.

Thomas, R.W. (1990). Introduction: Issues in Spatial Epidemiology. *In:* Thomas (Ed.), Spatial Epidemiology, (pp. 1–14). Pion Publication, London.

Thrall, G.I. (1999). The Future of GIS in Public Health Management and Practice. *Journal of Public Health Management & Practice*, **5(4)**, 82.

Tuncer, M. (2009). *National Cancer Programme 2009–2015* (Rep. No. 760). Turkish Ministry of Health, Department of Cancer Control, Ankara, Turkey.

Turkish Ministry of Health (2004). Turkey's National Health Information System Report. Turkish Ministry of Health, Ankara, Turkey.

UNSCEAR (2000). Sources and Effects of Ionizing Radiation, Annex B: Exposure from natural radiation sources (Rep. Vol. 1). UN Committee on the Effects of Atomic Radiation, New York.

Vieira, V., Webster, T., Aschengrau, A. and Ozonoff, D. (2002). A method for spatial analysis of risk in a population-based case-control study. *International Journal of Environmental Health*, **205**, 115–120.

Yomralioglu, T., Colak, H.E. and Aydinoglu, A.C. (2009). Geo-Relationship between Cancer Cases and the Environment by GIS: A Case Study of Trabzon in Turkey. *International Journal of Environmental Research and Public Health*, **6(12)**, 3190–3204.

# 15

# GIS for the Determination of Bioenergy Potential in the Centre Region of Portugal

**Tanya C.J. Esteves, Pedro Cabral[1], José Carlos Teixeira[2] and António J.D. Ferreira**

Centro de Estudos de Recursos Naturais, Ambiente e Sociedade
Escola Superior Agrária de Coimbra – Instituto Politécnico de Coimbra
Bencanta 3040-316 Coimbra, Portugal
[1]Instituto Superior de Estatística e Gestão de Informação – Universidade Nova de Lisboa, Campus de Campolide, 1070-312 Lisboa, Portugal
[2]Departamento de Engenharia Mecânica – Universidade do Minho
Campus de Azurém, 4800-058 Guimarães, Portugal

## Introduction

Every activity performed by mankind is directly or indirectly dependant on the use of energy. Fossil fuels are the main source used nowadays, a presumably limited energy source that may end in the near future (Boyle, 2004). World total annual consumption of all forms of primary energy increased drastically, and in the year 2006 it reached an estimated 10,800 Mtoe (million tons of oil equivalent) (U.S. Energy Information Administration [USEIA], 2009). The annual average energy consumption per person of the world population in 2006 was about 1.65 toe (ton of oil equivalent) (Population Reference Bureau, 2010). In 2010, the consumption of this energy may reach 12,800 Mtoe (USEIA, 2009) and in 2050 it is expected to achieve a range of 14,300 Mtoe to 23,900 Mtoe (International Energy Agency for Bioenergy [IEAB], 2009). We can also assume that it might possibly never end. The current energy crisis is affecting great part of the world population (U.S. Department of Energy, 2009).

The fluctuation of the oil price is causing a severe economic disruption worldwide, where steps must be taken as to guarantee mankind's future. Most fossil fuels must be substituted by other kinds of energy sources to preserve environmental and economic resources. This transformation may lead to a

J.K. Thakur et al. (eds.), *Geospatial Techniques for Managing Environmental Resources*,
DOI 10.1007/978-94-007-1858-6_15, © Capital Publishing Company 2012

much needed sustainability. Sustainable development is defined as being *the development that meets the needs of the present without compromising the ability of future generations to meet their own needs* (World Commission on Environment and Development, 1990), involving environmental, social and operational management strategies, an equilibrium not easily attained due to their interdependency. Boyle (2004) considers that a sustainable energy source is one that ideally does not deplete substantially by its continuous use, one that does not entail significant pollutant emissions or other environmental problems, or one that does not involve the perpetuation of substantial health hazards and/or social injustices. Renewable energies appear generally more sustainable than fossil fuels, once they are essentially inexhaustible and their use usually entails less green house gases (GHG) and pollutant emissions. By using renewables, a higher level of sustainability may be achieved by modern society (Richardson and Verwijst, 2005).

Portugal is extremely fortunate, as it is rich in bioenergy sources of many sorts. Solar, wind, hydro and tides are just a few of the rich sources that may be harnessed to produce bioenergy in this country. However, this chapter will focus solely on biomass, delineating a GIS-based strategy to comprehend the amount of available bioenergy resources commonly considered as residues. Hence, the aim is to analyze the potential of bioenergy in the Centre Region of Portugal (CRP) for several biomass resources, namely from energetic cultures, forest, agricultural and food residues and the biogas produced as by-product from some human activities. Spatial and non-spatial data are collected and transformed into a comparable energy unit (toe). Another goal is to determine the optimal location for the BCC. This entity encompasses a large range of services before and after bioenergy production, e.g., technical assistance throughout the production process, research, personnel training and product certification. Adequately implementing this infrastructure in the terrain is essential for a flourishing development of bioenergy use in the study area. The two overall outcomes of the developed work will be two maps: one depicting the bioenergy potential for the CRP and another with recommendations for the optimal implementation of the BCC.

## Bioenergy

This chapter presents the main considerations in the bioenergy study field, defining what bioenergy is, its sources, and the current situation in Portugal.

### Bioenergy: What is it?

The renewable energy directive defines biomass as "the biodegradable fraction of products, wastes and residues from biological origin from agriculture (including vegetable and animal substances), forestry and related industries including fisheries and aquaculture, as well as the biodegradable fraction of

industrial and municipal waste" (European Parliament and of the Council [EPC], 2009).

Obtaining a reliable estimate of the total world-wide energy contribution from bioenergy sources is not an easy task. Although the benefits from the use of bioenergy are irrefutable, there are still technical issues that have to be surpassed, e.g., the intermittency of some renewables. Nonetheless, the biggest obstacle has more to do with politics and policy issues than with technical ones. When these renewable technologies are developed in a sensitive way, they have the benefit of being environmentally benign, diverse, secure, locally based and abundant, promoting the involvement of the local communities. Numerous challenges need to be addressed for its untapped potential to be used in a sustainable way (IEAB, 2009). One has to take into account a large number of influencing factors, and not only the environmental aspect. Recently, "new" biomass sources have emerged, being composed of materials that are processed on a large, commercial scale, normally in the more industrialized countries. They are normally purpose-grown energy crops or organic wastes that are capable to create heat or any wide range of solid, liquid or gaseous biofuel (Boyle, 2004).

## Bioenergy Sources

Biomass accounts for about a third of total primary energy consumptions in developing countries. Wood plays an indubitable role as an energy source; nevertheless, its patterns of demand and supply, and its associated economic, social and environmental impacts are still poorly understood (Boyle, 2004; Masera, Ghilardi, Drigo and Trossero, 2006). There are many bioenergy sources, from which this chapter will only focus on some of the purpose-grown energy crops (agricultural crops) and wastes.

Farmers in Europe have been discovering the advantages of producing renewable energy and biomaterials. Due to changes in the food production and consumption in Europe, agriculture has shown potential to be a major bioenergy production contributor in the EU27, supporting the efforts to significantly increase the share of renewable energy sources production (European Environment Agency [EEA], 2007). The most widely grown crops for bioenergy purposes are maize, sugar cane, sunflowers, oilseed rape, soya beans, etc. However, future agricultural biomass production should not impose additional economic, social and environmental pressure on farmland biodiversity and environmental resources than is currently the case (EEA, 2007).

A multitude of wastes can be used to produce bioenergy. However, a main question remains: should this material be regarded as a renewable resource? Wood residues that come from thinning plantations and trimming operations generate large volumes of forest residues. It is customary to let these residues

rot on site. Although this fact has the environmental merit of retaining nutrients, they may enhance the forest fire risk in many regions. Reusing these residues for energy production is possible. Temperate crop wastes are also able to be used. Surplus in agricultural production often leads to burning in the field, even though air pollution concerns and legislation restrain such practices (Boyle, 2004). Despite animal manure being a major source of important pollutants, particularly methane ($CH_4$), their use is a viable form of energy production through anaerobic digestion (Ramachandra, 2008). Animal wastes from the confined animal feeding operations lead to new, state-of-the-art waste management systems (anaerobic digestion technology) that make animal operations economically viable and environmentally benign (Cantrell, Ducey, Ro and Hunt, 2008). This leads farmers to reduce their dependency on imported fossil fuels while concurrently improving the soil, water and air quality, and converting the treatment of livestock waste from a liability or cost into a profit centre that can simultaneously generate annual revenues, moderate the impacts of commodity prices and diversify farm income (Cantrell et al., 2008). Municipal solid waste (MSW) is generally considered to include all kind of residues generated from homes, businesses, and the cleaning of public places such as streets, parks, beaches and other recreational areas. They can also be used to produce energy, by recovering landfill gas, incineration, gasification, $H_2$ production, pyrolysis and anaerobic digestion of the organic fraction (Gómez, Zubizarreta, Rodrigues, Dopazo and Fueyo, 2010). A large proportion of MSW is biological material and its anaerobic digestion reproduces the natural process of degradation of the organic matter in the landfill. This process produces methane, and compost is also an often by-product. The produced gas in landfill biogas plants is increasingly used to generate electricity for local use or for sale and have been amongst the most financially attractive of the existing systems (Boyle, 2004; Gómez et al., 2010).

## Bioenergy in Portugal

Countries like Portugal that have low or inexistent access to fossil fuels are subject to the prices of international entities: in 2007, Portugal had an approximate consumption from oil of 54% of the primary energy. However, the country still has a final energy consumption per inhabitant lower than the mean of other EU-25 countries (1.7 toe/inhabitant versus 2.5 toe/inhabitant) (Agência Portuguesa do Ambiente [APA], 2008). But it still represents a constant exit of currency to supplying countries, with a consequent weakening of the economy. This is a very important reason to invest in alternative energies and energetic efficiency, to escape the dependence on the volatility of oil, natural gas and coal prices. The national renewable sector has been strongly developing (Associação das Energias Renováveis [APREN], 2010). The Directive 2001/77/CE of 27 September 2001 stipulated that Portugal would have to produce 39% of electricity from renewable energy sources until 2010

(EPC, 2001). By early 2007, this aim had already been achieved, having altered the stipulated target to an ambitious 45% (Direcção Geral de Energia e Geologia, 2005; European Commission, 2007).

Biomass dedicated power plants are of recognized importance for the global bioenergy balance. Portugal has nine biomass plants working in a cogeneration regime, with a total of 308 MW electric energy generation (APREN, 2010). In what refers to the national production of solid waste, between 1995 and 2008 the increase of these residues accompanied the Gross Domestic Product (GDP) growth, were a respective increase of approximately 32% and 33%. These values translate a production of 5059 million tonnes, a total higher than the one perceived in the Portuguese Strategic Plan for Municipal Solid Waste 2007-2016 – 4993 million tonnes (Ministério do Ambiente e Ordenamento do Território, 2007). In 2008, a mean of 1.3 kg/inhabitant.day was produced (European capitation – 1.4 kg/inhabitant.day) (APA, 2009). Landfills are the main destination for final disposal of municipal solid waste in Portugal. About 65% of the total produced waste is landfilled, followed by incineration with energy valorization (18%), separate collection (9%) and 8% for organic valorization (APA, 2009).

## The Centre Region of Portugal

Portugal is a 92,094 $km^2$ west coast European country, in the Iberian Peninsula. It benefits from its privileged geographic location, between Europe, America and Africa (Agência para o Investimento e Comércio Externo de Portugal [AICEP], 2008). The littoral, generally more flat, is distinguished from the inland sloped areas, where the higher altitudes are in the mountain range located in the Centre Region of the country (AICEP, 2008; Instituto Nacional de Estatística [INE], 2009). As for the territorial units for statistics (Nomenclature of Territorial Units for Statistics – NUTS), the country is at NUTS I level, divided into seven NUTS II territories (Regions), in which the CRP is included. This region is divided into 12 NUTS III areas (Fig. 1). It occupies 28,200 $km^2$, comprising a total of 100 municipalities (AICEP, 2008). As for the protected areas, there are 4,560.31 $km^2$ classified in the Natura 2000 network, as well as 1,981.67 $km^2$ of various types of protected areas (INE, 2009). The 2001 Census states that this region has 2,371,700 inhabitants (AICEP, 2008), which in 2006 produced 1,060,968 t of municipal urban waste (71,466 t from selective collection) (INE, 2009). The CRP is one of the richest, in terms of forest stands. Olive groves, pine and eucalyptus forest stands are prominent (AICEP, 2008). A massive yearly problem are forest fires: in 2007 and 2008, a total of 4,482 wildfires occurred, burning 77.88 $km^2$ of land (INE, 2009). In agriculture, there was a variety of crops planted (e.g., wheat, rice, cherries). Potato crops produced a total of 28,470 t in 2008, although the planted area was only of 152.08 $km^2$. Maize was the crop with most planted area (342.04 $km^2$), although the total production was 174,015 t.

Wine and olive oil production are also common in this region. In 2008, 1,507,444 hl of wine were produced, as well as 144,743 hl of olive oil, from 309 olive oil mills (INE, 2009).

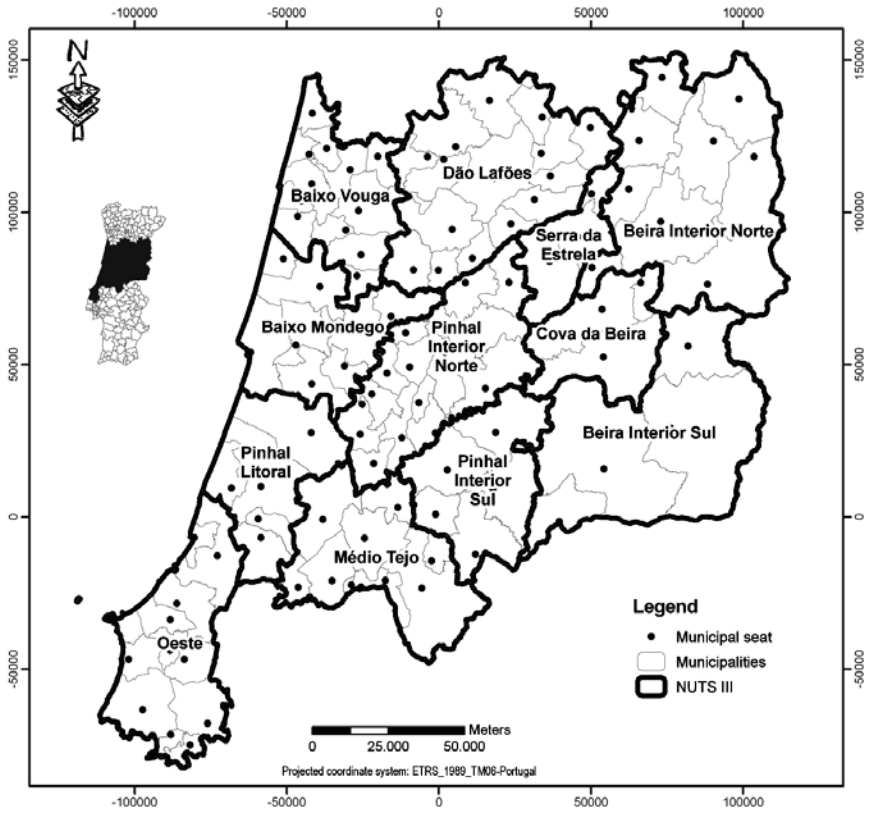


**Figure 1.** NUTS levels of the CRP.

Regional energy consumption can be categorized in *domestic*, *non-domestic*, *industrial*, *agriculture*, *lighting of public roads*, *inner lighting of State/public buildings* and *others*. In 2007, the *industrial* sector used most energy (547,085.76 toe), in contrast with the *others* sector (12,157.36 toe). The *domestic* and *agriculture* sector spent 256,006.69 toe and 25,946.79 toe, respectively. The consumption of electric energy per inhabitant was of 0.107 toe, as opposed to the national average of 0.112 toe. As expected, the *industrial* sector spends most energy per consumer (15.239 toe), whilst the *agriculture* sector spends 0.201 toe and the *domestic* uses 0.361 toe (INE, 2009). Gross production of electricity was of 1,387,955.62 toe, having 176,528.05 toe come from wind power, 123,427.47 toe from hydropower and 1.332 toe from photovoltaics. Thermal power was also produced (1,087,998.77 toe), from which 182,571.88 toe came from central cogeneration (INE, 2009).

## The Bioenergy Potential Map for the Centre Region of Portugal

The bioenergy map for the CRP is one of the two results of the present study that may help us attain a general overview of the amount of available biomass and to understand how that biomass is distributed throughout the region. To aid in this study, a multicriteria decision analysis will be used as to obtain a final result.

### Input Resource Collection and Treatment

The collection and treatment of the information presented a difficult task: the size of the study area, the dispersion and availability of data were real concerns to deal with upon this stage. Only freely available data was used to create this map. One of the main struggles faced was that recent data was seldom available (the 1999 information for the agricultural sector is used). Information from several sectors was collected, namely: forest residue biomass, agricultural residue biomass, energetic cultures, animal husbandry residues, municipal solid waste, used vegetable oils, agricultural and food industries. In what refers to geographical data, only the 2010 Official Administrative Map of Portugal was used (Instituto Geográfico Português [IGP], 2009).

The analysis scale is at the municipality level. A municipality is a political unit that has an incorporated local self-government. It was the level considered adequate to perform an analysis of the bioenergy potential, that at a larger scale (e.g., parish), too many details would have to be taken into consideration, not being compatible with the aim of the present study. Depending on the subsequent results, a more detailed analysis on a larger scale that is based on the results could be produced for some territorial clusters. On the contrary, a larger scale (e.g., district, NUTS III) would omit too much information, something not desirable at this point.

In general, bioenergy potential for each source was obtained by knowing the area occupied by the source in each municipality of the study region, the annual production of residues for each source and their Low Heat Value (LHV). Multiplying these values and transforming them into a unique unit (toe), bioenergy results appear for forest (maritime pine, cork oak, eucalyptus, holm oak, stone pine, Portuguese oak, sweet chestnut, other hardwood trees, other softwood trees); burned areas; shrublands; agriculture (fresh fruit, citron, nut, vineyard and olive grove permanent drops and maize, wheat, barley, rye, sorghum, oat and rice temporary crops); and energy crops (maize, wheat, barley, rye, sorghum, potato and sugar beet amylaceous crops and sunflower oleaginous crops). For this last production, two details differed from the previous: first, as to not compete with food production, only agricultural areas that have been abandoned throughout the last 20 years were used for these

crops; secondly, instead of using LHV values, an energy conversion index (l/t) was used and then the result was transformed into toe. For the energy potential from animal husbandry effluents, bovine, swine and bovine intensive farming are considered. Each animal has different physiology, producing a different daily amount of biogas. Determining this value for each animal and knowing how many are available, the yearly production of biogas is known. This value was then multiplied by the biogas LHV and the potential bioenergy for animal husbandry effluents is known.

For this study, a theoretical value for biogas generated from one ton of MSW in landfills was considered. Knowing the yearly amount of material deposited at a landfill site, the amount of biogas produced annually per municipality was obtained. This value is multiplied by the biogas' LHV and the bioenergy potential (toe) is estimated. Organic valorization is foreseen for most of the region in the near future. Knowing the average municipal production of organic residues, it was multiplied with the amount of biogas that a ton of residue produces. This result was then multiplied by the biogas LHV value, obtaining the final result for bioenergy potential (toe) for organic valorization. Some residues in MSW aren't anaerobically digested, where direct combustion of the inorganic part of the MSW may be a solution. Knowing the typical composition of the MSW in Portugal, the average amount of paper/cardboard, plastic, textile, fine matter and other materials were determined. Multiplying their percentage amount with the total values deposited in the landfill, the total amount of different inorganic material was known. Also having the LHV for each type of material, the energy potential (toe) resulting from this combustion was calculated. To calculate the amount of used vegetable oils (UVO) produced per municipality, the yearly average capita value in Portugal was used. By multiplying this value with the population in each municipality, the consumption/inhabitant.year was known. From the total amount of produced UVO, only 45% is actually considered as waste, and only 60-70% of that amount is the one that actually suffers transesterification. Thus, the amount of biodiesel produced per municipality per year was calculated. By transforming the obtained values in toe with the LHV value, the amount of potential bioenergy was calculated. As for energy obtained from the agricultural and food industries, the olive press cake residue is reused for bioenergy production by combustion. By knowing the amount of produced olives, the residue amount was also known and multiplying this value by the LHV value, the potential bioenergy was obtained for this residue. Similarly for wine production, there is also a residue composed of grape stems, where, by knowing the amount of wine production, we could calculate the amount of produced residue for combustion. Knowing the LHV value, the amount of potential bioenergy to be retrieved from this waste was obtained.

## Using GIS for the Multicriteria Decision Analysis for Bioenergy Potential

This study used the ArcInfo 9.3 software, produced by ESRI, to perform the multicriteria decision analysis. Most of the data used by managers and decision makers is somehow related to a geographical level. Data that is undigested, unorganized or unevaluated may be processed to obtain information in order to have some kind of significance. Doing so adds extra value to the original data, proving useful to decision makers to produce quality decisions (Malczewski, 1999). Typically, spatial decision problems involve a large set of feasible alternatives and multiple, conflicting and incommensurate evaluation criteria, while some are of the qualitative and other of the quantitative nature (Malczewski, 1999, 2006a, b). Multicriteria decision analysis is a useful tool to help solve this type of problems. It uses two types of criteria: *constraints* and *factors*. The former are based on boolean criteria restricting the analyses to specific regions while the latter define a degree of suitability for the whole geographical space, specifying areas or alternatives according to a continuous measure of suitability (Hansen, 2005). The decision making process involves the aggregation of selected criteria that need to be standardized to a common scale (Hansen, 2005). A boolean overlay approach involves the application of operators such as intersection (AND) or union (OR) resulting in binary maps where only the suitable (TRUE) and non-suitable (FALSE) locations are present. An alternative method is the *weighted linear combination* that weighs and combines the factor maps to evaluate the suitability of each cell (Jiang and Eastman, 2000). The suitability $s$ at the $k^{th}$ pixel may be determined by a weighted linear combination (Hansen. 2005):

$$s^k = \Sigma\, w_i\, x_i^k \tag{1}$$

where $w_i$ is the weight and $x_i^k$ is the value of criteria $i$ in the $k^{th}$ pixel. The weights $w_1, \ldots, w_n$ show each criteria's relative importance and their sum should not exceed 1.0 (Hansen. 2005). Here, a combination of the *boolean overlay* and the *weighted linear combination* was used.

The data described in Section 4.1 was introduced into a geographic database and, with the aid of the *ModelBuider* tool, input data turned into information. This functionality created the model to process the input data, allowing to chain together sequences of tools, feeding the output of one tool into another (Environmental Systems Research Institute [ESRI], 2010). Used functions in this model were merge, dissolve, feature to raster, weighted sum and divide tools. No personalized formulas were used in this particular model, only the standardized ones available by the ArcInfo 9.3 tools.

The merge tool merged the polygon data (municipalities with the bioenergy information) of the different input residue feature classes, and the dissolve tool aggregated the potential bioenergy field for each municipality feature class. The feature to raster tool transformed the vector data into raster so that

the weighted overlay tool could be used, overlaying the rasters, using a common scale and weights and outputting the final result of the model (ESRI, 2010).

## Results

Currently, there is no method to fully yield 100% of the potential that is available by each and every considered residue. Due to technology constantly progressing and presenting new solutions, these are frequently surpassing existing boundaries, so, whatever considered yield for bioenergy production in this study would rapidly be outdated. The outputted map can be found in Fig. 2. We find that the most promising area in terms of bioenergy production is the northern inland area, Beira Interior Norte, achieving a maximum of 98,912.40 toe in the Sabugal municipality. This fact may be due to the combination of climatic factors with the high amount of agricultural and forest areas, leading to higher biomass yield. The littoral part of the CRP has a much lower potential, where the lowest production is of 1,848.54 toe (Entroncamento). The general middle region of the study area and the Oeste NUTSIII are not appropriate for bioenergy production from biomass.

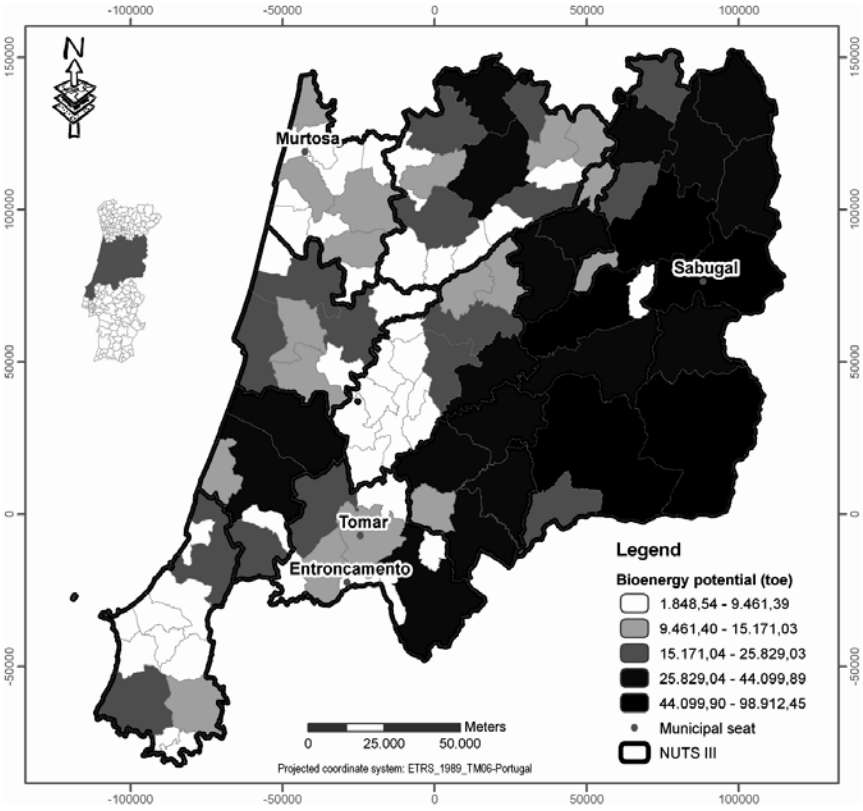


**Figure 2.** Bioenergy potential for the CRP.

The component that most influences this final map is the forest waste biomass. The source's produced amount is overtaking the remaining sources, mainly due to shrubland contribution.

Information confidentiality for some municipalities is a factor hampering the true potential analysis. For various waste sources, many municipalities (around 5%) had confidential data in the consulted bibliography. This fact may certainly alter the presented results drastically, once that the municipalities can produce enough waste to make a great difference in the final value for those municipalities, making the presented results rapidly obsolete.

## Location of the Bioenergy Competency Centre

The BCC will not produce energy itself. Rather, it will have several critical functions for the further development of bioenergy production. In general, it is thought to constantly manage and update information produced in the first section of this work and study the costs of production/collection and processing of the materials needed for the production of bioenergy, as well as the definition of the threshold of economic viability. Its tasks include product certification, research, development and innovation, consultancy, training and trials. It will integrate the main stakeholders in the CRP, as to maximize the profitability of the various laboratorial, management and economical infrastructures and available knowledge. Information flow will be key in this organization's work processes. Taking these important functions into consideration, the implementation of the BCC is of utmost importance. Acknowledging this fact, it should be located in a place of easy access to all stakeholders.

### Input Resource Collection and Treatment

For the implementation of the BCC, several suppositions had to be considered. As before, all information is freely available to the general public. The national network of the protected areas was used to determine the existing natural protected areas; the Corine Land Cover 2006 for Portugal (IGP, 2009) was used to determine land use; the itinerary map for Portugal (Instituto Geográfico do Exército, 2009) was used for road information; Shuttle Radar Topography Mission (SRTM) digital elevation data (Consultative Group on International Agricultural Research, 2008) was used to obtain slope information; the location of existing and future biomass power plants in the CRP was also used. Other information can be used, such as sight-seeing and recreation areas, as to exclude them from the final result (one does not want to implement the BCC in these areas). To the author's knowledge, there is no information of the sort available for the study region. What can be done is, when selecting the location from the final map, to compare this information with the Municipal Master Plan, once this document contains the previously stated information. If the map were done at a single municipal level, the information would certainly be easier to incorporate in the created model.

## Using GIS for the Multicriteria Decision Analysis for the BCC Implementation

The *ArcInfo 9.3 ModelBuilder* functionality was again a valued tool to locate the BCC. In general, all the information is classified into five different classes, being 1 the least favourable condition and 5 the most preferable one. Three approaches for using the roads were used: the first one expressed the importance of the existing types of roads, making sure that the BCC is easily accessible to all stakeholders; the second approach considered the distance to roads, preferably locating the BCC closer to the roads; and, finally, the use of service areas (with the *Network Analyst* extension) to know the time (hours) it takes the main stakeholders to access the BCC. The resulting map from bioenergy potential analysis is also used as input, so that the BCC can be located preferably in areas with higher production of biomass.

Some restricting conditions also influence the final map results. The protected areas information was used to exclude these areas, once it is illegal to build in such areas. In what refers to the land use, some features were excluded from this feature class once that a construction such as the BCC could not be located in the areas: continuous urban fabric; discontinuous urban fabric; wetlands; and airports. Having considered the aforementioned restrictions, these were merged and transformed into a raster information layer reclassified from 1 to 5. The restricted areas were excluded from the analysis (NoData).

Slope plays a major financial role in building an infrastructure. The steeper a terrain is, the higher will be the construction costs. It also influences travelling: steeper slopes bring more difficulties in transportation (with more fuel consumption). After reclassifying all the inputs in a 1 to 5 scale, a weighted overlay carried out using all the rasters. Table 1 shows four different scenarios for the inputs. Scenario 1 translates the fact that both stakeholders (biomass plants and waste producers) represent an important role for the BCC (higher weights, both with 25%). *Slope* and *restrictions* parameters were constant in all scenarios.

**Table 1.** Weighting of different inputs for determination of the location of the BCC

| *Inputs* | *Scenario 1* | *Scenario 2* | *Scenario 3* | *Scenario 4* |
|---|---|---|---|---|
| Restrictions | 5 | 5 | 5 | 5 |
| Slope | 10 | 10 | 10 | 10 |
| Road differentiation | 15 | 20 | 15 | 20 |
| Distance to roads | 20 | 15 | 20 | 15 |
| Network analysis from biomass plants | 25 | 25 | 30 | 30 |
| Bioenergy potential | 25 | 25 | 20 | 20 |

In Scenario 2, all parameters had the same weight as the first, besides the *road differentiation* and *distance to roads* ones (more emphasis for the first – 20% – than the second – 15%), as to verify the influence of both aspects on the final result, by comparison with Scenario 1. Scenario 3 considered the same weights as in Scenario 1, except for *network analysis from the biomass plants* and the *bioenergy potential*. In this case, business success is important for biomass plants (as opposed to farmers and other producer stakeholders, that face this more as a secondary business by selling their residues), so they may be more reliant on the services that the BCC may offer than the remaining stakeholders, thus having a higher percentage value (30%) than the bioenergy potential (20%). In the last scenario (4), all weights were changed in respect to Scenario 1. Basically, the *network analysis from the biomass plants* and the *potential bioenergy* were the same as Scenario 3 and the *road differentiation* and *distance to roads* were equal to Scenario 2. From the resulting information, areas with values 4 and 5, and with an area larger than 22,500 $m^2$ were chosen (projected area necessary for the BCC was 150 m × 150 m).

GIS tools such as buffers, merge, reclassify, weighted overlay, conditional and network analysis were used to materialize this model.

## Results

The proper implementation of the BCC will allow stakeholders to have easier access to the provided services. Road types, road distance, travel time, bioenergy potential and slope were the factors considered. The weighing process proved itself difficult, due to the high amount of inputs. One cannot make large differentiations between two comparing values once the remaining parameters would suffer a large reduction, influencing the final result. In Fig. 3, we can verify that different scenario results are very similar between them. Most of the suggested locations in the different scenarios are coincident, although with visible changes in the area amount for each scenario. Another factor that is clearly visible is that there are more areas to implement the BCC with a classification of 4 than there are with a classification of 5 (Table 2). Scenario 2 is the most limitative one, once less area with classification 5 is usable. Scenario 3 is the broadest of them, where more area is available, although the one with classification 5 is higher in Scenario 1. If it were preferable to use only locations with this classification, the solution would be almost the same in all scenarios. Generally, preferable locations would be situated in the Viseu, Covilhã, Guarda, Sabugal, Fundão, Castelo Branco, Sertã, Cantanhede, Coimbra, Pombal and Leiria municipalities. Note that, after a selection of the final area, it should be verified if the selected locations are in accordance with the planning options of the municipality's Municipal Master Plan.

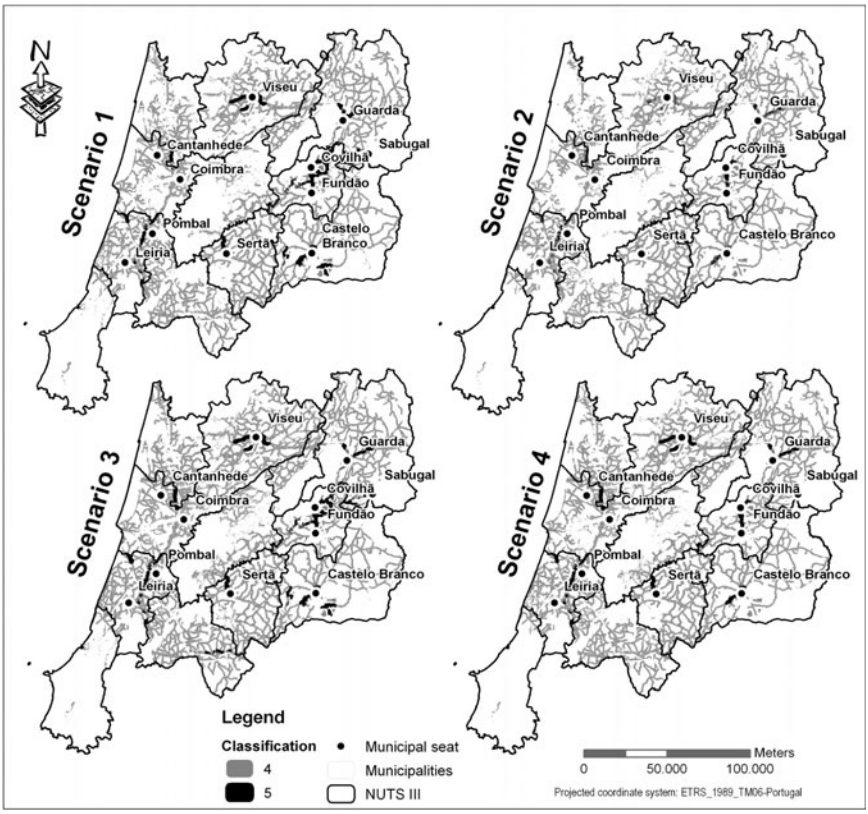


**Figure 3.** The four scenarios for the implementation of the Bioenergy Competency Centre.

**Table 2.** Summary of areas with classification 4 and 5

| *Scenarios* | *Total area* | *Areas with classification 4* | | *Areas with classification 5* | |
|---|---|---|---|---|---|
| | *(ha)* | *ha* | *%* | *ha* | *%* |
| Scenario 1 | 578,021.15 | 567,981.87 | 98.26 | 10,039.28 | 1.77 |
| Scenario 2 | 512,315.38 | 508,802.14 | 99.31 | 3,513.24 | 0.69 |
| Scenario 3 | 645,172.95 | 635,514.89 | 98.50 | 9,658.06 | 1.50 |
| Scenario 4 | 593,636.41 | 586,909.87 | 98.87 | 6,726.55 | 1.15 |

Choosing a determinate location depends on a variety of opinions. GIS and its results are socially constructed via negotiations between various social groups such as developers, practitioners, planners, decision-makers, special interest groups, citizens and others who may have interest in the planning and policy making process (Malczewski, 2004). Many of these issues have to be

pondered by the key actors of the future BCC. An appealing option would be locating the BCC in the inland area of the country (Viseu, Guarda, Covilhã, Belmonte, Sabugal, Fundão, Castelo Branco and Sertã). The aim is to confer some dynamism to the area, once this population is increasingly fleeing to the littoral, looking for better life conditions. This may lead to local employment, as well as the possibility of awakening the surrounding population to this new business and delay (or even mitigate) land abandonment.

## Future Research Directions

The complexity of the environmental sector depends on a wide variety of composite and comprehensive tools, in which GIS are included, to help solve problems and create new and innovative solutions for the environment. Being conventional energy a source of economic losses for countries, a strong challenge is imposed upon them to produce their own energy sources, mainly through green energies. Bioenergy use may be a sturdy step in that direction, guaranteeing the safeguard of environmental and economical resources of the countries. This study offers a step in this direction. Understanding what resources are in a given territory and using them to an economic and environmental advantage is one of the goals to achieve.

Although the presented results are valid, they could be enhanced. More recent information would bring authenticity to the results to represent today's reality, where certainly much has changed since then. It would be interesting to see how final results differ by using recent data.

By inserting transformation rates into the final results, these would give a realistic view of the bioenergy potential in the territory. Saying, e.g., that a given area has a bioenergy potential of 1500 toe doesn't really ring true; transformation yields for different technologies have to be taken into consideration to determine the actual potential for bioenergy.

Many waste typologies were not considered, being able to present a viable source for bioenergy, e.g. biogas from sludge treatment from wastewater treatment plants and industrial sources (residues from industries that use material such as bark, leather, wood, tyre fluff, etc.). The insertion of this data into the present study would be of great benefit.

An important step to validate the described study would be to make a Strengths, Weaknesses, Opportunities and Threats (SWOT) analysis. It would verify its feasibility, using different types of biomass to make a well-founded decision. This aspect is of extreme importance, once we desire our energy production to have a positive energy balance, as well as to be profitable. This type of study may promote the full use of bioenergy production in the CRP.

## Conclusion

New energy sources are necessary to ensure the sustainability of mankind's future. One of possible solutions is to use bioenergy waste from various sources as to yield energy from them. This was the base premise of this study. The use of this material may contribute to decrease the amount of imported fossil fuels, with economic advantages and to partially replace a pollutant energy source by a greener one.

A large amount of resources are present in the CRP, particularly forest waste, being a main contributor for the amount of bioenergy that may be produced. When compared to the other resources, it is the one present in higher amount. Using this material in particular has a double function: production of bioenergy and aid in the prevention of forest fires, saving lives, material goods, ecosystems and, ultimately, money. Yet other unconventional bioenergy sources exist that are of great interest for the future, such as agricultural residues, MSW, animal husbandry effluents, agricultural and food industries waste and energy crops. As analyzed in the final results, the inland region of the study area promotes higher bioenergy potential yield. This fact may bring positive consequences to these areas, in which local richness may be enhanced. With the yield of available biomass, local population will be employed, giving them better life conditions. This is important, once these areas have been seeing an increasing desertification to littoral urban centres. Reactivating these rural areas and providing a sustainable income would greatly help the local population's overall conditions. However, an important aspect has to be taken into consideration when producing bioenergy: the amount of energy used to produce, treat and transform the residues might not compensate their use. In this study, this refers to the use of energy crops. Perhaps the low value obtained for these crops is related to how the model was created. But still, maybe, and simply enough, energy crops are not a viable source for the CRP.

The location of the BCC was a second main result for this study. A correct implementation will help all interested parts in easily reaching this Centre. Results show more adequate implementation areas in the inland region, this outcome being highly desirable. Varying the weights of the different parameters had no great influence in the actual location of the BCC. In general, favourable results landed pretty much in the same municipalities for all four scenarios. Scaling issues should be taken into consideration. The used local data may have different interpretations, depending on the scale analysis. At a local scale, one would say that a given municipality has not enough production for bioenergy from a determinate source. But when considering the bordering municipalities, this municipality may be a contributor for production to be cost-effective and successful. Looking at the information with a regional perspective, several key issues may be tackled: environment ($CO_2$ emission

reduction, less wildfires, etc.), economic, society (employment, local development) and politics (more subsidies to promote bioenergy production from biomass).

## References

Agência para o Investimento e Comércio Externo de Portugal (2008). Portugal - Perfil país. AICEP Portugal Global, Lisboa.

Agência Portuguesa do Ambiente (2008). Relatório do Estado do Ambiente 2007. Agência Portuguesa do Ambiente, Amadora.

Agência Portuguesa do Ambiente (2009). Relatório do Estado do Ambiente 2009. Agência Portuguesa do Ambiente, Amadora:.

Associação das Energias Renováveis (2010). Roteiro Nacional das Energias Renováveis - Aplicação da Directiva 2009/28/CE. Associação de Energias Renováveis, Lisboa.

Boyle, G. (2004). Renewable energy: power for a sustainable future (2 ed.). Oxford University Press, United Kingdom.

Cantrell, K.B., Ducey, T., Ro, K.S. and Hunt, P.G. (2008). Livestock waste-to-bioenergy generation opportunities. *Bioresource Technology*, **99**, 7941–7953.

Consultative Group on International Agricultural Research (2008). CGIAR – Consortium for Spatial Information. Retrieved August 19, 2008, from http://srtm.csi.cgiar.org/

Direcção Geral de Energia e Geologia (2005). Direcção Geral de Energia e Geologia Homepage. Retrieved November 5, 2010, from http://www.dgge.pt/

Environmental Systems Research Institute (2010). ArcGis 9.3 Desktop Help. ESRI, USA.

European Commission (2007). Evaluation report on the implementation in Portugal of the European sustainable development strategy – June (No. Tech. Rep. SG/743/07-EN). European Commission, Brussels.

European Environment Agency (2007). Estimating the environmentally compatible bioenergy potential from agriculture (No. Tech. Rep. 12/2007). European Environment Agency, Copenhagen.

European Parliament and of the Council (2007). Directive 2001/77/EC. Promotion of electricity produced from renewable energy sources in the internal electricity market. *Official Journal of the European Communities*, Brussels.

European Parliament and of the Council (2009). Directive 2009/28/CE. Promotion of the use of energy from renewable sources and amending and subsequently repealing Directives 2001/77/EC and 2003/30/EC. *Official Journal of the European Communities*, Brussels.

Gómez, A., Zubizarreta, J., Rodrigues, M., Dopazo, C. and Fueyo, N. (2010). Potential and cost of electricity generation from human and animal waste in Spain. *Renewable Energy*, **35**, 495–505.

Hansen, H.S. (2005). GIS-based Multi-Criteria Analysis of Wind Farm Development. Paper presented at the ScanGis 2005 – 10th Scandinavian Research Conference on Geographical Information Science, Stockholm, Sweden.

Instituto Geográfico do Exército (2010). Instituto Geográfico do Exército. Retrieved October 7, 2010, from http://www.igeoe.pt

Instituto Geográfico Português (2009). Instituto Geográfico Português. Grupo de Detecção Remota. Retrieved September 12, 2009, from http://www.igeo.pt/gdr/

Instituto Nacional de Estatística (2009). Estatísticas Agrícolas 2008. Instituto Nacional de Estatística. I.P., Lisboa.

International Energy Agency for Bioenergy (2009). Bioenergy – A sustainable and reliable energy Source (No. Main Report). s.l.: IEA Bioenergy.

Jiang, H. and Eastman, J.R. (2000). Application of fuzzy measures in multi-criteria evaluation in GIS. *International Journal of Geographical Information Science*, **14(2)**, 173–184.

Malczewski, J. (1999). GIS and multicriteria decision analysis. John Wiley and Sons, Inc., USA.

Malczewski, J. (2004). GIS-based land-use suitability analysis: A critical overview. *Progress in Planning*, **62**, 3–65.

Malczewski, J. (2006a). GIS-based multicriteria decision analysis: A survey of the literature. *International Journal of Geographical Information Science*, **20(7)**, 703–726.

Malczewski, J. (2006b). Integrating multicriteria analysis and geographic information systems: the ordered weighted averaging (OWA) approach. *International Journal of Environmental Technology and Management*, **6(1/2)**, 7–19.

Masera, O., Ghilardi, A., Drigo, R. and Trossero, M.A. (2006). WISDOM: A GIS-based supply demand mapping tool for woodfuel management. *Biomass and Bioenergy*, **30**, 618–637.

Ministério do Ambiente e Ordenamento do Território. (2007). Plano Estratégico para os Resíduos Sólidos Urbanos 2007–2016. Ministério do Ambiente, do Ordenamento do Território e do Desenvolvimento Regional, Lisboa.

Population Reference Bureau (2010). 2006 World Population Data Sheet. Population Reference Bureau, Washington.

Ramachandra, T.V. (2008). Geographical information system approach for regional biogas potential assessment. *Research Journal of Environmental Sciences*, **3(2)**, 170–184.

Richardson, J. and Verwijst, T. (2005). Sustainable bioenergy production systems: Environmental, operational and social implications. *Biomass and Bioenergy*, **28** (Preface), 95–96.

U.S. Department of Energy (2009). Department of Energy. Retrieved June 23, 2009, from http://tonto.eia.doe.gov/oog/info/twip/twipcrvwall.xls#'Data 2'!A1

U.S. Energy Information Administration (2009). World Total Primary Energy Consumption by Region. Reference Case, 1990-2030. Energy Information Administration/International Energy Outlook. Retrieved July 27, 2010, from http://www.eia.doe.gov/oiaf/ieo/pdf/ieoreftab_1.pdf

World Commission on Environment and Development (1990). Our common future. Oxford University Press, USA.

# 16

# Use of Geospatial Data in Planning for Offshore Wind Development

**John Madsen, Alison Bates, John Callahan and Jeremy Firestone**
College of Earth, Ocean and Environment, University of Delaware
Newark, Delaware, US

## Introduction

Offshore wind projects currently provide over two gigawatts of power to the global energy market (Global Wind Energy Council, 2010). Nearly all of this is generated in the North Sea dominated by projects in the United Kingdom and Denmark (Global Wind Energy Council, 2010). The development of offshore wind energy is moving forward in the United States (US) with the recently approved Cape Wind project in federal waters off Massachusetts, the continued planning for offshore wind projects in the Great Lakes and the granting of limited leases for study and calls for requests for interest in leasing selected portions of the eastern outer continental shelf (e.g., Minerals Management Service, 2009; Bureau of Ocean Energy Management, Regulation and Enforcement, 2010; Great Lakes Wind Council, 2010). In addition to the United Kingdom in Europe, large-scale offshore wind projects are projected for France, Belgium and the Netherlands, as well as, in China (Global Wind Energy Council, 2010). The development of offshore wind projects further contributes to the existing pressures on the marine environment increasing the potential benefits of comprehensive, integrated, ecosystem-based planning. This type of marine spatial planning (MSP) is based on sound science and considers current and anticipated uses of the ocean and coastal environment (Ehler and Douvere, 2009). Geospatial techniques provide the framework by which data can be manipulated to aid in implementation of MSP.

The specific objective of this chapter is to use a "case study" approach to illustrate how the gathering, manipulation and interpretation of geospatial data are used in the implementation of MSP. The studies are from Massachusetts, Rhode Island and Delaware in the US and Belgium in Europe.

J.K. Thakur et al. (eds.), *Geospatial Techniques for Managing Environmental Resources*,
DOI 10.1007/978-94-007-1858-6_16, © Capital Publishing Company 2012

The Delaware study represents an initial effort at compiling data within a geospatial framework to assess the potential location of offshore wind projects within state and adjacent federal waters. The Belgian, Rhode Island and Massachusetts projects illustrate how geospatial data have been integrated and analyzed to provide the information that, in concert with policy, has been used in the MSP process to develop integrated plans concerning effective, and ecologically mindful, use of marine resources, including offshore wind.

## Background

A commonly accepted definition of marine spatial planning (MSP) is that it is a public process of analyzing and allocating the spatial and temporal distribution of human activities in marine areas to achieve ecological, economic, and social objectives that are usually specified through a political process (Ehler and Douvere, 2009). The six major characteristics of MSP are that it is: (1) ecosystem-based, (2) integrated, (3) place- or area-based, (4) adaptive, (5) strategic and anticipatory and (6) participatory (Ehler and Douvere, 2009). MSP was established in Europe, and plays a fundamental role in the management of the marine environment. The US Interagency Ocean Policy Task Force, established by President Obama, identifies coastal and marine spatial planning as one of its nine priority objectives in its final recommendations regarding sustainable stewardship of the ocean, coasts and Great Lakes (Interagency Ocean Policy Task Force, 2010).

MSP requires a governing framework: a set of goals, priorities and standards; a legal basis for authority and funding; and procedures defining the planning process, public and stakeholder participation, and the lifetime and extent of the plan (Ehler and Douvere, 2009). In concert with policy, MSP requires a significant data-compilation effort: information requirements must be identified and data gathered from disparate sources; these datasets must be checked for quality and synthesized into a common platform; data gaps must be identified; and results processed and presented in a usable format (e.g., Ehler and Douvere, 2009). It is this data-compilation effort that is best implemented using geospatial techniques. In planning for the location of offshore wind projects the vast majority of data that must be considered is spatial in nature. That is, the information contained in a data point is a function of its geographic position (both in a horizontal and a vertical sense). Geospatial techniques, such as those offered in Geographic Information Systems (GIS), are ideally suited to manipulate and represent these data. GIS allows users to view, understand, interpret and visualize data in many ways that can reveal relationships, patterns and trends in various forms including maps (e.g., Ehler and Douvere, 2009).

## Use of Geospatial Data in MSP for Offshore Wind—Case Studies

The following case studies of Massachusetts, Rhode Island and Delaware in the US and Belgium in Europe illustrate how through the use of GIS, MSP for offshore wind projects can be built upon the framework provided by the best available, science-based data. Examples of the geospatial techniques applied to integrate, manipulate and analyze the data in the case studies are described in the "Methods to Analyze Data for Offshore Wind Development" and "Methods of Data Sharing and Display for Users of MSP" sections of this chapter.

### Massachusetts Ocean Management Plan

The Commonwealth of Massachusetts passed the Oceans Act of 2008 to lay the framework for managing human activities in its state and adjacent federal waters using an ecosystem-based approach (Massachusetts Executive Office of Energy and Environmental Affairs [MA-EEA], 2009a). This Act required the MA-EEA to develop an Ocean Management Plan that includes the development of renewable energy facilities in appropriate locations. The plan calls for the use of scientific data and the setting forth of plans that are cognizant of marine biological and physical processes, that incorporate public input in the planning process and that identify goals and priorities. The plan must include current uses with valuation of those activities and locations and standards for activities that are allowable under the State's pre-existing Oceans Sanctuaries Act (MA-EEA, 2009a).

The Ocean Management Plan defines areas based upon existing uses and proposed allowable activities. It establishes three primary areas for future development: prohibited, renewable energy and multi-use (MA-EEA, 2009a). Prohibited areas are those protected under the Oceans Sanctuaries Act; no further development may occur. Renewable energy areas are delineated to provide the optimal location for both commercial and community scale renewable energy, including offshore wind development. Areas of multi-use comprise the vast majority of the state's ocean waters and they are open to all uses allowable under the Ocean Sanctuaries Act. Rather than being determined by spatially defined boundaries, multi-use areas are managed by siting and performance standards. These areas could support the development of community-scale offshore wind projects (MA-EEA, 2009a).

In the development of the plan, a baseline assessment was conducted to characterize the current status of the state's ocean waters (MA-EEA, 2009b). A scientific advisory council and six working groups consisting of experts from fisheries, marine habitat, ocean recreational and cultural services, regional sediment management, renewable energy and transportation, navigation and infrastructure were formed to gather, coordinate and analyze pertinent data

from their area of focus. The groups were also charged with identifying data gaps and proposing long term research goals (MA-EEA, 2009b).

The baseline data assessment was aided by the use of MORIS, a web-based GIS-mapping tool that was developed by the Massachusetts Office of Coastal Zone Management, the Massachusetts Office of Geographic and Environmental Information, the Massachusetts Ocean Partnership, and Applied Science Associates (Massachusetts Office of Coastal Zone Management [MA-CZM], 2011). MORIS utilizes a central repository of GIS data and allows users, such as resource managers, scientists and the general public, to create maps of selected layers (MA-CZM, 2011). As with most MSP efforts, the baseline assessment data had to be amassed from a variety of sources and it was incomplete for the entire study area. The details of how MORIS supports data storage, management, analysis and visualization is described in further detail in the "Methods of Data Sharing and Display for Users of MSP" section of this chapter.

After analysis of the data layers compiled by the working groups, and in concert with an assessment of priorities, three zones for future activities (prohibited, renewable energy and multi-use) were delineated. To identify potential areas for wind energy development, a screening process was applied which involved passing areas through "filters" that included exclusionary and constraint of potential impacts criteria (MA-EEA, 2009a). As a result of the screening process, two areas, the Gosnold Wind Energy Area and the Martha's Vineyard Wind Energy Area, have been designated as appropriate for commercial-scale wind energy facility siting (MA-EEA, 2009a). Each of the two wind energy areas is expected to support a maximum of 150, 3.6 megawatt turbines. Three additional areas, within the state's waters, were designated as provisional sites for wind energy development, although they have limitations and are not slated for near-future development. Within the framework of the state's ocean management plan, suitable locations for offshore wind facilities in federal waters have also been recommended (MA-EEA, 2009a).

## Rhode Island Ocean SAMP

The state of Rhode Island Coastal Resources Management Council used MSP to develop a Special Area Management Plan (SAMP) for the state's ocean environment (Rhode Island Coastal Resources Management Council [RI-CRMC], 2010). The Ocean SAMP lays out enforceable policies and recommendations that promote a balanced and comprehensive ecosystem-based management approach for the state's ocean-based resources. It protects current uses and habitats by establishing zones for commercial fishing, critical habitats for fish, marine animals and birds and marine transportation. It also includes comprehensive new regulatory standards for offshore development. In doing so, it delineates appropriate areas in the state's offshore waters for renewable energy and also suggests suitable sites in nearby federal waters.

The Ocean SAMP area includes approximately 3800 km$^2$ of portions of Block Island Sound, Rhode Island Sound and the Atlantic Ocean. It extends laterally across 48 km and abuts the state waters of neighbouring Massachusetts, Connecticut and New York (RI-CRMC, 2010). Currently, a 28.8 megawatt project southeast of Block Island, consisting of five to eight turbines, is in the planning and approvals phase with construction as early as 2012 (Deepwater Wind LLC, 2011).

The RI-CRMC acknowledges that one of the biggest challenges of the Ocean SAMP process was gathering the extensive amount of data needed to initiate the MSP process and turning it into usable GIS layers (RI-CRMC, 2010). In an effort to manage the database, the University of Rhode Island Environmental Data Center (EDC) provides guidelines for data submittal. Users are asked to provide data in an ESRI ArcGIS-ready format (e.g., shapefiles, coverages, GRIDs, LATTICEs, TINs, geodatabases or conventional georeferenced images). Non-GIS data are accepted in a limited capacity, as long as they are accompanied by proper metadata. The data that has been compiled is listed in Table 2. Through the EDC, many of the data layers are available for public use.

In terms of offshore wind development within the designation of a Renewable Energy Zone, the Ocean SAMP provides a technical analysis of wind resource, bathymetry and seabed geology, followed by exclusionary criteria (RI-CRMC, 2010). The wind resource was characterized in 2007 and again in 2010 (Applied Technology Management, 2007; Grilli, Spaulding, Crosby and Sharma, 2010). From these data, maps were developed to depict the regions of best wind resource within the Ocean SAMP area. This was followed by a comprehensive analysis using the Technology Development Index (TDI) developed by Spaulding, Grilli, Damon and Fugate (2010). The specifics of the TDI are described in the "Methods to Analyze Data for Offshore Wind Development" section of this chapter.

After using the TDI as a measure of determining general areas suitable for offshore wind development, the siting was further refined using exclusionary criteria. Each of the criteria was added as a data layer, progressively reducing the available preferred areas. The exclusionary data layers include: marine transportation routes, regulated uses including disposal sites, presence of potential unexploded ordinance, protected areas, conservation zones and military areas, licensed extractive development areas, airport setbacks and a coastal buffer zone (RI-CRMC, 2010).

Although the Renewable Energy Zone was delineated as a special use area within a broad multi-use region, renewable energy may be developed in other areas within state waters, provided no significant conflicts with existing human uses and natural resources are found (RI-CRMC, 2010). Prohibited areas from large- and small-scale development are named as Areas of Particular Concern (APCs) and Areas Designated for Preservation (ADPs). APCs are areas of high conservation value, important habitat features, sensitive cultural

resources, high human use value or areas important for activities such as shipping, military use, or navigation. ADPs are more stringently protected and include habitat of endangered species and other sensitive species zones (RI-CRMC, 2010).

## Delaware MSP for Offshore Wind

In an effort that is being undertaken by the University of Delaware to focus on the potential for offshore wind power development off the Delaware coast in state and adjacent federal waters up to 50 m deep, geospatial techniques are being employed to synthesize existing data, identify gaps, and develop projects to collect the necessary missing data to develop an initial framework for MSP that could form the basis of stakeholder engagement. The goal of the project is to generate interactive multi-layered maps, accompanied by a policy document, which will display current information about wind resources, ecological features, bathymetry and marine geology and existing use and users. Maps will indicate zones that are optimal for wind projects, as well as, exclusionary zones and zones where further data collection and investigation are needed to determine suitability for wind project developments. The project results will set the groundwork for Delaware's MSP efforts and may serve to direct initial proposals for locating new offshore wind projects.

The data layers and their sources that the Delaware MSP project seeks and intends to compile are summarized in Table 1. The data sources provide a good example of the various repositories including federal, state, academic and private that may contain data that must be obtained and integrated to apply MSP for offshore wind projects.

## Spatial Analysis of the Belgian Part of the North Sea

Belgium is one of the global leaders in implementing MSP as a method of ecosystem-based management for its territorial sea and exclusive economic zone. The Belgian part of the North Sea (BPNS) covers about 3600 $km^2$ with a coastline that is 66 km in length. Despite its relative small area (i.e., only 0.5% of the North Sea) the BPNS is intensely used (Maes et al., 2005). Belgium began to implement its Master Plan for the BPNS starting in 2003 using GIS to delineate areas for offshore wind development and sand/gravel extraction; this was followed by designation of marine protected areas (Douvere, Maes, Van Hulle and Schrijvers, 2007).

The criteria used to delineate these areas included fishing activity, nature and biodiversity and visual impacts from shore (Douvere et al., 2007). The effort produced a spatial plan that included a geo-referenced map of acceptable uses of the BPNS, with a 263.7 $km^2$ zone identified for potential offshore wind development (Degraer, Brabant and Rumes, 2010). This zone begins 22 km from the shoreline and extends seaward to the northern navigation route (Van Hulle et al., 2004). Belgium has continued to use this zone as the

**Table 1.** GIS data layers and sources for data to be used in the Delaware MSP for offshore wind

| *GIS data layer* | *Description of layer and notes* | *Source of data* |
|---|---|---|
| Vessel traffic | Observed ship movements, fairways and established shipping lanes, including pilot boarding areas and anchorages. Generally exclusionary to offshore wind projects. | International Comprehensive Ocean-Atmosphere Data Set; Waterway Network Ship Traffic, Energy and Environment Model; US Department of Transportation Commercially Navigable Waterways; Bureau of Ocean Energy Management, Regulation and Enforcement (BOEMRE) Marine Cadastre |
| Marine wildlife | Nesting, staging and important feeding areas for critical waterbirds; avian flyways; migratory pathways of marine mammals; and distribution of important species. Generally exclusionary to offshore wind projects. | Delaware Department of Natural Resources and Environmental Control (DNREC), North Atlantic Right Whale Catalog, Ocean Biogeographic Information System (OBIS)-SEAMAP |
| Prohibited areas | Prohibited areas include a minefield, chemical waste dump, and dredge spoil grounds. Exclusionary to offshore wind projects. | NOAA Electronic Navigation Charts (ENCs) |
| Regulated airspace | Airspace restricted by the US Federal Aviation Agency (FAA). Generally exclusionary to offshore wind projects. | FAA |
| Artificial reefs | Generally exclusionary to offshore wind projects. | DNREC |
| Sand borrow sites | Active and potential sand mining operations for beach replenishment. Generally exclusionary to offshore wind development. | DNREC, US Army Corps of Engineers, Delaware Geological Survey (DGS) |
| Bathymetry and marine geology | Water depth, characterization of seafloor sediments from grab samples and sub-bottom sediments from cores and seismic reflection profiles. Depths and sediment types have impact on foundation type and installation costs. | NOAA Bathymetry, USGS CONMAP, DGS, University of Delaware (UD) |
| Wind resource | Metric indicating strength of wind resource. | National Renewable Energy Lab (NREL), NOAA Buoy Data |
| Energy infrastructure | Location and capacities of onshore and offshore transmission critical for optimizing location of offshore energy projects. | NREL and PJM Interconnection LLC |
| MSP, State/Federal boundaries | Extent of MSP effort and boundaries for state/federal waters and federal OCS lease blocks. | UD, BOEMRE Marine Cadastre |

permissible area for offshore wind development as it adopts permitting guidelines. To date, Belgium has granted domain concessions to six wind projects, three of which have also obtained the appropriate environmental permits. Thus far, sixty-one offshore wind turbines have been installed, fifty-five on Bligh Bank and six on Thornton Bank; Eldepasco is expected to begin construction in 2011 (Royal Belgian Institute of Natural Sciences, 2011).

Following its initial MSP effort, Belgium conducted a comprehensive scientific study to set the framework for planning efforts into the future (Maes et al., 2005). This two-year study, the GAUFRE project, adapted land-based planning methods to the BPNS and produced an integrated vision for future use. The final recommendations of GAUFRE are a flexible structure that allows the government to adapt policies as needs change (Maes et al., 2005). The GAUFRE project involved substantial data gathering from a multitude of sources and integration of these data to produce GIS maps. The data compiled in the project is listed in Table 2. With exception of tourism, a geo-referenced map was generated for each component listed. During this process, areas of significant data gaps were identified and will be used to guide future data gathering efforts (Maes et al., 2005).

The second phase of the GAUFRE project analyzed the interaction among stakeholders where use overlapped spatially or temporally (Maes et al., 2005). Both positive interactions and conflict areas were identified and described. The MSP process in Belgium is set apart through the vision of the GAUFRE project. Rather than a final, end-use spatial plan, the project offers a strategic vision for development of the marine environment that incorporates the interconnectedness of each use and allows for continual adaptation over time. The vision is expressed through the integration of impact of use with three core values: well-being, ecological value and economic value. Six scenarios are displayed on structure maps with each map incorporating important use categories with core values. The scenarios include: the relaxed, playful, natural, mobile, rich and sailing sea; each with different emphasis on ecological value, economic value and well-being. As examples, the relaxed sea scenario places an emphasis on providing opportunities for tourism and recreational activities; the rich sea scenario places economic development as the most important objective in which many more resources can be exploited (Maes et al., 2005).

## Essential Techniques in Use of Geospatial Data for Offshore Wind

Table 2 provides an example of the types of geospatial data that are needed to provide the framework for implementing MSP for offshore wind projects. The two case studies, Belgium and Rhode Island, offer a good sampling of the types of data that are required.

**Table 2.** Examples of geospatial data for MSP for offshore wind projects

| *Geospatial Data* | *Case Study* | |
|---|---|---|
| | *Belgium* | *Rhode Island* |
| Wind | Planned wind parks | Wind resource, TDI, Tier 1 analyses, Renewable energy zones |
| Water depths, Marine geology and Oceanography | Bathymetry, Sand banks, Bottom and sub-bottom sediments, Ocean currents, Water pollution | Bathymetry, Bottom sediments, Benthic habitat, Subsurface geology, BOEMRE priority areas for geologic study, Meteorological data, Waves, tides, hydrography and circulation |
| Ecology | Benthic samples, Flora and fauna, Ecological valuation, Bird species, migratory routes and disturbance, Pollution/disturbed benthos, Areas of nature protection | Benthic ecosystem, Plankton, Fishes, Sea turtles, Marine mammals, Right whale management area, Avifanua, nutrients and toxins |
| Infrastructure | Buried cables and pipelines, Coastal defense, Towers/ platforms, Ports, anchorage areas | Cables and submarine cables, Anchorages, Ports/ harbours, airports and airport buffers |
| Navigation concerns | Shipping routes | NOAA ENC navigation lanes |
| Exclusional use | Dredging/dumping of dredge material, Sand/gravel extraction, Military use, Ammunition dumping | Disposal sites, NOAA regulated areas |
| Other use and concerns | Fishing and shipping intensity, Tourism/recreation, Aquaculture, Water pollution, Research zones | Fisheries and fish habitat, AIS vessel positions, Shipping activity, ferry routes, Unexploded ordnance, tourism and recreation |
| Cultural/Historical features | Shipwrecks | Submerged archaeological sites<br>Adjacent historic onshore sites |
| Boundaries | Territorial waters and EEZ | Coastal buffer zone, Ocean SAMP area, State waters boundary, BOEMRE OCS lease blocks |

Not included in Table 2, and of concern in siting offshore projects, is the influence of wind turbines on aviation and marine radar. In the US, the Federal Aviation Administration considers not only risks of aircraft collisions with blades, turbines or towers, but also the potential for wind projects to degrade radar performance. The Department of Homeland Security has issued an interim policy calling for federal opposition to the establishment of any wind project "within radar line of sight" of a Department of Defense or Homeland Security radar installation. Research on the effects of turbines on radar and ways to mitigate associated problems have been conducted and are on-going (e.g., Brenner et al., 2008; Hawk, 2009).

In addition to the identification, acquisition and compilation of the critical geospatial data described in the case studies and listed in Tables 1 and 2, geospatial techniques must be applied to make this data useable within an MSP framework. These techniques involve: (1) standardizing individual datasets into a common platform, (2) deciding upon and carrying out the methods (e.g., modelling vs. visual inspection) that are used to analyze the data in terms of offshore wind development, and (3) determining and applying the appropriate methods of data sharing and display that will create an output that is easy to use in MSP.

## Geospatial Techniques: Standardizing Datasets into a Common Platform

Offshore wind datasets are highly varied and typically compiled from disparate sources (Tables 1 and 2). After the significant initial work of identification and compilation are complete, bringing these datasets together in a useful technological platform is necessary. In some cases, digitization and georeferencing are required. This is the process of scanning or sketching the geospatial features on a hard-copy map or drawing into a digital format, and is usually done through any GIS package. However, most offshore wind geospatial data pre-exist in digital format, and thus translation of the datasets into a common spatial reference system (SRS) is generally the first step in processing.

SRSs define the type of coordinates used to represent the spatial data. Having all of the data georeferenced to a common SRS allows it to be easily manipulated within a comprehensive GIS, a geospatial data viewer such as Google Earth or NASA World Wind or any mapping software. Using a common SRS is critical when doing nearly any type of analysis, such as computing distance matrices, performing grid algebra or any vector-based geoprocessing (e.g., union, buffer, intersection). Within a SRS, the shape and orientation of the Earth are taken into account, and described by the horizontal reference datum. A common global datum is the WGS 84, World Geodetic System of 1984 and it is the datum used in the GAUFRE project in the BPNS. For the Massachusetts Ocean Management Plan, the MassGIS database associated with the MORIS mapping tool contains data that are referenced to the

Massachusetts State Plane Mainland NAD83 datum with units in metres. In the Rhode Island SAMP, the RIGIS data stored at the EDC are referenced to the Rhode Island State Plane Feet NAD83 coordinate system. Researchers may submit data to the EDC in either the RI State Plane Feet NAD83 or geographic (latitude/longitude) WGS84 coordinate systems. The Delaware MSP project will use Delaware State Plane NAD83 coordinates with units in metres.

SRSs also include the mathematical projection of 3D real-world geographic coordinates (latitude and longitude) to 2D planar coordinates (metres or feet) that are used for display. This is known as the projection of the SRS. The terms "projection" and "SRS" are often confused. It is important to note that a SRS incorporates all of the information about how a feature is referenced to the Earth. A projection is only the mathematical algorithms used to convert geographic to planar coordinates and has no bearing to the ellipsoid or the datum being applied. Because the data is being transformed from 3D to 2D, only some aspects of the data can be preserved, and therefore projections are usually classified by which aspects the transformation preserves. Projections may preserve distances (equidistant), areas (equal area), direction (azimuthal) or shape (conformal) (United States Geological Survey, 1989). For analyses that utilize distance calculations (e.g., distance to shore), it is optimal to keep the datasets in an equidistant projection. Likewise for analyses that visually compare regions (e.g., areas where development is prohibited, migratory paths/nesting grounds), keeping these data in an equal area projection is beneficial. Multiple types of analyses can be performed on the same data by projecting the source data to multiple output reference systems. However in terms of mapping these results, one common SRS should be used.

In addition to translating data to a common SRS, care must be taken to determine the appropriate file format and resolutions. These are typically determined by the analytical or distribution requirements. For example, if data will be distributed via the web, keeping data in widely supported formats is ideal, such as shapefiles for vectors or TIFFs for rasters. Data may also need to be converted to raster or vector formats, or generalized/down-sampled based upon the analysis techniques employed.

## Geospatial Techniques: Methods to Analyze Data for Offshore Wind Development

Once the data has been translated into a common platform, the types of analysis that will be performed need to be determined and then carried out. Depending on the analysis chosen, data may need to be further preprocessed in some way. General approaches include using data required for MSP in analytical modelling methods or in maps and drawings as illustrations for visual inspection (Beck, 2009). Both approaches may be used for different purposes, on different data sources, or on the same data source at different stages of the project life cycle.

Incorporating the data into analytical modelling methods usually means to apply numerical equations or logical algorithms to values within the source data. Within a GIS or programing environment, source datasets are typically converted to raster, cell-based formats. Vector-based data (points, lines and polygons) are converted to rasters using a variety of techniques, depending on the nature of the data. For example, for marine wildlife tracking (such as marine mammal or avian movement), data points may represent individual sightings. To convert these points to raster data, they may be summarized as the number of observations that occur within a given grid cell. Grid cell resolution is variable depending on the scale of study, with a 1 km × 1 km size being considered reasonable for local to regional coverage. Algorithms are then applied to each cell in the spatial domain of the study area. Resulting rasters may represent physical calculations, index values, priority ranking, or true/false values.

The analyses that are required must be run in capable and readily available software. In recent years, many free and open source software (FOSS) programs for geospatial use have become popular due to their maturity, advanced features, active communities and low barrier to adoption. FOSS that can be used to perform analyses that are needed for offshore wind development projects include GRASS GIS, Quantum GIS and GDAL/OGR (for display, conversion and GIS analysis); PostGIS (for data storage); R Geo (for statistical analysis); and Mapserver and Open Layers (for display).

The Technology Development Index (TDI) developed by Spaulding et al. (2010) for the Rhode Island SAMP is a good example of an analytical modelling approach that can be applied in the planning for offshore wind development. The TDI is expressed by the ratio between the Technical Challenge Index (TCI) and the Power Production Potential (PPP) of the energy extraction equipment (e.g., wind turbines). The TCI is a sum of the measures of how difficult it is to site an energy project at a given location plus the distance of the site to the nearest electrical grid connection. As suggested by Spaulding et al. (2010), TCI could be estimated from the structural design and installation including cabling to shore (influenced by local factors including bottom sediments and subsurface geology) and the associated costs for a given location. In this case, numerical values of TCI could be assigned to individual categories ranked in level of difficulty/expense, with lower numbers being assigned to locations that are the least difficult and/or expensive to develop. The PPP is defined as the annual mean power density for the energy project multiplied by the capacity factor for the facility. In the case of offshore winds, the mean annual power density ($kW/m^2$) is determined at the turbine's hub height and the capacity factor is approximately 35% (Renewable Energy Research Laboratory, 2008). Minimum values of the ratio TCI/PPP identify areas of optimum siting based on these factors (Spaulding et al., 2010).

In practice, the area of study is typically gridded (e.g., 100 m square grid size for the Rhode Island SAMP) and the TDI (TCI and PPP) is calculated for

each grid space. The results can be presented in the form of contours of TDI (Spaulding et al., 2010). As noted by Spaulding et al. (2010), this technique explicitly accounts for the spatial variability of all input data. In addition, simulations can be performed either deterministically or stochastically, using a Monte Carlo method, so that uncertainties in the underlying input data can be reflected in the estimated TDI values (Spaulding et al., 2010). The stochastic approach allows detailed assessment of the sensitivity of the estimates to the input data used to calculate the TCI and PPP values (Spaulding et al., 2010).

The most common application of visual inspection techniques for offshore wind projects is the determination of exclusionary zones based upon the locations of features that would preclude development. In the Massachusetts Ocean Management Plan, areas of exclusion as shown on GIS generated maps include: locations within 1.6 km from inhabited shorelines, Coast Guard-designated navigation areas (i.e., shipping channels and traffic lanes, precautionary areas, anchorage areas and pilot boarding areas), the presence of eelgrass and intertidal flats, ferry routes, high concentrations of avian resources (e.g., nesting, staging and critical foraging areas for Roseate Tern; nesting, staging and core foraging areas for special concern Arctic, Least and Common tern species), high concentrations of whale populations (i.e., North Atlantic Right Whale core habitat), areas of significant commercial and recreational fishing effort and value, direct transit navigation routes for shipping and fishing and regulated airspace. Also removed from further consideration were areas determined to have excessive cumulative effects, constraints of wind turbine technology, visual impacts and other existing uses as determined through qualitative assessment, public input and stakeholder feedback (MA-EEA, 2009a).

Visual inspection techniques also can be used to delineate preferred areas for development based on the absence of exclusionary features and the minimization of impact on ecological resources or competing uses. In the case of the Rhode Island SAMP, the results from numerical analyses and the TDI contours were combined with maps of exclusionary zones to delineate the most suitable areas for renewable energy development. A similar approach was used in the Belgian MSP effort. Intensity of use maps for categories that included fisheries, mineral extraction, aquaculture, dredging, dredge disposal, dumping, wrecks, anchoring, shipping, research, military, cables and pipes, wind projects, coastal defense, marine protected areas and recreation were generated for the BPNS area using a grid interval of 1 $km^2$. Each of the uses was qualitatively scored based on its intensity of occurrence within each grid interval. The intensity values assigned ranged from 3, high intensity of use, to 0, no activity (Maes et al., 2005). The expected impact of each category of use in terms of its disturbance based upon ecological, physical and chemical factors was then ranked qualitatively using a numerical scale. This scale also ranged from 3 to 0, with major impacts assigned a value of 3 and negligible or no impact a value of 0 (Maes et al., 2005). Maps delineating the full

environmental impact of each use were then generated by multiplying the intensity value by the impact value for each 1 $km^2$ grid interval. These GIS maps were used in a suitability analysis that incorporated technical and jurisdictional constraints, as well as ecological and socio-economic considerations to identify appropriate use areas within the BPNS (Maes et al., 2005).

Regardless of the approach, the scope, resolution and scale of the analysis must be considered and boundaries of the analysis clearly defined. This makes it easier to develop models and maps, and focuses the interpretation of results. Primarily within a modelling approach, grid cell resolution plays a key role. Beck (2009) argues that marine spatial plans should consider information at two spatial scales and resolutions: a sub-regional or 'state' scale with relatively fine resolution and a regional scale with coarser resolution. The sub-regional scale makes it feasible to use a resolution that approximates the largest scale (smallest area) used. Models can run at this resolution (typically a few km or less) to produce numerical results as is common for projects within state boundaries or smaller study areas. Both the Rhode Island and Belgium MSP examples to identify preferred areas for offshore wind development used a grid interval of 1 $km^2$ and thus were conducted at what would be considered the sub-regional scale.

Processes that happen or data aggregated at regional scales may have less spatial detail but are just as critical for planning purposes. Analyses at this scale (a few km or larger) are typically done through maps and illustrations for visual inspection. They can serve as a study mask and help focus prioritizing, coordinating and evaluating sub-regional investigations. For example, in examining ship vessel traffic within the Delaware MSP study area, a more regional scale analysis is required based upon the resolution of the available data. To understand where ships travel within the Delaware study area and where conflicts appear to be most prevalent, the International Comprehensive Ocean-Atmosphere Data Set (ICOADS) will be used. ICOADS is a data set of global marine surface conditions collected and reported by a fleet of about 4000 ships known as the Voluntary Observing Ships (VOS) (Corbett, Wang and Firestone, 2006). The ICOADS dataset and the Waterway Network Ship Traffic, Energy and Environment Model (STEEM) can be imported into a GIS to identify areas of high traffic within the Delaware MSP study area (Wang, Corbett and Firestone, 2007). Totals of ship transits are represented within a 4 km by 4 km grid, or 16 $km^2$. Any geospatial analysis methods incorporating this data must be performed with a resolution of 4 km × 4 km or larger. Thus, resolution becomes a factor when focussing on the Delaware study area given the global nature of the dataset, but it remains the best available to determine habitual shipping traffic patterns. Preliminary analysis of the ICOADS and STEEM data indicates that clear economic shipping lanes emerge. They will be incorporated into the Delaware MSP.

The discussed case studies and approaches used have limitations to the accuracy of the information. Inherent in geospatial analyses is that the GIS data and models represent approximations or indicators of the physical phenomena, not the phenomena itself (Longley, Goodchild, Maguire and Rhind, 2005). Ambiguity and vagueness are always introduced. It is non-trivial to generate probability of error or uncertainty maps in typical GIS programs. Additional steps must be taken, usually including installation of plug-ins or writing code with advanced technical or statistical expertise, to approximate associated errors. However, it is helpful to understand the errors associated with any analysis to improve understanding and help make better decisions. If MSP takes a scientific approach to the collection, manipulation, analysis and presentation of geographic information, it is then inappropriate that GIS users remain unable to describe how close their information is to the truth it represents (Hunter, 1998).

Uncertainty may come into play many times during a GIS-based offshore wind project. There is measurement error in the input source data and much uncertainty in the interpretation of that data. This varies widely among the types of data used. For example, the errors associated with estimating migrating bird populations from many years of individual sightings is much different than errors introduced when creating a smooth surface (i.e., digital elevation model) of ocean bathymetry. Yet, these data may be used in a common analysis to derive a single result (e.g., where to optimally locate offshore wind projects). Mowrer (2000) discusses the data life cycle and how inaccuracies can be introduced at many times during a project, from data collection to data conversion, to limitations in the algorithms applied, to approximations or categorizations used for aesthetic display. Accuracy assessments can be performed at any time in the cycle and modifications can be made to data models or methods applied (Mowrer, 2000).

The spatial and temporal scale at which analyses are conducted plays a role in the uncertainty of the results, although the scale is usually dictated by the availability of the data. Generally, the more averaging (aggregation or 'scaling up') done to the data, the stronger the perceived relationships tend to be (Longley et al., 2005). More uncertainty is introduced as further processing is done in order to prepare data for the selected analysis method or approach, particularly when converting from vector-based data to raster. It is difficult to assign appropriate fundamental units (e.g., grid cell resolutions for raster modelling, minimum mapping areas for vector drawings) for many natural and human phenomena, it is even more difficult when these are integrated. Data used as illustrative purposes will have errors in the details at the boundaries. Within MSP, these can be mitigated somewhat by using conservative estimates for inclusionary areas and over estimates for exclusionary areas. Performing analyses at two separate scales, each with their own sets of uncertainty, improves confidence if they indicate similar results.

Other measures can also be taken to reduce uncertainty. Proper metadata and complete descriptions of data collection methods and any preprocessing performed (with notes about associated errors) are extremely useful. In the case studies that are presented in this chapter, metadata are available for all of the complied GIS layers. The Massachusetts, Rhode Island and Delaware MSP projects utilize metadata that are Federal Geographic Data Committee (FGDC) complaint. Obtaining data from trusted sources and field checking information are obvious choices but are difficult, sometimes impossible, to achieve in practice. Establishing an independent scientific panel to evaluate methods and data, such as the working groups and advisory council in the Massachusetts case study, is recommended (Beck, 2009). Openshaw (1989) suggests uncertainty estimations might not require hard quantitative assessments, but instead may involve a more pragmatic approach of determining that errors and uncertainty levels are not so high as to doubt the validity of a particular result for a given set of data applied to a specific situation.

## Geospatial Techniques: Methods of Data Sharing and Display for Users of MSP

In order to implement MSP, decisions must be made on how best to share and display the data and results with other project participants, relevant stakeholders, and the general public. In all of the case studies that are discussed in this chapter, digital multi-layered maps in a GIS or maps embedded in PDF or as graphic images are used to present results. An approach to sharing data with varied audiences is to develop comprehensive web-based mapping applications with the ability for users to show/hide various data layers. An example of this is the MORIS tool developed for the Massachusetts MSP. MORIS is designed to provide spatial data that are accurate, scientifically sound and credible in an easily accessible and useful manner using a collaborative, interactive process that involves a variety of partners and data sources (MA-CZM, 2011). The MORIS implementation is open source and can be accessed via its website (http://www.mass.gov/czm/mapping/index.htm).

MORIS is a JavaScript web application, run through a client-side web browser that utilizes various components of OpenLayers/GeoExt, JavaScript toolkits for rich mapping applications (MA-CZM, 2011). It pulls data through GeoServer mapping software, a free, open-source, map-serving platform that serves data using Open Geospatial Consortium, Inc. (OGC) WMS and WFS formats, among others. OGC is a nonprofit, international, voluntary consensus standards organization that is involved in the development of standards for geospatial- and location-based services. The developers of MORIS note that an advantage of serving the data layers through OGC-compliant map services is that in addition to supplying the MORIS client, layers are available to be consumed by other clients including ArcMap, Quantum GIS and Google Earth (MA-CZM, 2011).

The EDC at the University of Rhode Island, working in concert with the RI-CRMC, has developed a web-based portal system in which users can view and access data related to the Rhode Island SAMP project (http://www.narrbay.org/). Options are available to view maps with data layers via a rapid watershed viewer, download images of maps in pdf format, or download data in shapefile or ARC/INFO interchange file formats. The initial effort of the Delaware MSP offshore wind project will be to generate maps in pdf format that will be web viewable and available for download.

Another method is to use KML for sharing data to large audiences. It is the default display format, and can be created and edited, in Google Earth. KML can store both individual geographic features with raw coordinates (for vectors: points, lines polygons) or links to geospatial data stored remotely, including georeferenced graphic images, WMS and WFS map services and 3D models. Many GIS programs can export more traditional formats to KML. If the datasets are small (less than a few MB), they can be completely contained inside a KML and no server side technology is required. This is ideal for situations where very little IT support is available. KML can serve large datasets easily by pointing to the server that houses the data. In addition to being easy to use and having native KML support, an advantage of using Google Earth is the availability of background data. Google Earth includes aerial imagery, subsurface ocean data, point of interest and georeferenced photographs with user contributed data.

## Conclusion

The case studies outlined in this chapter demonstrate the variety and quantity of geospatial data that is required for successfully implementing MSP for offshore wind projects. Far beyond simply requiring information about the wind resource, water depths, distance to shore and the local ecosystem, data pertaining to such diverse categories as coastal tourism, commercial and recreational fishing, established shipping lanes, sand borrow sites, disposal and unexploded ordinance sites, marine archaeological sites, submerged transmission lines, the locations of local and federal boundaries and nearby land-based energy infrastructure and local socio-economic and socio-cultural considerations need to be compiled.

Once gathered, geospatial techniques must be employed to first standardize individual datasets into a common platform and then apply analysis methods generally involving both visual comparisons and raster-based impact studies. As a final task in the application of geospatial techniques to offshore wind development projects, the relevant data and results of analyses must be displayed and shared with stakeholders and decision makers. As illustrated by the case studies, geospatial maps, especially those that are able to integrate multiple layers of data and that can be evaluated in the determination of

preferred locations for offshore wind development projects, provide invaluable input to the MSP process.

In addition to the case studies presented in this chapter, major MSP efforts pertaining to offshore wind development are on-going in countries such as the United Kingdom and the Netherlands in Europe, as well as states along the East Coast of the US and the Great Lakes. These efforts, in concert with the cases presented in this chapter, indicate the importance and increasing need for the application of geospatial techniques in the planning for offshore wind development.

## Acknowledgement

This chapter was prepared by the authors under award NA10OAR4170084 from the National Oceanic and Atmospheric Administration, US Department of Commerce. The statements, findings, conclusions and recommendations are those of the authors and do not necessarily reflect the views of the National Oceanic and Atmospheric Administration or the Department of Commerce.

## References

Applied Technology and Management (2007). Rhode Island Winds Summary Report. Retrieved from the State of Rhode Island Office of Energy Resources Web site: http://www.energy.ri.gov/documents/renewable/RIWINDS_RANKING.pdf

Beck, M., Ferdana, Z., Kachmar, J., Morrison, K.K. and Taylor, P. (2009). Best Practices for Marine Spatial Planning. The Nature Conservancy, Arlington, VA.

Brenner, M., Cazares, S., Cornwall, M.J., Dyson, F., Earley, D., Horowitz, P., Long, D., Sullivan, J., Vesecky, J. and Weinberger, P. (2008). Wind farms and radar. Retrieved from the Department of Defense Intelligence and Related Organizations Web site: http://fas.org/irp/agency/dod/jason/wind.pdf

Bureau of Ocean Energy Management, Regulation and Enforcement (2010). Cape Wind Associates, LLC Commercial lease of submerged lands for renewable energy development on the outer continental shelf. Retrieved from the Bureau of Ocean Energy Management, Regulation and Enforcement Web site: http://www.boemre.gov/offshore/RenewableEnergy/PDFs/CapeWind_signed_lease.pdf

Corbett, J., Wang, C. and Firestone, J. (2006). Estimation, validation, and forecasts of regional commercial marine vessel inventories. Retrieved from the University of Delaware, College of Earth, Ocean and Environment Web site: http://coast.CEOE.udel.edu/NorthAmericanSTEEM/ARBCEC_SECA_task1-2ReportMay2006.pdf

Deepwater Wind LLC (2011). Block Island Wind Farm Overview. Retrieved from http://dwwind.com /block-island/block-island-project-overview

Degraer, S., Brabant, R. and Rumes, B. (Eds.) (2010). Offshore wind farms in the Belgian part of the North Sea: Early environmental impact assessment and spatio-temporal variability. Royal Belgian Institute of Natural Sciences, Brussels, Belgium.

Douvere, F., Maes, A., Van Hulle, F. and Schrijvers, J. (2007). The role of marine spatial planning in sea use management: The Belgian case. *Marine Policy*, 31, 182–191.

Ehler, C. and Douvere, F. (2009). Marine spatial planning: A step-by-step approach toward ecosystem-based management. UNESCO Intergovernmental Oceanographic Commission and Man and the Biosphere Programme, Paris, France.

Global Wind Energy Council (2010). Global Wind 2009 Report. Brussels, Belgium, Author.

Great Lakes Wind Council (2010). Report of the Michigan Great Lakes Wind Council. Retrieved from the Michigan Great Lakes Wind Council Web site: http://www.michiganglowcouncil.org/GLOW Report 9-1-09_FINAL.pdf

Grilli, A., Spaulding, M.L., Crosby, A. and Sharma, R. (2010). Evaluation of wind statistics and energy resources in southern Rhode Island coastal waters for the Rhode Island Ocean Special Area Management Plan. Retrieved from the Rhode Island Sea Grant Web site: http://seagrant.gso.uri.edu/oceansamp/pdf/appendix/20-AGrilliEtAl-EvalWind.pdf

Hawk, S. (2009). Impact study of 130 offshore wind turbines in Nantucket Sound. Retrieved from the Federal Aviation Agency Web site: https://oeaaa.faa.gov/document /Study_of_Nantucket_Wind_Farm_Report.pdf

Hunter, G.J. (1998). Managing Uncertainty in GIS. Retrieved from the NCGIA Core Curriculum in Geographic Information Science Web site: http://www.ncgia.ucsb.edu/giscc/units/u187/u1871.html

Interagency Ocean Policy Task Force (2010). Final recommendations of the Interagency Ocean Policy Task Force. Executive Office of the President of the United States, Washington, DC.

Longley, P.A., Goodchild, M.F., Maguire, D.J. and Rhind, D.W. (2005). Geographic Information Systems and Science (2nd ed.). John F. Wiley and Sons, New York, NY.

Maes, F., Schrijvers, J., Van Lancker, V., Verfaillie, E., Degraer, S., Derous, S., De Wachter, B., Volckaert, A., Vanhulle, A., Vandenabeele, P., Cliquet, A., Douvere, F., Lambrecht, J. and Makgill, R. (2005). A flood of space: Towards a spatial structure plan for sustainable management of the North Sea. De Windroos, Beernem, Belgium.

Massachusetts Executive Office of Energy and Environmental Affairs (2009a). Massachusetts Ocean Management Plan, Volume 1: Management and Administration. Retrieved from Massachusetts Executive Office of Energy and Environmental Affairs Web site: http://www.env.state.ma.us/eea/mop/final-v1/v1-complete.pdf

Massachusetts Executive Office of Energy and Environmental Affairs (2009b). Massachusetts Ocean Management Plan, Volume 2: Baseline Assessment and Scientific Framework. Retrieved from Massachusetts Executive Office of Energy and Environmental Affairs Web site: http://www.env.state.ma.us/eea/mop/ final-v2/v2-complete.pdf

Massachusetts Office of Coastal Zone Management (2011). MORIS: Massachusetts Ocean Resource Information System: CZM's Online Mapping Tool. Retrieved from Massachusetts Office of Coastal Zone Management Web site: http://www.mass.gov/czm/mapping/index.htm

Minerals Management Service (2009). Bluewater Wind Delaware, LLC. Lease of submerged lands for alternative energy activities on the outer continental shelf. Retrieved from the Bureau of Ocean Energy Management, Regulation and Enforcement Web site: http://www.boemre.gov/offshore/RenewableEnergy/PDFs/LeaseA0474.pdf

Mowrer, T.H. and Congalton, R.G. (2000). Quantifying Spatial Uncertainty in Natural Resources: Theory and Applications for GIS and Remote Sensing. CRC Press, New York, NY.

Openshaw, S. (1989). Learning to live with errors in spatial databases. *In:* M. Goodchild and S. Gopal (Eds.), The accuracy of spatial databases (pp. 263–276). Taylor & Francis, London, England.

Rhode Island Coastal Resources Management Council (2010). Rhode Island Ocean Special Area Management Plan. Retrieved from the Rhode Island Sea Grant Web site: http://seagrant.gso.uri.edu/oceansamp/documents.html#samp

Royal Belgian Institute of Natural Sciences (2011). Offshore Wind Farms in Belgium. Retrieved from http://www.mumm.ac.be/EN/Management/Sea-based/windmills.php

Spaulding, M.L., Grilli, A., Damon, C. and Fugate, G. (2010). Application of Technology Development Index and Principal Component Analysis and Cluster Methods to Ocean Renewable Energy Facility Siting for the Rhode Island Ocean Special Area Management Plan 2010. Retrieved from the Rhode Island Sea Grant Web site: http://seagrant.gso.uri.edu/oceansamp/pdf/appendix/16-SpauldingTDI.pdf

United States Geological Survey (1989). Map Projections. Retrieved from the United States Geological Survey Web site: http://egsc.usgs.gov/isb/pubs/MapProjections/projections.pdf

Van Hulle, F., Le Bot, S., Cabooter, Y., Soens, J., Van Lancker, V., Deleu, S., Henriet, J.P., Palmers, G., Dewilde, L., Driesen, J., Van Roy, P. and Belmans, R. (2004). Optimal Offshore Wind Energy Developments in Belgium. Part I. Sustainable production and consumption patterns. Belgium Science Policy, Brussels, Belgium.

Wang, C., Corbett, J.J. and Firestone, J. (2007). Modeling energy use and emissions from North American shipping: An application of ship traffic, energy, and environment model. *Environmental Science & Technology*, **41**, 3226–3232.

# 17

# Social Vulnerability Assessment through GIS Techniques: A Case Study of Flood Risk Mapping in Mexico

**P. Krishna Krishnamurthy and L. Krishnamurthy**
Agroforestry Centre for Sustainable Development
University of Chapingo, Chapingo 56235, Mexico

## Introduction

The most significant impact of natural disasters is at the local level, where human settlements are destroyed and livelihoods are put at risk, economic losses are ensued, and there may be injuries or loss of life in the affected areas (Smith, 2004; Tran et al., 2009). Disaster potential can be conceptualised as the simultaneous occurrence of hazard (the geophysical environmental risk) *and* vulnerability (the social risk) (cf. Alexander, 1998). Within the context of climate change, in particular, hydrometeorological hazards are becoming more complex and the potential for greater adverse impacts increases (Pielke, 2005; IPCC WGI, 2007). One-in-one-hundred-years flooding events such as that of 2007 in the Gulf of Mexico are expected to become more frequent (SEMARNAT and INE, 2010). The number of recorded floods in Mexico has increased four-fold in the past fifty years and the associated economic losses have increased exponentially in the same period (EM-DAT, 2011). The policy challenge is complicated as coastal societies continue to settle in hazard-prone areas with as many as 600 million globally (and 50 million in the Gulf of Mexico) living in floodplains by 2100 (Nicholls and Mimura, 1998), and a replicable methodology for the analysis of *social* vulnerability is needed.

Social vulnerability is inherently complex and no consensual definition for the term exists (Ebert et al., 2009). As it is societies that define their vulnerabilities, the concept has different meanings to different people in different places at different times (Clark et al., 1998; Wisner et al., 2004). For the purposes of this essay, however, social vulnerability is defined as the

J.K. Thakur et al. (eds.), *Geospatial Techniques for Managing Environmental Resources*,
DOI 10.1007/978-94-007-1858-6_17, © Capital Publishing Company 2012

*characteristics* of a person (or group) that render them incapable of dealing with hazards (cf. Adger, 1999). Having operationalised vulnerability in terms of characteristics, it is possible to define spatial physical proxies that influence social vulnerability.

This chapter proposes an approach to assess and monitor social vulnerability at the municipal level by using open source data for vulnerability proxy indicators: population below the poverty line (socioeconomic structure), distance to hospitals, emergency shelters and federal roads (infrastructure), population density per municipality (population dynamics), and flood frequency (historical hazards). It is argued that these data, integrated onto a Geographic Information System (GIS), can provide useful vulnerability maps to inform policymaking.

This three-step analysis illustrates (i) distributional patterns of vulnerability at municipal, (ii) the impact of different proxy indicators on overall vulnerability, and (iii) what steps can be taken to reduce disaster risks. In doing so, this chapter models the vulnerability of the study site. The advantages and disadvantages of the mapping process are explored through a case study of the flood-prone State of Veracruz, Mexico.

## Geospatial Techniques: Vulnerability and Flood Risk Assessment

The use of geospatial techniques to assess vulnerability to hydrometeorological hazards has been comparatively unexamined because they are difficult to model and predict, especially in the context of climate change (Daniel and Abkowitz, 2005). At the time of printing, only one GIS-based study on flooding (Tran et al., 2009) was found in the literature (SCOPUS, Web of Knowledge, Google Scholar, key words = GIS AND flood*). Vulnerability studies using GIS tools are similarly limited, focussing on topographical and hydrological features, rather than social factors (e.g. Hart and Knight, 2009). In a study of coastal vulnerability to flooding in Vietnam, Tran et al. (2009), however, map six physical proxies that relate to local vulnerabilities: house type, flood levels in (i) 1999 and (ii) 2004, proximity to rivers, proximity to safe shelter, and proximity to main roads.

The use of Geographic Information Systems in disaster studies is relatively recent (Hart and Knight, 2009). The importance of integrating GIS in hazard assessment is recognized by Hatfield (2006): hazard maps are useful tools in the identification of disaster risk as they display the social vulnerabilities and can facilitate target policy to assist vulnerable populations. The use of GIS tools in hazard studies has been mainly restricted to geological hazard assessment such as landslide zonation (Nagarajan et al., 1998), volcanic risk management (Pareschi et al., 2000) and earthquake evacuation planning (Rashed and Weeks, 2003a).

GIS tools and maps are important for effective disaster management policy (Tran et al., 2009). Such integration is important for three reasons: (i) a vulnerability map can help in communicating available knowledge through a visual medium; (ii) context-specific information is crucial in reducing disaster risk at a relevant spatial resolution, such as the municipal level; and (iii) GIS maps are advantageous as they allow for complex spatial analysis (Hatfield, 2006).

First, mapping is one of the initial steps in understanding the factors leading to vulnerability and its distribution within a given context (Wisner et al., 2004). Maps provide clear pictures of the distribution of hazards and vulnerability that can be appreciated by people with no specialist knowledge (Tran et al., 2009). Further, maps can provide a compelling visual to motivate political action (Pradan, 2004). The mapping process, followed by a comprehensive spatial analysis, can also help in identifying areas that are particularly vulnerable and that require prioritisation. As such, a GIS-based analysis of vulnerability can help in allocating resources more efficiently (Morrow, 1999). Maps are thus an important way of communicating local perceptions of risk and vulnerability to policymakers through a simple and compelling visual mode.

Second, information at very detailed geographical level is often not available for the most vulnerable countries and communities where infrastructure for data collection is limited. Where it is available, it is often not presented in a clear manner that is useful to decision-makers. For this reason, the primary aim of GIS mapping is to make this knowledge visible by transferring information to a map (Tran et al., 2009). This type of communication allows policy-makers to rapidly understand the needs of local governments and communities as well as opportunities for disaster risk reduction (Twigg, 2001).

Third, technological advances have facilitated the creation of maps, and the development of GIS software has made spatial analysis easier. Producing conventional maps is a time-consuming process based on information gathered from historical data. Correction or expansion of maps has traditionally been complicated and that it has been difficult to update maps with data on (i) environmental change (erosion, hazard patterns) and (ii) anthropogenic change (land use change, development of infrastructure, human settlements). Consequently, vulnerability maps could potentially become obsolete as soon as they are published.

A limitation of conventional maps refers to the resolution: municipal-level data dealing with information about infrastructure, demographic conditions, and economic factors is lacking in conventional maps. All of these data are essential in mapping local vulnerability to flood risk. In contrast, GIS software allows for the integration of non-geographical attributes with graphic features through geographical referencing and allows for the management, display and query of socio-economic information (Dash, 1997).

Finally, GIS maps provide an illustration of different risks and how they interact to contribute to overall vulnerability. GIS technology can show thematic maps based on specific information such as infrastructure and poverty. The ability to produce thematic maps allows policymakers to focus on and tackle specific aspects of vulnerability. For instance, by identifying the relationship between vulnerability and infrastructure, it is possible to allocate financial resources to improve the quality and access to infrastructure for disaster management.

## Methods

### Study Area

The State of Veracruz is located in the south-eastern part of the Gulf of Mexico (Fig. 1). The State has an area of 71,699 km$^2$ and is divided into 210 administrative entities, or municipalities (Fig. 1). The population is 7,110,214, of which more than 4.5 million live in the North, near the political, cultural and economic capitals of the State. Much of the infrastructure lies in the coastal plain and around 79% of the population lives within 30 km of the coast (INEGI, 2010).

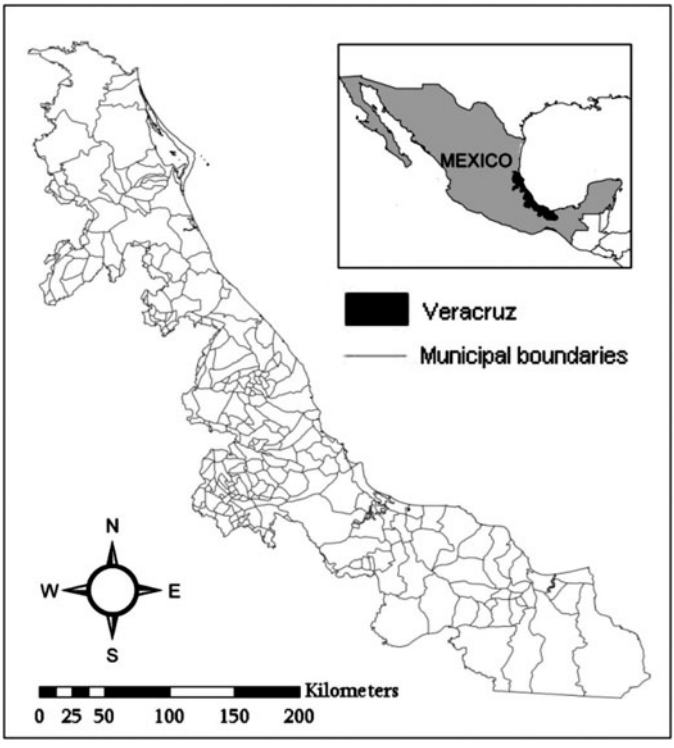


**Figure 1.** The geographical context of Veracruz, Mexico.

Like several coastal areas in Mexico, the State of Veracruz is vulnerable to hydrometeorological hazards including hurricanes and floods. Indeed, it is considered to be among the most disaster-prone areas in Mexico, losing up to 15% of its gross domestic product (GDP) annually due to hazards (CENAPRED, 2009). The main economic activity of Veracruz is citrus-based agriculture which accounts for 60% of its GDP. During the rainy season (October-December), crops are cyclically affected and huge economic losses are incurred due to flood events and migration is commonplace (Krishnamurthy and Krishnamurthy, 2011). Hazards, therefore, hinder the social and economic stability of the State. In September 2007, an early rainy season was accompanied with a one-in-one-hundred-years flood event occurred in the southern part of the State affecting 10,000 households, some 35,000 people, 17,000 hectares of agricultural land and incurring losses of around US$20 million.

## Scope and Limitations of the Study

The State of Veracruz suffers several hazards such as floods, hurricanes and drought; this study focuses only on flood risk mapping. While the inclusion of geophysical data (such as topography, soil type and rivers) may enhance the assessment of *overall* vulnerability (Rashed and Weeks, 2003b), this study is concerned with the *social* elements of vulnerability, and so the emphasis is on census and infrastructure data. Moreover, the study focuses on vulnerability at the municipal level, thereby disregarding vulnerabilities at smaller scales (i.e. at the community and household levels). This was necessary given the available data. However, the study demonstrates the potential for using GIS tools in disaster management and planning based on the assessment of *social* vulnerability at resolutions that are relevant for policymaking using open source data.

## Data

The principal data collected for this vulnerability assessment consisted of a poverty indicator, flood records, information about existing infrastructure (distribution of hospitals, federal roads and emergency shelters—public buildings such as schools assigned a 'safe' status under the Civil Protection Strategy)—and population density. These data were obtained from national (INEGI, SPC) and international (UNDP, CRED, EM-DAT) databases and were uploaded on the GIS software. The base map represents the boundaries of each municipality. All data were projected in UTM, WGS84, with a latitude-longitude coordinate system. Based on the existing literature and the recommendations of the Civil Protection Strategy and the National Centre for Disaster Prevention, six socially relevant physical proxies were selected: population density at the municipal level, historical flood frequency, distance to hospitals, distance to emergency shelters and proximity to federal roads (Table 1).

**Table 1.** Criteria for the assessment of social vulnerability.

| *Proxy indicator* | *Rationale* | *File type* | *Data source* |
|---|---|---|---|
| Population below the poverty line (percentage) | Poverty is one of the main factors contributing to vulnerability, although the relationship is complex (Cutter et al., 2003). One of the direct ways in which poverty influences vulnerability is through lack of financial resources, which leads to lower capacities to cope and recover from a disaster. | Polygon shapefile | UNDP, 2007 |
| Frequency of flood hazard | Hazards are characteristic of the places where they occur. Hence, municipalities that have been affected by floods are likely to be affected in the future. Any hazard assessment should consider areas that have been affected in the past (Jones, 1991). | Polygon shapefile | CRED, 2010; EM-DAT, 2010; SPC, 2010 |
| Population density | Densely populated areas are more affected by flood hazard as there is greater potential for loss. Conversely, where there are no people, there are no disasters (Wisner et al., 2008). | Polygon shapefile | INEGI, 2010 |
| Distance to hospitals | Populations that are near hospitals are more resilient as they are able to recover from injuries more quickly. Populations near hospitals are less affected. Under the Civil Protection Strategy, hospitals may also act as improvised shelters if necessary (SNPC, 2009). | Point shapefile | INEGI, 2010 |
| Distance to nearest emergency shelter | Shelters reduce vulnerability by reducing exposure to hazard during extreme weather events. Populations near emergency shelters are less vulnerable (CENAPRED, 2009). | Point shapefile | INEGI, 2010 |
| Distance to federal roads | Unlike highways, federal roads are free and connect municipalities and States, allowing for speedy evacuation from a risk-prone area. By this rationale, populations farther away from federal roads are more vulnerable (CENAPRED, 2009). | Polyline shapefile | INEGI, 2010 |

## Social Vulnerability Index

The risks from floods result from a combination of geographical factors (and their concomitant environmental impacts), demographic and technical conditions (Smith, 2004). Therefore, this research considers flood risk as the probability of loss resulting from the interaction between natural hazards, demographic and infrastructural conditions. The factors influencing social vulnerability can hence be described as follows:

Vulnerability = $f$ (hazard occurrence, exposure, infrastructure, socioeconomic capacity)

and are further explained by the following model (cf. Krishnamurthy et al., 2011):

$$\text{Vulnerability} = \sum_{i=1}^{m} a_i H_i \times \sum_{j=1}^{n} b_j \; E_j \times \sum_{k=1}^{p} c_k \; I_k \times \sum_{l=1}^{a} d_l \; S_l$$

where $a_i$, $b_j$, $c_k$ and $d_l$ are the weights of Hazard $i$ ($H_i$), Exposure $j$ ($E_j$), Infrastructure $k$ ($I_k$) and Socioeconomic structure $l$ ($S_l$) respectively. And $m$, $n$, $p$ and $q$ are the total numbers of hazard, exposure, infrastructure and socioeconomic factors respectively. No zero values can be assigned in this model, or certain municipalities are rendered not vulnerable at all. All values are normalised, with 1 as the maximum value for each indicator; indicators are thus expressed as percentages of the maximum value of each indicator divided by 100. Measuring hazards with an index ($H_i$) can be problematic as different hazards require different measures of "intensity" such as wind speeds for hurricanes or epicentres for earthquakes (Coch, 1995). Flood frequency is used as the proxy for hazard in this model. Conversely, unaffected municipalities were considered uniformly vulnerable and were given a value representing the proximity of the municipality to the flood boundaries, expressed in terms of percentage of maximum value (1 minus (distance as % of maximum/100)).

Exposure to the hazard ($E_j$) refers to the degree of the system's contact with the hazard. In the case of *human* systems, the exposure refers to populations that are likely to be affected by a hazard. For this model, population density is used as a proxy for exposure. Thus, densely populated municipalities are more exposed to hazards (Jones, 1991).

Infrastructure ($I_k$) relates to the ability to evacuate or find safe shelter during a hazard event. For the purposes of this research, infrastructure is measured in terms of distances to (i) hospitals, (ii) safe shelters and (iii) roads, all of which are crucial for evacuation and are considered to influence risk. As for the other indicators, distances are expressed in terms of percentage of maximum distance. Municipalities already containing hospitals, shelters and roads were given the minimum value for municipalities without this infrastructure, and then divided by the number of hospitals, shelters or roads

in the municipality. For the model, all distances were measured with the Measure Tool in the ArcMap software.

Socioeconomic structure ($S_l$) is a measure of adaptive capacity, and can provide information about the ability of communities to cope with disasters. For this chapter, the relevant socioeconomic indicator is poverty, which influences the ability of a household to manage risks. Poverty is measured in terms of the percentage of population in the municipality that is below the national poverty line ($52 Mexican pesos, ~ US$ 4.21).

The weightings attributed to each of the indicators were defined qualitatively on a scale of 1-5 through expert opinion. Population density and poverty were considered to be the most significant indicators (weighting = 5). Hazard incidence was considered to be the second most important indicator, and was given slightly lower weighting because vulnerable populations can mobilise during a hazard event and reduce their exposure accordingly (weighting = 4). Distance to hospitals and shelters were deemed equally significant but less important (weighting = 3). Distance to federal roads was regarded to be the least important of the indicators because alternate mobilisation mechanisms can be improvised by vulnerable communities (weighting = 2). The results of the calculation were again normalised so that the vulnerability scores range from 0 to 100 and these were divided into five different ranges using the quintile method, with each range cumulatively representing 20% of the maximum vulnerability.

## Results

The mapping process shows a skewed distribution of infrastructure and vulnerabilities across the study area. What becomes apparent from the analysis is that the northern and central parts of Veracruz have more institutions to cope with flood hazards: 29 out of the 45 hospitals (64%) and eight of the 25 emergency shelters (32%) are concentrated in this region; similarly, the road network in the central part is well developed, connecting all the major centres of tourism in the State (Gobierno de Veracruz, 2010). The southern part of the State is more vulnerable due to the co-incidence of poorer communities, weaker infrastructure and higher flood frequency. Crucially, however, it is also important to note that the more densely populated municipalities are located in the northern part of the State (and only four high-density municipalities are in the south).

Using the composite score obtained from the model outlined above, each polygon (municipality) was assigned a value which allowed for the ranking of its vulnerability to flooding. Values were divided into quintiles, with each quintile assigned a qualitative indication of severity (from very low to very high). The results of the calculations are shown in Fig. 2 where each polygon has been classified according to the severity of flood vulnerability. There are eight polygons associated with very high flood vulnerability and they are all

located in the southern part of Veracruz. Similarly, it is interesting to note that, in general, the municipalities on the coast of the State have higher vulnerabilities than those that are further inland.

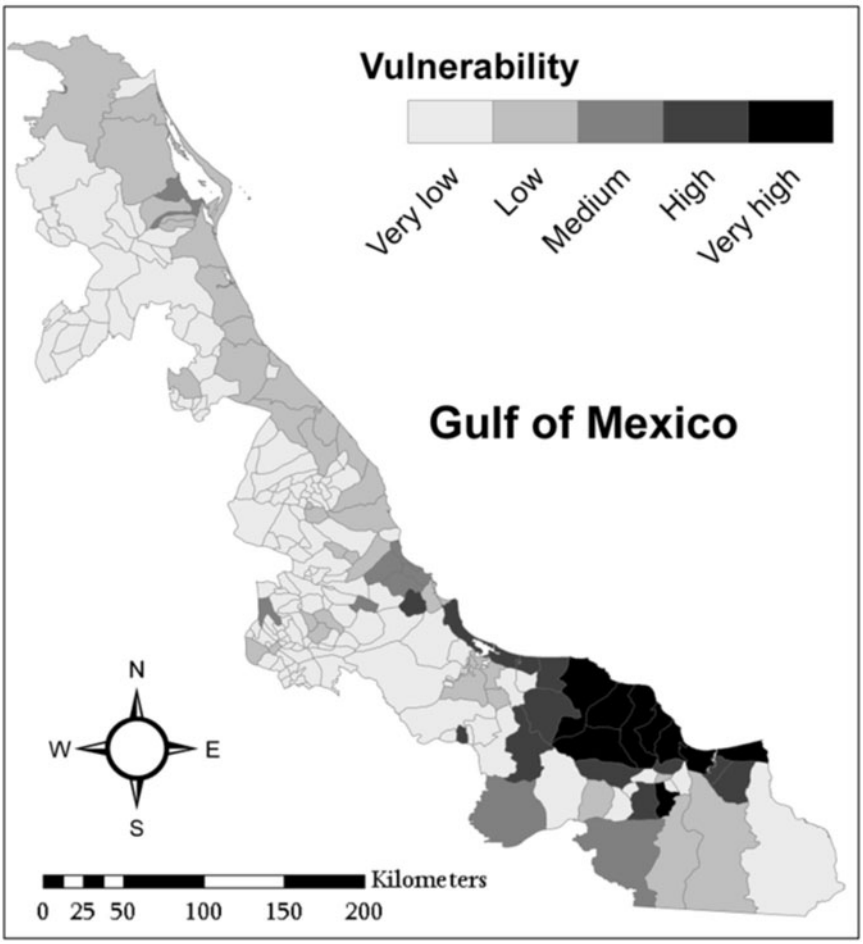


**Figure 2.** Social vulnerability map.

Geospatial analysis can also be useful for guiding and planning policy interventions: by identifying the factor that has the highest contribution to vulnerability in a particular polygon it is possible to isolate the single intervention with the highest potential for reducing risk. Figure 3 highlights the factors that are contributing to vulnerability in Hueyapan de Ocampo, a municipality that is extremely vulnerable to the adverse impacts of flooding through a spider diagram. The diagram highlights that low access to infrastructure, and particularly hospitals, has the highest contribution to vulnerability in the municipality, suggesting that building hospitals can reduce flood disaster risk in the area. High incidence of poverty is an important

contributing factor to overall vulnerability in the municipality; therefore, disaster risk reduction policy that includes effective poverty reduction strategies is essential in the context of the municipality. This type of information and analysis can be used to monitor and even anticipate the outcomes of a given intervention by altering the value of an indicator (as per expected or observed changes) and re-calculating the vulnerability score and can be very useful for planning. Similarly, vulnerability index analyses could be used to project future vulnerability under simple environmental change scenarios; for example, if flood frequency is expected to increase as a result of anthropogenic climate change, the values can be altered and the vulnerability score can be re-calculated (cf. Hahn et al., 2009).

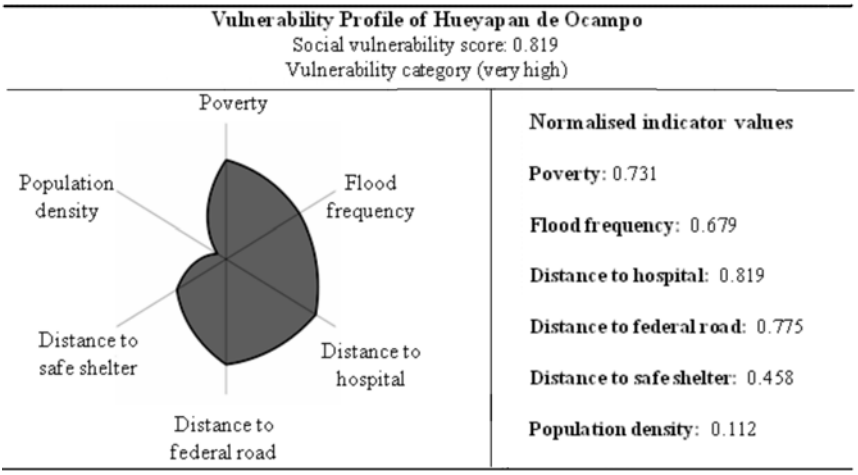


**Figure 3.** Spider diagram highlighting the contribution of indicators to the social vulnerability to floods in Hueyapan de Ocampo, a highly vulnerable municipality.

## Discussion

Social vulnerability is a critical aspect of hazard risk assessment. Yet it is rarely incorporated in hazard studies due to conceptual difficulties on the one hand, and a lack of suitable data on the other (Ebert et al., 2009). The principal aim of this study was to test the utility of indicators that could be obtained from spatial data in identifying social vulnerability for Veracruz. Six proxy variables, i.e. indicators that express the non-observable concept of social vulnerability were defined and their explanatory capacity was assessed. The indicators described social vulnerability with high accuracy. The final output of the model showed higher vulnerabilities to flood events in the southern part of the State than in the north. The skewed distribution of vulnerability resulted from poorer infrastructure in the southern part of the state. Moreover, the

model predicted higher social vulnerability on the coastal areas compared to inland municipalities. Methodologically, this can be explained by the higher population densities on the coastal municipalities (indeed, the three most densely populated municipalities were located on the coast). Conceptually, this is explained by the fact that coastal societies are more exposed to hydrometeorological hazards as they are closer to the source of the hazard (Wisner et al., 2004).

With the use of only six proxy variables (flood frequency, poverty rates, population density, distance to (i) hospitals, (ii) emergency shelters and (iii) roads), the model presented in this study generally corresponds with the expected vulnerabilities of the state. However, a number of limitations in the procedure must be pointed out. Although a literature review was conducted and consultation was held with experts in the field, the selection of proxy variables (and the weighting attributed to each variable) was a highly subjective exercise. Factors influencing social vulnerability vary geographically and temporally, and different societies are affected by hazards in different ways.

The number and selection of indicators is also subject to debate. The model used for this study considered "only" six variables. In a study of erosion risk in the South Downs region of England, Boardman et al. (2003) suggest a vulnerability index based on two factors: land use (crop choice) and slope. By contrast, Ebert et al. (2009) propose an index of social vulnerability to landslides in Tegucigalpa based on 47 variables. The argument can be made that consideration of more variables can enhance the explanatory power of a model, but it can also involve higher costs (for data collection) and higher computing power (for data analysis). Models which require fewer indicators may be preferred when time, resources and data are limited. Ultimately, the choice and number of indicators should relate to the end use of the tool: for policy purposes, indicators must have a relevant recommendation for disaster risk reduction interventions.

Further, it is possible that the model presented in this study overestimated vulnerability to flooding in the State of Veracruz. The initial predictions suggested that the central part of the state would be the least vulnerable to flood hazard due to the amount of infrastructure. However, attributing a higher weighting to population density resulted in the estimation that fourteen municipalities have medium vulnerability and one is highly vulnerable. Similarly, ten municipalities in the southern part had very low vulnerability scores due to low population densities (these municipalities had population densities of less than 15 inhabitants per kilometre square). This shows the crucial impact of population density on the modelled predictions.

Another way in which the model may overestimate vulnerability is by ignoring the distribution of infrastructure in the adjacent states: populations have the option of mobilising and temporarily resettling in the hospitals or shelters of adjacent, less affected states. Furthermore, infrastructure at the *local* level was not included. Such local institutions as clinics and improvised

shelters may play important roles in reducing social vulnerability. No suitable local datasets exist for clinics and *improvised* emergency shelters; for such data to be included a field study may be necessary. The scope of this study was therefore limited to data available through federal organisations. Nevertheless, inclusion of additional field data may be pertinent in the future for more accurate assessments of social vulnerability. Given the limitations outlined above, the final output must be taken to represent one of several tools that can inform flood risk assessment.

## Future Research Directions

Understanding social vulnerability is a significant first step in developing disaster risk reduction policies and in planning for hazard mitigation (Cutter et al., 2003). Contextualising vulnerability within a societal framework can help improve knowledge of the local institutions that enhance (or reduce) the ability of a community to cope with hazardous events (Wisner et al., 2004). The present study suggests that infrastructure (hospitals, safe shelter and roads) is an important element of social vulnerability. However, it is also important to recognize that social vulnerability is hazard-dependent (Tran et al., 2009): for example, the south of Veracruz is periodically disturbed by flood events but the adverse impacts of hurricane hazard affect on the northern part of the state more frequently. An important advancement in the understanding of vulnerability will therefore necessitate multiple-hazard assessment.

This chapter has proposed a methodology to integrate GIS tools in the assessment of social vulnerability to flood risk. The approach suggested in this essay can be replicated for other hazards and other comparable coastal zones provided that data *and* the technology to carry out an analysis are available. A map model such as the one presented in this chapter can be helpful in informing (i) local communities of their vulnerabilities and (ii) decision-makers of the factors that lead to social vulnerability.

To improve the quality of vulnerability assessments, it is important to obtain data—this research used open source data to illustrate the extent of data available at relatively high spatial resolution, but more data are required to do more complex analyses. Increasing access to geospatial information through online open source (for example, GeoCommons) can enhance the capacities to map and assess vulnerability. An important challenge, however, relates to the quality of data. This research used secondary data, for which it is impossible to estimate measurement errors or potential biases. To the extent that databases from international organisations and government-owned institutions were used for the research, potential biases are accounted for to a large extent. But as data for higher spatial resolution are collected, it will be important to collect high quality data that are reliable.

To overcome the challenges of secondary data collection, it is important to involve vulnerable communities themselves in the process: communities

have long-term links with their surroundings, but transmit this information orally. Hence, this knowledge is invisible (or unknown) to people outside the community. Different members of the community, including community leaders, professionals, women and children, can contribute by offering their perceptions on disaster risk and the factors that lead to vulnerability. Communities also have a strong cultural understanding of the risks associated with specific hazards. They can identify the crops that are most resilient and that are best adapted to the local conditions; the areas that are most affected during hurricane events (although satellite data is increasingly used to corroborate this information); the houses that are damaged either through inundation or through wind impacts; the families that are most vulnerable to hurricane hazard. Participatory GIS analyses can also be used to map social (e.g. caste), economics (e.g. income) and environmental (e.g. land use) differences that may not be already available and are therefore difficult to map without frequent field visits to the study site (Peters-Guarín et al., 2005). Beyond simply identifying risks, local people are also able to explain relationships between risk and vulnerability.

Vulnerability assessments through GIS analyses are being increasingly mainstreamed in disaster risk reduction strategies, and this trend is likely to continue over the coming decades as geospatial data becomes increasingly available and the technology increasingly accessible. More specifically, geospatial techniques for assessing vulnerability are likely to become a useful tool in guiding disaster risk reduction and in monitoring policy outcomes. In the context of Mexico, for instance, the *National Risk Atlas* (available online at http://www.atlasnacionalderiesgos.gob.mx/) highlights the hotspots for different risks in the country, including geological, hydrometeorological and chemical hazards. Further, in its fourth and latest National Communication to the United Nations Framework Convention on Climate Change, the Mexican Government highlights the importance of mapping techniques to identify adaptation priorities for vulnerable areas in the context of climate change (SEMARNAT and INE, 2010).

## Conclusion

This chapter demonstrates the needs, rationale and procedures for assessing social vulnerability through geospatial techniques. This information has been interpreted through a vulnerability map which outlines the factors that contribute to flood vulnerability at municipal level in the State of Veracruz, Mexico. By developing a GIS-based method based on open source data, this chapter proposes a framework for communicating vulnerability analysis to policy-making which can be replicated elsewhere. Here, it is important to note that modelling human systems is not necessarily universally robust: the model used for this research is based on the perceptions of the local community and should be seen as a visual representation of local risk perceptions in both time

and space. However, the incorporation of social indicators of vulnerability can illustrate vulnerability as well as feasible adaptation mechanisms. This knowledge can be conveyed to policy-makers to develop disaster management strategies that focus on specific vulnerabilities. Understanding vulnerability at high spatial resolutions can help improve knowledge of the social, environmental and institutional situations which enhance (or reduce) the ability of a community to cope with hazards.

## References

Adger, W.N. (1999). Social Vulnerability to Climate Change and Extremes in Coastal Vietnam. *World Development*, **27(2)**, 249–269.

Alexander, D. (1998). Natural Disasters. University College London Press, London, United Kingdom.

Boardman, J., Evans, R. and Ford, J. (2003). Muddy floods on the South Downs, Southern England: Problems and responses. *Environmental Science and Policy*, **6**, 69–83.

Centro Nacional de Prevención de Desastres [CENAPRED] (2009). Dirección de capacitación. Retrieved December 10, 2010, from http://www.cenapred.unam.mx/es/Capacitacion/

Clark, G.E., Moser, S.C., Ratick, S.J., Dow, K., Meyer, W.B., Emani, S., Jin, W., Kasperson, J.X. and Schwars, H.E. (1998). Assessing the vulnerability of coastal communities to extreme storms: the case of Revere, MA, USA. *Mitigation and Adaptation Strategies for Global Change*, **3(1)**, 59–82.

Coch, N.K. (1995). Geohazards: Natural and Human. Prentice Hall, New Jersey, United States.

Cutter, S.L., Boruff, B.J. and Shirley, W.L. (2003). Social vulnerability to environmental hazards. *Social Science Quarterly*, **82**, 242–260.

Daniel, E.B. and Abkowitz, M.D. (2005). Predicting storm-induced beach erosion in Caribbean Small Islands. *Coastal Management*, **33**, 53–69.

Dash, N. (1997). The use of geographic information system in disaster research. *International Journal of Mass Emergencies and Disasters*, **15(1)**, 135–146.

Ebert, A., Kerle, N. and Stein, A. (2009). Urban social vulnerability assessment with physical proxies and spatial metrics derived from air- and space-borne imagery and GIS data. *Natural Hazards*, **48**, 275–294.

Emergency Events Databases [EM-DAT] (2011). Retrieved January 2, 2011, from http://www.emdat.be/Database/CountryProfile/countryprofile2.php

Gobierno de Veracruz (2010). Cuarto Informe de Gobierno. Gobierno de Veracruz, Xalapa, Mexico.

Hahn, M.B., Riederer, A.M. and Foster, S.O. (2009). The Livelihood Vulnerability Index: A pragmatic approach to assessing risks from climate variability and change—A case study in Mozambique. *Global Environmental Change*, **19(1)**, 74–88.

Hart, D.E. and Knight, G.A. (2009). 'Geographic Information System assessment of tsunami vulnerability on a dune coast'. *Journal of Coastal Research*, **25(1)**, 131–141.

Hatfield Consultants (2006). Using Participatory Methodologies, Geographic Information Systems and Earth Observation Data to Map Traditional Ecological Knowledge in Hong Ha Commune, Thua Thien Hue, Viet Nam. EOSTEM Project Milestone 9 Report. Hatfield Consultants, West Vancouver, Canada.

Intergovernmental Panel on Climate Change Working Group I [IPCC WGI] (2007). Climate Change 2007 - The Physical Science Basis: Contribution of Working Group I to the Fourth Assessment Report of the IPCC. Cambridge University Press, Cambridge, United Kingdom.

National Institute for Geographic Studies and Informatics [INEGI] (2010). Retrieved January 3, 2011, from http://www.inegi.org.mx/

Jones, D.K.C. (1991). Environmental Hazards. *In:* Bennett, R. and Estall, R. (Eds) Global Change and Challenge (pp. 27–56). Routledge, London.

Krishnamurthy, P.K., Fisher, J.B. and Johnson, C. (2011). Mainstreaming local perceptions of hurricane risk into policymaking. *Global Environmental Change*, **21(1)**, 143–153.

Krishnamurthy, P.K. and Krishnamurthy, L. (2011). Agrobiodiversity for livelihood security: A case study of agroforestry technologies in Mexico. *Journal of Life Sciences*, **5(2)**, 108–119.

Morrow, B.H. (1999). Identifying and mapping community vulnerability. *Disasters*, **21(1)**, 1–18.

Nagarajan, R., Mukherjee, A., Roy, A. and Khire, M.V. (1998). Technical note: Temporal remote sensing data and GIS application in landslide hazard zonation of part of Western Ghat, India. *International Journal of Remote Sensing*, **19(4)**, 573–585.

Nicholls, R.J. and Mimura, N. (1998). Regional issues raised by sea-level rise and their policy implications. *Climate Research*, **11(1)**, 5–18.

Pareschi, M.T., Cavarra, L., Favalli, M., Giannini, F. and Meriggi, A. (2000). GIS and volcanic risk assessment. *Natural Hazards*, **21(2-3)**, 361–379.

Peters-Guarín, G., van Westen, C.J. and Monotya, L. (2005). Community-Based Flood Risk Assessment Using GIS for the Town of San Sebastián, Guatemala. *Journal of Human Security and Development*, **1(1)**, 29–49.

Pielke, Jr., R.A. (2005). Are there trends in hurricane destruction? *Nature*, **438**, E11.

Pradan, A. (2004, July 26-28). GIS and remote sensing for flood disaster identification: A case study of Koshi River basin in Nepal. Paper presented at the Global Symposium for Hazard Risk Reduction: Lessons Learned from the Applied Research Grants for Disaster Risk Reduction Program, Washington, DC, United States.

Rashed, T. and Weeks, J. (2003a). Assessing vulnerability to earthquake hazards through spatial multicriteria analysis of urban areas. *International Journal of Geographical Information Science*, **17(6)**, 547–576.

Rashed, T. and Weeks, J. (2003b). Exploring the spatial association between measures from satellite imagery and patterns of urban vulnerability to earthquake hazards. *The International Archives of the Photogrammetry, Remote Sensing and Spatial Information Sciences XXXIV*, **7(W9)**, 144–152.

Secretaría de Medio Ambiente y Recursos Naturales y el Instituto Nacional de Ecología [SEMARNAT and INE] (2008). Mexico's Third National Communication to the United Nations Framework Convention on Climate Change. SEMARNAT, Mexico City, Mexico.

Sistema Nacional de Protección Civil [SNPC] (2009). Normatividad de Protección Civil: Ley de Protección Civil para el Estado Libre y Soberano de Veracruz-Llave. SNPC, Mexico City, Mexico.

Smith, K. (2004). Environmental Hazards: Assessing Risk and Reducing Disaster. Routledge, London, United Kingdom.

Tran, P., Shaw, R., Chantry, G. and Norton, J. (2009). GIS and local knowledge in disaster management: A case study of flood risk mapping in Viet Nam. *Disasters*, **33(1)**, 152–169.

Twigg, J. (2001). Sustainable livelihoods and vulnerability to disasters. Working Paper 2. Benfield, London.

Wisner, B., Blaikie, P., Cannon, T. and Davis, I. (2004). At Risk: Natural hazards, people's vulnerability and disasters. Routledge, London, United Kingdom.

# Index



J.K. Thakur et al. (eds.), *Geospatial Techniques for Managing Environmental Resources*,
DOI 10.1007/978-94-007-1858-6, © Capital Publishing Company 2012